

# Heavy Flavor Coefficient Functions in Deep-Inelastic Scattering at $O(a_s^2)$ and Large Virtualities

Diplomarbeit  
zur Erlangung des wissenschaftlichen Grades  
Diplom-Physiker

vorgelegt von

Sebastian Werner Gerhard Klein<sup>a</sup>

geboren am 23.01.1980 in Karlsruhe

Betreuer: PD Dr. Johannes Blümlein<sup>b</sup>

<sup>a</sup>*Universität Potsdam, Institut für Physik  
Am Neuen Palais 10, D-14469 Potsdam*

<sup>b</sup>*Deutsches Elektronen-Synchrotron, DESY  
Platanenallee 6, D-15738 Zeuthen*

eingereicht am 27. Oktober 2006

Gutachter:

PD Dr. Johannes Blümlein, DESY, Zeuthen

Prof. Dr. Martin Wilkens, Universität Potsdam

# Contents

<b>1</b>	<b>Introduction</b>	<b>5</b>
<b>2</b>	<b>Deeply Inelastic Scattering</b>	<b>10</b>
2.1	Kinematics . . . . .	10
2.2	Cross Section . . . . .	11
2.3	The Tensor for Forward Compton Scattering . . . . .	15
2.4	Moment Structure of the Hadronic Tensor . . . . .	16
2.5	The Parton Model . . . . .	18
2.5.1	Validity of the Parton Model . . . . .	19
2.5.2	Scaling . . . . .	21
<b>3</b>	<b>Operator Product Expansion Near the Light Cone</b>	<b>23</b>
3.1	Light Cone Dominance . . . . .	23
3.2	Light Cone Expansion . . . . .	24
3.3	Operator Matrix Elements . . . . .	25
3.4	Structure of the Heavy Quark Coefficient Functions in the Limit $Q^2 \gg m^2$ up to $O(\alpha_s^2)$ . . . . .	26
3.5	Outline of the Computation of $\hat{A}_{ij}^{(k)}$ . . . . .	27
<b>4</b>	<b>Regularization and Renormalization</b>	<b>29</b>
4.1	Dimensional Regularization . . . . .	29
4.2	The $\overline{\text{MS}}$ Scheme . . . . .	29
4.3	Renormalization of $\hat{A}_{ij}$ . . . . .	30
<b>5</b>	<b><math>F_2^{Q\bar{Q}}</math> and <math>F_L^{Q\bar{Q}}</math> at Leading Order</b>	<b>35</b>
5.1	Complete Calculation of $H_{(2,L),g}^{(1)}$ at Leading Order . . . . .	36
5.2	The Limit $Q^2 \gg m^2$ . . . . .	38
<b>6</b>	<b>Heavy Flavor Coefficient Functions for Large <math>Q^2</math> at Leading Order</b>	<b>40</b>
6.1	LO Wilson Coefficients for Massless Quark $ep$ -Pair Production in the $\overline{\text{MS}}$ Scheme . . . . .	40
6.2	The Calculation of the Operator Matrix Element $\hat{A}_{Qg}^{(1)}$ . . . . .	41
6.3	The Heavy Flavor Wilson Coefficients for $Q^2 \gg m^2$ . . . . .	42
<b>7</b>	<b>Two-Loop Massive Operator Matrix Elements</b>	<b>44</b>
7.1	Feynman Diagrams . . . . .	44
7.2	Momentum Integrals . . . . .	47
7.2.1	1-Loop Insertions . . . . .	48
7.2.2	Genuine 2-Loop Diagrams . . . . .	51
7.3	Summation . . . . .	52
7.3.1	Summation Techniques . . . . .	55
7.4	Five-Propagator Integrals . . . . .	57
7.4.1	Mellin-Barnes Representation . . . . .	57
7.4.2	Hypergeometric Representation . . . . .	60
7.5	Reduced Integrals . . . . .	63
7.6	The Final Results for the 2-Loop Operator Matrix Elements . . . . .	66

8	The 2-Loop Heavy Flavor Wilson Coefficients	71
9	Summary	74
10	Appendix	75
A	Conventions	77
B	Feynman Rules	79
C	Kinematics of 2-to-2 particle scattering	81
D	Color Factors in $SU(N)$	83
E	Results for the Individual Diagrams	84
F	Momentum Integrals in $D$ dimensions	92
G	Sums	94
G.1	Sums involving Harmonic Sums	94
G.2	Sums involving Beta-Functions	97
G.3	Sums involving Beta-Functions and Harmonic Sums	98
G.4	Sums involving Beta-Functions and Harmonic Sums with two Free Indexes	102
G.5	Sums involving Binomials	102
G.6	Sums involving Binomials and Harmonic Sums	103
G.7	Sums involving Binomials with Two Free Indexes	106
G.8	Other Sums	106
G.9	Some Techniques	106
H	The $\Gamma$ -Function and Related Functions	108
I	Generalized Hypergeometric Series	110
J	Parameter Integrals	115
K	Mellin Transforms and Polylogarithms	120
L	Splitting Functions	122

## List of Figures

1	Schematic graph of deeply inelastic scattering for single boson exchange.	10
2	Schematic picture of the optical theorem.	15
3	Deeply inelastic electron-proton scattering in the parton model.	19
4	Feynman diagrams contributing to the photon gluon fusion process at LO.	35
5	Feynman diagrams contributing to $\hat{A}_{Qg}^{(1)}$ .	41
6	Feynman diagrams contributing to the gluonic OME $\hat{A}_{Qg}^{(2)}$ .	46
7	1-particle reducible diagrams contributing to the gluonic OME $\hat{A}_{Qg}^{(2)}$ .	47

8	Feynman diagrams contributing to the pure-singlet OME $\hat{A}_{Qq}^{(2),PS}$ . . . . .	47
9	Feynman diagrams contributing to the non-singlet OME $\hat{A}_{qq}^{(2),NS}$ . . . . .	47
10	Feynman diagrams contributing to $\hat{A}_{Qg}^{(1)}$ and acting as 1-loop insertion for $\hat{A}_{ij}^{(2)}$ . . . . .	48
11	1-loop insertions in computing $\hat{A}_{ij}^{(2)}$ . . . . .	50
12	Labeling of the propagators of diagrams $f$ and $n$ . . . . .	64
13	Feynman rules for QCD. . . . .	79
14	Feynman rules for composite operators. . . . .	80

## List of Tables

1	The first four Mellin moments for the scalar five propagator integrals of graphs $e, f, h, l, m, n, o$ using M. Czakon's MB package. . . . .	58
2	Analytic results for the first four Mellin moments for the scalar five propagator integrals of graphs $e, f, h, l, m, n, o$ . . . . .	59
3	Analytic results for general $N$ for the scalar five propagator integrals of graphs $e, f, h, l, m, n, o$ . . . . .	60
4	The analytic results for the reduced scalar integrals of graphs $f$ and $n$ . . . . .	65
5	Complexity of the results in Mellin space and in $z$ -space for each diagram . . . . .	66
6	Functions contributing to the results in $z$ -space . . . . .	70



# 1 Introduction

During the last century, the substructure of matter has been investigated at increasingly shorter distances. In 1911 in his famous scattering experiments, E. Rutherford discovered the substructure of the atom, [1]. Most of the mass of the atom was found to be contained in a small, positively charged nucleus being surrounded by negatively charged, point-like electrons. Subsequently, the proton, [2], and the neutron, [3], were identified to be the constituents of the atomic nucleus, bound together by pions [4]. In the following R. Frisch and O. Stern (1933) and R. Bacher, L. Alvarez and F. Bloch (1933/40) discovered the anomalous magnetic moments of the proton and neutron, [5], which gave first evidence for a possible compositeness of nucleons. With the availability of electron beams of much higher energy during the 1950's, R. Hofstadter et. al. revealed the charge substructure of the nucleons [6].

Parallel to the investigations of the nucleon structure, a large amount of hadrons was discovered in cosmic ray and accelerator experiments. Hadrons are strongly interacting particles which occur as mesons (spin = 0, 1) or baryons (spin = 1/2, 3/2). In the beginning of the 1960's investigations were undertaken to systematize the hadrons, based on their properties as quantum numbers or masses. In 1964, M. Gell-Mann, [7], and G. Zweig, [8], proposed the quark model as a mathematical description for these hadrons<sup>1</sup>. Three quark flavors, up( $u$ ), down( $d$ ) and strange( $s$ ), were sufficient to give a group-theoretic description of all hadrons known at that time. The quarks were considered as fractionally charged, spin-1/2 states. Baryons thus consist of three quarks and mesons of a quark-antiquark pair. Assuming  $SU(3)$  flavor symmetry, properties for hadrons such as their anomalous magnetic moment and, to some extent, mass relations between groups of hadrons could be derived. The mass of the  $\Omega^-$ -baryon could be predicted before it was finally observed, [9], marking a great success for the quark model. A problem occurred in describing baryons containing quarks of the same flavor and spin, as is the case for the  $\Delta^{++} = |u \uparrow u \uparrow u \uparrow\rangle$  state. This apparently violated the Pauli-principle. Greenberg, [10], proposed parastatistics to solve this problem. Another solution consisted in maintaining the Pauli-principle and introducing a new quantum number for the quarks being otherwise identical, called color. The lack of direct experimental evidence of this new degree of freedom prompted the assumption that all physical observables must be color-neutral [11–13]. At this stage, the quark model provided a static description of hadrons but did not explain whether quarks are the constituents of hadrons and, if so, which force would bind them to colorless states.

At the end of the 1960's the Stanford Linear Accelerator SLAC, cf. [14], allowed to perform deeply inelastic lepton-nucleon scattering experiments at much higher resolutions than previously possible. Deeply inelastic scattering is one of the cleanest ways to resolve the inner structure of any composite object. A beam of well-known, structureless particles, which are not interacting strongly, is scattered off the object of interest and one measures momentum and energy of the outgoing particles. The scale which thus can be resolved decreases with increasing beam energy and is inversely proportional to the modulus of the momentum exchanged between the interacting particles. The SLAC-MIT experiments measured the structure functions of nucleons which depend both on the energy transfer  $\nu$  and the 4-momentum transfer  $q^2 = -Q^2$  from the lepton to the nucleon. In the case of unpolarized electron-proton scattering via the exchange of a single virtual photon, the cross section can be described by two structure functions,  $F_2(\nu, Q^2)$  and  $F_L(\nu, Q^2)$ . In the high energy limit,  $Q^2, \nu \rightarrow \infty, Q^2/\nu = \text{fixed}$ , it was found that both structure

---

<sup>1</sup>In contrast to Gell-Mann, Zweig considered quarks as real physical building blocks of the hadrons.

functions  $F_2(\nu, Q^2)$  and  $F_L(\nu, Q^2)$  depend on the ratio of  $Q^2$  and  $\nu$  only. This phenomenon was called scaling [15]. Some time before, J. Bjorken predicted this behavior in a field theoretic analysis based on current algebra, which describes hadrons under the influence of electromagnetic and weak interactions [16]. As the relevant parameter in the deep-inelastic limit he introduced the Bjorken-scaling variable  $x = Q^2/2M\nu$ , where  $M$  is the mass of the nucleon. Shortly after, R. Feynman could give a phenomenological explanation for this behavior of structure functions within the parton model [17]. According to this model, the proton consists of several point-like constituents, the partons. His assumption was that during the interaction time - which is very short since high energies are involved - these partons behave as free particles off which the electrons scatter elastically. Therefore the total cross section is just the incoherent sum of the individual electron-parton cross-sections, weighted with the probability to find the particular parton inside the proton. The latter is given for parton  $i$  of the proton by the parton density  $f_i(z)$ . It denotes the probability to find the parton  $i$  in the proton carrying the fraction  $z$  of the total proton momentum  $P$ . In the limit considered by Feynman,  $z$  becomes equal to  $x$ , giving an explanation for scaling. Bjorken and E.A. Paschos, [18], identified quarks and partons.

In 1967 S. Weinberg proposed the electroweak  $SU_L(2) \times U_Y(1)$  standard model based on gauge interactions, [19], extending earlier work by S. Glashow, [20], cf. also [21], for the leptonic sector. This theory was proved to be renormalizable by G. t'Hooft and M. Veltman in 1972, [22], cf. [23, 24], if anomalies are canceled including quarks in appropriate representations. G. t' Hooft also proved renormalization for massless Yang-Mills theories [25]. These gauge theories had first been studied by C.N. Yang and R.L. Mills in 1954, [26], and have the distinctive property that their gauge group is non-abelian, contrary to Quantum Electrodynamics. In 1973, M. Gell-Mann, H. Fritzsch and H. Leutwyler, [27], cf. also [13], proposed to gauge color which leads to an extension of the standard model to  $SU_L(2) \times U_Y(1) \times SU_c(3)$ , including the strongly interacting sector. The dynamical theory of quarks and gluons, Quantum Chromodynamics, is thus a massless Yang-Mills theory which describes the interaction of different quark flavors via massless gluons. Among the semi-simple compact Lie-groups,  $SU(3)$  turns out to be the only possible gauge group for this theory, cf. [28]. In 1973 D. Gross and F. Wilczek, [29], and H. Politzer, [30], proved in a 1-loop calculation that Quantum Chromodynamics is an asymptotically free gauge theory, which allows to perform perturbative calculations for processes at high enough energies scales. There the strong coupling constant becomes sufficiently small and a perturbative parameter.

The cross section of deeply inelastic processes receives contributions from two different resolution scales  $Q^2$ . One is the large energy - or small distance - region, to which perturbative techniques can be applied. The other is the low energy - or long distance - region, which describes the hadronic bound state effects and cannot be treated perturbatively due to the large coupling at these scales. The operator product expansion near the light-cone, [31], can be applied to separate these two effects. Thus the two energy scales of the process are associated with two different quantities, the Wilson coefficients and the operator matrix elements. The former contain the large scale contributions and can therefore be calculated perturbatively, whereas the latter describe the low scale behavior and are quantities which have to be extracted from experimental data. Using this technique, one can recover Feynman's parton model and show the equivalence of the approaches by Feynman and Bjorken in the twist-2 approximation [32].

The light-cone expansion also allows to explain the logarithmic scaling violations of the deep



inelastic cross section, which had to be expected since QCD is not an essentially free field theory [33–37]. In fact, the prediction of scaling violations is one of the strongest experimental evidences of QCD.

Thus deeply inelastic scattering played a crucial role in formulating and testing QCD as the theory governing the dynamics of quark systems. Its two most important properties are the confinement postulate - all physical states have to be color singlets - and asymptotic freedom - the strength of the interaction gets weaker at higher scales, i.e. shorter distance.

An important step toward completing the standard model were the observations of the three heavy quarks charm, bottom and top. In 1974 two narrow resonances, called  $\Psi$  and  $\Psi'$ , were observed at SLAC in  $e^+e^-$  collisions at 3.1 GeV and 3.7 GeV, respectively [38]. At the same time at Brookhaven in proton-proton collisions a new particle called  $J$  was discovered at the same energy as  $\Psi$  [39]. The  $\Psi$  and the  $J$  resonance were identified to describe the same particle, called  $J/\Psi$ . Its existence could not be explained in terms of the three known quark flavors and was interpreted as a meson consisting of a new quark, the charm quark. This was an important success of the standard model, since the existence of the charm was postulated before, [40], and is necessary to cancel anomalies for the 2nd family. With its mass of  $m_c \approx 1.3$  GeV it is much heavier than the light quarks,  $m_u \approx 2$  MeV,  $m_d \approx 5$  MeV,  $m_s \approx 100$  MeV, [41], and heavier than the proton. In later experiments, two other heavy quarks were detected. In 1977 the  $\Upsilon$  ( $= b\bar{b}$ ) resonance was observed at Fermilab, [42], and interpreted as a bound state of an even heavier quark, the bottom, with  $m_b \approx 4.2$  GeV [41]. Ultimately, the quark picture was completed by the discovery of the heaviest quark, the top-quark, in  $p\bar{p}$  collisions at the Tevatron in 1995 [43]. Its mass is given by roughly  $m_t \approx 175$  GeV [41]. The heavy quarks cannot be considered as constituents of hadrons bound in atomic nuclei. They are excited in high energy experiments and may form short-lived hadrons with the exception of the top-quark, which decays before it can form a bound state.

The production mechanisms of heavy quarks give an important contribution to the structure functions of deeply inelastic scattering [44–47]. A precise Mellin-space representation of the heavy flavor Wilson coefficients was given in Ref. [48]. The structure function  $F_2(x, Q^2)$  is measured in a wide kinematic region, [41], whereas  $F_L(x, Q^2)$  was mainly measured in fixed target experiments, [49], and determined in the region of large  $\nu$  [50]. The last running period of the Hadron-Elektron-Ring-Anlage HERA at DESY in Hamburg is devoted to the measurement of  $F_L(x, Q^2)$  in both experiments, H1 and ZEUS, and currently in progress [51]. The most important factor to increase accuracy is to enrich luminosity at large enough scales in future experiments. In the foreseeable future, experiments at the proposed US Electron-Ion-Collider (EIC) could be able to measure  $F_L(x, Q^2)$  at a much larger luminosity than HERA.

In order to derive theoretical predictions, a first step in calculating the heavy flavor contributions to the structure functions consists in applying the renormalization group equation to obtain mass factorization, cf. [52, 53], between the heavy flavor Wilson coefficients and the light flavor parton densities. These parton densities carry all information on the structure of the proton at short distances and the level of twist-2. They are not calculable perturbatively and have to be extracted from experimental data. However, since they are process independent quantities, the same parton densities can be used to describe not only deeply inelastic events, but also the proton-proton collisions at the upcoming Large-Hadron-Collider (LHC) at CERN. The need for considering heavy quark production has therefore several aspects. One of them is to obtain a better description of heavy flavor production and its contribution to the structure

functions of the nucleon. On the other hand, increasing our knowledge on the perturbative part of deep-inelastic processes allows for a more precise determination of the parton-densities from experimental data. Thus one learns more about the structure of the proton and can use the parton densities for the description of different processes, and along with this obtain a more precise determination of the scale of Quantum Chromodynamics,  $\Lambda_{QCD}^{\overline{MS}}$ . This also serves as a test for QCD, since one can compare the parton densities obtained from different experiments and analyzes.

This thesis will concentrate on extrinsic unpolarized charm-production in deep-inelastic scattering. The charm is the lightest of the heavy quarks and therefore requires lower energies to be produced. In the case considered, the charm quark appears either through virtual corrections in fermion loops or in the final state of the radiative processes. It is well suited to extract the gluon density since at leading order (LO) only the photon-gluon fusion process contributes to the cross section [44, 45]. next-to-leading order (NLO) calculations as performed in Ref. [46] showed that this process is still dominant, although now other processes contribute as well. The gluon density plays a special role, since roughly 50 percent of the proton momentum can be attributed to it, as data from Fermilab and CERN showed already in the seventies [54]. Improved knowledge on  $g(x, Q^2)$  is also necessary to describe gluon-initiated processes at the Tevatron and at the LHC. Additionally, the study of heavy quark production will help to understand the small- $x$  behavior of the structure functions, since they show a steep rise, which is mainly attributed to the gluon density.

At present the unpolarized heavy flavor corrections to the structure functions are known up to NLO and partly to next-to-next-to-leading order (NNLO). The LO terms have been derived in the late seventies, [44, 45], and a semi-analytical result at NLO in the mid-90's [46]. In the asymptotic limit  $Q^2 \gg m_c^2$ , a similar factorization as described above for the heavy Wilson coefficients can be obtained. Using the light-cone expansion, they are then given by a Mellin-convolution of the massless Wilson coefficients  $C(Q^2/\mu^2)$  and heavy partonic operator matrix elements  $A(m^2/\mu^2)$ ,  $\mu^2$  being the factorization scale. This allows to calculate all contributions but the power-suppressed terms  $(m^2/Q^2)^k$ , as has first been outlined in Ref. [55]. The former are process dependent quantities, whereas the latter are process independent and describe the heavy quark mass effects. The Wilson coefficients for massless quarks were calculated in LO [56], NLO [57–59], and NNLO [60–62]. An analytic result for the NLO heavy operator matrix elements was derived in Ref. [55], thereby giving a full NLO analytic result in the asymptotic limit. The asymptotic NNLO heavy flavor longitudinal Wilson coefficients have been derived recently [47].

The aim of this thesis is the calculation of the photon-light-parton fusion processes and their contributions to the heavy Wilson coefficients in analytic form in the limit  $Q^2 \gg m_c^2$ . Its main part consists of recalculating the 2-loop heavy operator matrix elements, which are needed to describe the asymptotic NLO contributions to  $F_2(x, Q^2)$  and the NNLO result for  $F_L(x, Q^2)$ . The respective matrix elements have been calculated for the first time in Ref. [55] but have not yet been confirmed by an independent calculation. In doing so, massive 2-loop 2-point functions have to be calculated with an additional operator insertion in the Feynman diagrams. Note that applying the renormalization group equation allows for the calculation of the logarithmic heavy flavor corrections and the constant in the asymptotic limit. However, the logarithmic orders are given in terms of the known splitting functions, [33–35, 59, 63–66], and massless Wilson coefficients [56–62]. The main purpose of this thesis is therefore to calculate the constant term. As a by-product LO and NLO splitting functions are obtained as well. These calculations finally allow

to calculate the heavy flavor contributions  $F_2^{Q\bar{Q}}(x, Q^2)$  and  $F_L^{Q\bar{Q}}(x, Q^2)$  in the region  $Q^2 \gg m_c^2$ . The problem to be solved is a single scale problem, since the external particles are gluons and light quarks, respectively, on their mass-shell. The approach in Ref. [55] heavily relied on the integration-by-parts method, [67], thereby reducing 5-propagator integrals to integrals with only four propagators or less. In doing so, however, one artificially increases the number of integrals and produces many terms which cancel in the end. Additionally, this calculation was performed in  $z$ -space and not in Mellin-space, resulting in expressions containing a vast amount of different Nielsen-integrals, [68]. In this work, a different approach is followed, which overcomes these problems.

The thesis is organized as follows. Deeply inelastic scattering and how to treat it in the framework of the parton model is described in detail in section 2. We discuss the framework of factorization in the asymptotic limit  $Q^2 \gg m_c^2$  using the light-cone expansion in section 3. The renormalization procedure involved in this calculation and the regularization scheme is explained in section 4. The complete leading order results, [44, 45], are recalculated in section 5. In section 6 we apply the light-cone expansion and calculate the light flavor coefficient functions and the 1-loop massive operator matrix element and thus obtain the asymptotic result of section 5. The main part of this thesis is the calculation of the two-loop massive operator matrix elements in section 7. Contrary to Ref. [55], integration-by-parts is thoroughly avoided, thereby compacting and reducing the complexity of the calculation. By working in Mellin-space rather than in  $z$ -space, the problem is shifted from integrating Nielsen-integrals with partly sophisticated arguments to calculating sums with one free integer parameter,  $N$ . This is done by making use of integral representations of generalized hypergeometric series and Mellin-Barnes integrals [69]. The final result can then be expressed in terms of harmonic sums [70, 71]. Both approaches can be mapped to each other, but the latter has several advantages. For instance, the number of different functions in the final result is reduced significantly. Another aspect is that this calculation could be automatized to a large extent using the algebraic manipulation programs FORM, [72], and MAPLE, contrary to Ref. [55], where a large part of the calculation had to be done by hand. In section 8 the respective physical observables are described to  $O(a_s^2)$ . Section 9 contains the conclusion. Several technical aspects and sample calculations are given in the appendices.

## 2 Deeply Inelastic Scattering

Scattering high energy leptons off hadrons provides one of the cleanest possibilities to investigate the nucleon structure at short distances. Usually the 4-momentum transfers  $q^2 = -Q^2$  involved are at least of the order  $Q^2 \geq 1 \text{ GeV}^2$ , at which the target nucleonic states are destroyed during the interaction. Hence the process is called inelastic. The resolution of spatial scales in deeply inelastic scattering (DIS) is approximately given by  $1/\sqrt{Q^2}$ . Charged leptons ( $e^\pm$ ,  $\mu^\pm$ ) as well as neutrinos  $\nu$ ,  $\bar{\nu}$  can be used as probes of the hadrons and thus one is able to measure a variety of scattering cross sections containing different flavor combinations of quarks. Additionally, polarized lepton scattering at polarized targets can be performed in order to investigate the spin structure of hadrons [73].

DIS has been very important in establishing QCD as an asymptotically free field theory. The experiments performed at SLAC in 1968 prompted the introduction of the parton model, [17,18], and lead to the acceptance of the quark hypothesis [7, 8, 18].

In section 2.1 we discuss the kinematics of the process. A general expression for the cross section of unpolarized electromagnetic electron-proton scattering is given in section 2.2. The cross section can then be related to the forward Compton amplitude via the optical theorem as will be described in 2.3, which allows to make quite general statements on the mathematical structure of the result, cf. section 2.4. Up to this point, all considerations are quite general, based on the well-known electroweak theory and a description of the hadron using current algebra, [11], only. This section concludes with the motivation and phenomenological description of the parton model, cf. subsection 2.5, which explains many properties of DIS processes and was historically a breakthrough in establishing QCD. Most importantly it can describe the scaling behavior of the structure functions observed at SLAC.

### 2.1 Kinematics

We describe DIS at tree level (LO) in electroweak theory, see Figure 1. A lepton with momentum

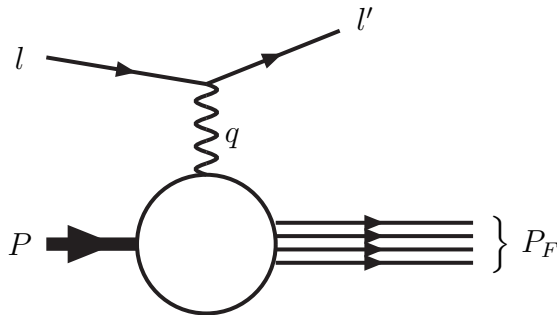


Figure 1: Schematic graph of deeply inelastic scattering for single boson exchange.

$l$  scatters off a nucleon of mass  $M$  and momentum  $P$  via the exchange of a virtual vector boson with momentum  $q$ . The momentum of the outgoing lepton is given by  $l'$  and the outgoing hadronic jet is denoted by  $F$  with total momentum  $P_F$ . Here  $F$  can consist of any combination

of hadronic states allowed by quantum number conservation. The virtual vector boson is space-like and one defines the virtuality  $Q^2$  as

$$Q^2 := -q^2, \quad (1)$$

$$q = l - l'. \quad (2)$$

Further important Lorentz-invariants are

$$s := (P + l)^2, \quad (3)$$

$$W^2 := (P + q)^2 = P_F^2. \quad (4)$$

In order to describe this process, one usually refers to the scaling variable Bjorken- $x$ , the variable  $y$  and the total energy transfer  $\nu$  of the lepton to the nucleon in the nucleon's rest frame [16]. They are given by

$$\nu := \frac{P \cdot q}{M} = \frac{W^2 + Q^2 - M^2}{2M}, \quad (5)$$

$$x := \frac{-q^2}{2P \cdot q} = \frac{Q^2}{2M\nu} = \frac{Q^2}{W^2 + Q^2 - M^2}, \quad (6)$$

$$y := \frac{P \cdot q}{P \cdot l} = \frac{2M\nu}{s - M^2} = \frac{W^2 + Q^2 - M^2}{s - M^2}. \quad (7)$$

Note that lepton masses are neglected throughout this analysis. In general, the virtual vector boson exchanged can be a  $\gamma$ ,  $Z$  or  $W^\pm$ -boson with the in- respectively outgoing lepton being an electron, muon or neutrino, respectively. This thesis is restricted to electron-proton scattering. Thus weak effects caused by the exchange of a  $Z$ -boson can be neglected as long as the virtuality is not too large, i.e.  $Q^2 \leq 500 \text{ GeV}^2$ , cf. [74]. For these values of  $Q^2$  this reaction is dominated by single photon exchange, which from now on will be considered only.

The physical region of this process is given by the condition

$$W^2 \geq M^2, \quad (8)$$

which can be inferred from the fact that the incoming hadron is taken to be stable and cannot decay into a system of smaller invariant mass [75]. By further considering the proton's rest frame and demanding a positive energy transfer from the lepton to the proton one obtains

$$\nu \geq 0, \quad 0 \leq y \leq 1, \quad s \geq M^2. \quad (9)$$

From (8) follows the kinematic region for Bjorken- $x$  via

$$\begin{aligned} W^2 = (P + q)^2 &= M^2 - Q^2 \left(1 - \frac{1}{x}\right) \geq M^2 \\ \implies 0 &\leq x \leq 1. \end{aligned} \quad (10)$$

Note that  $x = 1$  describes the elastic process, whereas  $x < 1$  is the inelastic region [76].

## 2.2 Cross Section

The transition matrix element of deeply inelastic  $ep$ -scattering in Born-approximation is given by [28, 77]

$$M_{fi} = \langle l', \lambda', P_F | T | l, \lambda, P, \sigma \rangle = e^2 \bar{u}(l', \lambda') \gamma^\mu u(l, \lambda) \frac{1}{q^2} \langle P_F | J_\mu^{em}(0) | P, \sigma \rangle. \quad (11)$$

Here the spin components of the electron are denoted by  $\lambda$  and of the initial state proton by  $\sigma$ . The initial proton state and the final hadronic one are denoted by  $|P, \sigma\rangle$  and  $|P_F\rangle$ , respectively. The  $\gamma$ -matrices are denoted by  $\gamma_\mu$ ,  $u$  is the bi-spinor of the electron and  $\bar{u}$  its conjugate, see Appendix A. Further  $e$  is the electric charge and  $J_\mu^{em}(\xi)$  the quarkonic part of the electromagnetic current. At the moment, it is not necessary to specify this current any further. Note, however, that we consider neutral currents, which are self-adjoint

$$J_\mu^\dagger(\xi) = J_\mu(\xi) . \quad (12)$$

In view of QCD, the electromagnetic quark current is given by

$$J_\mu^{em}(\xi) = \sum_f \bar{\Psi}_f(\xi) \gamma_\mu \lambda^{em} \Psi_f(\xi) , \quad (13)$$

where  $\Psi_f(\xi)$  denotes the quark field of flavor  $f$ . For three light flavors,  $\lambda^{em}$  is given by the following combination of generators of the flavor group  $SU(3)_{flavor}$ , cf. [78, 79],

$$\lambda^{em} = \frac{1}{2} \left( \lambda_f^3 + \frac{1}{\sqrt{3}} \lambda_f^8 \right) . \quad (14)$$

The kinematics of the process can be measured from the scattered lepton or the hadronic final states, [80], depending on the experiment. The unpolarized cross section is obtained by averaging over the spin degrees of freedom of the leptonic and hadronic states [28, 77]. According to standard definitions, [81], the differential inclusive cross section is then given by

$$l'_0 \frac{d\sigma}{d^3l'} = \frac{1}{32(2\pi)^3(l.P)} \sum_{\lambda', \lambda, \sigma, F} (2\pi)^4 \delta^4(P_F + l' - P - l) |M_{fi}|^2 . \quad (15)$$

Inserting the transition matrix element (11) into the relation for the cross section, one notices that the trace over the leptonic states forms a separate tensor,  $L^{\mu\nu}$ . Similarly, the hadronic tensor  $W_{\mu\nu}$  is formed,

$$L_{\mu\nu}(l, l') = \sum_{\lambda', \lambda} \left[ \bar{u}(l', \lambda') \gamma^\mu u(l, \lambda) \right]^* \left[ \bar{u}(l', \lambda') \gamma^\nu u(l, \lambda) \right] , \quad (16)$$

$$W_{\mu\nu}(q, P) = \frac{1}{4\pi} \sum_{\sigma, F} (2\pi)^4 \delta^4(P_F - q - P) \langle P, \sigma | J_\mu^{em}(0) | P_F \rangle \langle P_F | J_\nu^{em}(0) | P, \sigma \rangle . \quad (17)$$

Thus one arrives at the following relation for the cross section

$$\begin{aligned} l'_0 \frac{d\sigma}{d^3l'} &= \frac{1}{4P.l} \frac{\alpha^2}{Q^4} L^{\mu\nu} W_{\mu\nu} \\ &= \frac{1}{2(s - M^2)} \frac{\alpha^2}{Q^4} L^{\mu\nu} W_{\mu\nu} , \end{aligned} \quad (18)$$

where  $\alpha$  is the fine-structure constant, see Appendix A. The leptonic tensor in (18) can be computed easily in the context of the standard model. Using relations given in Appendix A one obtains

$$L_{\mu\nu}(l, l') = Tr[\not{l} \gamma^\mu \not{l}' \gamma^\nu] = 4(l_\mu l'_\nu + l'_\mu l_\nu - \frac{Q^2}{2} g_{\mu\nu}) . \quad (19)$$

The description of the hadronic tensor, which represents all produced hadronic states, forms the heart of the problem. It cannot be calculated perturbatively within the framework of a field-theory as QCD. In the following, quite general considerations on the hadronic tensor will be performed, based on a description using current-algebra, [11], and elementary quantum mechanics. As will be shown in subsequent sections, parts of the hadronic tensor can in fact be calculated perturbatively.

In order to rewrite the hadronic tensor to obtain a form more suitable for calculation, one uses the well-known integral representation of the  $\delta$ -distribution

$$\delta^4(x) = \frac{1}{(2\pi)^4} \int d^4\xi \exp(-ix\xi) \quad (20)$$

and the translation operator, [82],

$$\hat{O}(\xi) = \exp(i\hat{P}\xi)\hat{O}(0)\exp(-i\hat{P}\xi) . \quad (21)$$

Here  $\hat{O}$  is any operator dependent on the 4-vector  $\xi$ .  $\hat{P}$  is the 4-momentum operator. To shorten notation, the following abbreviation for spin-averaging of the initial proton state is introduced

$$\sum_{\sigma} \langle P, \sigma | \hat{O} | P, \sigma \rangle \equiv \langle P | \hat{O} | P \rangle . \quad (22)$$

One arrives at

$$\begin{aligned} W_{\mu\nu}(q, P) &= \frac{1}{4\pi} \sum_F \int d^4\xi \exp(-i(P_F - q - P)\xi) \langle P | \exp(-i\hat{P}\xi) J_{\mu}^{em}(\xi) \exp(i\hat{P}\xi) | P_F \rangle \\ &\quad \langle P_F | J_{\nu}^{em}(0) | P \rangle \\ &= \frac{1}{4\pi} \int d^4\xi \exp(iq\xi) \langle P | J_{\mu}^{em}(\xi) \left[ \sum_F | P_F \rangle \langle P_F | \right] J_{\nu}^{em}(0) | P \rangle \\ &= \frac{1}{4\pi} \int d^4\xi \exp(iq\xi) \langle P | J_{\mu}^{em}(\xi) J_{\nu}^{em}(0) | P \rangle . \end{aligned} \quad (23)$$

Here we used the completeness relation

$$\sum_F | P_F \rangle \langle P_F | = 1 . \quad (24)$$

The hadronic tensor has now been obtained as Fourier-transform of the expectation value of the non-local operator  $J_{\mu}^{em}(\xi) J_{\nu}^{em}(0)$ . One may further simplify this expression due to the fact that the product of the two currents vanishes if one exchanges their ordering. In order to show this, one applies the same manipulations as in (23) in reverse way in the following expression

$$\begin{aligned} &\frac{1}{4\pi} \int d^4\xi \exp(iq\xi) \langle P | J_{\mu}^{em}(0) J_{\nu}^{em}(\xi) | P \rangle \\ &= \frac{1}{4\pi} \int d^4\xi \exp(iq\xi) \sum_F \langle P | J_{\mu}^{em}(0) | P_F \rangle \langle P_F | \exp(i\hat{P}\xi) J_{\nu}^{em}(0) \exp(-i\hat{P}\xi) | P \rangle \\ &= \frac{1}{4\pi} \int d^4\xi \exp(-i\xi(-q - P_F + P)) \sum_F \langle P | J_{\mu}^{em}(0) | P_F \rangle \langle P_F | J_{\nu}^{em}(0) | P \rangle \\ &= \frac{1}{4\pi} \sum_F (2\pi)^4 \delta^4(-q - P_F + P) \langle P | J_{\mu}^{em}(0) | P_F \rangle \langle P_F | J_{\nu}^{em}(0) | P \rangle . \end{aligned} \quad (25)$$

The  $\delta$ -distribution in (25) enforces

$$P_F^2 = (P - q)^2 = M^2 - Q^2 - \frac{Q^2}{x} \leq M^2 , \quad (26)$$

since  $Q^2 \geq 0$ . However, (26) contradicts (8) and is therefore unphysical. Hence the expression (25) vanishes and one arrives at the following final form of the hadronic tensor

$$W_{\mu\nu}(q, P) = \frac{1}{4\pi} \int d^4\xi \exp(iq\xi) \langle P | [J_\mu^{em}(\xi), J_\nu^{em}(0)] | P \rangle , \quad (27)$$

where the bracket  $[a, b]$  denotes the commutator of  $a$  and  $b$ .

Using symmetry and conservation laws, the hadronic tensor can be decomposed into a variety of different scalar structure functions and thus be stripped of its Lorentz-structure. In the most general case, there are 14 independent structure functions [83, 84]. However, in the case considered here only two structure functions contribute. One requires Lorentz and time-reversal invariance, [31], and additionally makes use of the fact that the electromagnetic current is conserved

$$\partial_\mu J_\mu^{em}(\xi) = 0 . \quad (28)$$

By using a well-known property of the Fourier-transform, one can show that electromagnetic gauge invariance of the hadronic tensor follows

$$q_\mu W^{\mu\nu} = 0 . \quad (29)$$

The leptonic tensor (19) is symmetric and thus cancels all antisymmetric parts of  $W_{\mu\nu}$ . The only quantities which can contribute to the Lorentz-structure of the hadronic tensor in the unpolarized case are then given by

$$g_{\mu\nu} , \quad q_\mu q_\nu , \quad P_\mu P_\nu , \quad q_\mu P_\nu + q_\nu P_\mu . \quad (30)$$

By making a general ansatz for the hadronic tensor using (30) and imposing gauge invariance, one expresses the hadronic tensor by two dimensionless structure functions

$$W_{\mu\nu} = \frac{1}{2x} \left( g_{\mu\nu} - \frac{q_\mu q_\nu}{q^2} \right) F_L(x, Q^2) + \frac{2x}{Q^2} \left( P_\mu P_\nu + \frac{q_\mu P_\nu + q_\nu P_\mu}{2x} - \frac{Q^2}{4x^2} g_{\mu\nu} \right) F_2(x, Q^2) . \quad (31)$$

The structure functions  $F_2(x, Q^2)$ ,  $F_L(x, Q^2)$  depend on two variables, Bjorken- $x$  and  $Q^2$ , contrary to the case of elastic scattering, in which only one variable, e.g. the energy, determines the cross section. Due to hermiticity of the hadronic tensor, the structure functions are real. The decomposition (31) of the hadronic tensor allows to express the differential cross section (18) of unpolarized DIS in case of single photon exchange

$$\frac{d\sigma}{dx dy} = \frac{2\pi\alpha^2}{xyQ^2} \left\{ \left[ 1 + (1-y)^2 \right] F_2(x, Q^2) - y^2 F_L(x, Q^2) \right\} . \quad (32)$$

All information on the structure of the proton is contained in the structure functions, and this is generally also the case for polarized electroweak interactions. A third structure function,  $F_1(x, Q^2)$ , which is not independent of the previous ones, may be considered

$$F_1(x, Q^2) = \frac{1}{2x} \left[ F_2(x, Q^2) - F_L(x, Q^2) \right] . \quad (33)$$



When evaluating the hadronic tensor in the context of QCD, one usually treats  $F_2$  and  $F_L$  separately. It is therefore useful to derive explicit expressions relating these two structure functions to the hadronic tensor by the projections  $g^{\mu\nu}W_{\mu\nu}$  and  $P^\mu P^\nu W_{\mu\nu}$ :

$$\begin{aligned} g^{\mu\nu}W_{\mu\nu}(q, P) &= \frac{D-1}{2x}F_L(x, Q^2) - \frac{D-2}{2x}F_2(x, Q^2), \\ P^\mu P^\nu W_{\mu\nu}(q, P) &= \frac{Q^2}{8x^3}F_L(x, Q^2). \end{aligned} \quad (34)$$

Here  $D$  denotes the space-time dimension, see Appendix A. Target mass corrections are neglected throughout this thesis, i.e. we set  $P^2 = 0$ . Solving (34) for the structure functions yields

$$\begin{aligned} F_L(x, Q^2) &= \frac{8x^3}{Q^2}P^\mu P^\nu W_{\mu\nu}(q, P), \\ F_2(x, Q^2) &= \frac{2x}{D-2} \left[ (D-1) \frac{4x^2}{Q^2}P^\mu P^\nu W_{\mu\nu}(q, P) - g^{\mu\nu}W_{\mu\nu}(q, P) \right]. \end{aligned} \quad (35)$$

### 2.3 The Tensor for Forward Compton Scattering

In quantum field theory one usually considers a time-ordered product, denoted by  $\mathbb{T}$ , rather than a commutator. By interpreting the final state  $|P_F\rangle$  in DIS as a virtual intermediate one, the hadronic tensor can be expressed as the imaginary part of the virtual forward Compton amplitude, denoted by  $T_{\mu\nu}(x, Q^2)$ . This is done by applying the optical theorem as depicted graphically in Figure 2. Using this description one can perform the light-cone expansion, [31], starting from a time-ordered product and derive quite general statements on the moments of the structure functions as will be shown in the subsequent section.

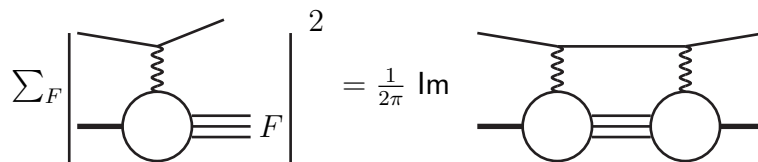


Figure 2: Schematic picture of the optical theorem.

The optical theorem states

$$W_{\mu\nu}(q, P) = \frac{1}{2\pi} \text{Im} T_{\mu\nu}(q, P), \quad (36)$$

where the Compton amplitude is given by, cf. [78],

$$T_{\mu\nu}(q, P) = i \int d^4\xi e^{iq\xi} \langle P | \mathbb{T} J^{\mu\eta\dagger}(\xi) J_\nu^{em}(0) | P \rangle. \quad (37)$$

Since in the present case the current is self-adjoint, see (12), the  $\dagger$  will be omitted from now on. In (37) the time ordered product of two bosonic operators  $A(x)$ ,  $B(x)$  is given by, cf. [28],

$$\mathbb{T} ( A(x) B(y) ) = \theta(x_0 - y_0)A(x)B(y) + \theta(y_0 - x_0)B(y)A(x). \quad (38)$$

In order to prove (36), one uses similar manipulations as in (23). Thus one obtains

$$\begin{aligned}
T_{\mu\nu}(q, P) &= i \int d^4\xi e^{iq\xi} \langle P | \mathbb{T} J_\mu^{em}(\xi) J_\nu^{em}(0) | P \rangle \\
&= i \int d^4\xi e^{iq\xi} \langle P | \theta(\xi_0) J_\mu^{em}(\xi) J_\nu^{em}(0) + \theta(-\xi_0) J_\nu^{em}(0) J_\mu^{em}(\xi) | P \rangle \\
&= \lim_{\varepsilon \rightarrow 0} i \sum_F (2\pi)^3 \int d\xi_0 \left( \exp(-i\xi_0(-q_0 - P_0 + P_{F,0} - i\varepsilon)) \delta^3(\mathbf{P}_F - \mathbf{P} - \mathbf{q}) \theta(\xi_0) \right. \\
&\quad \left. \langle P | J_\mu^{em}(0) | P_F \rangle \langle P_F | J_\nu^{em}(0) | P \rangle + \exp(-i\xi_0(-q_0 + P_0 - P_{F,0} + i\varepsilon)) \right. \\
&\quad \left. \delta^3(-\mathbf{P}_F + \mathbf{P} - \mathbf{q}) \theta(-\xi_0) \langle P | J_\nu^{em}(0) | P_F \rangle \langle P_F | J_\mu^{em}(0) | P \rangle \right) \\
&= \lim_{\varepsilon \rightarrow 0} \sum_F (2\pi)^3 \left( \frac{\delta^3(\mathbf{P}_F - \mathbf{P} - \mathbf{q})}{-q_0 - P_0 + P_{F,0} - i\varepsilon} \langle P | J_\mu^{em}(0) | P_F \rangle \langle P_F | J_\nu^{em}(0) | P \rangle \right. \\
&\quad \left. + \frac{\delta^3(-\mathbf{P}_F + \mathbf{P} - \mathbf{q})}{q_0 - P_0 + P_{F,0} - i\varepsilon} \langle P | J_\nu^{em}(0) | P_F \rangle \langle P_F | J_\mu^{em}(0) | P \rangle \right)
\end{aligned} \tag{39}$$

Now one can use the distribution identity, [85],

$$\lim_{\varepsilon \rightarrow 0} \frac{1}{x - i\varepsilon} = \mathbf{P}\left(\frac{1}{x}\right) + i\pi\delta(x), \tag{40}$$

where  $\mathbf{P}$  denotes Cauchy's principal value. The imaginary part of the Compton amplitude then becomes

$$\begin{aligned}
\text{Im } T_{\mu\nu} &= \sum_F (2\pi)^3 \pi \left( \delta^4(P_F - P - q) \langle P | J_\mu^{em}(0) | P_F \rangle \langle P_F | J_\nu^{em}(0) | P \rangle \right. \\
&\quad \left. + \delta^4(-P_F + P - q) \langle P | J_\mu^{em}(0) | P_F \rangle \langle P_F | J_\nu^{em}(0) | P \rangle \right).
\end{aligned} \tag{41}$$

Similarly to (25), the last term of the upper equation is unphysical and therefore equal to zero. The final result is

$$\text{Im } T_{\mu\nu} = \sum_F (2\pi)^3 \pi \delta^4(P_F - P - q) \langle P | J_\mu^{em}(0) | P_F \rangle \langle P_F | J_\nu^{em}(0) | P \rangle. \tag{42}$$

Comparing (42, 17) yields the optical theorem (36).

## 2.4 Moment Structure of the Hadronic Tensor

By applying the same invariance and conservation conditions as for the hadronic tensor, the Compton amplitude can be expressed in the unpolarized case similarly by two amplitudes  $T_L(Q^2, \nu)$  and  $T_2(Q^2, \nu)$ . It is then given by

$$T_{\mu\nu}(q, P) = \left( g_{\mu\nu} + \frac{q_\mu q_\nu}{Q^2} \right) \frac{\nu T_L(Q^2, \nu)}{2xM} + \left( P_\mu P_\nu + \frac{q_\mu P_\nu + q_\nu P_\mu}{2x} - \frac{Q^2}{4x^2} g_{\mu\nu} \right) \frac{T_2(Q^2, \nu)}{M^2}. \tag{43}$$

Using translational invariance, one can show that (37) is crossing symmetric under  $q \rightarrow -q$ , cf. [83],

$$T_{\mu\nu}(q, P) = T_{\mu\nu}(-q, P). \tag{44}$$

Note that  $q \rightarrow -q$  is equivalent to  $\nu, x \rightarrow (-\nu), (-x)$ , as can be inferred from (5, 6). The corresponding relations for the amplitudes are then obtained by considering (43)

$$T_{(L,2)}(Q^2, \nu) = T_{(L,2)}(Q^2, -\nu) . \quad (45)$$

By (36) these amplitudes relate to the structure functions  $F_L$  and  $F_2$  as

$$F_{(L,2)}(x, Q^2) = \frac{1}{2\pi} \frac{\nu}{M} \text{Im} T_{(L,2)}(Q^2, \nu) . \quad (46)$$

Another general property of the Compton amplitude is that  $T_L$  and  $T_2$  are real analytic functions of  $\nu$  at fixed  $Q^2$ , cf. [86], i.e.

$$T_{(L,2)}(Q^2, \nu^*) = T_{(L,2)}^*(Q^2, \nu) . \quad (47)$$

By applying (subtracted) dispersion relations, one can further analyze the Compton amplitude. In doing so, one of the crucial assumptions is that scattering amplitudes are analytic in the complex plane except at values of kinematic variables allowing intermediate states to be on their mass-shell, i.e. physical. This general feature has been proved to all orders in perturbation theory [87]. In QCD, however, the intermediate states are quarks and gluons, which are not observable due to confinement. Therefore they cannot be regarded as physical asymptotic states and for QCD the theorem is an assumption only, which is justified on grounds of the parton model. When  $\nu \geq Q^2/2M$ , the virtual photon-proton system can produce a physical hadronic intermediate state, so the  $T_{(L,2)}(Q^2, \nu)$  have cuts along the positive real  $\nu$ -axis. More precisely, there is a pole at  $\nu = Q^2/2M$  corresponding to elastic scattering and a cut beginning at the pion production threshold, [86]. For this analysis, however, the pion mass is neglected and the cut begins at the pole. The discontinuity along the cut is then just given by (36). For the amplitudes  $T_2, T_L$  the following forward dispersion relation holds, cf. [83],

$$T_{(L,2)}(Q^2, \nu) = 4M \int_{Q^2/2M}^{\infty} d\nu' \frac{1}{\nu'^2 - \nu^2} F_{(L,2)}(Q^2, \nu') . \quad (48)$$

By using  $x = Q^2/2\nu M$  and shifting  $y := Q^2/2\nu' M$  one arrives at

$$T_{(L,2)}(Q^2, \nu) = \frac{4M}{\nu x} \int_0^1 dy \frac{F_{(L,2)}(Q^2, y)}{1 - \frac{y^2}{x^2}} . \quad (49)$$

After a Laurent expansion one obtains the following moment decomposition, cf. [83],

$$T_{(L,2)}(Q^2, \nu) = \frac{4M}{\nu} \sum_{N=0,2,4,\dots}^{\infty} \frac{1}{x^{N+1}} \int_0^1 dy y^N F_{(L,2)}(Q^2, y) . \quad (50)$$

Note that the sum runs over even  $N$  only. The last formula yields a natural connection to the Mellin-moments of the structure functions. The Mellin transform of a function  $f$  is defined by

$$\mathbf{M}[f](N) := \int_0^1 dz z^{N-1} f(z) . \quad (51)$$

The Mellin-convolution of two functions  $f, g$ , denoted by  $f \otimes g$ , is given in  $z$ -space via

$$[f \otimes g](z) = \int_0^1 dz_1 \int_0^1 dz_2 \delta(z - z_1 z_2) f(z_1) g(z_2) , \quad (52)$$

and decomposes in Mellin-space into a simple product of the Mellin-transforms of the two functions, i.e.

$$\mathbf{M}[f \otimes g](N) = \mathbf{M}[f](N)\mathbf{M}[g](N) . \quad (53)$$

In (51,53),  $N$  is taken to be an integer, however, later on one may perform analytic continuation to arbitrary complex values of  $N$  [88, 89].

From (50), one can infer that in Mellin-space only even moments contribute to the hadronic tensor. This is important for the symmetry of the problem under consideration, since in the subsequent calculation often terms emerge differing by a factor  $(-1)^N$  only and can therefore be taken to be a priori equal.

## 2.5 The Parton Model

The structure functions, see Eq. (31), do in general depend on two kinematic variables,  $x$  and  $Q^2$ . Bjorken was the first who found scaling, cf. [16], i.e. in the Bjorken limit  $\{Q^2, \nu\} \rightarrow \infty$ ,  $x$  fixed, the structure functions depend on the ratio of these variables only

$$\lim_{\{Q^2, \nu\} \rightarrow \infty, x=const.} F_{(L,2)}(x, Q^2) = F_{(L,2)}(x) . \quad (54)$$

Soon after this prediction, scaling was observed experimentally in electron-proton collisions at SLAC (1968). Similar to the  $\alpha$ -particle scattering experiments by Rutherford in 1911, the cross section remained large at high momentum transfer  $Q^2$ . This suggested point-like targets. However, only in rare cases a single proton was detected in the final state, consisting of a large number of hadrons. To account for these observations, Feynman introduced the parton model [17]. He assumed the proton to be an extended object, consisting of several point-like particles, which he called partons. They are held together by their mutual interaction and behave like free particles during the interaction with the highly virtual photon in the Bjorken-limit. This is another way of demanding the fundamental property of QCD, asymptotic freedom. Note that the success of these assumptions prompted the search for a field theory enjoying this property. One arrives at the picture of the proton being “frozen” while the scattering takes place. The electron scatters elastically off the partons and this process does not interfere with the other partonic states, the “spectators”. The proton is destroyed during this interaction, forming the final-state hadrons. The DIS cross section is then given by the incoherent sum over the individual virtual electron-parton cross sections. Since no information on the particular proton structure is known, Feynman described parton  $i$  by the parton distribution function (PDF)  $f_i(z)$ . It gives the probability to find parton  $i$  in the “frozen” proton, carrying the fraction  $z$  of its momentum. Figure 3 gives a schematic picture of the parton model in the Born approximation. The parton momentum is denoted by  $p$ ,  $p'$  being its momentum after the interaction. Similar to the scaling variable  $x$  one can define the partonic scaling variable  $\tau$ . It plays the same role as the Bjorken-variable, but in the partonic subprocess only. It is given by

$$\tau := \frac{Q^2}{2p \cdot q} , \quad (55)$$

where the superscript  $i$  for the individual partons has been suppressed. In the collinear parton model<sup>2</sup>, which is applied throughout this thesis,  $p = zP$  holds, i.e. the momentum of the partons

---

<sup>2</sup>For other parton models as the covariant parton model cf. [90].

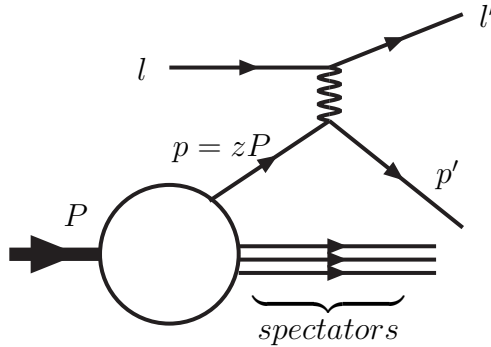


Figure 3: Deeply inelastic electron-proton scattering in the parton model.

is taken to be parallel to the proton momentum. By (55) one obtains

$$\tau z = x . \quad (56)$$

Feynman's original parton model, referred to as the naive parton model, neglects the mass of the partons and enforces the strict correlation

$$\delta \left( \frac{q \cdot p}{M} - \frac{Q^2}{2M} \right) , \quad (57)$$

due to the experimentally observed scaling behavior, which leads to  $z = x$ . This means that the momentum fraction carried by the partons is just given by Bjorken- $x$ . Further the proton is considered to be made up of three valence-partons, two  $u$  and one  $d$  type. The QCD improved parton model drops this restriction and allows virtual quark states (sea-quarks) and gluons as partons as well. It can be proved by applying the light-cone expansion, as will be shown in section 3. In section 2.5.1 the validity of Feynman's parton model will be considered. The factorization theorem of the QCD improved parton, cf. section 3, will be motivated in section 2.5.2 and used to derive the naive parton model at LO and the scaling behavior of the structure functions.

### 2.5.1 Validity of the Parton Model

The validity of the parton picture can be justified by considering an impulse approximation of the scattering process as seen from a certain class of reference frames, in which the proton momentum is taken to be very large ( $P_\infty$ -frames). This limit together with the Bjorken-limit cause two important facts to happen to the proton: The internal interactions of its partons are time dilated, and it is Lorentz contracted in the direction of the collision. As the center-of-mass (cms) energy increases, the parton lifetimes are lengthened and the time it takes the electron to interact with the proton is shortened. Therefore the condition for the validity of the parton model is given by, cf. [18, 91],

$$\frac{\tau_{\text{int}}}{\tau_{\text{life}}} \ll 1 . \quad (58)$$

Here  $\tau_{\text{int}}$  denotes the interaction time and  $\tau_{\text{life}}$  the average life time of a parton. If (58) holds, the proton will be in a single virtual state characterized by a certain number of partons during the

entire interaction time. This justifies the assumption of parton  $i$  carrying a definite momentum fraction  $z_i$  of the proton in the cms.  $z_i$  is expected to satisfy  $0 \leq z_i \leq 1$ , since otherwise there would be partons moving in opposite directions. Therefore this parton model is also referred to as the collinear parton model, since the proton is assumed to consist out of a stream of partons with parallel momenta. Further  $\sum_i z_i = 1$  holds. In order to derive the fraction of times in (58), one aligns the coordinate system parallel to the proton's momentum. Thus one obtains in the limit  $\mathbf{P}^2 \gg M^2$

$$P = \left( \sqrt{P_3^2 + M^2}; 0, 0, P_3 \right) \approx \left( P_3 + \frac{M^2}{2 \cdot P_3}; 0, 0, P_3 \right) . \quad (59)$$

The photon momentum can be written in general as

$$q = (q_0; q_3, \vec{q}_\perp) , \quad (60)$$

where  $\vec{q}_\perp$  denotes its transverse momentum with respect to the proton. From (59,60) constraints follow on the choice of  $q$

$$M\nu = q.P = (q_0 - q_3)P_3 + \frac{M^2}{2P_3}q_0 , \quad -q^2 = (q_3 + q_0)(q_3 - q_0) + |\vec{q}_\perp|^2 . \quad (61)$$

By the requirement that both  $\nu M$  and  $q^2$  approach a limit independent of  $\mathbf{P}$  as  $\mathbf{P} \rightarrow \infty$ , one finds

$$q_0 - q_3 = \frac{u}{P_3} , \quad q_0 = vP_3 . \quad (62)$$

There are many possibilities to choose  $u$  and  $v$ . This reflects the fact that there are many possible infinite momentum frames. The cms system of the initial states yields

$$v = \left( 2M\nu + \frac{q^2}{4P_3^2} \right) , \quad u = M\nu . \quad (63)$$

Thus one obtains for the characteristic interaction time scale using an (approximate) time-energy uncertainty relation

$$\tau_{\text{int}} \simeq \frac{1}{q_0} = \frac{4P_3x}{Q^2(1-x)} . \quad (64)$$

The life time of the individual partons is estimated accordingly to be inversely proportional to the energy fluctuations of the partons around the average energy  $E$

$$\tau_{\text{life}} \simeq \frac{1}{\sum_i E_i - E} . \quad (65)$$

Here  $E_i$  denote the energies of the individual partons. By introducing the two-momentum  $\vec{k}_{\perp i}$  of the partons perpendicular to the direction of motion of the proton as given in (59), one derives constraints on the validity of the collinear parton model. Eq. (65) can then be rewritten as

$$\sum_i E_i - E = \sum_i \sqrt{z_i^2 P_3^2 + m_i^2 + \vec{k}_{\perp i}^2} - \sqrt{P_3^2 + M^2} , \quad (66)$$

where  $m_i$  denotes the mass of the  $i$ -th parton. Further calculation yields the parton life time, cf. [92],

$$\begin{aligned}
\sum_i E_i - E &= \sum_i z_i P_3 \sqrt{1 + \frac{m_i^2 + k_{\perp i}^2}{z_i^2 P_3^2}} - P_3 - \frac{M^2}{2P_3} \\
&\approx \sum_i z_i P_3 + \sum_i \frac{m_i^2 + k_{\perp i}^2}{2z_i P_3} - P_3 - \frac{M^2}{2P_3} \\
&= \frac{1}{2P_3} \cdot \left( \sum_i \frac{m_i^2 + k_{\perp i}^2}{z_i} - M^2 \right), \\
\Rightarrow \tau_{\text{life}} &= \frac{2P_3}{\sum_i \frac{m_i^2 + k_{\perp i}^2}{z_i} - M^2}. \tag{67}
\end{aligned}$$

Together with (65) one finds

$$\frac{\tau_{\text{int}}}{\tau_{\text{life}}} = \frac{2x}{Q^2(1-x)} \left( \sum_i (m_i^2 + k_{\perp i}^2)/z_i - M^2 \right). \tag{68}$$

This expression is independent of  $P_3$ . The above procedure allows therefore to estimate the probability of deeply inelastic scattering to occur independently of the momentum of the proton. Accordingly, consider now the case of two partons with momentum fractions  $x$  and  $1-x$  and equal perpendicular momentum, neglecting all masses. One obtains

$$\frac{\tau_{\text{int}}}{\tau_{\text{life}}} \approx \frac{Q^2}{(1-x)^2} \cdot \frac{1}{2k_{\perp}^2}. \tag{69}$$

The above example therefore leads to the conclusion, that deeply inelastic scattering probes single partons if the virtual mass of the virtual photon is much larger than the transverse momenta squared of the partons and Bjorken- $x$  is neither close to one nor zero, since in the latter case  $xP_3$  would be the large momentum to be considered.

### 2.5.2 Scaling

In the QCD improved parton model, besides the  $\delta$ -distribution a function  $w_{\mu\nu}^i(\tau, Q^2)$  contributes to the hadronic tensor. One factorizes the hadronic tensor into the PDFs and the equivalent of the hadronic tensor at the parton level, the partonic tensor  $w_{\mu\nu}^i$ . The PDFs are non-perturbative quantities and have to be extracted from experiment, whereas the partonic tensors are calculable perturbatively. The hadronic tensor is then given by, [75],

$$W_{\mu\nu}(x, Q^2) = \frac{1}{4\pi} \sum_i \int_0^1 dz \int_0^1 d\tau z (f_i(z) + \bar{f}_i(z)) w_{\mu\nu}^i(\tau, Q^2) \delta(x - z\tau). \tag{70}$$

Here the number of partons and their respective type are not yet specified and we have included the corresponding PDF of the respective anti-parton, denoted by  $\bar{f}(z)$ . Comparing (70) to (52) one notices, that the hadronic tensor is just a Mellin-convolution of the PDFs with the partonic tensor. This tensor belongs to the particular subprocess of parton  $i$ . Let us assume that the electromagnetic parton current takes the simple form

$$\langle i | j_{\mu}^i(\tau) | i \rangle = -ie_i \bar{u}^i \gamma_{\mu} u^i, \tag{71}$$

similar to the leptonic current as present in (11). Here  $e_i$  is the charge of parton  $i$ . At LO one finds for the partonic structure tensor

$$w_{\mu\nu}^i(\tau, Q^2) = \frac{2\pi e_i^2}{q \cdot p^i} \delta(1 - \tau) \left[ 2p_\mu^i p_\nu^i + p_\mu^i q_\nu - g_{\mu\nu} q \cdot p^i \right]. \quad (72)$$

Note that the  $\delta$ -distribution in (72) together with the  $\delta$ -distribution in (70) just reproduces Feynman's assumption of the naive parton model,  $z = x$ . Substitution of (72) into the general expression for the hadronic tensor (31) and projecting onto the structure functions via (35) yields

$$\begin{aligned} F_L(x, Q^2) &= 0, \\ F_2(x, Q^2) &= \sum_i e_i^2 x (f_i(x) + \bar{f}_i(x)). \end{aligned} \quad (73)$$

This result, at LO, is the same as one obtains in the naive parton model. It predicts that

- The Callan-Gross relation, cf. [93], holds:

$$F_L(x, Q^2) = F_2(x, Q^2) - 2xF_1(x, Q^2) = 0. \quad (74)$$

- The structure functions are scale-independent

These predictions were a success of the parton model, reproducing the general properties of the data as observed at **SLAC**.



### 3 Operator Product Expansion Near the Light Cone

In the Bjorken limit DIS structure functions can be described within the light-cone expansion (LCE), [31], which allows a systematic consideration of the contributions of different twist. At leading twist  $\tau = 2$  the unpolarized nucleon structure functions  $F_i(x, Q^2)$  are obtained as Mellin convolutions between the parton densities  $f_j(x, \mu^2)$  and the Wilson coefficients  $C_i^j(x, Q^2/\mu^2)$

$$F_i(x, Q^2) = \sum_j C_i^j \left( x, \frac{Q^2}{\mu^2} \right) \otimes f_j(x, \mu^2) \quad (75)$$

to all orders in perturbation theory. This property is also formulated in the factorization theorems [52, 53]. Here  $\mu^2$  denotes the factorization scale and  $\otimes$  the Mellin convolution, cf. (53). Since the distributions  $f_j$  refer to massless partons, the heavy flavor effects are contained in the Wilson coefficients only. The Wilson coefficients themselves can be viewed as quasi cross-sections in  $pV^*$ -scattering, where  $V^*$  denotes the virtual vector boson exchanged. We are interested in the massive contributions to  $F_{(2,L)}(x, Q^2)$  in the region  $Q^2 \gg m^2$ . These are the non-power corrections in  $m^2/Q^2$ , i.e. all logarithmic contributions and the constant term. In the limit  $Q^2 \gg m^2$  the massive Wilson coefficients  $H_{(2,L),i}^{\text{S,NS}}(Q^2/m^2, m^2/\mu^2, x)$ , likewise the case for the structure functions (75), factorize

$$H_{(2,L),i}^{\text{S,NS}} \left( \frac{Q^2}{m^2}, \frac{m^2}{\mu^2}, x \right) = C_{(2,L),k}^{\text{S,NS}} \left( \frac{Q^2}{\mu^2}, x \right) \otimes A_{k,i}^{\text{S,NS}} \left( \frac{m^2}{\mu^2}, x \right) \quad (76)$$

into the Wilson coefficients  $C_{(2,L),k}^{\text{S,NS}}(Q^2/\mu^2, x)$  accounting for light flavors and the massive operator matrix elements  $A_{k,i}^{\text{S,NS}}(m^2/\mu^2, x)$ , see section 3.3.

#### 3.1 Light Cone Dominance

In the Bjorken limit,  $Q^2 \rightarrow \infty$ ,  $\nu \rightarrow \infty$ , and  $x$  fixed, it can be shown that the hadronic tensor is dominated by its contribution near the light-cone, i.e. by the values of the integrand in (27) at  $\xi^2 \approx 0$ , cf. [31]. This can be understood by considering the infinite momentum frame, see section 2.5.1,

$$P = (p^0; 0, 0, p^0), \quad (77)$$

$$q = \left( \frac{\nu}{2p^0}; \sqrt{Q^2}, 0, \frac{\nu}{2p^0} \right), \quad (78)$$

$$p^0 \approx \sqrt{\nu} \rightarrow \infty. \quad (79)$$

According to the Riemann-Lebesgue theorem, the integral in (27) is dominated by the region where  $q \cdot \xi \approx 0$  due to the rapidly oscillating exponential  $\exp(iq \cdot \xi)$ . One can now rewrite the dot product as

$$q \cdot \xi = \frac{1}{2}(q^0 - q^3)(\xi^0 + \xi^3) + \frac{1}{2}(q^0 + q^3)(\xi^0 - \xi^3) - q^1 z^1, \quad (80)$$

and infer that the condition  $q \cdot \xi \approx 0$  in the Bjorken-limit is equivalent to

$$\xi^0 \pm z^3 \approx \frac{1}{\sqrt{\nu}}, \quad \xi^1 \approx \frac{1}{\sqrt{\nu}}, \quad (81)$$

resulting in

$$\xi^2 \approx 0, \quad (82)$$

which means light-cone dominance, i.e. for DIS in the Bjorken-limit the dominant contribution to the hadronic tensor  $W_{\mu\nu}(q, P)$  comes solely from the region where  $\xi^2 \approx 0$ .

### 3.2 Light Cone Expansion

In the cross section of DIS, (18), the hadronic tensor (27) can be decomposed into two structure functions, see Eq. (31),

$$\begin{aligned} W_{\mu\nu}(q, P) &= \frac{1}{4\pi} \int d^4\xi \exp(iq\xi) \langle P | [J_\mu^{em}(\xi), J_\nu^{em}(0)] | P \rangle \\ &= \frac{2x}{Q^2} \left( P_\mu P_\nu + \frac{q_\mu P_\nu + q_\nu P_\mu}{2x} - \frac{Q^2}{4x^2} g_{\mu\nu} \right) F_2(x, Q^2) \\ &\quad + \frac{1}{2x} \left( g_{\mu\nu} + \frac{q_\mu q_\nu}{Q^2} \right) F_L(x, Q^2). \end{aligned} \quad (83)$$

In the Bjorken limit, the integrand of (83) is dominated by its contribution near the light-cone and one can write the light-cone expansion of the current-current correlation as, cf. [31],

$$\lim_{\xi^2 \rightarrow 0} [J(\xi), J(0)] \propto \sum_{i, N, \tau} c_{i, \tau}^N(\xi^2, \mu^2) \xi_{\mu_1} \dots \xi_{\mu_N} O_{i, \tau}^{\mu_1 \dots \mu_N}(0, \mu^2). \quad (84)$$

Here the Lorentz indexes of the currents have been suppressed for brevity. In (84) the local operators  $O_{i, \tau}(\xi, \mu^2)$  are finite as  $\xi^2 \rightarrow 0$ . The singularities which appear for the product of two operators as their arguments become equal are shifted to the  $c$ -number coefficients  $c_{i, \tau}^N(\xi^2, \mu^2)$  and can therefore be treated separately. The summation index  $i$  runs over the set of allowed operators in the model, while the sum over  $N$  extends to infinity. Dimensional analysis shows that the degree of divergence of the functions  $c_{i, \tau}^N$  as  $\xi^2 \rightarrow 0$  is given by

$$c_{i, \tau}^{(N)} \left( \xi^2 \right) \propto \left( \frac{1}{\xi^2} \right)^{-\tau + 2d_J}. \quad (85)$$

Here,  $d_J$  denotes the canonical dimension of the current  $J(\xi)$  and  $\tau$  is the twist of the local operator  $O_{i, \tau}^{\mu_1 \dots \mu_N}(z)$ , which is defined by, cf. [32],

$$\tau := D_O - N. \quad (86)$$

$D_O$  is the canonical (mass) dimension of  $O_{i, \tau}^{\mu_1 \dots \mu_N}(z, \mu^2)$  and  $N$  is called its spin. From (85) one can infer that the most singular coefficients are those of lowest twist related to the operators stemming from the LCE of the electromagnetic currents (13), i.e. in the case considered here twist  $\tau = 2$ . Operators with higher twist lead to suppression factors  $(\bar{\mu}^2/Q^2)^k$ , with  $\bar{\mu}$  a typical mass scale of  $O(1 \text{ GeV})$ . We consider only the lowest twist contributions in the following. Both the operators and the coefficient functions are renormalized, which is indicated by the renormalization scale  $\mu^2$ . Within QCD, all twist-2 operators can be classified according to their flavor group representation. There are two classes. The twist-2 singlet operators are given by

$$O_q^{\mu_1 \dots \mu_N}(z) = \frac{1}{2} i^{N-1} S[\bar{q}(x) \gamma^{\mu_1} D^{\mu_2} \dots D^{\mu_N} q(x)] - \text{TraceTerms}, \quad (87)$$

$$O_g^{\mu_1 \dots \mu_N}(z) = \frac{1}{2} i^{N-2} S[F_\alpha^{a, \mu_1}(z) D^{\mu_2} \dots D^{\mu_{N-1}} F^{a, \alpha, \mu_N}(z)] - \text{TraceTerms}, \quad (88)$$

and the flavor non-singlet operator is

$$O_{q,r}^{\mu_1 \dots \mu_N}(z) = \frac{1}{2} i^{N-1} S[\bar{q}(x) \gamma^{\mu_1} D^{\mu_2} \dots D^{\mu_N} \frac{\lambda_r}{2} q(x)] - \text{TraceTerms} . \quad (89)$$

Here  $D_\mu = \partial_\mu + ig_s T_a A_\mu^a$  denotes the covariant derivative and  $S$  is the symmetrization operator for the Lorentz indexes  $\mu_i$ . Further  $a$  denotes the color index,  $F_{\mu\nu}^a$  is the field strength tensor of the gluon field and the matrices  $\lambda_r/2$  represent the generators of the flavor group  $SU(N_f = 3)$ .  $q$  denotes the quark fields. The classification of the composite operators (87–89) in terms of flavor singlet and non-singlet refers to their symmetry properties with respect to the flavor group  $SU(N_f)$ . Since the electromagnetic current  $J_\mu(z)$  belongs to the singlet and adjoint representation of  $SU(N_f)$ , the twist-2 operators, derived from the products of two currents, do so as well. Operators (87,88) are singlets under  $SU(N_f)$ . Further (87) is referred to as pure-singlet (PS) operator. Since (89) is the only operator carrying flavor quantum number due to the presence of  $\lambda_r$ , it belongs to the adjoint representation of  $SU(N_f)$  and is hence referred to as the non-singlet (NS) operator [28].

Inserting the LCE (84) into the hadronic tensor (83) leads to the following result in Mellin-space for the structure functions

$$F_i^N(Q^2) \propto \sum_{i=q,g} A_i^N(\mu^2/M^2) C_i^N(Q^2/\mu^2) , \quad (90)$$

where the operator matrix element (OME) and the coefficient function are defined by

$$\begin{aligned} A_i^N(\mu^2/M^2) &= \langle P | O_i^N(0, \mu^2) | P \rangle , \\ C_i^N(Q^2/\mu^2) &= \int d^4\xi \exp(-iq\xi) c_i^N(\xi^2, \mu^2) . \end{aligned} \quad (91)$$

Note that by identifying the nucleonic OME with the PDF one obtains Eq. (75).

### 3.3 Operator Matrix Elements

We denote the contributions to the coefficient functions in (75) stemming from heavy flavor production by  $H_{(2,L),i}^{\text{S,NS}}(Q^2/m^2, m^2/\mu^2, x)$ . As has been first outlined in Ref. [55], these massive Wilson coefficients factorize in the limit  $Q^2 \gg m^2$

$$H_{(2,L),i}^{\text{S,NS}} \left( \frac{Q^2}{m^2}, \frac{m^2}{\mu^2}, x \right) = C_{(2,L),k}^{\text{S,NS}} \left( \frac{Q^2}{\mu^2}, x \right) \otimes A_{k,i}^{\text{S,NS}} \left( \frac{m^2}{\mu^2}, x \right) \quad (92)$$

into the light flavor Wilson coefficients  $C_{(2,L),k}^{\text{S,NS}}(Q^2/\mu^2, x)$  and massive operator matrix elements  $A_{k,i}^{\text{S,NS}}(m^2/\mu^2, x)$ . The latter take a similar role as the parton densities in (75), but they are calculable perturbatively. Note that in (92) for the singlet case  $i, k = g, q$  and for the non-singlet case  $i, k = q$ . The factorization (92) is a consequence of the renormalization group and the fact that we restrict the investigation to non-power corrections to  $H_{(2,L),i}^{\text{S,NS}}(Q^2/m^2, m^2/\mu^2, x)$ . The operator matrix elements  $A_{k,i}^{\text{S,NS}}$  obey the expansion

$$A_{k,i}^{\text{S,NS}} \left( \frac{m^2}{\mu^2} \right) = \langle i | O_k^{\text{S,NS}} | i \rangle = \delta_{k,i} + \sum_{l=1}^{\infty} a_s^l A_{k,i}^{\text{S,NS},(l)} \left( \frac{m^2}{\mu^2} \right) , \quad i = q, g \quad (93)$$

of the twist-2 singlet and non-singlet operators  $O_k^{S,NS}$  (87-89) between partonic states  $|i\rangle$ , which are related to the initial-state nucleon states  $|N\rangle$  by collinear factorization. Here  $a_s = \alpha_s(\mu^2)/(4\pi)$  denotes the strong coupling constant. The operator matrix elements are process-independent quantities. The process dependence of  $H_{(2,L),i}^{S,NS}$  is described by the associated massless coefficient functions

$$C_{(2,L),k}^{S,NS} \left( \frac{Q^2}{\mu^2} \right) = \sum_{l=l_0}^{\infty} a_s^l C_{(2,L),k}^{(l),S,NS} \left( \frac{Q^2}{\mu^2} \right), \quad k = g, q, \quad (94)$$

calculated in the  $\overline{\text{MS}}$  scheme. For later use we introduce the notation

$$\widehat{C}_{(2,L),k} \left( \frac{Q^2}{\mu^2} \right) = C_{(2,L),k} \left( \frac{Q^2}{\mu^2}, N_L + N_H \right) - C_{(2,L),k} \left( \frac{Q^2}{\mu^2}, N_L \right). \quad (95)$$

Here  $N_H, N_L$  are the number of heavy and light flavors, respectively. In the following we will consider the case of a single heavy quark, i.e.  $N_H = 1$ . The formalism is easily generalized to more than one heavy quark species. The heavy flavor Wilson coefficient is obtained as the expansion of the product of (93, 94) to the respective order in  $a_s$ .

### 3.4 Structure of the Heavy Quark Coefficient Functions in the Limit $Q^2 \gg m^2$ up to $O(a_s^2)$

In order to obtain expressions for the heavy quark coefficient functions up to  $O(a_s^2)$ , one expands the heavy quark coefficient functions into a perturbative series

$$H_{(2,L),i}^{S,NS} \left( \frac{Q^2}{m^2}, \frac{m^2}{\mu^2} \right) = \sum_{k=0}^{\infty} a_s^k H_{(2,L),i}^{(k),S,NS} \left( \frac{Q^2}{m^2}, \frac{m^2}{\mu^2} \right). \quad (96)$$

$$(97)$$

By inserting the perturbative expansions (93, 94, 96) into (92) one obtains for the coefficients  $H_{2,(g,q)}^{S,PS,NS}$  corresponding to the structure function  $F_2$  up to  $O(a_s^2)$ , [55],

$$H_{2,g}^S \left( \frac{Q^2}{m^2}, \frac{m^2}{\mu^2} \right) = a_s \left[ A_{Qg}^{(1)} \left( \frac{m^2}{\mu^2} \right) + \widehat{C}_{2,g}^{(1)} \left( \frac{Q^2}{\mu^2} \right) \right] + a_s^2 \left[ A_{Qg}^{(2)} \left( \frac{m^2}{\mu^2} \right) + A_{Qg}^{(1)} \left( \frac{m^2}{\mu^2} \right) \otimes C_{2,q}^{(1)} \left( \frac{Q^2}{\mu^2} \right) + \widehat{C}_{2,g}^{(2)} \left( \frac{Q^2}{\mu^2} \right) \right], \quad (98)$$

$$H_{2,q}^{PS} \left( \frac{Q^2}{m^2}, \frac{m^2}{\mu^2} \right) = a_s^2 \left[ A_{Qq}^{\text{PS},(2)} \left( \frac{m^2}{\mu^2} \right) + \widehat{C}_{2,q}^{\text{PS},(2)} \left( \frac{Q^2}{\mu^2} \right) \right], \quad (99)$$

$$H_{2,q}^{\text{NS}} \left( \frac{Q^2}{m^2}, \frac{m^2}{\mu^2} \right) = a_s^2 \left[ A_{qq,Q}^{\text{NS},(2)} \left( \frac{m^2}{\mu^2} \right) + \widehat{C}_{2,q}^{\text{NS},(2)} \left( \frac{Q^2}{\mu^2} \right) \right]. \quad (100)$$

To  $O(a_s^3)$  the longitudinal heavy quark Wilson coefficients  $H_{L,g(q)}^{S,PS,NS}$  read, [47],

$$H_{L,g}^S \left( \frac{Q^2}{m^2}, \frac{m^2}{\mu^2} \right) = a_s \widehat{C}_{L,g}^{(1)} \left( \frac{Q^2}{\mu^2} \right) + a_s^2 \left[ A_{Q,g}^{(1)} \left( \frac{\mu^2}{m^2} \right) \otimes C_{L,q}^{(1)} \left( \frac{Q^2}{\mu^2} \right) + \widehat{C}_{L,g}^{(2)} \left( \frac{Q^2}{\mu^2} \right) \right] \\ + a_s^3 \left[ A_{Q,g}^{(2)} \left( \frac{\mu^2}{m^2} \right) \otimes C_{L,q}^{(1)} \left( \frac{Q^2}{\mu^2} \right) + A_{Q,g}^{(1)} \left( \frac{\mu^2}{m^2} \right) \otimes C_{L,q}^{(2)} \left( \frac{Q^2}{\mu^2} \right) + \widehat{C}_{L,g}^{(3)} \left( \frac{Q^2}{\mu^2} \right) \right] \quad (101)$$

$$H_{L,q}^{PS} \left( \frac{Q^2}{m^2}, \frac{m^2}{\mu^2} \right) = a_s^2 \widehat{C}_{L,q}^{PS,(2)} \left( \frac{Q^2}{\mu^2} \right) + a_s^3 \left[ A_{Qq}^{PS,(2)} \left( \frac{\mu^2}{m^2} \right) \otimes C_{L,q}^{(1)} \left( \frac{Q^2}{\mu^2} \right) + \widehat{C}_{L,q}^{PS,(3)} \left( \frac{Q^2}{\mu^2} \right) \right] \quad (102)$$

$$H_{L,q}^{NS} \left( \frac{Q^2}{m^2}, \frac{m^2}{\mu^2} \right) = a_s^2 \widehat{C}_{L,q}^{NS,(2)} \left( \frac{Q^2}{\mu^2} \right) + a_s^3 \left[ A_{qq,Q}^{NS,(2)} \left( \frac{\mu^2}{m^2} \right) \otimes C_{L,q}^{(1)} \left( \frac{Q^2}{\mu^2} \right) + \widehat{C}_{L,q}^{NS,(3)} \left( \frac{Q^2}{\mu^2} \right) \right], \quad (103)$$

where

$$C_{L,q}^{(2)} = C_{L,q}^{NS} + C_{L,q}^{PS} \quad (104)$$

and

$$H_{L,q}^S = H_{L,q}^{NS} + H_{L,q}^{PS}. \quad (105)$$

The functions  $C_{(2,L),i}^{(k)}(Q^2/\mu^2)$  are the scale dependent Wilson coefficients in the  $\overline{\text{MS}}$  scheme with  $C_{2,L,i}^{(k)}(Q^2/\mu^2) = c_{(2,L),i}^{(k)}$  for  $Q^2 = \mu^2$  given in Refs. [56–62].  $A_{ij}^{(k)}(m^2/\mu^2)$  are the operator matrix elements defined in Eq. (93) and have been calculated up to  $O(a_s^2)$  in Ref. [55]. Note that due to the structure of the longitudinal heavy flavor coefficients, up to  $O(a_s^3)$  only the  $O(a_s^2)$  operator matrix elements contribute [47]. This allows to obtain a NNLO result for  $H_{L,(g,q)}$  involving the 2-loop OMEs  $A_{ij}^{(2)}$ , unlike the case of  $H_{2,(g,q)}$ . The relations (98-103) are given for renormalized quantities. Unrenormalized OMEs emerging from the calculation will be denoted by a hat later on. The renormalization procedure will be discussed in section 4.

### 3.5 Outline of the Computation of $\hat{A}_{ij}^{(k)}$

In this section we describe the computation of the unrenormalized OMEs  $\hat{A}_{Qg}$ ,  $\hat{A}_{Qq}^{PS}$ , and  $\hat{A}_{qq,Q}^{NS}$  in perturbation theory. First we consider the singlet OME  $\hat{A}_{Qg}$ , defined by (93)

$$\hat{A}_{Qg} \left( \frac{m^2}{\mu^2}, \epsilon \right) = \langle g | O_q^{\mu_1 \dots \mu_N} | g \rangle. \quad (106)$$

Here  $|g\rangle$  represents the external on-shell gluon state and  $O_q^{\mu_1 \dots \mu_N}$  is the twist-2 heavy quark local operator as defined in Eq. (87). In perturbation theory, (106) can be evaluated order by order in the coupling constant by applying the standard QCD Feynman-rules and the Feynman-rules for composite operators as given in Appendix B. The Green's function needed for  $\hat{A}_{Qg}$  is obtained by considering the vacuum expectation value of the time-ordered product of the composite operator, inserted between the external gluon fields. Since an S-Matrix element is calculated, one needs to amputate the external field and arrives at the following equation in momentum space

$$\epsilon^\mu(p) G_{Q,\mu\nu}^{ab} \epsilon^\nu(p) = \langle 0 | T(A_\mu^a(x) O_q^{\mu_1 \dots \mu_N}(0) A_\nu^b(y)) | 0 \rangle, \quad (107)$$

where  $G_{Q,\mu\nu}^{ab}$  is the connected Green's function. In (107),  $A_{\mu,\nu}^{a,b}$  denote the external gluon fields with color indexes  $a, b$ , Lorentz indexes  $\mu, \nu$  and momentum  $p$ . The local operators are traceless symmetric tensors under the Lorentz group. The computation of the Green's functions will reveal trace terms, which have to be projected out by multiplying with an external source  $J_{\mu_1 \dots \mu_N} = \Delta_{\mu_1} \dots \Delta_{\mu_N}$ , where  $\Delta_\mu$  is a light-like vector,  $\Delta^2 = 0$ . One obtains

$$J_{\mu_1 \dots \mu_N} O_q^{\mu_1 \dots \mu_N}(z) = \frac{1}{2} i^{N-1} \bar{q}(x) \not{\Delta} \Delta_{\mu_2} D^{\mu_2} \dots \Delta_{\mu_N} D^{\mu_N} q(x) . \quad (108)$$

The tensor  $G_{Q,\mu\nu}^{ab}$  then relates to the OME as

$$G_{Q,\mu\nu}^{ab} = \hat{A}_{Qg} \left( \frac{m^2}{\mu^2}, \varepsilon \right) \delta^{ab} (\Delta \cdot p)^N \left( -g_{\mu\nu} + \frac{\Delta_\mu p_\nu + \Delta_\nu p_\mu}{\Delta \cdot p} \right) . \quad (109)$$

The unrenormalized matrix element is thus given by

$$\hat{A}_{Qg} \left( \frac{m^2}{\mu^2}, \varepsilon \right) = \frac{1}{N_c^2 - 1} \frac{1}{D - 2} (-g_{\mu\nu}) \delta^{ab} (\Delta \cdot p)^{-N} G_{Q,\mu\nu}^{ab} . \quad (110)$$

The corresponding relations for an external quark field in the non-singlet case  $\hat{A}_{qq,Q}^{NS}$  and the pure-singlet case  $\hat{A}_{Qq}^{PS}$  read

$$\bar{u}(p) G_Q^{ij} u(p) = \langle 0 | \mathbb{T}(\bar{q}_i(x) O_Q^{\mu_1 \dots \mu_N}(0) q_j(y)) | 0 \rangle , \quad (111)$$

$$\bar{u}(p) G_q^{ij} \lambda_r u(p) = \langle 0 | \mathbb{T}(\bar{q}_i(x) O_{q,r}^{\mu_1 \dots \mu_N}(0) q_j(y)) | 0 \rangle . \quad (112)$$

By the same argument as above one arrives at the following projector for the OMEs

$$\hat{A}_{fq} \left( \frac{m^2}{\mu^2}, \varepsilon \right) = \frac{1}{N_c} \delta^{ij} \frac{1}{4} (\Delta \cdot p)^{-N} \text{Tr}(\not{p} G_f^{ij}) . \quad (113)$$

The computation of the OMEs in this thesis is done in Mellin-space, other than in Ref. [55], where the calculation was thoroughly performed in  $z$ -space. From section 2.4, (Eq. 50) we infer that only even Mellin-moments contribute to the heavy coefficient functions in the LCE. This is reflected by the fact that the results of the OMEs for the singlet and pure-singlet case appear with the universal factor

$$\frac{1 + (-1)^N}{2} . \quad (114)$$

Therefore one defines the Mellin-transform of the singlet and pure-singlet OMEs by

$$\mathbf{M}[A_{fk}](N) := \frac{1 + (-1)^N}{2} \int_0^1 dz z^{N-1} A_{fk}(z) . \quad (115)$$

## 4 Regularization and Renormalization

### 4.1 Dimensional Regularization

When evaluating momentum integrals of Feynman diagrams in  $D = 4$  dimensions, one usually encounters singularities, which have to be regularized. A convenient method is to apply  $D$ -dimensional regularization [94–97]. The dimensionality of space–time is analytically continued to values  $D \neq 4$ , for which the corresponding integrals converge. After performing the Wick rotation Euclidean space integrals, see Appendix F, of the form

$$\int \frac{d^D k}{(2\pi)^D} \frac{(k^2)^r}{(k^2 + R^2)^m} = \frac{1}{(4\pi)^{D/2}} \frac{\Gamma(r + D/2)\Gamma(m - r - D/2)}{\Gamma(D/2)\Gamma(m)} (R^2)^{r+D/2-m} \quad (116)$$

are obtained. The properties of the  $\Gamma$ -function in the complex plane are well known, see Appendix H, and therefore one can analytically continue the right-hand side of (116) from integer  $D$  to arbitrary complex values of  $D$ . In order to recover the space-time dimension, one sets

$$D = 4 + \varepsilon . \quad (117)$$

The singularities can now be isolated by expanding the  $\Gamma$ -functions into a Laurent-series around  $\varepsilon = 0$ . They appear as poles in  $\varepsilon$ . One has to keep in mind that the parameter integrals which have to be introduced to bring a multi-dimensional integral into the form (116), see Eq. (F.2), usually diverge as well as  $\varepsilon \rightarrow 0$ . However, by introducing  $\varepsilon$ , one also continues these parameter integrals analytically and the same argument holds. Accordingly, all quantities have to be considered in  $D$  dimensions. This applies for the metric tensor  $g_{\mu\nu}$  in  $D$  dimensions and the Clifford-Algebra of  $\gamma$  matrices, see Appendix A.

Also the bare coupling constant  $\hat{g}_s$ , being dimensionless for  $D = 4$ , has to be continued to  $D$ -dimensions. Due to this it acquires a mass dimension

$$\hat{g}_{s,D} = \mu_0^{-\varepsilon/2} \hat{g}_s , \quad (118)$$

which is absorbed in the arbitrary scale factor  $\mu_0$ . From now on, (118) is understood to have been applied and we set

$$\frac{\hat{g}_s^2}{(4\pi)^2} = \hat{a}_s . \quad (119)$$

Dimensional regularization has the advantage that it obeys all physical requirements such as Lorentz-invariance, gauge invariance and unitarity [95, 98]. Hence it is suitable to be applied in perturbative quantum field theory.

### 4.2 The $\overline{\text{MS}}$ Scheme

Using dimensional regularization, the poles of the unrenormalized results appear as terms  $1/\varepsilon^i$ , where in 2-loop calculations  $i = 1, 2$ . In order to remove these singularities, one has to perform renormalization and mass factorization. To do this, a suitable renormalization scheme has to be chosen. The most commonly used schemes in perturbation theory are the MS-scheme, [99], and the  $\overline{\text{MS}}$ -scheme, [100], the latter being used in this thesis.

In the renormalization procedure the  $\overline{\text{MS}}$ -scheme subtracts only the pole terms in  $\varepsilon$ . More generally, the  $\overline{\text{MS}}$ -scheme makes use of the observation that terms  $1/\varepsilon$  always appear in combination with the spherical factor

$$S_\varepsilon \equiv \exp\left[\frac{\varepsilon}{2}(\ln(4\pi) - \gamma_E)\right], \quad (120)$$

which may be bracketed out for each loop order. Here  $\gamma_E$  denotes the Euler-Mascheroni constant

$$\gamma_E := \lim_{N \rightarrow \infty} \left( \sum_{k=1}^{\infty} \frac{1}{N} - \ln(N) \right) \approx 0.577215664901 \dots \quad (121)$$

By subtracting the poles in the form  $S_\varepsilon/\varepsilon$  in the  $\overline{\text{MS}}$ -scheme, no terms containing  $\ln^k(4\pi)$ ,  $\gamma_E^k$  will appear in the renormalized result, simplifying the expression [28].

### 4.3 Renormalization of $\hat{A}_{ij}$

In this section we describe how the bare OMEs  $\hat{A}_{ij}$  defined in Eq. (93) are renormalized. The renormalization proceeds in three steps. First mass and coupling constant renormalization will be performed. Also the composite operators require renormalization since the bare operators exhibit ultraviolet singularities. After renormalization the OMEs are denoted by  $\hat{A}_{ij}$ . Since the OMEs are calculated for an incoming gluon or light quark which is on-shell,  $p^2 = 0$ , collinear (C)-divergences appear as well. These singularities are removed by mass factorization, [52, 53], and give the renormalized OMEs  $A_{ij}$ . We will not distinguish between UV- and C- singularities in the following but deal with them in the same way, introducing a common value of  $\varepsilon$ . In the end, the OMEs will be represented in such a way that the coefficients of the pole terms are given by products of the splitting functions, [33–35, 59, 63–66], and in terms of the  $\beta$ -function, [29, 30, 101]. Thus our result can not only be compared with the results in Ref. [55], but for the pole terms also with other results in the literature. If not stated otherwise, the  $\overline{\text{MS}}$ -scheme will be used for the renormalization.

For the OME  $\hat{A}_{ij}$ , the perturbative series in the bare coupling constant  $\hat{a}_s$ , see Eq. (119), reads

$$\hat{A}_{ij} = \sum_{k=0}^{\infty} \hat{a}_s^k A_{ij}^{(k)}. \quad (122)$$

In order to perform mass renormalization, the on-mass-shell scheme is chosen, i.e. the renormalized quark propagator is required to be equal to the free propagator at  $p^2 = m_q^2$  and the gluon propagator obeys  $p^2 = 0$ . In this scheme, the mass  $Z$ -Factor reads, [79],

$$Z_m = 1 + \hat{a}_s C_F S_\varepsilon \left( \frac{m^2}{\mu^2} \right)^{\varepsilon/2} \left[ \frac{6}{\varepsilon} - 4 \right], \quad (123)$$

where  $C_F$  is a color factor of  $SU(N)$ , cf. Appendix D,

$$C_F = \frac{N^2 - 1}{2N}. \quad (124)$$

Due to (123), the bare mass  $\hat{m}$ , which appears in  $\hat{A}_{ij}$  has to be replaced by the renormalized mass  $m$  via

$$\hat{m} = Z_m m = m + (Z_m - 1)m = m + \hat{a}_s \delta m. \quad (125)$$



In order to do this, one notices that the bare mass can be factored out of the unrenormalized OMEs via

$$\hat{A}_{ij}^{(k)} = \left( \frac{\hat{m}^2}{\mu^2} \right)^{\frac{\varepsilon}{2}k} \hat{A}'_{ij}{}^{(k)} ,$$

where the elements  $\hat{A}'_{ij}{}^{(k)}$  have no mass dependence. Up to  $O(\hat{a}_s^2)$ , mass renormalization proceeds now as follows

$$\begin{aligned} \hat{A}_{ij} &= \hat{A}'_{ij}{}^{(0)} + \hat{a}_s \left( \frac{\hat{m}^2}{\mu^2} \right)^{\frac{\varepsilon}{2}} \hat{A}'_{ij}{}^{(1)} + \hat{a}_s^2 \left( \frac{\hat{m}^2}{\mu^2} \right)^{\varepsilon} \hat{A}'_{ij}{}^{(2)} \\ &= \hat{A}'_{ij}{}^{(0)} + \hat{a}_s \left( \frac{m + \hat{a}_s \delta m}{\mu} \right)^{\varepsilon} \hat{A}'_{ij}{}^{(1)} + \hat{a}_s^2 \left( \frac{m + \hat{a}_s \delta m}{\mu} \right)^{2\varepsilon} \hat{A}'_{ij}{}^{(2)} \\ &= \hat{A}_{ij}^{(0)} + \hat{a}_s \hat{A}_{ij}^{(1)} + \hat{a}_s^2 \left[ \delta m \frac{d}{dm} \hat{A}_{ij}^{(1)} + \hat{A}_{ij}^{(2)} \right] . \end{aligned} \quad (126)$$

Notice that in (126) the zeroth order OME  $\hat{A}_{ij}^{(0)}$  has no mass dependence.

In order to renormalize the strong coupling constant  $\hat{a}_s$ , one proceeds in different ways for the light and heavy quark contributions. The light quark flavors are the  $u$ ,  $d$  and  $s$ -quark ( $N_f = 3$ ). The heavy quark flavors are labeled by  $c = 1$ ,  $b = 2$ ,  $t = 3$  and their masses are given by  $m_i$ ,  $i = 1..3$ . The coupling constant  $\hat{a}_s$  is renormalized via the  $Z$ -factor  $Z_g^2$  as

$$\begin{aligned} \hat{g}_s &= g_s Z_g , \\ \hat{a}_s &= a_s Z_g^2 . \end{aligned} \quad (127)$$

In order to obtain  $Z_g$ , one applies the Slavnov-Taylor identity, [23],

$$Z_g = \frac{Z_1}{Z_3^{3/2}} . \quad (128)$$

Therefore, one needs to know the  $Z$ -factors of the gluon propagator,  $Z_3$ , and of the 3-gluon vertex,  $Z_1$ . To obtain the contributions to  $Z_1$  and  $Z_3$  from the counterterm and the light quark, gluon and Faddeev–Popov ghosts loops, the  $\overline{\text{MS}}$ -scheme is applied. These parts read, in Feynman gauge,

$$Z_1^l = 1 + a_s \frac{2}{\varepsilon} S_\varepsilon \left[ -\frac{2}{3} C_A + \frac{4}{3} T_R N_f \right] , \quad (129)$$

$$Z_3^l = 1 + a_s \frac{2}{\varepsilon} S_\varepsilon \left[ -\frac{5}{3} C_A + \frac{4}{3} T_R N_f \right] . \quad (130)$$

The color invariants in (129, 130) of  $SU(N)$  are given by, cf. Appendix D,

$$C_A = N \quad , \quad T_R = \frac{1}{2} . \quad (131)$$

The heavy quark loop contribution to  $Z_1$  and  $Z_3$  are obtained by requiring that the corresponding gluon self energy  $\Pi(p^2, m_i)$  vanishes at light-like momentum, i.e.  $\Pi(0, m_i) = 0$ . They are equal to

$$Z_1^H = Z_3^H = a_s \frac{S_\varepsilon}{\varepsilon} \frac{8}{3} T_R \left[ 1 + \frac{\zeta_2}{8} \varepsilon^2 \right] \sum_{i=1}^3 \left( \frac{m_i^2}{\mu^2} \right)^{\varepsilon/2}. \quad (132)$$

The condition  $\Pi(0, m_i) = 0$  leads to the factor  $(1 + \zeta_2 \varepsilon^2 / 8)$ , where  $\zeta_n$  are the values of Riemann's  $\zeta$ -function at integer values of  $n$ , cf. Appendix (H.8). Inserting (132, 130, 129) into (128) and expanding up to  $O(a_s)$  yields

$$Z_g = \frac{Z_1^l + Z_1^H}{(Z_3^l + Z_3^H)^{3/2}} = 1 + a_s S_\varepsilon \left\{ \frac{\beta_0}{\varepsilon} + \frac{\beta_{0,Q}}{\varepsilon} \left[ 1 + \frac{\zeta_2}{8} \varepsilon^2 \right] \sum_{i=1}^3 \left( \frac{m_i^2}{\mu^2} \right)^{\varepsilon/2} \right\}. \quad (133)$$

In (133),  $\beta_0$  is the lowest order term of the expansion of the  $\beta$ -function [29, 30, 101]

$$\beta(g_s) = -g_s \sum_{k=0}^{\infty} \beta_k \left( \frac{g_s}{4\pi} \right)^{2k+2}, \quad (134)$$

$$\beta_0 := \frac{11C_A - 4T_R N_f}{3}. \quad (135)$$

The contribution of one heavy quark of species  $i$  to the  $\beta$ -function is then given by

$$\beta_{0,i} = -\frac{4}{3} T_R. \quad (136)$$

Finally one arrives at the following expression for the renormalized strong coupling constant  $a_s$  up to  $O(a_s^2)$

$$a_s = a_s Z_g^2 = a_s \left\{ 1 + a_s \delta a_s \right\}, \quad (137)$$

$$\delta a_s := S_\varepsilon \left\{ \frac{2\beta_0}{\varepsilon} + \frac{2\beta_{0,Q}}{\varepsilon} \left[ 1 + \frac{\zeta_2}{8} \varepsilon^2 \right] \sum_{i=1}^3 \left( \frac{m_i^2}{\mu^2} \right)^{\varepsilon/2} \right\}. \quad (138)$$

Using (137) and (126), the OME  $\hat{A}_{ij}$  reads, after mass and coupling constant renormalization up to  $O(a_s^2)$ ,

$$\hat{A}_{ij} = \delta_{ij} + a_s \hat{A}_{ij}^{(1)} + a_s^2 \left\{ \hat{A}_{ij}^{(2)} + \delta m \frac{d}{dm} \hat{A}_{ij}^{(1)} + \delta a_s \hat{A}_{ij}^{(1)} \right\}. \quad (139)$$

The strong coupling constant obeys the evolution equation

$$\frac{da_s}{d \ln(\mu^2)} = - \sum_{k=0}^{\infty} \beta_k a_s^{k+2}, \quad (140)$$

where  $\beta_k$  are the expansion coefficients of the  $\beta$ -function (134).  $\beta_0$  to  $\beta_3$  were calculated in the  $\overline{\text{MS}}$ -scheme in Ref. [29, 30, 101]. Solving the evolution equation (140) in the  $\overline{\text{MS}}$ -scheme, [100],

the running coupling constant is then given in 4-loop approximation by, cf. [102, 103],

$$\begin{aligned}
a_s(Q^2) &= \frac{1}{\beta_0(Q^2/\Lambda_{\overline{\text{MS}}}^2)} - \frac{1}{\beta_0^3(Q^2/\Lambda_{\overline{\text{MS}}}^2)^2} \beta_1 \ln(Q^2/\Lambda_{\overline{\text{MS}}}^2) \\
&+ \frac{1}{\beta_0^3(Q^2/\Lambda_{\overline{\text{MS}}}^2)^3} \left\{ \frac{\beta_1^2}{\beta_0^2} \left[ \ln^2(Q^2/\Lambda_{\overline{\text{MS}}}^2) - \ln(Q^2/\Lambda_{\overline{\text{MS}}}^2) - 1 \right] + \frac{\beta_2}{\beta_0} \right\} \\
&+ \frac{1}{\beta_0^4(Q^2/\Lambda_{\overline{\text{MS}}}^2)^4} \left\{ \frac{\beta_1^3}{\beta_0^3} \left[ -\ln^3(Q^2/\Lambda_{\overline{\text{MS}}}^2) + \frac{5}{2} \ln^2(Q^2/\Lambda_{\overline{\text{MS}}}^2) + 2 \ln(Q^2/\Lambda_{\overline{\text{MS}}}^2) - \frac{1}{2} \right] \right. \\
&\left. - 3 \frac{\beta_1 \beta_2}{\beta_0^2} \ln(Q^2/\Lambda_{\overline{\text{MS}}}^2) + \frac{\beta_3}{2\beta_0} \right\}. \tag{141}
\end{aligned}$$

Here the QCD scale  $\Lambda_{\overline{\text{MS}}}$  has been introduced. Note that the expansion coefficients of the  $\beta$ -function depend on the number of active quark flavors  $N_f$ . At the production threshold of heavy quarks, this leads to matching conditions for the values of  $a_s(N_f - 1)$  and  $a_s(N_f)$  [103].

Operator renormalization in Mellin-space is performed by multiplying with the operator  $Z$ -factor  $\mathbf{Z}_O$

$$\hat{A}_{ij} \left( \frac{m^2}{\mu^2}, a_s, \varepsilon \right) = Z_{O,ik}(a_s, \varepsilon) \otimes \tilde{A}_{kj} \left( \frac{m^2}{\mu^2}, a_s, \varepsilon \right). \tag{142}$$

In the singlet case, (142) is a matrix equation, since the gluon and quark-singlet OMEs mix under renormalization, because they have the same quantum numbers [79]. In the non-singlet case, no mixing occurs.  $\mathbf{Z}_O$  is related to the anomalous dimension matrix of the composite operators (87-89) as

$$\gamma_{ij}^N = -(Z_O(\mu))_{ik}^{-1} \frac{\partial}{\partial \mu} Z_{O,kj}(\mu) \tag{143}$$

in Mellin-space. In  $z$ -space, the latter are given by the splitting functions.

$$\gamma_{ij}^N = - \int_0^1 dz z^{N-1} P_{ij}(z). \tag{144}$$

For the Mellin-space representation of the LO and NLO splitting functions, see Appendix L. The matrix elements  $Z_{O,ij}$  can then be expanded in a perturbative series

$$Z_{O,ij} = \sum_{k=0}^{\infty} a_s^k Z_{O,ij}^k. \tag{145}$$

By using (142) and inverting the matrix  $\mathbf{Z}_O$ , one obtains the OMEs  $\tilde{A}_{ij}$  up to  $O(a_s^2)$ , [55],

$$\begin{aligned}
\tilde{A}_{ij} &= \delta_{ij} + a_s \left[ \hat{A}_{ij}^{(1)} + Z_{O,ij}^{-1,(1)} \right] \\
&+ a_s^2 \left[ \hat{A}_{ij}^{(2)} + \delta m \frac{d}{dm} \hat{A}_{ij}^{(1)} + \delta a_s \hat{A}_{ij}^{(1)} + Z_{O,ik}^{-1,(1)} \hat{A}_{kj}^{(1)} + Z_{O,ij}^{-1,(2)} \right]. \tag{146}
\end{aligned}$$

The structure of the expansion coefficients  $Z_{O,ij}^{-1,(k)}$  of the inverse  $\mathbf{Z}_O$  matrix can be inferred from the literature, cf. e.g. [104], see Appendix L. The collinear divergences are removed in much the same way by performing mass factorization, cf. Ref. [55],

$$\tilde{A}_{ij} \left( \frac{m^2}{\mu^2}, a_s \right) = A_{ik} \left( \frac{m^2}{\mu^2}, a_s, \varepsilon \right) \otimes \Gamma_{kj}(a_s, \varepsilon). \quad (147)$$

Here,  $A_{ij}$  denote the finite OMEs and  $\Gamma_{ij}$  are the transition functions. Expanding the latter in a power series in  $a_s$  yields

$$\Gamma_{ij} = \sum_{k=0}^{\infty} a_s^k \Gamma_{ij}^{(k)}. \quad (148)$$

By inverting the  $\Gamma$ -matrix in (147) one obtains the finite OMEs up to  $O(a_s^2)$ , [55],

$$\begin{aligned} A_{ij} = \delta_{ij} &+ a_s \left[ \hat{A}_{ij}^{(1)} + Z_{O,ij}^{-1,(1)} + \Gamma_{ij}^{-1,(1)} \right] \\ &+ a_s^2 \left[ \hat{A}_{ij}^{(2)} + \delta m \frac{d}{dm} \hat{A}_{ij}^{(1)} + \delta a_s \hat{A}_{ij}^{(1)} + Z_{O,ik}^{-1,(1)} \hat{A}_{kj}^{(1)} + Z_{ij}^{-1,(2)} \right. \\ &\quad \left. + \left\{ \hat{A}_{ik}^{(1)} + Z_{O,ik}^{-1,(1)} \right\} \otimes \Gamma_{kj}^{-1,(1)} + \Gamma_{ij}^{-1,(2)} \right]. \end{aligned} \quad (149)$$

Here  $\Gamma_{ij}^{-1,k}$  are the expansion coefficients of the inverse  $\Gamma$ -matrix up to  $O(a_s^2)$ , given in the literature, [105], and listed in Appendix L.

## 5 $F_2^{Q\bar{Q}}$ and $F_L^{Q\bar{Q}}$ at Leading Order

At leading order (LO) the structure functions  $F_2^{Q\bar{Q}}$  and  $F_L^{Q\bar{Q}}$  derive from the tree level cross-section of virtual photon-gluon scattering

$$\gamma^* + G \rightarrow Q + \bar{Q} + X . \quad (150)$$

This reaction is referred to as Bethe-Heitler fusion process and has been calculated first in Ref. [44, 45]. The structure functions can be calculated using the collinear parton model, i.e. the constituents (partons) of the proton are viewed as free particles during the interaction time and their 4-momentum is taken to be parallel to the proton momentum [17]. The perturbative and non-perturbative part of the scattering cross section can then be separated due to the factorization theorems, [52, 53], see Eq. (75). At LO two Feynman-diagrams contribute to the process, see Figure 4.

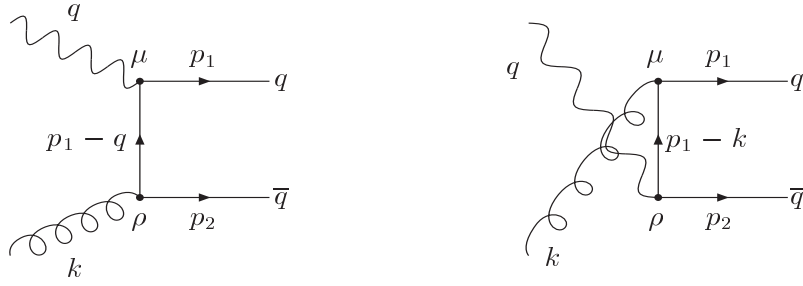


Figure 4: Feynman diagrams contributing to the photon gluon fusion process at LO.

Here  $k$  denotes the 4-momentum of the gluon and

$$k = zP , \quad (151)$$

i.e.  $z$  is the fraction of the proton momentum carried by the gluon. The scaling variable  $\tau$  is the ratio of the Bjorken-variable  $x$  and  $z$

$$\tau := \frac{x}{z} , \quad (152)$$

see section 2.5. The cms velocity  $v$  of the produced quarks is given by, cf. [45],

$$v = \left( 1 - 4 \frac{m^2}{Q^2} \frac{\tau}{1 - \tau} \right)^{1/2} . \quad (153)$$

The condition  $v \geq 0$  defines the threshold  $a$

$$v \geq 0 \Leftrightarrow \frac{z}{x} \leq a \equiv 1 + \frac{4m^2}{Q^2} . \quad (154)$$

According to the factorization theorems, [52, 53], the structure functions are given by the Mellin-convolution of the non-perturbative parton densities and the perturbative coefficient functions. The integration boundaries are determined by condition (154). The heavy quark coefficient functions are denoted by  $H_{(2,L),g}(\tau, Q^2/m^2, m^2/\mu^2)$  and their contribution to the structure functions is [55], see section 3,

$$F_{(2,L)}^{Q\bar{Q}}\left(x, \frac{Q^2}{m^2}\right) = x \int_{ax}^1 \frac{dz}{z} G(z, \mu^2) H_{(2,L),g}\left(\tau, \frac{Q^2}{m^2}, \frac{m^2}{\mu^2}\right), \quad (155)$$

with  $G(z, \mu^2)$  being the gluon density. In this section the LO term  $H_{(2,L),g}^{(1)}(\tau, Q^2/m^2, m^2/\mu^2)$  of the heavy quark coefficient functions is calculated. Later, the limit  $Q^2 \gg m^2$  is performed. As has been discussed in section 2, the matrix element of this process can be obtained by separating the leptonic and the hadronic parts. One obtains the structure functions by projecting the hadronic tensor, Eq. (35),

$$\frac{1}{x} F_2^{Q\bar{Q}}\left(x, \frac{Q^2}{m^2}\right) = \frac{2}{D-2} \left[ 4(D-1) \frac{x^2}{Q^2} k^\mu k^\nu W_{\mu\nu} - g^{\mu\nu} W_{\mu\nu} \right] \quad (156)$$

$$F_L^{Q\bar{Q}}\left(x, \frac{Q^2}{m^2}\right) = \frac{8x^3}{Q^2} k^\mu k^\nu W_{\mu\nu}, \quad (157)$$

where  $D$  denotes the space-time dimension,  $D = 4 + \varepsilon$ . By applying (155) and factorizing the hadronic tensor, one obtains similar projection relations for the heavy quark structure functions

$$H_{2,g}\left(\tau, \frac{Q^2}{m^2}, \frac{m^2}{\mu^2}\right) = \frac{2}{D-2} \left[ 4(D-1) \frac{\tau^2}{Q^2} k^\mu k^\nu w_{\mu\nu} - g^{\mu\nu} w_{\mu\nu} \right] \quad (158)$$

$$H_{L,g}\left(\tau, \frac{Q^2}{m^2}, \frac{m^2}{\mu^2}\right) = \frac{8\tau^2}{Q^2} k^\mu k^\nu w_{\mu\nu}, \quad (159)$$

where  $w_{\mu,\nu}$  is now the purely perturbative part of the hadronic tensor, cf. section 2.5.2, and is derived from the Feynman diagrams of Figure 4 at LO.

## 5.1 Complete Calculation of $H_{(2,L),g}^{(1)}$ at Leading Order

Using the Feynman rules of Appendix B, the matrix element contributing to  $H_{(L,2),g}^{(1)}$  reads

$$M_{\rho\mu} = \bar{u}(p_2) i g_s \gamma_\rho i \frac{\not{p}_1 - \not{q} + m}{(p_1 - q)^2 - m^2} i e_q \gamma_\mu v(p_1) + \bar{u}(p_2) i g_s \gamma_\rho i \frac{\not{p}_1 - \not{q} + m}{(p_1 - k)^2 - m^2} i e_q \gamma_\mu v(p_1). \quad (160)$$

Throughout this thesis the Feynman gauge is used. Squaring the matrix element yields a quantity depending on four indexes

$$H^{\rho\mu\sigma\nu} := M^{\rho\mu} M^{*\sigma\nu}. \quad (161)$$

Since one considers the case of unpolarized gluons, one has to sum over the polarization states of the gluons via a contraction with the metric tensor  $-g_{\rho\sigma}$ . This average results into an overall

factor  $1/(D-2)$  due to the fact that a vector particle has  $(D-2)$  spin degrees of freedom in  $D$  dimensions. According to the optical theorem, the hadronic tensor is now given by

$$w_{\mu\nu} = \frac{1}{2\pi} \text{Im } t_{\mu\nu} = \frac{1}{2\pi} \left[ \frac{-g_{\rho\sigma}}{D-2} H^{\rho\mu\sigma\nu} \right], \quad (162)$$

where  $t_{\mu\nu}$  is the partonic equivalent of the forward Compton amplitude. Since we consider the inclusive cross section, the quark–antiquark momenta are integrated over. All integrals are non-singular, hence we set  $D = 4$  and obtain, [81],

$$H_{2,g}^{(1)} \left( \tau, \frac{Q^2}{m^2}, \frac{m^2}{\mu^2} \right) = \frac{T_R}{4\pi} \int dR_2 \left( g_{\mu\nu} - 12 \frac{\tau^2}{Q^2} k_\mu k_\nu \right) H^{\mu\nu\rho\sigma} g_{\mu\rho} \quad (163)$$

$$H_{L,g}^{(1)} \left( \tau, \frac{Q^2}{m^2}, \frac{m^2}{\mu^2} \right) = \frac{T_R}{4\pi} \int dR_2 \left( -8 \frac{\tau^2}{Q^2} k_\mu k_\nu H^{\mu\nu\rho\sigma} g_{\mu\rho} \right). \quad (164)$$

Here  $T_R$  is a color factor, cf. Appendix D, given by  $T_R = 1/2$  for  $SU(N)$ . Note that the quark charge  $e_q$  is not included in Eqs. (163, 164). The phase space element is given in Appendix C. The expression for the coefficient functions simplifies to

$$H_{2,g}^{(1)} \left( \tau, \frac{Q^2}{m^2}, \frac{m^2}{\mu^2} \right) = \frac{T_R}{4\pi} \int_{t^-}^{t^+} \frac{dt}{64\pi s p_{cm}^2} \left( g_{\mu\nu} - 12 \frac{\tau^2}{Q^2} k_\mu k_\nu \right) H^{\mu\nu\rho\sigma} g_{\rho\sigma} \quad (165)$$

$$H_{L,g}^{(1)} \left( \tau, \frac{Q^2}{m^2}, \frac{m^2}{\mu^2} \right) = \frac{T_R}{4\pi} \int_{t^-}^{t^+} dR_2 \frac{dt}{64\pi s p_{cm}^2} \left( -8 \frac{\tau^2}{Q^2} k_\mu k_\nu H^{\mu\nu\rho\sigma} g_{\rho\sigma} \right). \quad (166)$$

Here  $p_{cm}$  denotes the center-of-mass 3-momentum of the initial state particles, cf. (C.6). The Mandelstam-variables are defined by

$$s = (q+k)^2 = (p_1+p_2)^2 = -Q^2 + 2q \cdot k + k^2 = m_1^2 + m_2^2 + p_1 \cdot p_2 \quad (167)$$

$$u = (q-p_2)^2 = (k-p_1)^2 = m_1^2 - 2k \cdot p_1 + k^2 = m_2^2 - 2q \cdot p_2 - Q^2 \quad (168)$$

$$t = (q-p_1)^2 = (k-p_2)^2 = -Q^2 - 2q \cdot p_1 + m_1^2 = m_2^2 - 2k \cdot p_2 + k^2, \quad (169)$$

with

$$s + t + u = k^2 - Q^2 + m_1^2 + m_2^2. \quad (170)$$

In the present case, we specify these relations with  $k^2 = 0$ ,  $p_1^2 = m_1^2 = p_2^2 = m_2^2 = m^2$ . The integration boundaries  $t^\pm$  are determined by the physical regions of the phase space and are given by, (C.27),

$$t^\pm = \frac{s+Q^2}{2} \pm \frac{s+Q^2}{2} \cdot v. \quad (171)$$

The calculation has been performed using the computer algebra program FORM [72]. After the  $t$ -integration one obtains the heavy quark coefficient functions

$$H_{2,g}^{(1)} \left( \tau, \frac{Q^2}{m^2}, \frac{m^2}{\mu^2} \right) = 8T_R \cdot \left\{ v \left[ -\frac{1}{2} + 4\tau - 4\tau^2 + 2\frac{m^2}{Q^2}(\tau^2 - \tau) \right] + \left[ -\frac{1}{2} + \tau - \tau^2 + 2\frac{m^2}{Q^2}(3\tau^2 - \tau) + 4\frac{m^4}{Q^4}\tau^2 \right] \ln \left( \frac{1-v}{1+v} \right) \right\}, \quad (172)$$

$$H_{L,g}^{(1)} \left( \tau, \frac{Q^2}{m^2}, \frac{m^2}{\mu^2} \right) = 16T_R \cdot \left[ v \cdot \tau(1-\tau) + 2\frac{m^2}{Q^2}\tau^2 \ln \left( \frac{1-v}{1+v} \right) \right]. \quad (173)$$

Eqs. (172, 173) agree with the results of Ref. [45] except for a factor of  $\tau/Q^2$ , which is due to different definitions of  $F_2$  and  $F_L$ , see Eq. (155).

## 5.2 The Limit $Q^2 \gg m^2$

We consider the asymptotic limit  $Q^2 \gg m^2$ . For large scales  $Q^2$ , the expansion of  $v$  reads

$$v = 1 - \frac{2m^2}{Q^2} \frac{\tau}{1-\tau} + O\left(\frac{m^4}{Q^4}\right). \quad (174)$$

The logarithm in (172) becomes

$$\ln\left(\frac{1-v}{1+v}\right) = \ln\left(\frac{m^2}{Q^2}\right) + \ln\left(\frac{\tau}{1-\tau}\right) + O\left(\frac{m^2}{Q^2}\right). \quad (175)$$

Using the Taylor-expansion in  $m^2/Q^2$ , one arrives at

$$\begin{aligned} H_{2,g}^{(1)}\left(\tau, \frac{Q^2}{m^2}, \frac{m^2}{\mu^2}\right) &= 4T_R \cdot \left\{ 8\tau(1-\tau) - 1 + [\tau^2 + (1-\tau)^2] \ln\left(\frac{Q^2}{m^2}\right) \right. \\ &\quad \left. + [\tau^2 + (1-\tau)^2] \ln\left(\frac{1-\tau}{\tau}\right) \right\} \\ &\quad + 4T_R \frac{m^2}{Q^2} \left\{ -10\tau^2 - \tau + 4(3\tau^2 - \tau) \left[ \ln\left(\frac{\tau}{1-\tau}\right) \right. \right. \\ &\quad \left. \left. + \ln\left(\frac{m^2}{Q^2}\right) \right] \right\} + O\left(\frac{m^4}{Q^4}\right) \end{aligned} \quad (176)$$

$$\begin{aligned} H_{L,g}^{(1)}\left(\tau, \frac{Q^2}{m^2}, \frac{m^2}{\mu^2}\right) &= 16T_R \cdot \tau(1-\tau) \\ &\quad + 16T_R \tau^2 \frac{m^2}{Q^2} \left\{ -1 + \left[ \ln\left(\frac{\tau}{1-\tau}\right) + \ln\left(\frac{m^2}{Q^2}\right) \right] \right\} \\ &\quad + O\left(\frac{m^4}{Q^4}\right). \end{aligned} \quad (177)$$

The limit  $m^2/Q^2 \rightarrow 0$  can be performed and only the first terms in (176, 177) remain. In case of  $H_{2,g}^{(1)}$  the leading logarithmic contribution is

$$H_{2,g}^{(1)}\left(\tau, \frac{Q^2}{m^2}, \frac{m^2}{\mu^2}\right) \propto \frac{1}{2} \widehat{P}_{gg}^{(0)}(\tau) \ln\left(\frac{Q^2}{m^2}\right). \quad (178)$$

Here

$$\widehat{P}_{gg}^{(0)}(\tau) = 8T_R[\tau + (1-\tau)^2] \quad (179)$$

is the LO scheme independent splitting function, see Appendix L. Likewise

$$H_{L,g}^{(1)}\left(\tau, \frac{Q^2}{m^2}, \frac{m^2}{\mu^2}\right) \propto 16T_R \cdot \tau(1-\tau) \quad (180)$$



denotes the 1-loop scheme-invariant gluonic Wilson coefficient for the longitudinal structure function in the massless limit [56]. In the longitudinal case no collinear singularity is present, unlike the case for  $H_2$ , which is signaled by the occurrence of  $\ln(Q^2/m^2)$  along with the corresponding splitting function.

## 6 Heavy Flavor Coefficient Functions for Large $Q^2$ at Leading Order

As has been described in Section 3, the heavy quark coefficient functions  $H_{(2,L),g}$  can be calculated in the limit  $Q^2 \gg m^2$  by applying the factorization theorems, see (92). At LO they are then given by, cf. (98, 101),

$$H_{L,g}^{(1)}\left(\frac{Q^2}{m^2}, \frac{m^2}{\mu^2}\right) = \widehat{C}_{L,g}^{(1)}\left(\frac{Q^2}{\mu^2}\right), \quad (181)$$

$$H_{2,g}^{(1)}\left(\frac{Q^2}{m^2}, \frac{m^2}{\mu^2}\right) = A_{Qg}^{(1)}\left(\frac{m^2}{Q^2}\right) + \widehat{C}_{2,g}^{(1)}\left(\frac{Q^2}{\mu^2}\right), \quad (182)$$

where  $\widehat{C}_{(2,L)}^{(1)}$ ,  $A_{Qg}^{(1)}$  are the massless LO Wilson coefficients and the LO singlet OME, respectively. In section 6.1 the unrenormalized massless Wilson coefficients are calculated and in section 6.2 the contributing unrenormalized massive OME in the  $\overline{\text{MS}}$ -scheme. In section 6.3 we will compute the renormalized asymptotic heavy quark coefficient functions and discuss the result.

### 6.1 LO Wilson Coefficients for Massless Quark $ep$ -Pair Production in the $\overline{\text{MS}}$ Scheme

The unrenormalized massless LO Wilson coefficients are denoted by  $\overline{C}_{(2,L),g}^{(1)}(\tau, Q^2)$ . At LO they are calculated similar to the LO heavy quark coefficient functions  $H_{(2,L),g}^{(1)}(\tau, Q^2)$ , see section 5, setting  $m \equiv 0$  at the beginning. Due to this, the collinear singularity present in (176) will cause  $\overline{C}_{2,g}^{(1)}(\tau, Q^2)$  to diverge. This divergence is treated in the  $\overline{\text{MS}}$ -scheme, see section 4.2. No singularity is present for  $\overline{C}_{L,g}^{(1)}$ .

The Feynman-diagrams contributing are again given in Figure 4. The projections of the hadronic tensor are the same as in (156) and (157). The phase space integral is given by (C.21), where  $y \in [-1, 1]$ . The relations for  $v$  and  $a$ , see (153, 154), simplify in the massless case to

$$v = 1, \quad a = 1. \quad (183)$$

The matrix element  $M_{\mu\nu}$  is given by (160) with  $m = 0$ . The sub-system cross sections  $\overline{C}_{(2,L),g}^{(1)}$  read

$$\overline{C}_{2,g}^{(1)}\left(\tau, \frac{Q^2}{\mu^2}\right) = \frac{2T_R}{2\pi(D-2)^2} \int_{-1}^1 \frac{dy(p'_{cm})^{D-3}}{32\pi sp_{cm}} \left[ g_{\mu\nu} - 4\left(D-1\right) \frac{\tau^2}{Q^2} k_\mu k_\nu \right] H^{\mu\nu\rho\sigma} g_{\rho\sigma} \cdot \frac{(1-y^2)^{D/2-2}}{2^{D-4}\pi^{D/2-2}\Gamma(D/2-1)} \quad (184)$$

$$\overline{C}_{L,g}^{(1)}\left(\tau, \frac{Q^2}{\mu^2}\right) = \frac{T_R}{2\pi(D-2)} \int_{-1}^1 \frac{dy(p'_{cm})^{D-3}}{32\pi sp_{cm}} \left( -8 \frac{\tau^2}{Q^2} k_\mu k_\nu H^{\mu\nu\rho\sigma} g_{\rho\sigma} \right) \cdot \frac{(1-y^2)^{D/2-2}}{2^{D-4}\pi^{D/2-2}\Gamma(D/2-1)}, \quad (185)$$

where  $\mu$  is the factorization scale. The calculation has again been done using FORM [72]. After performing the  $\varepsilon$ -expansion, the result of the calculation can be written as

$$\overline{C}_{2,g}^{(1)}\left(\tau, \frac{Q^2}{\mu^2}\right) = S_\epsilon \left\{ \frac{\widehat{P}_{qg}^{(0)}(\tau)}{\epsilon} + \frac{\widehat{P}_{qg}^{(0)}(\tau)}{2} \left[ \ln\left(\frac{1-\tau}{\tau}\right) + \ln\left(\frac{Q^2}{\mu^2}\right) - 4 \right] + 12T_R \right\} \quad (186)$$

$$\overline{C}_{L,g}^{(1)}\left(\tau, \frac{Q^2}{\mu^2}\right) = 16T_R\tau(1-\tau). \quad (187)$$

For the definition of the LO splitting function, see Eq. (179). These results are the same as have been derived in Ref. [55]. Since the longitudinal massless Wilson coefficient is finite at LO, no renormalization is necessary and one can identify  $\overline{C}_{L,g}^{(1)} = \widehat{C}_{L,g}^{(1)}$ . The renormalized massless Wilson coefficient  $\widehat{C}_2^{(1)}$  is then given by, [55],

$$\widehat{C}_{2,g}^{(1)}\left(\tau, \frac{Q^2}{\mu^2}\right) = \frac{1}{2}\widehat{P}_{qg}^{(0)}(\tau) \ln\left(\frac{Q^2}{\mu^2}\right) + \widehat{c}_{2,g}^{(1)}, \quad (188)$$

$$\widehat{c}_{2,g}^{(1)} = \frac{\widehat{P}_{qg}^{(0)}(\tau)}{2} \left[ \ln\left(\frac{1-\tau}{\tau}\right) - 4 \right] + 12T_R. \quad (189)$$

## 6.2 The Calculation of the Operator Matrix Element $\widehat{A}_{Qg}^{(1)}$

The unrenormalized massive singlet OME at LO is denoted by  $\widehat{A}_{Qg}^{(1)}$ . It receives contributions from the two Feynman-graphs given in Figure 5.

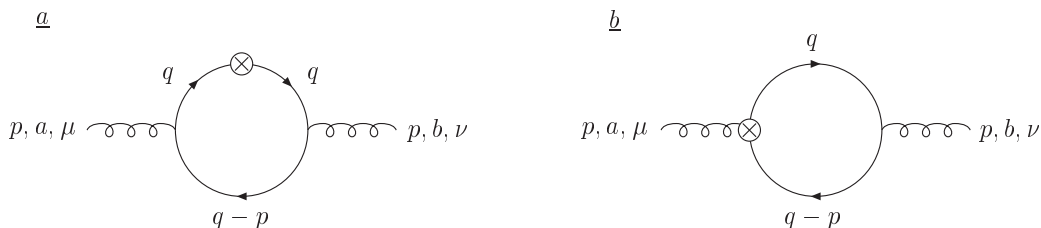


Figure 5: Feynman diagrams contributing to  $\widehat{A}_{Qg}^{(1)}$ .

Here  $N$  is the Mellin-moment,  $\mu, \nu$  denote Lorentz-indexes and  $a, b$  are color-indexes. One has to add the results for both fermion directions due to crossing, which yields a factor

$$\frac{1 + (-1)^N}{2}. \quad (190)$$

As it turns out, the two momentum directions differ by a factor  $(-1)^N$  only. In section 2.4 we saw that only even values of  $N$  contribute. Therefore, the two momentum directions are equal a priori and a symmetry factor 1/2 is included according to our convention. The computation is straightforward. One applies the projection (110) and uses the standard Feynman rules of QCD

and for the composite operators, as given in Appendix B. The loop integrals are evaluated by applying the integral relations for momentum integrals given in Appendix F. We denote by  $A_i^{Qg}$  the results for the individual 1-loop diagrams. Having applied the projector (110), one arrives at

$$A_a^{Qg} = -8a_s T_R S_\epsilon \left( \frac{m^2}{\mu^2} \right)^{\epsilon/2} \frac{1}{(2+\epsilon)\epsilon} \exp \left\{ \sum_{l=2}^{\infty} \frac{\zeta_l}{l} \left( \frac{\epsilon}{2} \right)^l \right\} \frac{2(N^2 + 3N + 2) + \epsilon(N^2 + N + 2)}{N(N+1)(N+2)}, \quad (191)$$

$$A_b^{Qg} = 32a_s T_R S_\epsilon \left( \frac{m^2}{\mu^2} \right)^{\epsilon/2} \frac{1}{(2+\epsilon)\epsilon} \exp \left\{ \sum_{l=2}^{\infty} \frac{\zeta_l}{l} \left( \frac{\epsilon}{2} \right)^l \right\} \frac{1}{(N+1)(N+2)}. \quad (192)$$

The unrenormalized 1-loop OME  $\hat{A}_{Qg}^{(1)}$  up to  $O(\epsilon)$  is given by

$$\begin{aligned} \hat{A}_{Qg}^{(1)} &= \frac{1}{a_s} \left[ A_a^{Qg} + A_b^{Qg} \right] \\ &= -S_\epsilon T_R \left( \frac{m^2}{\mu^2} \right)^\epsilon \frac{1}{\epsilon} \exp \left\{ \sum_{l=2}^{\infty} \frac{\zeta_l}{l} \left( \frac{\epsilon}{2} \right)^l \right\} \frac{8(N^2 + N + 2)}{N(N+1)(N+2)} \\ &= S_\epsilon T_R \left( \frac{m^2}{\mu^2} \right)^\epsilon \left( -\frac{1}{\epsilon} - \frac{\zeta_2}{8} \epsilon \right) \frac{8(N^2 + N + 2)}{N(N+1)(N+2)}. \end{aligned} \quad (193)$$

One now may transform back to  $z$ -space and introduce the LO splitting function  $\hat{P}_{qg}^{(0)}(z)$ , see (179), yielding

$$\hat{A}_{Qg}^{(1)} = S_\epsilon \left( \frac{m^2}{\mu^2} \right)^{\epsilon/2} \left[ -\frac{1}{\epsilon} \hat{P}_{qg}^{(0)}(z) + a_{Qg}^{(1)} + \epsilon \bar{a}_{Qg}^{(1)} \right], \quad (194)$$

where

$$a_{Qg}^{(1)} = 0, \quad (195)$$

$$\bar{a}_{Qg}^{(1)} = -\frac{\zeta_2}{8} \hat{P}_{qg}^{(0)}(z). \quad (196)$$

Note that the coefficient  $a_{Qg}^{(1)}$  of  $O(\epsilon^0)$  vanishes. The  $O(\epsilon^1)$  coefficient  $\bar{a}_{Qg}^{(1)}$  will be needed for the renormalization of the  $O(a_s^2)$  OME  $\hat{A}_{Qg}^{(2)}$  later on. Performing an  $\epsilon$  expansion up to the constant term yields

$$\hat{A}_{Qg}^{(1)} = S_\epsilon \left[ -\frac{\hat{P}_{qg}(z)}{\epsilon} - \ln \left( \frac{m^2}{\mu^2} \right) \frac{\hat{P}_{qg}(z)}{2} \right]. \quad (197)$$

### 6.3 The Heavy Flavor Wilson Coefficients for $Q^2 \gg m^2$

In order to calculate the heavy flavor coefficient functions, the result of section 6.2 has to be renormalized. Coupling constant and mass renormalization are performed according to equation

(139) but have no effect at  $O(a_s)$ . As described in section 4.3, UV divergences are removed by the operator renormalization constants  $Z_{ik}(\varepsilon, a_s)$ , whereas the collinear-divergences are removed by the transition functions  $\Gamma_{ik}(\varepsilon, a_s)$ . Here the subscripts  $ik$  denote the parton types and in the singlet-case these indexes are equal to  $ik = qg$ . According to Eq. (149), the renormalized OME  $A_{Qg}^{(1)}$  is then given by

$$A_{Qg}^{(1)} = \hat{A}_{Qg}^{(1)} + Z_{O,qg}^{-1,(1)}, \quad (198)$$

where the operator renormalization constant can be taken from Appendix L,

$$Z_{qg}^{-1,(1)} = S_\varepsilon \frac{1}{\varepsilon} P_{qg}^{(0)}. \quad (199)$$

Note that the term  $\Gamma_{qg}^{-1,(1)}$ , which would have to be present according to Eq. (149), vanishes since massive quarks do not contribute to the transition functions. One obtains

$$A_{Qg}^{(1)} = -\ln\left(\frac{m^2}{\mu^2}\right) \frac{\hat{P}_{qg}(z)}{2}. \quad (200)$$

The heavy flavor coefficient functions at  $O(a_s)$  are then given by considering Eqs. (181, 182)

$$H_{L,g}^{(1)}\left(z, \frac{Q^2}{m^2}, \frac{m^2}{\mu^2}\right) = \hat{C}_{L,g}^{(1)}\left(\frac{Q^2}{\mu^2}\right), \quad (201)$$

$$H_{2,g}^{(1)}\left(z, \frac{Q^2}{m^2}, \frac{m^2}{\mu^2}\right) = A_{Qg}^{(1)}\left(\frac{m^2}{Q^2}\right) + \hat{C}_{2,g}^{(1)}\left(\frac{Q^2}{\mu^2}\right). \quad (202)$$

Inserting the massless Wilson coefficients given in Eqs. (187, 189) and the renormalized OME  $A_{Qg}^{(1)}$  into (201, 202) yields the LO heavy flavor coefficient functions in the asymptotic limit up to  $O(\varepsilon^0)$

$$H_{L,g}^{(1)}\left(\frac{Q^2}{m^2}\right) = 16T_R z(1-z) \quad (203)$$

$$H_{2,g}^{(1)}\left(\frac{Q^2}{m^2}\right) = T_R \left\{ 4(2z^2 - 2z + 1) \left[ \ln\left(\frac{1-z}{z}\right) + \ln\left(\frac{Q^2}{m^2}\right) \right] - 32z^2 - 4 + 32z \right\}. \quad (204)$$

These two final results are equal to the results obtained in the asymptotic limit  $Q^2 \gg m^2$  of the exact result, see (176) and (177), and agree with [55].

For the longitudinal coefficient function, one notices that the massless Wilson coefficient (187) is not divergent and is equal to the heavy flavor coefficient function in the  $\overline{\text{MS}}$ -scheme. This gives an explanation for the observation of section 5, that the longitudinal coefficient function has no collinear divergence. It is a scheme invariant-quantity at this order in the coupling constant. For the coefficient function  $H_{2,g}^{(1)}$  one observes that there is no correction at  $O(\varepsilon^0)$  in  $A_{Qg}^{(1)}$ . Hence the term proportional to  $(m^2/Q^2)^0$  in  $H_{2,g}^{(1)}$  is already given by the term  $\propto \varepsilon^0$  of the massless Wilson coefficient  $\hat{C}_{2,g}$ .

## 7 Two–Loop Massive Operator Matrix Elements

In this section, our computation of the unrenormalized 2–loop massive operator matrix elements  $\hat{A}_{i,j}^{(2)}(\mu^2/m^2)$  will be described. This calculation has already been performed by M. Buza et. al. in Ref. [55]. There, the calculation was performed using integration–by–part technique of Ref. [67], which leads to a large number of terms. Expressing the result in  $z$ -space in terms of Nielsen integrals, cf. [68], yields rather lengthy expressions for most individual diagrams and the final result.

The present approach differs from the former in two major points :

- We did not apply the integration–by–parts formalism. Thus the calculation was compactified, though partly being more demanding. In this way the creation of a large number of different terms and functions which cancel in the end could be avoided.
- We worked in Mellin-space rather than in  $z$ -space, shifting the main work from calculating Nielsen integrals to calculating finite or infinite nested harmonic sums. Thus the number of independent functions in the final result could be reduced from 48 in Ref. [55] to only 6 harmonic sums, cf. [47, 106, 107].

The calculation was performed widely in an automatized manner, using the algebraic manipulation program FORM, [72], in order to obtain an expression for the individual diagrams in terms of (generalized) hypergeometric series, [69], cf. Appendix I. The individual Feynman diagrams contributing were taken from Ref. [55] and are given in section 7.1. There one can also find a description on how to obtain an expression for the OMEs, starting from a diagram. The steps encoded in a FORM program are described in section 7.2, using two different approaches

- Diagrams containing 2-point 1-loop insertions were treated using scalar or tensor integrals, cf. section 7.2.1.
- In the remaining diagrams some propagators were canceled and only scalar integrals had to be dealt with, cf. section 7.2.2.

The expressions obtained for each diagram were then taken to MAPLE and expanded in the dimensional regularization parameter  $\varepsilon$ . In section 7.3 several techniques are explained how the emerging sums can be calculated. An interesting part of this calculation is that of the 5–propagator 2–loop integrals, since there the difference to Ref. [55] is most apparent. Section 7.4 is devoted to this part of the calculation, using Mellin-Barnes integrals to obtain numerical results for fixed values of  $N$  as a check. The results of this calculation are published in Ref. [108]. As it turns out, the most complex results of scalar momentum integrals are not given by the former, but rather by reduced 2-loop integrals in which only 4 propagators emerge in a nested form, see section 7.5. Finally, the result for the OMEs will be given and discussed in section 7.6.

### 7.1 Feynman Diagrams

In order to obtain an expression for the unrenormalized OMEs at 2-loop order, one has to calculate the amputated Green's functions  $G_{ij}^{(2)}(p^2)$  to  $O(a_s^2)$  in perturbation theory, see section 3.5. Here  $p$  denotes the external momentum. Three different cases contribute : diagrams with external gluons, the quark singlet and non-singlet case. The OMEs are then obtained by applying the following projections

- Gluon contribution

$$\hat{A}_{Qg}^{(2)}\left(\varepsilon, \frac{m^2}{\mu^2}, a_s\right) = \frac{1}{N_c^2 - 1} \frac{1}{D - 2} (-g_{\mu\nu}) \delta^{ab} (\Delta \cdot p)^{-N} G_{Q,\mu\nu}^{ab,(2)}, \quad (205)$$

- Pure-Singlet

$$\hat{A}_{Qq}^{(2)}\left(\varepsilon, \frac{m^2}{\mu^2}, a_s\right) = \frac{1}{N_c} \delta^{ij} \frac{1}{4} (\Delta \cdot p)^{-N} \text{Tr}(\not{p} G_Q^{ij,(2)}), \quad (206)$$

- Non-Singlet

$$\hat{A}_{qq,Q}^{(2)}\left(\varepsilon, \frac{m^2}{\mu^2}, a_s\right) = \frac{1}{N_c} \delta^{ij} \frac{1}{4} (\Delta \cdot p)^{-N} \text{Tr}(\not{p} G_q^{ij,(2)}). \quad (207)$$

Here,  $N_c$  denotes the number of colors,  $a, b$  are color indexes,  $i, j$  indexes of the generators of  $SU(N_c)$ , and  $N$  is the Mellin moment.  $\Delta$  is a light-like vector used to project out the antisymmetric parts of the composite operators and does not appear in the final result.  $D$  denotes the space-time dimension,  $D = 4 + \varepsilon$ . Note that since we work in Feynman gauge, the summation over the Lorentz indexes  $\mu, \nu$  in (205) includes unphysical transverse gluon polarizations. This has to be compensated by adding the corresponding ghost-graphs. For them, the projection is given by

$$\hat{A}_{Qg}^{(2),ghost}\left(\varepsilon, \frac{m^2}{\mu^2}, a_s\right) = \frac{1}{N_c^2 - 1} \frac{1}{D - 2} \delta^{ab} (\Delta \cdot p)^{-N} G_Q^{ab,(2),ghost}. \quad (208)$$

The diagrams contributing were taken from Ref. [55] and are given in Figures 6-9. Note that the operator insertion on a line in these figures is to be read as  $-\otimes-$  =  $\rightarrow\otimes\rightarrow$ .

The calculation is performed for each diagram individually by first writing down an explicit expression for the amputated diagrams according to the Feynman rules, cf. Appendix B. Then the projectors (205-208) are applied and traces and contractions of indexes are calculated, followed by the calculation of the loop-momentum integrals. The final result consists of the sum over all diagrams, considering symmetry factors, which have already been accounted for in Figures 6-9.

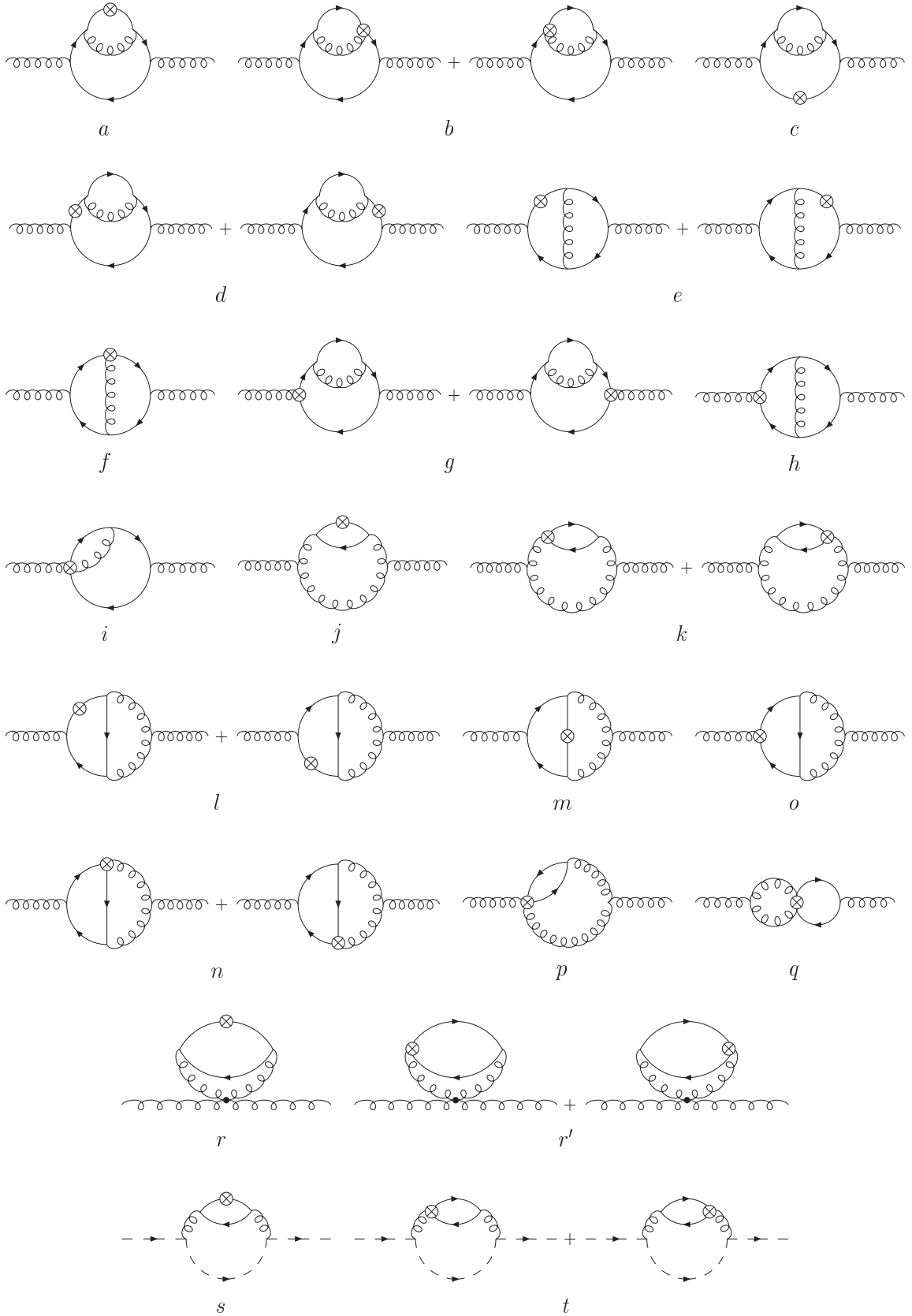


Figure 6: Diagrams contributing to the gluonic OME  $\hat{A}_{Qg}^{(2)}$ . The solid line represents the heavy quark  $Q$ , wavy lines the gluons and dashed lines the ghosts



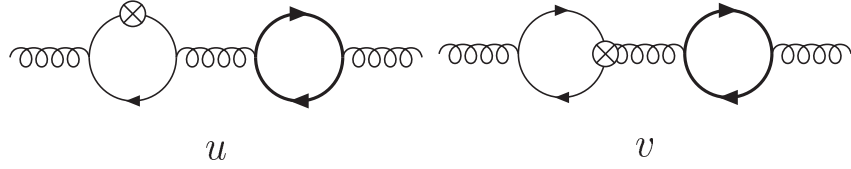


Figure 7: 1-particle reducible diagrams contributing to the singlet OME  $\hat{A}_{Qg}^{(2)}$ . They are removed during the renormalization procedure. The thin line represents the heavy quark  $Q$ , the solid line any heavy flavor.

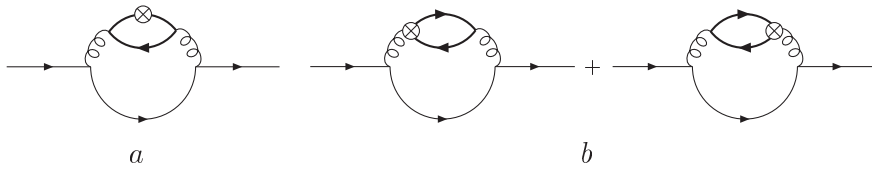


Figure 8: Diagrams contributing to the pure-singlet OME  $\hat{A}_{Qq}^{(2),PS}$ . The thin lines represent the light quark  $q$  and the thick lined the heavy quark  $Q$ .

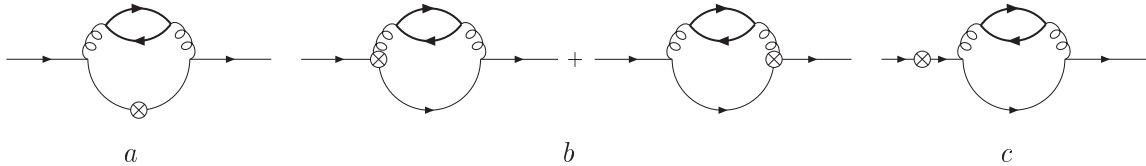


Figure 9: Diagrams contributing to the non-singlet OME  $\hat{A}_{qq}^{(2),NS}$ . The thin lines represent the light quark  $q$ . The heavy quark is contained in the respective contribution to the gluon self-energy only.

## 7.2 Momentum Integrals

The calculation of the momentum integrals was done in a procedural manner, using the algebraic manipulation program FORM, [72], to calculate traces of  $\gamma$ -matrices and contractions of Lorentz-indexes. Further, it could be used in most of the cases up to the point at which the result is given in terms of sums containing one parameter, the Mellin-variable  $N$ . The calculation was split into two parts. We made use of the fact that diagrams  $a - d$ ,  $g$ ,  $j - k$  and  $p - t$  as well as all non-singlet and pure-singlet ones, cf. Figures 6–9, are no genuine 2-loop diagrams but contain 2-point 1-loop insertions. These insertions are given in Figures 10 and 11. Thus the 1-loop insertions were computed first and inserted afterwards into the original diagram, as described

in section 7.2.1. Diagrams  $e, f, h, l, m, n$  and  $o$  are the genuine 2-loop diagrams, which will be dealt with in section 7.2.2. Note that due to the double sum contained in the operator insertion, diagram  $i$  is one of the most complicated diagrams and had to be treated on a similar level as the pure 2-loop diagrams. In the following,  $p$  denotes the external on-shell gluon momentum and  $q, k$  are the internal momenta which have to be integrated over.

### 7.2.1 1-Loop Insertions

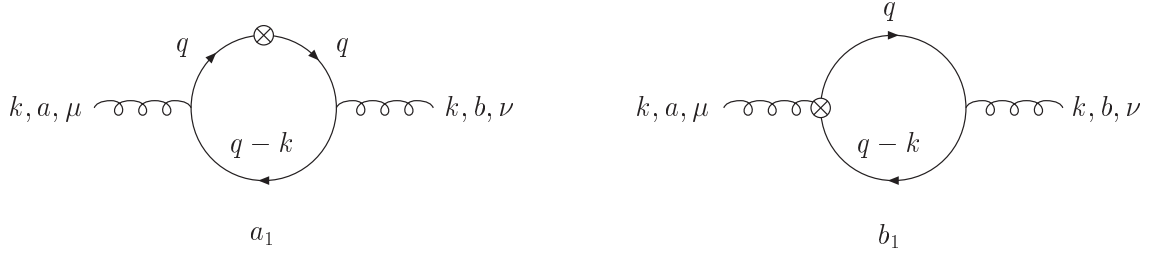


Figure 10: Feynman diagrams contributing to  $\hat{A}_{Qg}^{(1)}$  and acting as 1-loop insertion for  $\hat{A}_{ij}^{(2)}$

We choose the momentum flow in such a way that the external momentum  $p$  of the overall diagram does not enter the 2-point 1-loop insertion (if possible). A Wick rotation is performed in the beginning to shift the integration to Euclidean space. Feynman-parameters were assigned in an automated manner to combine the two propagators, see Appendix F. One obtains

$$\int \frac{dq}{(2\pi)^D} \frac{f(q, k, \Delta, N)}{(q^2 + m_1^2)((q \pm k)^2 + m_2^2)} = \int \frac{dq'}{(2\pi)^D} \int_0^1 dx \frac{f(q', k, \Delta, N)}{(q_\pm'^2 + R^2)^2},$$

$$R^2 = x(1-x) \left( k^2 + \frac{(1-x)m_1^2 + xm_2^2}{x(1-x)} \right). \quad (209)$$

Here  $f$  denotes any function of  $q, k, \Delta, N$ . It may carry Lorentz-indexes and contain  $\gamma$ -matrices, depending on the particular insertion. Further the transformation

$$q'_\pm := q \pm xk \quad (210)$$

has been made. The two masses  $m_1$  and  $m_2$  denote the mass of the heavy quark and are only labeled in order to distinguish the different kinds of insertions present. Both masses are zero only in the case of diagram  $q$ , cf. insertion  $f_1$ , Figure 11. In this case one can immediately see that the  $q'$ -integral vanishes, since no scale enters the loop integration, cf. [109]. For further use, we define

$$M_1^2 := \frac{m^2}{x(1-x)}, \quad (211)$$

$$M_2^2 := \frac{m^2}{x}. \quad (212)$$

After the change of variable to  $q'$  and writing  $\gamma$ -matrices in front of the integrals, the next step is the evaluation of integrals of the type

$$I_{A,B,N} := \int \frac{d^D q}{(2\pi)^D} (q \cdot k)^A (\Delta q \pm x \Delta k)^N q^{\alpha_1} \dots q^{\alpha_B} f(q^2), \quad (213)$$

where we again write  $q$  instead of  $q'$ . Here  $N$  is an integer variable and  $A, B$  are integers of fixed value, usually  $A, B = 0, 1, 2$ . These integrals are evaluated by expanding  $(\Delta q \pm x \Delta k)^N$  via a binomial series and applying the formula to reduce tensor integrals to scalar ones, cf. Appendix F. Thus at maximum 3 terms of the series may contribute, since otherwise a factor  $\Delta^2 = 0$  emerges always. Let us Consider e.g.

$$\begin{aligned} I_{1,1,N} &= \int \frac{d^D q'}{(2\pi)^D} (q \cdot k) (\Delta q' + x \Delta k)^N q^\alpha f(q^2) \\ &= x^N (\Delta k)^N k_\beta \frac{g^{\alpha\beta}}{D} \int \frac{d^D q'}{(2\pi)^D} q^2 f(q^2) + \\ &\quad \frac{N(N-1)}{2} x^{N-2} (\Delta k)^{N-2} k_\beta \Delta_\rho \Delta_\sigma \frac{g^{\beta\alpha} g^{\rho\sigma} + g^{\beta\rho} g^{\alpha\sigma} + g^{\beta\sigma} g^{\alpha\rho}}{D(D+2)} \int \frac{d^D q'}{(2\pi)^D} q^4 f(q^2) \\ &= \frac{(x \Delta k)^N k^\alpha}{D} \int \frac{d^D q'}{(2\pi)^D} q^2 f(q^2) + \frac{N(N-1) x^{N-2} (\Delta k)^{N-1} \Delta^\alpha}{D(D+2)} \int \frac{d^D q'}{(2\pi)^D} q^4 f(q^2). \end{aligned} \quad (214)$$

Eq. (214) can now be calculated using the expressions for scalar integrals as given in Eq. (F.7). The reduction to scalar integrals could be performed in a FORM-program, since the indexes  $A, B$  in (213) are fixed numbers. It is sufficient to decompose all dot-products containing  $q$  into sums and providing the program with the formulae of Eq. (F.5), which terminates the binomial expansion after 3 steps.

In Figures 10 and 11,  $a, b, c, d$  denote color indexes and  $\mu, \nu, \rho, \sigma$  are Lorentz-indexes. The results of the 2-point 1-loop insertions of Figure 10 in Minkowski-space then read

$$\begin{aligned} I_{a_1}^{\mu\nu,ab}(k) &= 4\delta_{ab} T_R \frac{g_s^2 (\Delta k)^{N-2}}{(4\pi)^{D/2}} \Gamma(3 - D/2) \int_0^1 dx x^{N+D/2-3} (1-x)^{-2+D/2} \left[ \right. \\ &\quad - 2x(1-x) \frac{g_{\mu\nu} k^2 - 2k_\mu k_\nu}{(-k^2 + M_1^2)^{3-D/2}} (\Delta k)^2 - \frac{2m^2 g_{\mu\nu}}{(-k^2 + M_1^2)^{3-D/2}} (\Delta k)^2 \\ &\quad + (1-x) \frac{2Nx + 1 - N}{2 - D/2} \cdot \frac{k_\mu \Delta_\nu + \Delta_\mu k_\nu}{(-k^2 + M_1^2)^{2-D/2}} (\Delta k) \\ &\quad + (1-x) \frac{(N-1)(1-2x) - Dx}{2 - D/2} \cdot \frac{g_{\mu\nu}}{(-k^2 + M_1^2)^{2-D/2}} (\Delta k)^2 \\ &\quad \left. - (1-x)(N-1) \frac{N(1-x) - 1}{(1-D/2)(2-D/2)} \cdot \frac{\Delta_\mu \Delta_\nu}{(-k^2 + M_1^2)^{1-D/2}} \right], \end{aligned} \quad (215)$$

$$\begin{aligned} I_{b_1}^{\mu\nu,ab}(k) &= 4\delta_{ab} T_R \frac{g_s^2 (\Delta k)^{N-2}}{(4\pi)^{D/2}} \Gamma(2 - D/2) \int_0^1 dx (x - x^2)^{D/2-2} (x^{N-1} + (1-x)^{N-1}) \left[ \right. \\ &\quad \left. - 2x(1-x) \frac{k^2 \Delta_\mu \Delta_\nu}{(-k^2 + M_1^2)^{2-D/2}} + 2x(1-x) \frac{(\Delta k) \Delta_\mu k_\nu}{(-k^2 + M_1^2)^{2-D/2}} \right]. \end{aligned} \quad (216)$$

These terms appear also in the calculation of the 1-loop OME  $A_{Qg}^{(1)}$ , which thus can be obtained by setting  $k = p$ , applying the projection (205) to (215, 216) and integrating the remaining Feynman parameter.

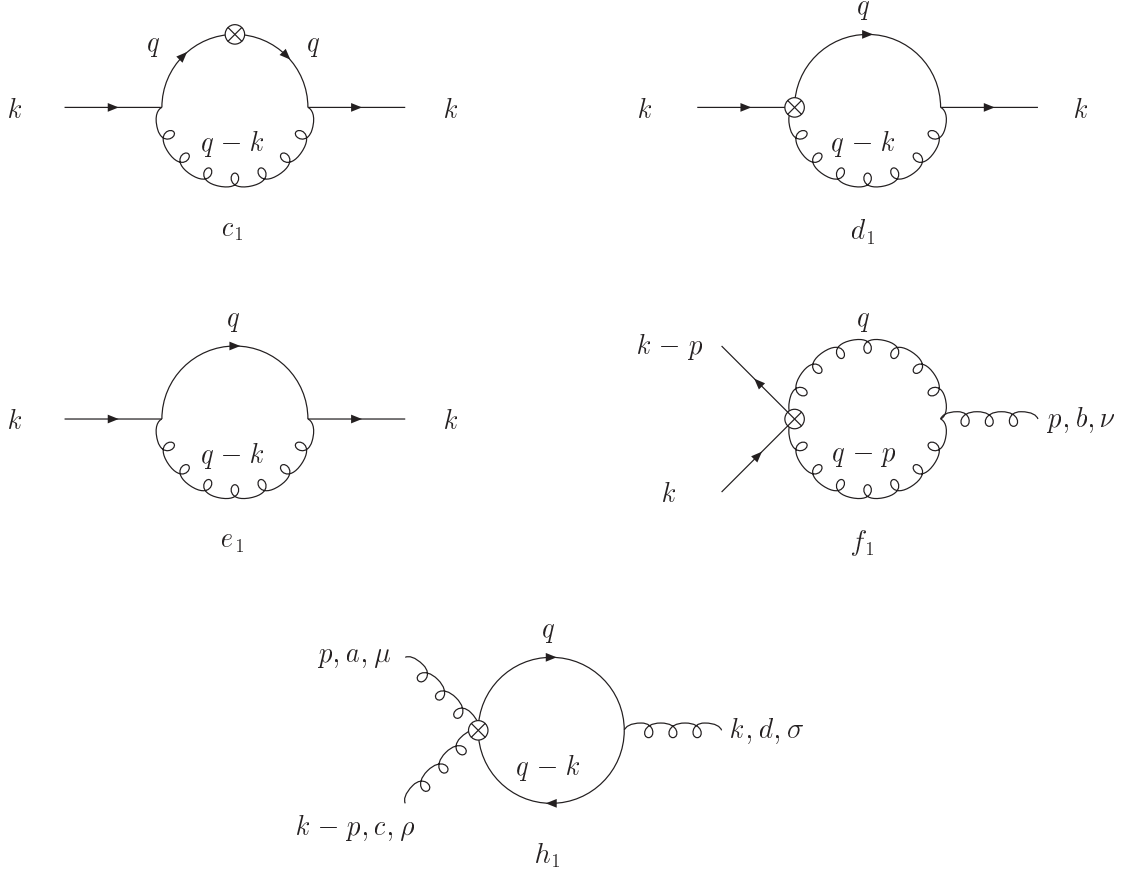


Figure 11: 1-loop insertions in computing  $\hat{A}_{ij}^{(2)}$

The results for the diagrams of Figure 11 are given by

$$\begin{aligned}
I_{c_1}(k) &= C_F \frac{g_s^2 (\Delta k)^{N-1}}{(4\pi)^{\frac{D}{2}}} \int_0^1 dx x^{-3+\frac{D}{2}+N} (1-x)^{-2+\frac{D}{2}} \left[ -\frac{2Dm(\Delta k)}{(-k^2 + M_2^2)^{3-\frac{D}{2}}} \Gamma\left(3 - \frac{D}{2}\right) \right. \\
&\quad \left. + \frac{2x(D-2)(\Delta k)\not{k}}{(-k^2 + M_2^2)^{3-\frac{D}{2}}} \Gamma\left(3 - \frac{D}{2}\right) + \frac{(D-2)(1-N(1-x))\not{\Delta}}{(-k^2 + M_2^2)^{2-\frac{D}{2}}} \Gamma\left(2 - \frac{D}{2}\right) \right], \quad (217)
\end{aligned}$$

$$I_{d_1}(k) = -2C_F \frac{g_s^2 (\Delta k)^{N-1}}{(4\pi)^{\frac{D}{2}}} \Gamma\left(2 - \frac{D}{2}\right) \not{\Delta} \int_0^1 dx \frac{x^{-1+\frac{D}{2}} (1-x)^{-3+\frac{D}{2}} (1-x^{N-1})}{(-k^2 + M_2^2)^{2-\frac{D}{2}}}, \quad (218)$$

$$I_{e_1}(k) = iC_F \frac{g_s^2}{(4\pi)^{\frac{D}{2}}} \Gamma\left(2 - \frac{D}{2}\right) \int_0^1 dx x^{\frac{D}{2}-2} (1-x)^{\frac{D}{2}-2} \left[ \frac{x(D-2)\not{k} - mD}{(-k^2 + M_2^2)^{2-\frac{D}{2}}} \right], \quad (219)$$

$$I_{f_1}(k) = 0, \quad (220)$$

$$\begin{aligned}
I_{h_1}^{\mu\rho\sigma,abc}(k) &= \frac{4g_s^3\Delta_\rho\Delta_\mu}{(4\pi)^{\frac{D}{2}}} \sum_{0\leq j<l}^{N-2} (\Delta k)^{N-2+j-l} \Gamma(2-\frac{D}{2})(-1)^l \int_0^1 dx x^{\frac{D}{2}-3+j} (1-x)^{\frac{D}{2}-3+N-l} \\
&\quad \left\{ (x\Delta k - \Delta p)^{l-1-j} \text{Tr}[t^b t^a t^c] + (-(1-x)\Delta k + \Delta p)^{l-1-j} \text{Tr}[t^a t^b t^c] \right\} \\
&\quad \left[ \frac{\Delta_\sigma m^2}{(-k^2 + M_1^2)^{2-\frac{D}{2}}} - \frac{\Delta_\sigma x(1-x)}{(-k^2 + M_1^2)^{1-\frac{D}{2}}} + \frac{\Delta_\sigma x(1-x)k^2}{(-k^2 + M_1^2)^{2-\frac{D}{2}}} \right. \\
&\quad \left. - 2 \frac{k_\sigma x(1-x)(\Delta k)}{(-k^2 + M_1^2)^{2-\frac{D}{2}}} \right]. \tag{221}
\end{aligned}$$

As has been lined out in section 2.4 already, only even Mellin moments contribute in the light-cone expansion in the present case. Therefore we set  $(-1)^N \equiv 1$ . Having computed the 2-point 1-loop insertions, the calculation of the whole diagram proceeds in much the same way. The results (215-221) are inserted into the respective parent diagram. The same steps as described above are performed to integrate the second momentum and derive an expression in terms of 3-fold parameter integrals. One of these variables could always be integrated trivially, see e.g. Eq. (J.3). In case of diagrams  $j, k, s, t$  and all non-singlet and pure-singlet diagrams, the two remaining parameter integrals were independent of each other and of the form of Euler-Beta-functions, cf. Appendix H. Thus a closed expression in terms of the regularization parameter  $\varepsilon$  could be obtained. In the remaining diagrams, the last two parameters were nested in the form

$$\int_0^1 \int_0^1 \frac{x^a(1-x)^b y^c(1-y)^d}{(1-xy)^e}. \tag{222}$$

In the case of diagram  $a$ , a Mellin-Barnes transformation was applied, see Eq. (I.20), in order to factorize the denominator. The complex contour integral could then be performed analytically using Eq. (I.24) of Appendix I. In the other cases, a closed expression in  $\varepsilon$  could not be derived easily. Eq. (J.8) was then applied to rewrite the integrals of the type (222) in terms of the generalized hypergeometric series  ${}_3F_2[a, b; c, d, e; 1]$ , see Appendix J. These expressions were then further computed using MAPLE. There, the  $\varepsilon$ -expansion could be performed since all divergences were contained in Beta-functions in front of the hypergeometric series. For the analytic continuation of the Beta-function see Appendix H. The calculation of the emerging infinite sums required most of the work and is described in section 7.3.

## 7.2.2 Genuine 2-Loop Diagrams

Diagrams  $e, f, h, l, m, o$  and  $n$ , which do not contain a 2-point 1-loop insertion we refer to as genuine 2-loop diagrams. Like diagram  $i$ , they could not be treated in the same way as described in section 7.2.1. The traces of  $\gamma$ -matrices and contractions of Lorentz-indexes were again calculated using FORM. After performing a Wick rotation, the expression was decomposed by canceling numerator terms with factors in the denominator. A simple example of this procedure is

$$\frac{2q \cdot p}{(q^2 + m^2)((q-p)^2 + m^2)} = \frac{1}{(q-p)^2 + m^2} - \frac{1}{q^2 + m^2}, \quad p^2 = 0. \tag{223}$$

Thus we could reduce tensor integrals to scalar ones, except for few simple cases, which, however, could be calculated in the same way as in section 7.2.1.

One expects that the complexity of a diagram depends on the position of the operator insertion, see Figure 14, Appendix B. In case of diagram  $h$  and  $o$ , however, the sum contained in the insertion can be performed trivially. It reads

$$\sum_{i=0}^{N-2} (\Delta q)^j (\Delta k)^{N-j-2} = \frac{1}{\Delta k - \Delta q} \left[ (\Delta k)^{N-1} - (\Delta q)^{N-1} \right], \quad (224)$$

where  $k - q$  is the gluon momentum, which in case of diagrams  $h$ ,  $o$  is the external momentum and hence does not have to be integrated over. Therefore diagrams  $e, h, l, m$  and  $o$  belong to the same class, whereas  $f, n$  and  $i$  are more complicated.

For each of the individual scalar integrals belonging to the former diagrams, a FORM procedure was written, performing the momentum integration and giving single generalized hypergeometric series as output. These procedures are similar to the ones described in section 7.2.1 and do not differ very much from each other. Hence we could use them with only slight changes for several integrals. An example for the calculation of the 5-propagator scalar integral belonging to diagram  $e$  is given in Appendix J. The other integrals belonging to this class were calculated correspondingly. The result in terms of generalized hypergeometric series was then again transported to MAPLE, where the summation was performed, cf. section 7.3.

Diagrams  $f, n$  and  $i$  required a more specific treatment. Due to the operator insertion on an inner vertex, the sum of the corresponding Feynman-rule can not be performed as easily as in Eq. (224) for diagrams  $n$  and  $f$ . For diagram  $i$ , only one of the two sums of the corresponding operator insertion could be done as in (224), yielding the same complexity as for diagrams  $n$  and  $f$ . In order to minimize the number of integrals containing the sum (224), which have to be calculated differently, one can rewrite the operator sums. After evaluating the traces and contracting the indexes, there are more terms  $\Delta k, \Delta q$  present than in the corresponding Feynman rule for the insertion. In order to bring these sums into the standard form (224), one can add and subtract boundary terms, e.g.

$$\sum_{i=0}^{N-2} (\Delta q)^{i+1} (\Delta k)^{N-i-1} = \sum_{i=0}^N (\Delta q)^i (\Delta k)^{N-i} - (\Delta k)^N - (\Delta q)^N. \quad (225)$$

Thus one is left with two types of integrals: The more complex ones still contain a sum of the type (224), but no further factors  $\Delta k, \Delta q$ . Hence one can calculate the corresponding integral once and then plug it into the program using the respective value of the upper summation boundary ( $N, N - 1, N - 2, \dots$ ). The boundary terms emerging in (225) are the same as the integrals of diagrams  $e, h, l, m, o$  and one can use the respective FORM procedures to arrive at an expression in terms of generalized hypergeometric series. Thus the only integrals which could not be calculated in an automatized manner and had to be added by hand into the FORM programs were the scalar integrals of diagrams  $n, f$  and  $i$  containing the operator insertion in the numerator as given in Figure 14.

### 7.3 Summation

Having performed the momentum integrations, the expressions of all diagrams but  $n, f$  and  $i$  were given in terms of single generalized hypergeometric series'  ${}_3F_2$ , cf. Appendix I. In case of diagrams  $n, f, i$ , parts were given in this form as well, see section 7.2.2, but the main integrals

had to be added to the respective FORM program and are discussed in sections 7.4 and 7.5, respectively. The expansion in the dimensional regularization parameter  $\varepsilon$  was performed by a MAPLE program. By partial fractioning, the emerging sums were split into smaller pieces, each of which were calculated individually.

Due to the  $\varepsilon$ -expansion of the  $\Gamma$ -functions, its logarithmic derivative, the  $\psi$ -function, emerges, see Appendix H. Therefore infinite sums containing  $\Psi$ -functions and  $\Gamma$ -functions had to be calculated, the latter in almost all cases being given in terms of Beta-functions or binomials.

In many applications of perturbative QCD and QED, [70, 71], harmonic sums emerge, which can be considered as generalization of the  $\psi$ -function and the  $\beta$ -function, see Appendix H<sup>3</sup>. The results are then given in terms of finite nested harmonic sums only, which are defined by

$$S_{a_1, \dots, a_m}(N) = \sum_{n_1=1}^N \sum_{n_2=1}^{n_1} \cdots \sum_{n_m=1}^{n_{m-1}} \frac{(\text{sign}(a_1))^{n_1}}{n_1^{|a_1|}} \frac{(\text{sign}(a_2))^{n_2}}{n_2^{|a_2|}} \cdots \frac{(\text{sign}(a_m))^{n_m}}{n_m^{|a_m|}},$$

$$N \in \mathbb{N}, \forall l, a_l \in \mathbb{Z} \setminus 0. \quad (226)$$

The depth  $d$  and the weight  $w$  of a harmonic sum are given by

$$d := m, \quad (227)$$

$$w := \sum_{i=1}^m |a_i|. \quad (228)$$

Harmonic sums of depth  $d = 1$  are also referred to as single harmonic sums. The complete set of algebraic relations connecting harmonic sums to other harmonic sums of the same or lower weight is known [70, 110]. Thus the number of independent harmonic sums can be reduced significantly, e.g. for  $w = 3$  the 18 possible harmonic sums can be expressed algebraically in terms of 8 basic harmonic sums only. One can introduce a product for the harmonic sums, the shuffle product  $\sqcup\sqcup$ , cf. [110]. For the product of a single and a general finite harmonic sum it is given by

$$S_{a_1}(N) \sqcup\sqcup S_{b_1, \dots, b_m}(N) = S_{a_1, b_1, \dots, b_m}(N) + S_{b_1, a_1, b_2, \dots, b_m}(N) + \cdots + S_{b_1, b_2, \dots, b_m, a_1}(N). \quad (229)$$

For sums  $S_{a_1, \dots, a_n}(N)$  and  $S_{b_1, \dots, b_m}(N)$  of arbitrary depth, the shuffle product is then the sum of all harmonic sums of depth  $m + n$  in the index set of which  $a_i$  occurs left of  $a_j$  for  $i < j$ , likewise for  $b_k$  and  $b_l$  for  $k < l$ . Note that the shuffle product is symmetric.

One can show that the following relation holds, cf. [110],

$$S_{a_1}(N) \cdot S_{b_1, \dots, b_m}(N) = S_{a_1}(N) \sqcup\sqcup S_{b_1, \dots, b_m}(N) - S_{a_1 \wedge b_1, b_2, \dots, b_m}(N) - \cdots - S_{b_1, b_2, \dots, a_1 \wedge b_m}(N), \quad (230)$$

where the  $\wedge$  symbol is defined as

$$a \wedge b = \text{sign}(a)\text{sign}(b) (|a| + |b|). \quad (231)$$

By summing (230) over permutations, one obtains the symmetric algebraic relations between harmonic sums. At depth 2 and 3 these read, [70],

$$S_{m,n} + S_{n,m} = S_m S_n + S_{m \wedge n}, \quad (232)$$

$$\sum_{\text{perm}\{l,m,n\}} S_{l,m,n} = S_l S_m S_n + \sum_{\text{inv perm}\{l,m,n\}} S_l S_{m \wedge n} + 2 S_{l \wedge m \wedge n}, \quad (233)$$

---

<sup>3</sup>One should not confuse the  $\beta$ -function determining the running of  $a_s$ , see Eq. (140) and the  $\beta$ -function in context of harmonic sums, see Eq. (H.13)

which we used extensively to simplify our expressions. In (232, 233), “perm” denotes all permutations and “inv perm” invariant ones. The sum  $S_{1,\dots,1}(N)$  can further be expressed at arbitrary depth in terms of a determinant as, cf. [70],

$$S_{\underbrace{1,\dots,1}_k} = \frac{1}{k!} \begin{vmatrix} S_1(N) & 1 & 0 & 0 & \dots & 0 \\ -S_2(N) & S_1(N) & 2 & 0 & \dots & 0 \\ S_3(N) & -S_2(N) & S_1(N) & 3 & \dots & 0 \\ \vdots & \vdots & \vdots & \vdots & & \vdots \\ (-1)^{k+1}S_k(N) & (-1)^k S_{k-1}(N) & (-1)^{k-1}S_{k-2}(N) & (-1)^{k-2}S_{k-3}(N) & \dots & S_1(N) \end{vmatrix}. \quad (234)$$

The limit  $N \rightarrow \infty$  of finite harmonic sums exists only if  $a_1 \neq 1$  in (226). However, it is useful to define all  $\sigma$ -values symbolically as

$$\sigma_{k_l,\dots,k_1} = \lim_{N \rightarrow \infty} S_{a_1,\dots,a_l}(N). \quad (235)$$

The finite  $\sigma$ -values are related to multiple  $\zeta$ -values, [70,71,111–113], Eq. (H.8). Further we define the symbol

$$\sigma_0 := \sum_{i=1}^{\infty} 1. \quad (236)$$

It is useful to work with these  $\sigma$ -values, since they allow to treat parts of sums individually, accounting for the respective divergences. These divergent pieces cancel in the end if the overall sum is finite.

The relation of single harmonic sums with positive or negative indexes to the  $\Gamma$ -function is then given by, see Appendix H,

$$S_1(N) = \psi(N+1) + \gamma_E, \quad (237)$$

$$S_a(N) = \frac{(-1)^{a-1}}{\Gamma(a)} \psi^{(a-1)}(N+1) + \zeta_a, \quad k \geq 2, \quad (238)$$

$$S_{-1}(N) = (-1)^N \beta(N+1) - \ln(2), \quad (239)$$

$$S_{-a}(N) = (-1)^{N+a} \beta^{(a)}(N+1) - (1 - 2^{1-a}) \zeta_a, \quad k \geq 2. \quad (240)$$

Thus single harmonic sums can be continued analytically to complex values of  $N$  by these relations. At higher depths, harmonic sums can be expressed in terms of Mellin-transforms of Nielsen-integrals, [68], which can be continued analytically as well, [88, 89, 114].

The Nielsen-integrals  $S_{n,p}(z)$  are defined by

$$S_{n,p}(z) = \frac{(-1)^{n+p-1}}{(n-1)!p!} \int_0^1 \frac{dx}{x} \log^{n-1}(x) \log^p(1-zx). \quad (241)$$

They fulfill the relation

$$\frac{dS_{n,p}(x)}{d \log(x)} = S_{n-1,p}(x). \quad (242)$$

If  $p = 1$ , one obtains the polylogarithms

$$\text{Li}_n(x) = S_{n-1,1}(x), \quad (243)$$



where

$$\text{Li}_0(x) = \frac{x}{1-x} . \quad (244)$$

The harmonic sums up to depth  $d = 4$  can then be expressed in terms of Mellin-transforms of logarithms, dilogarithms, trilogarithms, the Nielsen integral  $S_{1,2}$  and polynomials in  $z$ -space. These and further integral representations can be found in Refs. [70, 88, 115] and some examples are given in Appendix K.

### 7.3.1 Summation Techniques

All finite and infinite sums we had to calculate are given in Appendix G. Few of these sums can be calculated using general theorems as Gauss' theorem, (I.3), Dixon's theorem, (I.12), or summation tables in the literature, cf. [71, 115–117]. The remaining sums had to be newly calculated by us, using different techniques.

#### Difference Equations

Difference equations are the discrete equivalent of differential equations, cf. [118]. Only equations of simplest type occurred. Let  $T(N)$  be a sum which depends on an integer variable  $N$ . One considers the sum or difference

$$D_{\pm}(j) := T(j) \pm T(j-1) . \quad (245)$$

In many cases (245) is easier to calculate than  $T(N)$ . The original sum can be recovered via

$$T(N) = T(0) + \sum_{j=1}^N D_-(j) , \quad (246)$$

or

$$T(N) = (-1)^N \left( T(0) + \sum_{j=1}^N (-1)^j D_+(j) \right) , \quad (247)$$

depending on which form of (245) was used. This technique was applied to almost all sums involving harmonic sums only, cf. Appendix (G.1), and for some other sums as (G.144). As an example we consider the sum (G.10)

$$T(N) := \sum_{i=1}^{\infty} \frac{S_1(i+N)}{i^2} . \quad (248)$$

One obtains

$$\begin{aligned} D_-(j) &= \sum_{i=1}^{\infty} \frac{S_1(i+j) - S_1(i+j-1)}{i^2} = \sum_{i=1}^{\infty} \left( \frac{1}{ji^2} - \frac{1}{ij^2} + \frac{1}{(i+j)j^2} \right) \\ &= \sum_{i=1}^{\infty} \left( \frac{\zeta_2}{j} - \frac{\sigma_1}{j^2} + \frac{\sigma_1 - S_1(j)}{j^2} \right) = \sum_{i=1}^{\infty} \left( \frac{\zeta_2}{j} - \frac{S_1(j)}{j^2} \right) , \end{aligned} \quad (249)$$

$$T(0) = \sum_{i=1}^{\infty} \frac{S_1(i)}{i^2} = \sigma_{2,1} = 2\zeta_3 . \quad (250)$$

In (250) we made use of one of the various relations connecting  $\sigma$ - and  $\zeta$ -values, [116]. The sum over (249) is then given by the definition of harmonic sums, yielding

$$\sum_{i=1}^{\infty} \frac{S_1(i+N)}{i^2} = 2\zeta_3 + \zeta_2 S_1(N) - S_{2,1}(N) . \quad (251)$$

A somewhat more general example of this type of difference equations involving Beta-functions is given in Appendix (G.9).

### Derivatives

Harmonic sums containing the index which is not summed over can be obtained by differentiating with respect to that index. Assuming that differentiation and summation can be exchanged, one is left with a sum of less complexity. Using Eqs. (237-240) one obtains

$$\frac{d}{dN} B(N, i) = B(N, i) \left( \psi(N) - \psi(N+i) \right) = B(N, i) \left( S_1(N-1) - S_1(N+i-1) \right) . \quad (252)$$

We consider the following examples

$$\begin{aligned} \sum_{i=1}^{\infty} \frac{S_2(N+i)}{i^2} &= \sum_{i=1}^{\infty} \frac{-\psi^{(1)}(N+i+1) + \zeta_2}{i^2} = -\frac{d}{dN} \sum_{i=1}^{\infty} \frac{S_1(N+i)}{i^2} + \zeta_2^2 \\ &= -S_{2,2}(N) - 2S_{3,1}(N) + 2\zeta_2 S_2(N) + \frac{7}{10} \zeta_2^2 , \\ \sum_{i=1}^{\infty} B(N, i) S_1(N+i-1) &= -\frac{d}{dN} \sum_{i=1}^{\infty} B(N, i) + S_1(N) \sum_{i=1}^{\infty} B(N, i) \\ &= -\frac{d}{dN} \frac{1}{N-1} + \frac{S_1(N)}{N-1} \\ &= \frac{1}{(N-1)^2} + \frac{S_1(N)}{N-1} . \end{aligned} \quad (253)$$

Here we made used of relations (G.10) and (G.98) to obtain the sums (G.23) and (G.69).

### Integral representations

Using the well-known integral representation of the Euler-Beta-function, see Appendix H, and integral representations of harmonic sums as given in [70, 115], one can rewrite sums as integrals:

$$\begin{aligned} \sum_{i=1}^{\infty} \frac{B(N, i)}{i} &= \int_0^1 x^{N-1} \sum_{i=1}^{\infty} \frac{(1-x)^{i-1}}{i} = -\int_0^1 x^{N-1} \frac{\ln(x)}{1-x} \\ &= -\int_0^1 x^{N-1} \frac{\ln(x)}{1-x} = \frac{d}{dN} \int_0^1 \frac{1-x^{N-1}}{1-x} \\ &= \frac{d}{dN} S_1(N-1) = \zeta_2 - S_2(N-1) . \end{aligned} \quad (254)$$

In many cases the integrals emerging can be integrated in a similar way as above. Otherwise, we used available integral tables, cf. [70, 115–117]. Some integrals had to be done newly, especially

those relating to double sums. In these cases, the following two methods were useful. We observe that for  $A \geq B$ ,  $A \geq N$

$$\frac{\Gamma(A)}{\Gamma(B)} = x^{1-B} \frac{d^{A-B}}{dx^{A-B}} x^{A-1}, \quad (255)$$

$$\frac{d^A}{dx^A} x^N = \frac{\Gamma(N+1)}{\Gamma(N-A+1)} x^{N-A} \quad (256)$$

holds. Thus one can rewrite fractions of  $\Gamma$ -functions in terms of a differential operator under the integral. This is especially useful if the differential operator does not depend on the summation index, allowing to interchange these operations. After the summation, the differential operator can either be rewritten as a sum via

$$\frac{d^N}{dx^N} \left[ f(x)g(x) \right] = \sum_{i=0}^N \binom{N}{i} \left[ \frac{d^i}{dx^i} f(x) \right] \left[ \frac{d^{N-i}}{dx^{N-i}} g(x) \right], \quad (257)$$

or shifted under the integral to act on a different function by repeated partial integration

$$\begin{aligned} \int_a^b f(x) \left\{ \frac{d^N}{dx^N} g(x) \right\} &= \sum_{i=1}^N (-1)^i \left[ \left\{ \frac{d^{i-1}}{dx^{i-1}} f(x) \right\} \left\{ \frac{d^{N-i}}{dx^{N-i}} g(x) \right\} \right]_a^b \\ &+ (-1)^N \int_a^b g(x) \left\{ \frac{d^N}{dx^N} f(x) \right\}. \end{aligned} \quad (258)$$

In the cases we encountered, the sum in (258) always vanished, leaving only one integral.

## 7.4 Five-Propagator Integrals

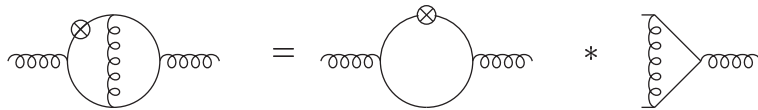
In this section, the calculation of the scalar 5-propagator integrals belonging to diagrams  $e, f, h, l, m, n$  and  $o$ , see Figure 6, is described. Here, the difference to the calculation in Ref. [55] is most apparent, since we did not use integration-by-parts. We performed an independent numerical check of our results using Mellin-Barnes integrals. Their use became a widespread technique for calculating Feynman diagrams for a series of Mellin moments  $N$  throughout the last years [119, 120]. In particular double and triple box-diagrams were calculated in this way. In Ref. [121], it was possible to expand the scalar two-loop two-point function in all orders in the dimensional regularization parameter  $\varepsilon$ , using additionally the gluing operation of Feynman diagrams, defined by Kreimer [122]. The analytic evaluation as used for the calculation of the OMEs is then described in section 7.4.2, where we again make use of a representation in terms of generalized hypergeometric series. We adopt the notation that  $I_A$  denotes the scalar integral belonging to diagram  $A$  and do not consider symmetry factors for the moment. Exponents of propagators are denoted by  $\nu_1, \nu_2, \dots$ . For their labeling see Figure 12.

### 7.4.1 Mellin-Barnes Representation

We apply the technique of the gluing operation with subsequent Mellin-Barnes transformation to a more complex problem than in Ref. [122], namely to the calculation of massive 5-propagator 2-loop Feynman diagrams with operator insertions on a line or at a vertex. Graphically this operation reads as follows:

Table 1: The first four Mellin moments for graphs  $e, f, h, l, m, n, o$  using M. Czakon's MB package [123]. All  $\nu_i = 1$  except for  $e, 2$ :  $\nu_1 = 2$ .

$N$	2	3	4	5
$I_{e,1}$	+0.49999	+0.31018	+0.21527	+0.16007
$I_{e,2}$	-0.09028	-0.04398	-0.02519	-0.01596
$I_l$	+0.49999 $\varepsilon^{-1}$ +0.53861	+0.30544 $\varepsilon^{-1}$ +0.33609	+0.20832 $\varepsilon^{-1}$ +0.23483	+0.15222 $\varepsilon^{-1}$ +0.17573
$I_m$	$O(10^{-17}) \varepsilon^{-1}$ $O(10^{-6})$	+0.08332 $2\varepsilon^{-1}$ +0.06893	$O(10^{-16}) \varepsilon^{-1}$ $O(10^{-6})$	+0.02222 $\varepsilon^{-1}$ +0.016527
$I_h$	+0.99999	0.	+0.43055	$O(10^{-6})$
$I_o$	+0.99999 $2\varepsilon^{-1}$ +1.07722	$O(10^{-17}) \varepsilon^{-1}$ + $O(10^{-12})$	+0.41666 $\varepsilon^{-1}$ +0.46967	$O(10^{-17}) \varepsilon^{-1}$ + $O(10^{-9})$
$I_f$	+0.99999	+0.99999	+0.90277	+0.80555
$I_n$	+0.99999 $\varepsilon^{-1}$ +1.07723	+0.49999 $\varepsilon^{-1}$ +0.53862	+0.41666 $\varepsilon^{-1}$ +0.44189	+0.27776 $\varepsilon^{-1}$ +0.30616



and similar for the remaining 6 diagrams. Details of the calculation can be found in Ref. [108]. Compared to Ref. [121, 122], the two-point function now carries an operator insertion, while the three-point function is unaltered. In order to take care of terms  $(\Delta q)^A$  stemming from the operator insertion, the steps as given in Appendix F, Eqs. (F.9-F.11) are performed. Depending on the insertion one has  $A = N - 1$ ,  $N - 2$ . Thus we obtain for graph  $e$ :

$$\begin{aligned}
I_{e,\nu_1} &= \frac{(\Delta p)^{N-1}}{(4\pi)^D (m^2)^{\nu_{12345}-D}} \frac{1}{(2\pi i)^2} \frac{(-1)^{\nu_{12345}+1}}{\Gamma(\nu_2)\Gamma(\nu_3)\Gamma(\nu_5)\Gamma(D-\nu_{235})} \int_{\gamma_1-i\infty}^{\gamma_1+i\infty} d\sigma \int_{\gamma_2-i\infty}^{\gamma_2+i\infty} d\tau \Gamma(-\sigma)\Gamma(\nu_3+\sigma) \\
&\times \frac{\Gamma(-\sigma+\nu_4+N-1)}{\Gamma(-\sigma+\nu_4)} \Gamma(-\tau)\Gamma(\nu_2+\tau) \frac{\Gamma(\sigma+\tau+\nu_{235}-D/2)\Gamma(\sigma+\tau+\nu_5)}{\Gamma(\sigma+\tau+\nu_{23})} \\
&\times \Gamma(-\sigma-\tau+D-\nu_{23}-2\nu_5) \frac{\Gamma(-\sigma-\tau+\nu_{14}-D/2)}{\Gamma(-\sigma-\tau+\nu_{14}+N-1)}, \tag{259}
\end{aligned}$$

where we use  $\nu_{14} \equiv \nu_1 + \nu_4$ , etc. Note that the overall constant factor

$$\frac{(\Delta p)^A}{(4\pi)^D (m^2)^{\nu_{12345}-D}} \tag{260}$$

is omitted in Tables 1-3. Analogously, we built the Mellin-Barnes integrals for the remaining six graphs and used the `mathematica` package `MB` by M. Czakon, [123], to numerically produce the

Table 2: The first four Mellin moments for graphs  $e, f, h, l, m, n, o$ .  $\nu_i = 1$ ;  $e, 2$ :  $\nu_1 = 2$ .

N	2	3	4	5
$I_{e,1}$	$\frac{1}{2}$	$\frac{67}{216}$	$\frac{31}{144}$	$\frac{2161}{13500}$
$I_{e,2}$	$-\frac{13}{144}$	$-\frac{19}{432}$	$-\frac{17}{675}$	$-\frac{431}{27000}$
$I_l$	$\frac{1}{2\varepsilon} + \frac{1}{4} + \frac{1}{2}\gamma_E$	$\frac{11}{36\varepsilon} + \frac{23}{144} + \frac{11}{36}\gamma_E$	$\frac{5}{24\varepsilon} + \frac{11}{96} + \frac{5}{24}\gamma_E$	$\frac{137}{900\varepsilon} + \frac{949}{10800} + \frac{137}{900}\gamma_E$
$I_m$	0	$\frac{1}{12\varepsilon} + \frac{1}{48} + \frac{1}{12}\gamma_E$	0	$\frac{1}{45\varepsilon} + \frac{1}{270} + \frac{1}{45}\gamma_E$
$I_h$	1	0	$\frac{31}{72}$	0
$I_o$	$\frac{1}{\varepsilon} + \frac{1}{2} + \gamma_E$	0	$\frac{5}{12\varepsilon} + \frac{11}{48} + \frac{5}{12}\gamma_E$	0
$I_f$	1	1	$\frac{65}{72}$	$\frac{29}{36}$
$I_n$	$\frac{1}{\varepsilon} + \frac{1}{2} + \gamma_E$	$\frac{1}{2\varepsilon} + \frac{1}{4} + \frac{\gamma_E}{2}$	$\frac{5}{12\varepsilon} + \frac{29}{144} + \frac{5}{12}\gamma_E$	$\frac{5}{18\varepsilon} + \frac{7}{48} + \frac{5}{18}\gamma_E$

results for the first few Mellin moments, given in Table 1. They serve as a check for our analytic result. One notices, that the integrals  $I_{h,o}$  are given by the integrals  $I_{e,l}$ , cf. Table 3. This is due to the fact that the operator insertion is located at the outer vertex with a gluon external line, Eq. (224). Obtaining an analytical result starting from double Mellin-Barnes integrals as in (259) turned out to be non-trivial. By applying the residue theorem we obtained double sums that contain the symbolic parameter  $N$ :

$$\begin{aligned}
I_{e,1} \Rightarrow & \frac{\Gamma(N+1)}{\Gamma(1+\varepsilon)} \sum_{k=0}^{\infty} \sum_{j=0}^{\infty} \frac{\Gamma(k+1)}{\Gamma(k+2+N)} \\
& \times \left[ \Gamma(-\varepsilon/2)\Gamma(1+\varepsilon/2) \frac{\Gamma(j+1+\varepsilon)\Gamma(j+1-\varepsilon/2)}{\Gamma(j+1+\varepsilon/2)\Gamma(j+2+N)} \frac{\Gamma(k+j+1+N)}{\Gamma(k+j+2)} \right. \\
& \left. + \Gamma(\varepsilon/2)\Gamma(1-\varepsilon/2) \frac{\Gamma(j+1-\varepsilon)\Gamma(j+1+\varepsilon/2)}{\Gamma(j+1)\Gamma(j+2-\varepsilon/2+N)} \frac{\Gamma(k+j+1-\varepsilon/2+N)}{\Gamma(k+j+2-\varepsilon/2)} \right]. \quad (261)
\end{aligned}$$

Sums like these cannot be done via `nestedsums`, [124] or `Xsummer`, [125], except for the most simple cases, fixing  $N$ . For other more complicated cases, however, we had to use special transformations. As a computer algebra system we used `MAPLE`. For the first four Mellin moments the results are shown in Table 2 and agree with the numeric results obtained by the use of `MB`. Finally, the complete analytic result for general values of  $N$  could be obtained for diagrams  $e, h, l, m, o$  by calculating double infinite sums of the type (261). To obtain this, we had to use extensively algebraic and analytic relations to convert the sums obtained in evaluating the Mellin-Barnes integrals into expressions containing (nested) harmonic sums and related objects in intermediary steps. The final results depend on harmonic sums only and are summarized in Table 3. For diagrams  $f, n$  this method to obtain analytic results for general values of  $N$

Table 3: The analytic results for general values of  $N$ , with all  $\nu_i = 1$ ,  $e, 2$ :  $\nu_1 = 2$ .

$I_{e,1}$	$\frac{S_1^2(N) + 3S_2(N)}{2N(N+1)}$
$I_{e,2}$	$\frac{S_1(N) - S_2(N) - S_{1,1}(N)}{N(N+1)(N+2)} - \frac{1}{(N+1)^2(N+2)}$
$I_l$	$\frac{2S_1(N)}{N(N+1)} \left( \frac{1}{\varepsilon} + \gamma_E \right) + 2 \frac{S_1(N)}{(N)(N+1)^2} + \frac{S_1^2(N) - S_2(N)}{2N(N+1)}$
$I_m$	$2 \frac{[1 - (-1)^N]}{N(N+1)^2} \left( \frac{1}{\varepsilon} + \frac{1}{(N+1)} + \gamma_E \right)$
$I_h$	$[1 + (-1)^N] \times I_{e,1}$
$I_o$	$[1 + (-1)^N] \times I_l$
$I_f$	$\frac{4}{N} \left[ S_2(N) - \frac{S_1(N)}{N} \right]$
$I_n$	$2 \left[ \frac{(-1)^N - 1}{N^2(N+1)} + \frac{2S_1(N)}{N(N+1)} \right] \left( \frac{1}{\varepsilon} + \gamma_E \right)$ $+ \left[ 2 \frac{(-1)^N - 1}{N^2(N+1)^2} + \frac{S_1^2(N) - S_2(N) + 2S_{-2}(N)}{N(N+1)} + \frac{2(3N+1)S_1(N)}{N^2(N+1)^2} \right]$

failed. They could only be evaluated analytically using a representation in terms of generalized hypergeometric series, as will be discussed in section 7.4.2.

### 7.4.2 Hypergeometric Representation

The 5-propagator integrals of diagrams  $e, h, l, m$  and  $o$  could be obtained in form of a single generalized hypergeometric series  ${}_3F_2$ . The calculation is straightforward and is given in Appendix J, in which as an example the complete calculation of the scalar integral corresponding to diagram  $e$  is presented, see Eqs. (J.12-J.22). The method is applied in a very similar way to the evaluation of the 5-propagator scalar integrals of diagrams  $h, l, m, o$  and could be well implemented into a FORM procedure, up to the point at which the  $\varepsilon$ -expansion of the result is performed. With minor changes, these procedures also allow for the calculation of integrals containing terms like

$$(\Delta k)(\Delta q)^{N-1}, (\Delta k)^2(\Delta q)^{N-1}, \quad (262)$$

which emerge in the calculation of the complete diagram due to its Lorentz-structure. Although not necessary in the present calculation, higher fixed-integer propagator powers can be treated by adjusting the procedures. The result always consists of single generalized hypergeometric series  ${}_3F_2$  and Beta-functions. Our results for the scalar integrals are given in Table 3 and are the same as the ones obtained by summing the double infinite sums as in Eq. (261).

In the case of the scalar 5–propagator integrals corresponding to diagrams  $n, f$ , we used generalized hypergeometric functions only. The momentum integrals can be performed using standard techniques, cf. Appendix F, giving the result in form of a 4–fold parameter integral on the unit cube. The structure of the integrand is such that none of the remaining parameters can be integrated trivially. Therefore one has to resort to variable transformations, leaving the integration boundaries intact. The transformations we used were given in Ref. [75]:

- To define the product  $xy$  as the new integration variable, one shifts

$$\begin{aligned} x' &:= xy, & y' &:= \frac{x(1-y)}{1-xy}, \\ x &= x' + y' - x'y', & y &= \frac{x'}{y' + x' - x'y'}, \\ \frac{\partial(x, y)}{\partial(x', y')} &= \frac{1-x'}{x' + y' - x'y'}, \end{aligned} \quad (263)$$

yielding

$$\int_0^1 \int_0^1 dx dy f(x, y) (xy)^N = \int_0^1 \int_0^1 dx' dy' \frac{(1-x')(x')^N}{x' + y' - x'y'} f\left(y' + x' - x'y', \frac{x'}{x' + y' - x'y'}\right). \quad (264)$$

- Terms of the form  $(x - y)^N$  can be combined by

$$\begin{array}{ll} \underline{x > y} : & \underline{x < y} : \\ x' := x - y, & x' := y - x, \\ y' := \frac{y}{1 - x + y}, & y' := \frac{1 - y}{1 + x - y}, \\ x = x' + y' - x'y', & x = (1 - x')(1 - y'), \\ y = (1 - x')y', & y = 1 - (1 - x')y', \\ \frac{\partial(x, y)}{\partial(x', y')} = 1 - x'. & \frac{\partial(x, y)}{\partial(x', y')} = 1 - x'. \end{array} \quad (265)$$

Thus, one obtains

$$\begin{aligned} \int_0^1 \int_0^1 dx dy f(x, y) (x - y)^N &= \int_0^1 \int_0^1 dx' dy' x'^N (1 - x') \left( f(y' + x' - x'y', (1 - x')y') \right. \\ &\quad \left. + (-1)^N f((1 - y')(1 - x'), 1 - (1 - x')y') \right). \end{aligned} \quad (266)$$

Eq. (265) is especially useful if the factor  $(x - y)$  occurs in the denominator. In this case, however, one has to take special care of possible divergences. Both of these transformations had to be applied to render the integrals  $I_f$  and  $I_n$  into the form of generalized hypergeometric series.

Consider  $I_f$  as an example. After the momentum integration, it becomes

$$\begin{aligned}
I_f &= \sum_{i=0}^{N-2} \iint \frac{dq dk}{(2\pi)^D(2\pi)^D} \frac{(\Delta q)^i (\Delta k)^{N-2-i}}{(q^2 - m^2)(q-p)^2 - m^2)(k^2 - m^2)(k-p)^2 - m^2)^2 (k-q)^2} \quad (267) \\
&= \frac{(\Delta p)^{N-2} \Gamma(1-\varepsilon)}{(4\pi)^{4+\varepsilon} (m^2)^{1-\varepsilon}} \iiint \int dudzdydx \frac{(1-u)^{-\varepsilon/2} z^{-\varepsilon/2} (1-z)^{\varepsilon/2-1}}{(1-u+uz)^{1-\varepsilon} (x-y)} \\
&\quad \left[ \left(zyu + x(1-zu)\right)^{N-1} - \left((1-u)x + uy\right)^{N-1} \right]. \quad (268)
\end{aligned}$$

Here and below, the Feynman-parameter integrals are carried out over the respective unit-cube. Applying now transformation (263) by defining  $u' := uz$  and shifting  $z' \rightarrow 1-z$ ,  $u' \rightarrow 1-u$  afterwards, yields

$$\begin{aligned}
I_f &= \frac{(\Delta p)^{N-2} \Gamma(1-\varepsilon)}{(4\pi)^{4+\varepsilon} (m^2)^{1-\varepsilon}} \iiint \int dudzdydx \frac{(1-u)^{-\varepsilon/2} z^{-\varepsilon/2} (1-z)^{\varepsilon/2-1}}{(1-u+uz)^{1-\varepsilon} (x-y)} \\
&\quad \left[ \left((1-u)y + ux\right)^{N-1} - \left((1-u)x + uy\right)^{N-1} \right]. \quad (269)
\end{aligned}$$

Now transformation (265) is used by setting  $x' := \pm(x-y)$ . Thus

$$\begin{aligned}
I_f &= \frac{(\Delta p)^{N-2} \Gamma(1-\varepsilon)}{(4\pi)^{4+\varepsilon} (m^2)^{1-\varepsilon}} \iiint \int dudzdy'dx' \frac{(1-u)^{-\varepsilon/2} z^{-\varepsilon/2} (1-z)^{\varepsilon/2-1}}{(1-u+uz)^{1-\varepsilon}} \frac{1-x'}{x'} \\
&\quad \left[ \left(y'(1-x') + ux'\right)^{N-1} - \left(y'(1-x') + x'(1-u)\right)^{N-1} - \left(1-ux' - y'(1-x')\right)^{N-1} \right. \\
&\quad \left. + \left(1-x' + ux' - y'(1-x')\right)^{N-1} \right]. \quad (270)
\end{aligned}$$

This form allows to perform the  $y'$  integration. Further we set  $x = x'$ ,  $u \rightarrow 1-u$ , giving

$$\begin{aligned}
&= \frac{2(\Delta p)^{N-2} \Gamma(1-\varepsilon)}{(4\pi)^{4+\varepsilon} (m^2)^{1-\varepsilon} N} \iiint \int dudzdx \frac{u^{-\varepsilon/2} z^{-\varepsilon/2} (1-z)^{\varepsilon/2-1}}{(u+z-uz)^{1-\varepsilon} x} \left[ x^N u^N - x^N (1-u)^N \right. \\
&\quad \left. + (1-ux)^N - (1-x(1-u))^N \right] \\
&= \frac{2(\Delta p)^{N-2} \Gamma(1-\varepsilon)}{(4\pi)^{4+\varepsilon} (m^2)^{1-\varepsilon} N} \left[ \frac{1}{N} \iint dudz \frac{u^{-\varepsilon/2} z^{-\varepsilon/2} (1-z)^{\varepsilon/2-1}}{(u+z-uz)^{1-\varepsilon}} \left[ u^N - (1-u)^N \right] \right. \\
&\quad \left. + \sum_{i=1}^N \binom{N}{i} \frac{(-1)^i}{i} \frac{u^{-\varepsilon/2} z^{-\varepsilon/2} (1-z)^{\varepsilon/2-1}}{(u+z-uz)^{1-\varepsilon}} \left[ u^i - (1-u)^i \right] \right] \\
&= \frac{2(\Delta p)^{N-2} \Gamma(1-\varepsilon)}{(4\pi)^{4+\varepsilon} (m^2)^{1-\varepsilon} N} \sum_{i=1}^N \left\{ \binom{N}{i} (-1)^i + \delta_{i,N} \right\} \frac{1}{i} \iint dudz \frac{u^{-\varepsilon/2} z^{-\varepsilon/2} (1-z)^{\varepsilon/2-1}}{(u+z-uz)^{1-\varepsilon}} \\
&\quad \left[ u^i - (1-u)^i \right]. \quad (271)
\end{aligned}$$



The latter expression can now be rewritten in terms of a generalized hypergeometric series by applying Eq. (J.8):

$$\begin{aligned}
&= \frac{S_\varepsilon^2(\Delta p)^{N-2}}{(4\pi)^4(m^2)^{1-\varepsilon}} \exp\left\{\sum_{l=2}^{\infty} \frac{\zeta_l}{l} \varepsilon^l\right\} \frac{2\pi}{N \sin(\frac{\pi}{2}\varepsilon)} \sum_{j=1}^N \left\{ \binom{N}{j} (-1)^j + \delta_{j,N} \right\} \\
&\quad \times \left\{ \frac{\Gamma(j)\Gamma(j+1-\frac{\varepsilon}{2})}{\Gamma(j+2-\varepsilon)\Gamma(j+1+\frac{\varepsilon}{2})} - \frac{B(1-\frac{\varepsilon}{2}, 1+j)}{j} {}_3F_2\left[\begin{matrix} 1-\varepsilon, \frac{\varepsilon}{2}, j+1 \\ 1, j+2-\frac{\varepsilon}{2} \end{matrix}; 1\right] \right\}. \quad (272)
\end{aligned}$$

Note that although (272) is a double sum, the summation parameters and  $N$  are not nested. This expression can be expanded in  $\varepsilon$  and calculated using the sums given in Appendix G. The final result one obtains (omitting  $(\Delta p)^{N-2}/(4\pi)^D/(m^2)^{1-\varepsilon}$ ) is given in Table 3 and agrees with the numerical checks. The same kind of manipulations we performed to obtain a result for the 5-propagator integral of diagram  $n$ . Although a little more work is involved, it could be treated in the same manner as diagram  $f$ . One of the most important things is to write all sums which have to be introduced in such a way that there is **no nesting** of summation indexes with  $N$ . The result is given in Table 3 and again agrees with the numerical check. Note that in case of only 3 massive propagators, analytic results for fixed values of  $N$  can be obtained quite easily by choosing the momentum flow in such a way that one momentum follows the massive propagators. Thus no denominator structure emerges in the parameter integral. Let us consider as an example integral  $I_n$ :

$$\begin{aligned}
I_n &= \sum_{j=0}^{N-2} \int \frac{dq}{(2\pi)^D} \int \frac{dk}{(2\pi)^D} \frac{(\Delta q)^j (\Delta q - \Delta k)^{N-2-j}}{(q^2 - m^2)((q-p)^2 - m^2)((k-q)^2 - m^2)(k-p)^2 k^2} \\
&= \frac{\Gamma(1-\varepsilon)(\Delta p)^{N-2}}{(4\pi)^{4+\varepsilon}(m^2)^{1-\varepsilon}} \iiint\int dw dy dv dz \sum_{i=0}^{N-2} (1-w)w^{\varepsilon/2-1}(1-y)^{1-\varepsilon/2}y^{-\varepsilon/2}(1-y)^j \\
&\quad (1-w)^j(z-v)^j(y((1-w)v+wz)+(1-y)z)^{N-j-2}. \quad (273)
\end{aligned}$$

Calculating (273) for arbitrary values of  $N$  analytically involves some work. However, by plugging in fixed values of  $N$ , (273) decomposes into a finite sum of Beta-functions, which can even be handled by MAPLE.

## 7.5 Reduced Integrals

In this section we describe the calculation of the scalar integrals corresponding to diagrams  $n$  and  $f$  in which one propagator dropped out due to numerator factors. Since the operator insertion is located at an inner vertex, we could not evaluate these integrals in an automatic way. Integral transformations as (263, 265) had to be applied in various cases. Thus the results could be expressed in terms of up to three-fold sums, allowing to expand in  $\varepsilon$ . The summations were performed using the sums contained in Appendix G. The notation is as follows:

$$I_{A,i} \quad (274)$$

denotes the scalar integral belonging to diagram  $A$  ( $= f, n$ ) in which the  $i$ th propagator is not present, see Figure 12. For the Feynman rules of the operator insertion see Figure 14. By writing down the corresponding momentum integrals,

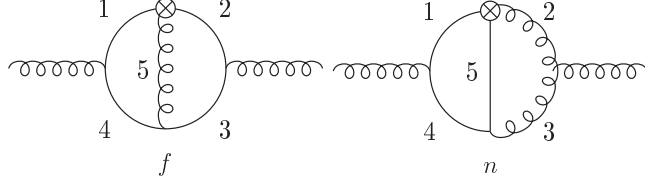


Figure 12: Labeling of the propagators of diagrams  $f$  and  $n$

one immediately notices that

$$\begin{aligned} I_{f,1} &= I_{f,2} , \\ I_{f,3} &= I_{f,4} = I_{n,3} , \end{aligned} \quad (275)$$

and one is thus left with only seven integrals. Further,  $I_{f,5}$ ,  $I_{n,4}$  and  $I_{n,5}$  turn out to be trivial, hence only four complicated integrals had to be calculated. The result of each integral is given in Table 4, dropping the overall factor

$$\frac{S_\varepsilon^2(\Delta p)^{N-2}}{(4\pi)^4(m^2)^{-\varepsilon}} . \quad (276)$$

In order to obtain an analytic result for fixed values of  $N$  as a check, we proceeded as in section 7.4.2, Eq. (273). By choosing the momentum flow in such a way that one momentum follows the massive propagator, the integral turns into a finite sum of Beta-functions. Let us consider as the most complex example  $I_{n,2}$ . The integral becomes

$$\begin{aligned} I_{n,2} &= \frac{(\Delta p)^{N-2}\Gamma(1-\varepsilon)}{(4\pi)^{4+\varepsilon}(m^2)^{-\varepsilon}} \frac{1}{\varepsilon} \sum_{j=0}^{N-2} (-1)^j \iiint dv dy dz (1-v)^{\varepsilon/2} v^j y^{-1-\varepsilon/2} (1-y)^{-\varepsilon/2+j} \\ &\quad \times z^j (1-z+yz)^{N-j-2} , \end{aligned} \quad (277)$$

which can be evaluated for arbitrary fixed  $N$  using MAPLE.

In order to derive the analytic result, as given in Table 4, a lot more work was involved. Rewriting  $I_{n,2}$  as a sum yields

$$\begin{aligned} I_{n,2} &= \frac{(\Delta p)^{N-2}\Gamma(1-\varepsilon)}{(4\pi)^{4+\varepsilon}(m^2)^{-\varepsilon}} \frac{1}{\varepsilon} \left[ \sum_{l=0}^{N-1} \binom{N-1}{l} (-1)^l \sum_{k=0}^{\infty} \frac{B(1-\varepsilon/2, k+1+\varepsilon/2) B(l+2+k, -\varepsilon/2)}{l+k+1} \right. \\ &\quad \times {}_3F_2 \left[ \begin{matrix} -\varepsilon, k+1+\varepsilon/2, l+2+k \\ k+2, l+k+2-\varepsilon/2 \end{matrix} ; 1 \right] \\ &\quad \left. + (-1)^N B(-\varepsilon/2, N-\varepsilon/2) \sum_{k=0}^{\infty} \frac{B(k+1+\varepsilon/2, N)}{N+k} \right] . \end{aligned} \quad (278)$$

The single infinite sum in (278) is given in Eq. (G.144) and was calculated as described in Appendix (G.9). We could not avoid introducing a three-fold nested sum in setting up (278). However, the Mellin-parameter  $N$  does not appear in the inner two sums, simplifying the calculation. This was done using integral representations, where double sums of the type given in

Eqs. (G.44, G.97, G.99–G.101) had to be calculated. The remaining integrals  $I_{f,1}$ ,  $I_{n,(1,3)}$  could be rewritten as double or single sums, being less complex than (278). After these calculations, diagram  $i$  could be obtained immediately. One of the operator sums of the corresponding Feynman rule could be performed right away, since the insertion is located at an outer vertex. Hence there is only one operator sum left and it turned out that all integrals needed for diagram  $i$  are given in Table 4.

Table 4: The analytic results for the reduced scalar integrals of graphs  $f$  and  $n$

$I_{f,1}$	$\frac{1}{\varepsilon^2}(-2S_2(N-1)) + \frac{1}{\varepsilon}(2S_{2,1}(N-1) - S_3(N-1)) + S_{2,1,1}(N-1) - S_4(N-1)$ $-\frac{1}{2}S_2^2(N-1) - \frac{1}{2}S_2(N-1)\zeta_2$
$I_{f,2}$	$= I_{f,1}$
$I_{f,3}$	$= I_{n,3}$
$I_{f,4}$	$= I_{n,3}$
$I_{f,5}$	$\frac{1}{\varepsilon^2}\left\{-\frac{8}{N}S_1(N-1)\right\} - \frac{2\zeta_2}{N}S_1(N-1)$
$I_{n,1}$	$\frac{1}{N}\left\{\frac{1}{\varepsilon^2}(4S_1(N-1)) + \frac{1}{\varepsilon}\left[-S_2(N-1) + S_1^2(N-1) + \frac{4}{N}S_1(N-1)\right] + 2S_{2,1}(N-1) - \frac{2}{3}S_3(N-1)\right.$ $\left. + \frac{1}{2}S_1(N-1)S_2(N-1) + \frac{1}{6}S_1^3(N-1) + \zeta_2S_1(N-1) - \frac{S_2(N-1)}{N} + \frac{S_1^2(N-1)}{N} + \frac{4S_1(N-1)}{N^2}\right\}$
$I_{n,2}$	$\frac{1}{\varepsilon^2}\left[4S_{-2}(N-1) + 2S_2(N-1)\right] + \frac{1}{\varepsilon}\left[-4S_{-2,1}(N-1) - 2S_{2,1}(N-1) + 2S_{-3}(N-1) + 3S_3(N-1)\right.$ $\left. + 4S_{-2}(N-1)S_1(N-1) + 2S_2(N-1)S_1(N-1)\right] + S_{1,1,-2}(N-1) + S_{-2,1,1}(N-1) - S_{1,-2,1}(N-1)$ $+ 2S_{1,1,2}(N-1) + S_{1,3}(N-1) - 2S_{-2,1}(N-1)S_1(N-1) + S_1(N-1)S_{-3}(N-1)$ $+ \frac{3}{2}S_{-2}(N-1)S_2(N-1) + \frac{3}{2}S_{-2}(N-1)S_1^2(N-1) - \frac{1}{2}S_2^2(N-1) + \left[\frac{1}{2}S_2(N-1) + S_{-2}(N-1)\right]\zeta_2$
$I_{n,3}$	$\frac{1}{N-1}\left\{\frac{1}{\varepsilon^2}(-2S_1(N-1)) + \frac{1}{\varepsilon}\left[\frac{3}{2}S_2(N-1) - \frac{1}{2}S_1^2(N-1)\right] - S_{2,1}(N-1) - \frac{1}{4}S_2(N-1)S_1(N-1)\right.$ $\left. + \frac{5}{6}S_3(N-1) - \frac{1}{12}S_1^3(N-1) - \frac{\zeta_2}{2}S_1(N-1)\right\}$
$I_{n,4}$	$\frac{1+(-1)^N}{N-1}\left\{\frac{2}{N\varepsilon^2} + \frac{2}{N^2\varepsilon} + \frac{S_2(N-1)}{N} + \frac{1}{2N}\zeta_2 + \frac{2}{N^3}\right\}$
$I_{n,5}$	$= 0$

The result of integral  $I_{n,2}$  is the most complex expression we encountered in our calculation. Even several harmonic sums of weight 4 are present, which do not appear in the final result, however. One observes that by adding boundary terms to complete the operator sum, cf. Eq. (225),  $I_{n,2}$  appears three times in the complete diagram  $n$  with differing upper summation boundaries. The

coefficients thereof just add up to zero, hence the leading index of the harmonic sums drops out as in

$$S_{1,-2,1}(N) - S_{1,-2,1}(N-1) = \frac{S_{-2,1}(N)}{N}. \quad (279)$$

Thus at most sums of depth 2 and weight 3 remain.

## 7.6 The Final Results for the 2–Loop Operator Matrix Elements

Our results of the individual diagrams of Figures 6–9 are given in Appendix E. These results are found to agree with the results obtained in  $z$ -space in [55]<sup>4</sup>. The expressions in  $z$ -space in terms of Nielsen-integrals turn out to be rather long, which may be partly due to the integral basis chosen. In some cases, functions of the type  $f_1(z)/(1+z)$  could be simplified to functions  $f_2(z)$  without this denominator. Our results in Mellin space are more compact. In Table 5 we list the harmonic sums contributing to the individual diagrams to illustrate the respective complexity and the number of different functions in  $z$ -space.

Table 5: Complexity of the results in Mellin space and in  $z$ -space for each diagram

Diagram	$S_1$	$S_2$	$S_3$	$S_{-2}$	$S_{-3}$	$S_{2,1}$	$S_{-2,1}$	# $z$ -space fct.
A		+						8
B	+	+	+			+		10
C		+						4
D	+	+						5
E	+	+						9
F	+	+	+			+		24
G	+	+						6
H	+	+						7
I	+	+	+	+	+	+	+	20
J		+						7
K		+						7
L	+	+	+			+		13
M		+						7
N	+	+	+	+	+	+	+	38
O	+	+	+			+		13
P	+	+	+			+		14
S		+						7
T		+						7
PS <sub>a</sub>		+						7
PS <sub>b</sub>		+						7
NS <sub>a</sub>								5
NS <sub>b</sub>	+	+	+					5

<sup>4</sup>We thank W.L. van Neerven and J. Smith for the opportunity to compare with their results in  $z$ -space for the individual diagrams.

In counting the number of  $z$ -space functions, those with different power prefactors are considered to be equivalent since their Mellin transform shifts in the argument only. In our results, there occur only polynomials out of maximally seven harmonic sums in the individual diagrams with a depth of up to two, with rational prefactors and supplement rational functions in  $N$  and  $\zeta_2$ . Intermediary sums of depth three contributed for some of the diagrams but canceled for each diagram due to algebraic relations [70, 110]. Note that harmonic sums with an index  $\{i = -1\}$  do not even occur for individual diagrams. This is in accordance with observations made before for all known single-scale Wilson-coefficients and anomalous dimensions, [89, 106, 107, 126].

The final result for the unrenormalized OMEs  $\hat{A}_{ij}^{(2)}$  is then obtained by summing the corresponding results of the individual diagrams. In the following expressions, mass renormalization, cf. Eq. (126), has already been carried out. The two loop singlet OME at  $O(a_s^2)$  becomes

$$\begin{aligned}
\hat{A}_{Qg}^{(2)}\left(\frac{m^2}{\mu^2}, \varepsilon\right) &= S_\varepsilon^2 \left(\frac{m^2}{\mu^2}\right)^\varepsilon \left( \frac{1}{\varepsilon^2} \left\{ 8T_R C_F \frac{N^2 + N + 2}{N(N+1)(N+2)} \left[ -4S_1(N) + \frac{3N^2 + 3N + 2}{N(N+1)} \right] \right. \right. \\
&\quad \left. \left. + 32T_R C_A \frac{N^2 + N + 2}{N(N+1)(N+2)} \left[ S_1(N) - 2 \frac{N^2 + N + 1}{(N-1)N(N+1)(N+2)} \right] \right\} \right. \\
&\quad \left. + \frac{1}{\varepsilon} \left\{ 4T_R C_F \left[ 2 \frac{N^2 + N + 2}{N(N+1)(N+2)} (S_2(N) - S_1^2(N)) + 4 \frac{S_1(N)}{N^2} \right. \right. \right. \\
&\quad \left. \left. - \frac{5N^6 + 15N^5 + 36N^4 + 51N^3 + 25N^2 + 8N + 4}{N^3(1+N)^3(2+N)} \right] \right. \\
&\quad \left. + T_R C_A \left[ 8 \frac{N^2 + N + 2}{N(N+1)(N+2)} (-2\beta'(1+N) + S_2(N) + S_1^2(N) - \zeta_2) \right. \right. \\
&\quad \left. \left. - 32 \frac{2N+3}{(N+1)^2(N+2)^2} S_1(N) - 8 \frac{P_1(N)}{(N-1)N^3(N+1)^3(2+N)^3} \right] \right\} \\
&\quad \left. + a_{Qg}^{(2)}(N) \right) + S_\varepsilon \frac{8}{3\varepsilon} T_R \left( 1 + \frac{\zeta_2}{8} \varepsilon^2 \right) \sum_{i=1}^3 \left( \frac{m_i^2}{\mu^2} \right)^{\varepsilon/2} \hat{A}_{Qg}^{(1)}, \tag{280}
\end{aligned}$$

where the expansion coefficient at  $O(\varepsilon^0)$  is given by, cf. [47],

$$\begin{aligned}
a_{Qg}^{(2)}(N) &= 4C_F T_R \left\{ \frac{N^2 + N + 2}{N(N+1)(N+2)} \left[ -\frac{1}{3} S_1^3(N-1) + \frac{4}{3} S_3(N-1) \right. \right. \\
&\quad \left. \left. - S_1(N-1)S_2(N-1) - 2\zeta_2 S_1(N-1) \right] + \frac{2}{N(N+1)} S_1^2(N-1) \right. \\
&\quad \left. + \frac{N^4 + 16N^3 + 15N^2 - 8N - 4}{N^2(N+1)^2(N+2)} S_2(N-1) \right. \\
&\quad \left. + \frac{3N^4 + 2N^3 + 3N^2 - 4N - 4}{2N^2(N+1)^2(N+2)} \zeta_2 \right. \\
&\quad \left. + \frac{N^4 - N^3 - 16N^2 + 2N + 4}{N^2(N+1)^2(N+2)} S_1(N-1) + \frac{P_2(N)}{2N^4(N+1)^4(N+2)} \right\}
\end{aligned}$$

$$\begin{aligned}
& +4C_A T_R \left\{ \frac{N^2 + N + 2}{N(N+1)(N+2)} \left[ 4\mathbf{M} \left[ \frac{\text{Li}_2(x)}{1+x} \right] (N+1) + \frac{1}{3} S_1^3(N) + 3S_2(N)S_1(N) \right. \right. \\
& \quad \left. \left. + \frac{8}{3} S_3(N) + \beta''(N+1) - 4\beta'(N+1)S_1(N) - 4\beta(N+1)\zeta_2 + \zeta_3 \right] \right. \\
& \quad - \frac{N^3 + 8N^2 + 11N + 2}{N(N+1)^2(N+2)^2} S_1^2(N) - 2 \frac{N^4 - 2N^3 + 5N^2 + 2N + 2}{(N-1)N^2(N+1)^2(N+2)} \zeta_2 \\
& \quad - \frac{7N^5 + 21N^4 + 13N^3 + 21N^2 + 18N + 16}{(N-1)N^2(N+1)^2(N+2)^2} S_2(N) \\
& \quad - \frac{N^6 + 8N^5 + 23N^4 + 54N^3 + 94N^2 + 72N + 8}{N(N+1)^3(N+2)^3} S_1(N) \\
& \quad \left. - 4 \frac{(N^2 - N - 4)}{(N+1)^2(N+2)^2} \beta'(N+1) + \frac{P_3(N)}{(N-1)N^4(N+1)^4(N+2)^4} \right\}. \quad (281)
\end{aligned}$$

The unrenormalized 1-loop singlet operator matrix element, cf. section 6.2, is given by

$$\hat{A}_{Qg}^{(1)}\left(\frac{m^2}{\mu^2}, \epsilon\right) = S_\epsilon\left(\frac{m^2}{\mu^2}\right)^{\epsilon/2} \left[ -\frac{1}{\epsilon} \hat{P}_{qg}^{(0)}(z) + a_{Qg}^{(0)} + \epsilon \bar{a}_{Qg}^{(1)} \right], \quad (282)$$

where

$$a_{Qg}^{(1)} = 0, \quad (283)$$

$$\bar{a}_{Qg}^{(1)} = -\frac{\zeta_2}{8} \hat{P}_{qg}^{(0)}(z). \quad (284)$$

The polynomials in Eqs. (280, 281) read

$$P_1(N) = N^9 + 6N^8 + 15N^7 + 25N^6 + 36N^5 + 85N^4 + 128N^3 + 104N^2 + 64N + 16, \quad (285)$$

$$P_2(N) = 12N^8 + 54N^7 + 136N^6 + 218N^5 + 221N^4 + 110N^3 - 3N^2 - 24N - 4, \quad (286)$$

$$\begin{aligned}
P_3(N) &= 2N^{12} + 20N^{11} + 86N^{10} + 192N^9 + 199N^8 - N^7 - 297N^6 - 495N^5 \\
&\quad - 514N^4 - 488N^3 - 416N^2 - 176N - 32. \quad (287)
\end{aligned}$$

The sum over heavy quarks in Eq. (281) stems from the reducible diagrams  $u$ ,  $v$ , see Figure 7, and is removed during the renormalization procedure due to the specific scheme chosen, cf. section 4.3. Note that we express single harmonic sums with negative index in terms of  $\beta$ -functions, see Eq. (240). Further the equality, cf. [70],

$$\mathbf{M} \left[ \frac{\text{Li}_2(x)}{1+x} \right] (N+1) - \zeta_2 \beta(N+1) = (-1)^{N+1} \left[ S_{-2,1}(N) + \frac{5}{8} \zeta_3 \right] \quad (288)$$

can be applied<sup>5</sup>. Therefore, the operator matrix element  $\hat{A}_{Qg}^{(2)}$  depends on one non-trivial basic function only [107, 126]. Rewriting (281) in terms of splitting functions, see Appendix L, yields

$$\begin{aligned}
\hat{A}_{Qg}^{(2)} &= S_\epsilon^2\left(\frac{m^2}{\mu^2}\right)^\epsilon \left[ \frac{1}{\epsilon^2} \left\{ \frac{1}{2} \hat{P}_{qg}^{(0)} \otimes (P_{qg}^{(0)} - P_{gg}^{(0)}) + \beta_0 \hat{P}_{qg}^{(0)} \right\} + \frac{1}{\epsilon} \left\{ -\frac{1}{2} \hat{P}_{qg}^{(1)} \right\} + a_{Qg}^{(2)} \right] \\
&\quad - \frac{2}{\epsilon} S_\epsilon \beta_{0,Q} \sum_{i=1}^3 \left(\frac{m_i^2}{\mu^2}\right)^{\epsilon/2} \left(1 + \frac{\epsilon^2}{8} \zeta(2)\right) \hat{A}_{Qg}^{(1)}. \quad (289)
\end{aligned}$$

<sup>5</sup>We correct a typo in [47]. The argument of the Mellin-transform in (281) reads  $N+1$ , not  $N$ .

For the expansion coefficients of the  $\beta$ -function for the case of light and heavy ( $Q$ ) flavors, see Eqs. (134, 135).

For the light quarks we obtain in the pure-singlet case

$$\begin{aligned} \hat{A}_{Qq}^{\text{PS},(2)}\left(\frac{m^2}{\mu^2}, \varepsilon\right) &= S_\varepsilon^2\left(\frac{m^2}{\mu^2}\right)^\varepsilon \left\{ -\frac{1}{\varepsilon^2} T_R C_F \frac{16(N^2 + N + 2)^2}{(N-1)N^2(N+1)^2(N+2)} \right. \\ &\quad \left. - \frac{1}{\varepsilon} T_R C_F \frac{8(5N^5 + 32N^4 + 49N^3 + 38N^2 + 28N + 8)}{(N-1)N^3(N+1)^3(N+2)^2} + a_{Qq}^{\text{PS},(2)}(N) \right\}, \end{aligned} \quad (290)$$

with

$$\begin{aligned} a_{Qq}^{\text{PS},(2)}(N) &= T_R C_F \left\{ -4 \frac{(N^2 + N + 2)^2}{(N-1)N^2(N+1)^2(N+2)} (2S_2(N) + \zeta_2) \right. \\ &\quad \left. + \frac{4P_4(N)}{(N-1)N^4(N+1)^4(N+2)^3} \right\}, \end{aligned} \quad (291)$$

$$\begin{aligned} P_4(N) &= N^{10} + 8N^9 + 29N^8 + 49N^7 - 11N^6 - 131N^5 - 161N^4 \\ &\quad - 160N^3 - 168N^2 - 80N - 16. \end{aligned} \quad (292)$$

In terms of splitting functions, (291) reads

$$\hat{A}_{Qq}^{\text{PS},(2)} = S_\varepsilon^2\left(\frac{m^2}{\mu^2}\right)^\varepsilon \left[ \frac{1}{\varepsilon^2} \left\{ -\frac{1}{2} \hat{P}_{qg}^{(0)} \otimes P_{gq}^{(0)} \right\} + \frac{1}{\varepsilon} \left\{ -\frac{1}{2} \hat{P}_{qq}^{\text{PS},(1)} \right\} + a_{Qq}^{\text{PS},(2)} \right]. \quad (293)$$

The non-singlet OME becomes

$$\begin{aligned} \hat{A}_{qq,Q}^{\text{NS},(2)}\left(\frac{m^2}{\mu^2}, \varepsilon\right) &= S_\varepsilon^2\left(\frac{m^2}{\mu^2}\right)^\varepsilon \left\{ \frac{1}{\varepsilon^2} T_R C_F \left[ -\frac{32}{3} S_1(N) + 8 \frac{3N^2 + 3N + 2}{3N(N+1)} \right] \right. \\ &\quad \left. + \frac{1}{\varepsilon} T_R C_F \left[ \frac{16}{3} S_2(N) - \frac{80}{9} S_1(N) + 2 \frac{3N^4 + 6N^3 + 47N^2 + 20N - 12}{9N^2(N+1)^2} \right] \right. \\ &\quad \left. + a_{qq,Q}^{\text{NS},(2)}(N) \right\}, \end{aligned} \quad (294)$$

with

$$\begin{aligned} a_{qq,Q}^{\text{NS},(2)}(N) &= C_F T_R \left\{ -\frac{8}{3} S_3(N) - \frac{8}{3} \zeta_2 S_1(N) + \frac{40}{9} S_2(N) + 2 \frac{3N^2 + 3N + 2}{3N(N+1)} \zeta_2 - \frac{224}{27} S_1(N) \right. \\ &\quad \left. + \frac{219N^6 + 657N^5 + 1193N^4 + 763N^3 - 40N^2 - 48N + 72}{54N^3(N+1)^3} \right\}. \end{aligned} \quad (295)$$

Further we obtain

$$\hat{A}_{qq,Q}^{\text{NS},(2)} = S_\varepsilon^2\left(\frac{m^2}{\mu^2}\right)^\varepsilon \left[ \frac{1}{\varepsilon^2} \left\{ -\beta_{0,Q} P_{qq}^{(0)} \right\} + \frac{1}{\varepsilon} \left\{ -\frac{1}{2} P_{qq,Q}^{\text{NS},(1)} \right\} + a_{qq,Q}^{\text{NS},(2)} \right]. \quad (296)$$

In all results, no sum with index  $\{-1\}$  contributes. Concerning the non-trivial harmonic sums emerging, the operator matrix elements are finally of similar complexity as the 2-loop anomalous

dimensions. The results for the pole terms and for the constant terms agree as well with [55]. Note, that the complexity of the final result reduced significantly, since the harmonic sum  $S_{2,1}(N)$ , which is still present in the individual results of diagrams  $b, f, i, l, n, o$  and  $p$ , canceled exactly. This means that in Mellin-space, only 6 different harmonic sums contribute to the result. Forming equivalence classes as done in Refs. [106, 107], there are only two main functions,  $S_1(N)$  and  $S_{-2,1}(N)$ . All other single harmonic sums can be obtained by structural relations [107]. On the other hand we count a total number of 48 functions in the  $z$ -space representations of Ref. [55], which are listed in Table 6. Note, that the pole terms in the unrenormalized results are not the main objective of this calculation. They are removed via renormalization and contribute to the logarithmic heavy flavor corrections proportional to  $\ln^k(Q^2/m^2)$  only. They are given in terms of the splitting functions, see section 4.3. These splitting functions are well known and have been calculated several times, [33–35, 59, 63–66]. The main focus is hence on the determination of the expansion coefficients  $a_{ij}^{(2)}$  at  $O(\varepsilon^0)$ , which give rise to the constant term of the heavy flavor corrections. They have been calculated only once in Ref. [55], the result of which we could confirm.

Table 6: Functions contributing to the results in  $z$ -space

$\delta(1-x)$	1	$\ln(x)$	$\ln^2(x)$	$\ln^3(x)$
$\ln(1-x)$	$\ln^2(1-x)$	$\ln^3(1-x)$	$\ln(x)\ln(1-x)$	$\ln(x)\ln^2(1-x)$
$\ln^2(x)\ln(1-x)$	$\ln(1+x)$	$\ln(x)\ln(1+x)$	$\ln^2(x)\ln(1+x)$	$\text{Li}_2(1-x)$
$\ln(x)\text{Li}_2(1-x)$	$\ln(1-x)\text{Li}_2(1-x)$	$\text{Li}_3(1-x)$	$S_{1,2}(1-x)$	$S_{1,2}(-x)$
$\frac{1}{1-x}$	$\frac{1}{1+x}$	$\frac{\ln(x)}{1-x}$	$\frac{\ln^2(x)}{1-x}$	$\frac{\ln^3(x)}{1-x}$
$\frac{\ln(x)}{1+x}$	$\frac{\ln^2(x)}{1+x}$	$\frac{\ln^3(x)}{1+x}$	$\frac{\ln(1+x)}{1+x}$	$\frac{\ln(x)\ln(1+x)}{1+x}$
$\frac{\ln(x)\ln^2(1+x)}{1+x}$	$\frac{\ln^2(x)\ln(1+x)}{1+x}$	$\frac{\ln(x)\ln(1-x)}{1-x}$	$\frac{\ln(x)\ln^2(1-x)}{1-x}$	$\frac{\ln(1-x)\text{Li}_2(x)}{1-x}$
$\frac{\text{Li}_2(1-x)}{1-x}$	$\frac{\ln(x)\text{Li}_2(1-x)}{1-x}$	$\frac{\ln(x)\text{Li}_2(1-x)}{1+x}$	$\frac{\ln(1+x)\text{Li}_2(-x)}{1+x}$	$\ln(1+x)\text{Li}_2(-x)$
$\text{Li}_2(-x)$	$\frac{\text{Li}_2(-x)}{1+x}$	$\frac{\ln(x)\text{Li}_2(-x)}{1+x}$	$\frac{\text{Li}_3(1-x)}{1-x}$	$\frac{\text{Li}_3(-x)}{1+x}$
$\frac{S_{1,2}(1-x)}{1-x}$	$\frac{S_{1,2}(1-x)}{1+x}$	$\frac{S_{1,2}(-x)}{1+x}$		



## 8 The 2-Loop Heavy Flavor Wilson Coefficients

In DIS experiments the physical observables are the cross section and the structure functions, respectively, see Eq. (32). In the case of spin-averaged pure photoproduction considered here, there are only two structure functions,  $F_2$  and  $F_L$ . These relate to the parton distribution functions and the Wilson coefficients, Eqs. (75, 90). The heavy flavor Wilson coefficients then factorize into light flavor Wilson Coefficients  $C_{(L,2),i}^{S,NS}(Q^2/\mu^2, z)$  and the massive operator matrix elements  $A_{ij}^{S,NS}(m^2/\mu^2, z)$ , see Eqs. (76, 92). In the previous section, we calculated the unrenormalized OMEs  $\hat{A}_{ij}^{S,NS}$  up to  $O(a_s^2)$ , see Eqs. (289, 293, 296). In order to relate our results to measurable quantities, renormalization has to be performed. The renormalized OMEs are obtained by using Eq. (149) and inserting the respective operator renormalization constants and transition functions, see Appendix L. Thus we arrive at the renormalized operator matrix elements

$$A_{Qg}^{(1)} = -\frac{1}{2}\hat{P}_{qg}^{(0)} \ln\left(\frac{m^2}{\mu^2}\right) \quad (297)$$

$$A_{Qg}^{(2)} = \frac{1}{8}\left\{\hat{P}_{qg}^{(0)} \otimes [P_{qq}^{(0)} - P_{gg}^{(0)} + 2\beta_0]\right\} \ln^2\left(\frac{m^2}{\mu^2}\right) - \frac{1}{2}\hat{P}_{qg}^{(1)} \ln\left(\frac{m^2}{\mu^2}\right) + \bar{a}_{Qg}^{(1)} [P_{qq}^{(0)} - P_{gg}^{(0)} + 2\beta_0] + a_{Qg}^{(2)} \quad (298)$$

$$A_{Qq}^{\text{PS},(2)} = -\frac{1}{8}\hat{P}_{qg}^{(0)} \otimes P_{qg}^{(0)} \ln^2\left(\frac{m^2}{\mu^2}\right) - \frac{1}{2}\hat{P}_{qg}^{\text{PS},(1)} \ln\left(\frac{m^2}{\mu^2}\right) + a_{Qq}^{\text{PS},(2)} + \bar{a}_{Qg}^{(1)} \otimes P_{qg}^{(0)} \quad (299)$$

$$A_{qq,Q}^{\text{NS},(2)} = -\frac{\beta_{0,Q}}{4}P_{qq}^{(0)} \ln^2\left(\frac{m^2}{\mu^2}\right) - \frac{1}{2}\hat{P}_{qq}^{\text{NS},(1)} \ln\left(\frac{m^2}{\mu^2}\right) + a_{qq,Q}^{\text{NS},(2)} + \frac{1}{4}\beta_{0,Q}\zeta_2 P_{qq}^0. \quad (300)$$

In order to obtain the heavy flavor contributions to the massive coefficient functions in the asymptotic limit  $Q^2 \gg m^2$ , we choose the uniform factorization scale  $\mu^2 = Q^2$ . Generalizations to other factorization scales are easily obtained. Then the massless Wilson coefficients become equal to their respective constant term in the  $\overline{\text{MS}}$ -scheme, see section 3.3,

$$C_{(L,2),i}^{(k)} = c_{(L,2),i}^{(k)}. \quad (301)$$

Applying equations (98–103) yields the contribution of single heavy quark production to the heavy Wilson coefficients in the asymptotic limit,

$$\begin{aligned} H_{2,g}^S\left(z, a_s, \frac{Q^2}{m^2}\right) &= a_s \left[ \frac{1}{2}\hat{P}_{qg}^{(0)} \ln\left(\frac{Q^2}{m^2}\right) + \hat{c}_{2,g}^{(1)} \right] \\ &+ a_s^2 \left[ \frac{1}{8}\left\{\hat{P}_{qg}^{(0)} \otimes [P_{qq}^{(0)} - P_{gg}^{(0)} + 2\beta_0]\right\} \ln^2\left(\frac{Q^2}{m^2}\right) \right. \\ &+ \frac{1}{2}\left\{\hat{P}_{qg}^{(0)} \otimes c_{2,q}^{(1)} + \hat{P}_{qg}^{(1)}\right\} \ln\left(\frac{Q^2}{m^2}\right) \\ &\left. + \bar{a}_{Qg}^{(1)} [P_{qq}^{(0)} - P_{gg}^{(0)} + 2\beta_0] + a_{Qg}^{(2)} + \hat{c}_{2,g}^{(2)} \right], \quad (302) \end{aligned}$$

$$\begin{aligned}
H_{2,q}^{PS} \left( z, a_s, \frac{Q^2}{m^2} \right) &= a_s^2 \left[ -\frac{1}{8} \widehat{P}_{qq}^{(0)} \otimes P_{gg}^{(0)} \ln^2 \left( \frac{Q^2}{m^2} \right) + \frac{1}{2} \widehat{P}_{qq}^{PS,(1)} \ln \left( \frac{Q^2}{m^2} \right) \right. \\
&\quad \left. + \bar{a}_{Qg}^{(1)} \otimes P_{gg}^{(0)} + a_{Qq}^{PS,(2)} + \widehat{c}_{2,q}^{PS,(2)} \right], \tag{303}
\end{aligned}$$

$$\begin{aligned}
H_{2,q}^{NS} \left( z, a_s, \frac{Q^2}{m^2} \right) &= a_s^2 \left[ -\frac{\beta_{0,Q}}{4} P_{qq}^{(0)} \ln^2 \left( \frac{Q^2}{m^2} \right) + \frac{1}{2} \widehat{P}_{qq}^{NS,(1)} \ln \left( \frac{Q^2}{m^2} \right) \right. \\
&\quad \left. + \frac{1}{4} \beta_{0,Q} \zeta_2 P_{qq}^0 + a_{qq,Q}^{NS,(2)} + \widehat{c}_{2,q}^{NS,(2)} \right]. \tag{304}
\end{aligned}$$

$$\begin{aligned}
H_{L,g}^S \left( z, a_s, \frac{Q^2}{m^2} \right) &= a_s \widehat{c}_{L,g}^{(1)} + a_s^2 \left[ \frac{1}{2} \widehat{P}_{qq}^{(0)} c_{L,q}^{(1)} \ln \left( \frac{Q^2}{m^2} \right) + \widehat{c}_{L,g}^{(2)} \right] \\
&+ a_s^3 \left\{ \left[ \frac{1}{8} \widehat{P}_{qq}^{(0)} [P_{qq}^{(0)} - P_{gg}^{(0)} + 2\beta_0] \ln^2 \left( \frac{Q^2}{m^2} \right) + \frac{1}{2} \widehat{P}_{qq}^{(1)} \ln \left( \frac{Q^2}{m^2} \right) \right. \right. \\
&\quad \left. \left. + a_{Qg}^{(2)} + \bar{a}_{Qg}^{(1)} [P_{qq}^{(0)} - P_{gg}^{(0)} + 2\beta_0] \right] c_{L,q}^{(1)} + \frac{1}{2} \widehat{P}_{qq}^{(0)} \ln \left( \frac{Q^2}{m^2} \right) c_{L,q}^{(2)} + \widehat{c}_{L,g}^{(3)} \right\} \tag{305}
\end{aligned}$$

$$\begin{aligned}
H_{L,q}^{PS} \left( z, a_s, \frac{Q^2}{m^2} \right) &= a_s^2 \widehat{c}_{L,q}^{PS,(2)} + a_s^3 \left\{ \left[ -\frac{1}{8} \widehat{P}_{qq}^{(0)} P_{gg}^{(0)} \ln^2 \left( \frac{Q^2}{m^2} \right) \right. \right. \\
&\quad \left. \left. + \frac{1}{2} \widehat{P}_{qq}^{PS,(1)} \ln \left( \frac{Q^2}{m^2} \right) + a_{Qq}^{PS,(2)} - \bar{a}_{Qg}^{(1)} P_{gg}^{(0)} \right] c_{L,q}^{(1)} + \widehat{c}_{L,q}^{PS,(3)} \right\} \tag{306}
\end{aligned}$$

$$\begin{aligned}
H_{L,q}^{NS} \left( z, a_s, \frac{Q^2}{m^2} \right) &= a_s^2 \left[ -\beta_{0,Q} c_{L,q}^{(1)} \ln \left( \frac{Q^2}{m^2} \right) + \widehat{c}_{L,q}^{NS,(2)} \right] \\
&+ a_s^3 \left\{ \left[ -\frac{1}{4} \beta_{0,Q} P_{qq}^{(0)} \ln^2 \left( \frac{Q^2}{m^2} \right) - \frac{1}{2} \widehat{P}_{qq}^{NS,(1)} \ln \left( \frac{Q^2}{m^2} \right) + a_{qq,Q}^{NS,(2)} + \frac{1}{4} \beta_{0,Q} \zeta_2 P_{qq}^{(0)} \right] \right. \\
&\quad \left. \times c_{L,q}^{(1)} + \widehat{c}_{L,q}^{NS,(3)} \right\}. \tag{307}
\end{aligned}$$

It was shown in Ref. [127] that in the kinematic region of HERA, the logarithms  $\ln(Q^2/m^2)$  emerging in Eqs. (302-307) need not to be resummed. As one sees, the logarithmic contributions to the heavy quark coefficient functions in the asymptotic limit are given in terms of splitting functions, the  $\beta$ -function and the expansion coefficients of the light Wilson coefficients  $C_{(2,L),i}^{S,NS}$  only. These terms are known from the literature. What is genuine to the present approach is the possibility to access the constant terms,  $a_{ij}(N)$ . Further, we would like to stress that we have obtained, for the first time, a NNLO result for the longitudinal asymptotic heavy Wilson coefficient in this way, cf. [47]. This is possible, since it requires the 2-loop OME  $A_{Qg}^{(2)}$  only. Note, however, that the limit  $Q^2 \gg m^2$  applies to  $H_L$  only at scales of  $Q^2 \geq 500 \text{ GeV}^2$ , which is not yet accessible by experiment. All terms in the above equations are known. The Wilson coefficients for massless quarks were calculated in LO [56], NLO [57–59], and NNLO [60–62]. For the LO massless Wilson coefficients, see also section 5. The splitting functions were calculated in Ref. [33–35, 59, 63–66], and the  $\beta$  function in Ref. [29, 30, 101], see section 4. Thus one is able to describe the perturbative contribution of heavy flavor production to the physical structure

functions in the asymptotic limit via the Mellin-convolution

$$F_{2,L}(z, Q^2) = \sum_j H_{2,L}^j \left( a_s, \frac{Q^2}{m^2}, \frac{m^2}{\mu^2} \right) \otimes f_j(\mu^2), \quad j = PS, NS, g \quad (308)$$

up to  $O(a_s^2)$  for  $F_2$  and to  $O(a_s^3)$  for  $F_L$ , respectively. This allows for precision analyzes of QCD as for the extraction of the non-perturbative universal parton-densities  $f_j(z)$  and the measurement of the QCD scale  $\Lambda_{QCD}$ .

## 9 Summary

We have recalculated the heavy flavor operator matrix elements  $A_{ij}^{(k)}$  at 2-loop order in perturbation theory in the singlet, non-singlet and pure-singlet case for the first time. We confirmed the result obtained by M. Buza et. al. in 1996, [55]. Together with the light Wilson coefficients, the operator matrix elements allow for a determination of the logarithmic and constant terms of the heavy flavor coefficient functions of deeply inelastic scattering in the asymptotic region  $Q^2 \gg m^2$ . This applies to the twist-2 approximation and reaches up to  $O(a_s^2)$  in perturbation theory. The motivation for this calculation is to handle the heavy flavor contributions to the structure functions, which are rather large. These results increase our knowledge on the perturbative part of Quantum Chromodynamics, allowing for a better determination of non-perturbative, universal quantities as the parton-distribution functions and to diminish the theory error on  $\Lambda_{QCD}$ . By not applying the integration-by-parts technique as used in Ref. [55] and working in Mellin-space, we were able to compactify the calculation and the results significantly. The natural representation of the problem seems to be in terms of harmonic sums, allowing for a dramatic reduction of complexity. This is mainly due to algebraic relations, which are not obvious in  $z$ -space. We observed also in the present case the empirical fact that harmonic sums with index  $\{-1\}$  do not appear at all, which is something to be recognized very hard in  $z$ -space. Additionally, large parts of the calculation could be automatized using computer algebra programs, allowing for a fast evaluation also in case of further problems, as the polarized case. We learned that for this type of problem, the Feynman-parameter integrals should be studied carefully before performing further steps as Mellin-Barnes-transformations or expanding in the dimensional regularization parameter. By using variable transformations leaving the integration boundaries intact, we were able to show that almost all integrals can be expressed in terms of generalized hypergeometric series, most importantly the series  ${}_3F_2$ , which is a well known function and therefore good to handle. The few remaining diagrams could be written as well in terms of multiple sums, which, in general, did not pose a bigger problem. Further study should show, whether the present approach using the representation outlined works also for very different, or in even more complicated cases.

## 10 Appendix



# A Conventions

We use natural units

$$\hbar = 1, \quad c = 1, \quad \varepsilon_0 = 1, \quad (\text{A.1})$$

where  $\hbar$  denotes Planck's constant,  $c$  the vacuum speed of light and  $\varepsilon_0$  the permittivity of free space. The electromagnetic fine-structure constant  $\alpha$  is then given by

$$\alpha = \alpha'(\mu^2 = 0) = \frac{e^2}{4\pi\varepsilon_0\hbar c} = \frac{e^2}{4\pi} \approx \frac{1}{137.03599911(46)}. \quad (\text{A.2})$$

In this convention, energies and momenta are given in the same units, electron volt (eV).

The space-time dimension is taken to be  $D$  and the metric tensor  $g_{\mu\nu}$  in Minkowski-space is defined as

$$g_{00} = 1, \quad g_{ii} = -1, \quad i = 1 \dots D-1, \quad g_{ij} = 0, \quad i \neq j. \quad (\text{A.3})$$

Einstein's summation convention is used, i.e.

$$x_\mu y^\mu := \sum_{\mu=1}^D x_\mu y^\mu. \quad (\text{A.4})$$

Bold-faced symbols represent  $D-1$ -dimensional spatial vectors:

$$x = (x_0, \mathbf{x}). \quad (\text{A.5})$$

If not stated otherwise, Greek indexes refer to the  $D$ -component space-time vector and Latin ones to the  $D-1$  spatial components only. The dot product of two vectors is defined by

$$p \cdot q = p_0 q_0 - \sum_{i=1}^{D-1} p_i q_i. \quad (\text{A.6})$$

The  $\gamma$ -matrices  $\gamma_\mu$  are taken to be of dimension  $D$  and fulfill the anti-commutation relation

$$\{\gamma_\mu, \gamma_\nu\} = 2g_{\mu\nu}. \quad (\text{A.7})$$

It follows that

$$\gamma_\mu \gamma^\mu = D \quad (\text{A.8})$$

$$\text{Tr}(\gamma_\mu \gamma_\nu) = 4g_{\mu\nu} \quad (\text{A.9})$$

$$\text{Tr}(\gamma_\mu \gamma_\nu \gamma_\alpha \gamma_\beta) = 4[g_{\mu\nu} g_{\alpha\beta} + g_{\mu\beta} g_{\nu\alpha} - g_{\mu\alpha} g_{\nu\beta}]. \quad (\text{A.10})$$

The dagger-symbol for a  $D$ -momentum  $p$  is defined by

$$\not{p} := \gamma_\mu p^\mu. \quad (\text{A.11})$$

The conjugate of a bi-spinor  $u$  of a particle is given by

$$\bar{u} = u^\dagger \gamma_0, \quad (\text{A.12})$$

where † denotes Hermitian and \* complex conjugation, respectively. The bi-spinor  $u$  and  $v$  fulfill the Dirac-equation,

$$(\not{p} - m)u(p) = 0, \quad \bar{u}(p)(\not{p} - m) = 0 \quad (\text{A.13})$$

$$(\not{p} + m)v(p) = 0, \quad \bar{v}(p)(\not{p} + m) = 0. \quad (\text{A.14})$$

Bi-spinors and polarization vectors are normalized to

$$\sum_{\sigma} u(p, \sigma)\bar{u}(p, \sigma) = \not{p} + m \quad (\text{A.15})$$

$$\sum_{\sigma} v(p, \sigma)\bar{v}(p, \sigma) = \not{p} - m \quad (\text{A.16})$$

$$\sum_{\lambda} \epsilon^{\mu}(k, \lambda)\epsilon^{\nu}(k, \lambda) = -g^{\mu\nu}, \quad (\text{A.17})$$

where  $\lambda$  and  $\sigma$  represent the spin.

The commonly used caret “^” to signify an operator, e.g.  $\hat{O}$ , is omitted if confusion is not to be expected.



## B Feynman Rules

The Feynman-rules for QCD and composite operators are taken from [79, 128]. We work in Feynman gauge.  $D$ -momenta are denoted by  $p_i$  and Lorentz-indices by Greek letters. Color indices are  $a, b, c, d, e$  and  $i, j$  are indices of the color matrices. Solid lines represent fermions, wavy lines gluons and dashed ones ghosts. Arrows denote the direction of the respective momenta. The rules for QCD are given in Figure 13 and those for the composite operators in Figure 14. A factor  $(-1)$  has to be included for each closed fermion or ghost loop.

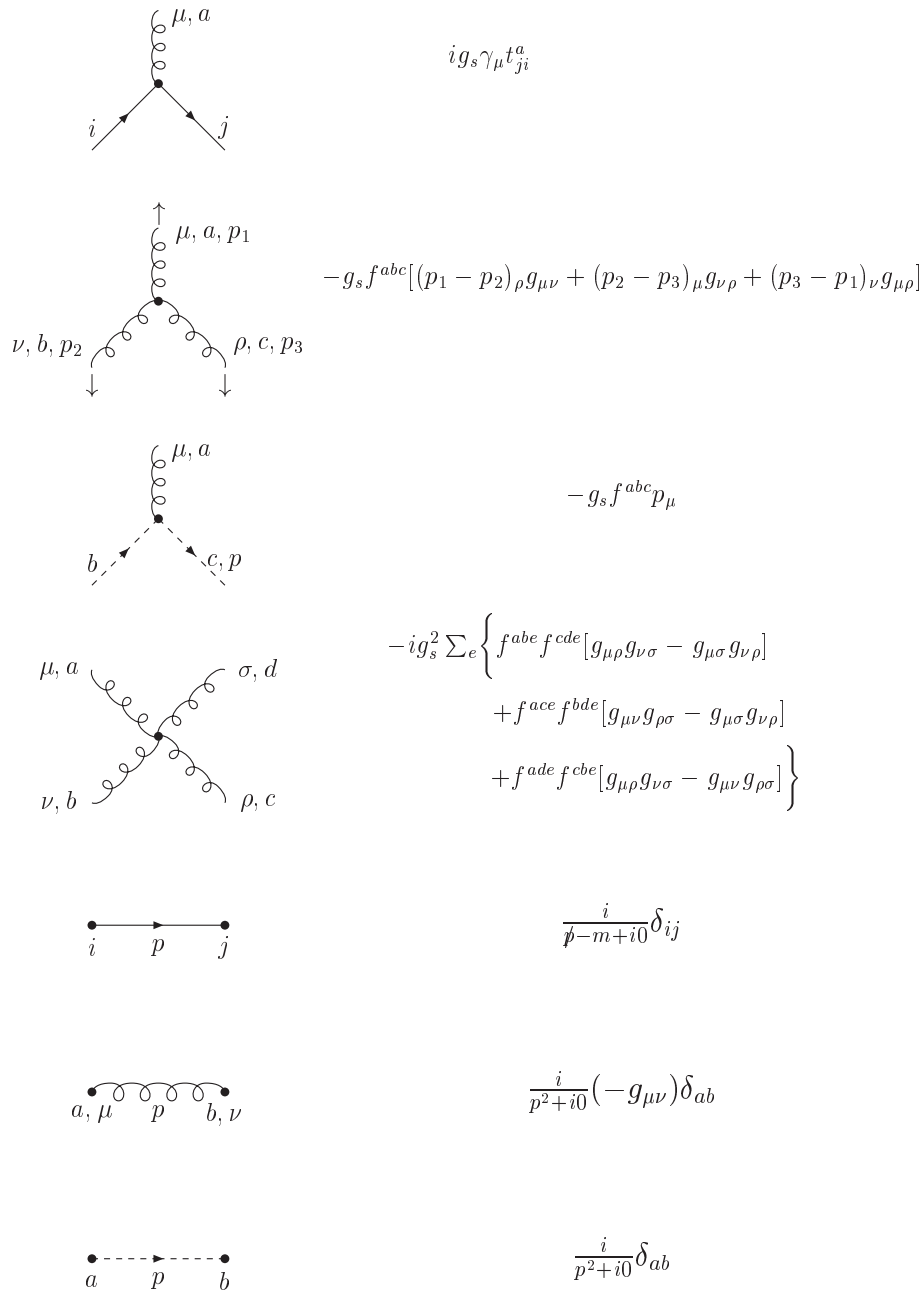
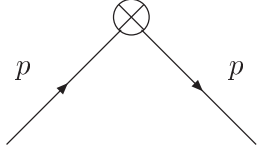
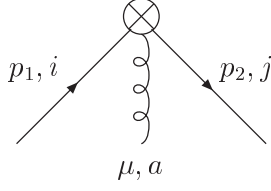


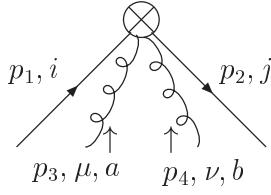
Figure 13: Feynman rules for QCD.



$$\not\Delta(\Delta \cdot p)^{N-1}, \quad N \geq 1$$



$$gt_{ji}^a \Delta^\mu \not\Delta \sum_{j=0}^{N-2} (\Delta \cdot p_1)^j (\Delta \cdot p_2)^{N-j-2}, \quad N \geq 2$$



$$g^2 \Delta^\mu \Delta^\nu \not\Delta \sum_{0 \leq j < l}^{N-2} \left[ (\Delta p_1)^{N-l-2} (\Delta p_1 + \Delta p_4)^{l-j-1} (\Delta p_2)^j (t^a t^b)_{ji} \right. \\ \left. + (\Delta p_1)^{N-l-2} (\Delta p_1 + \Delta p_3)^{l-j-1} (\Delta p_2)^j (t^b t^a)_{ji} \right], \\ N \geq 3$$

Figure 14: Feynman rules for composite operators.  $\Delta$  denotes a light-like 4-vector,  $\Delta^2 = 0$ ;  $N$  is an integer.

## C Kinematics of 2-to-2 particle scattering

Let  $q$ ,  $k$  and  $p_1$ ,  $p_2$  denote the  $D$ -momenta of the incoming and the outgoing particles in  $D$ -dimensional space-time. Their masses are given by  $m_q$ ,  $m_k$  and  $m_1$ ,  $m_2$ , respectively. In the cms-frame the momenta are given by

$$q = (E_q; \vec{0}_{D-2}, p_{cm}) \quad (\text{C.1})$$

$$k = (E_k; \vec{0}_{D-2}, -p_{cm}) \quad (\text{C.2})$$

$$p_1 = (E_1; \vec{p}_{cm}') \quad (\text{C.3})$$

$$p_2 = (E_1; -\vec{p}_{cm}') . \quad (\text{C.4})$$

The above quantities are expressed as follows, [129]:

$$p_{cm} = \frac{\lambda^{1/2}(s, m_q^2, m_k^2)}{2\sqrt{s}} \quad (\text{C.5})$$

$$|\vec{p}_{cm}'| = \frac{\lambda^{1/2}(s, m_1^2, m_2^2)}{2\sqrt{s}} \quad (\text{C.6})$$

$$E_q = \frac{s + m_q^2 - m_k^2}{2\sqrt{s}} \quad (\text{C.7})$$

$$E_k = \frac{s + m_k^2 - m_q^2}{2\sqrt{s}} \quad (\text{C.8})$$

$$E_1 = \frac{s + m_1^2 - m_2^2}{2\sqrt{s}} \quad (\text{C.9})$$

$$E_2 = \frac{s + m_2^2 - m_1^2}{2\sqrt{s}} . \quad (\text{C.10})$$

Here, the kinematic function  $\lambda$  is given by

$$\lambda(x, y, z) = (x - y - z)^2 - 4yz . \quad (\text{C.11})$$

The variable  $s$  denotes the cms energy squared, see (167). The two-particle phase space integral in  $D$  dimensions reads

$$\int dR_2 = \int \frac{d^{D-1}p_1}{(2\pi)^{D-1}(2E_1)} \frac{d^{D-1}p_2}{(2\pi)^{D-1}(2E_2)} \frac{1}{4q.k} (2\pi)^D \delta(p_1 + p_2 - q - k) . \quad (\text{C.12})$$

Using the  $D$ -dimensional  $\delta$ -distribution and integrating over  $p_2$  yields

$$\int dR_2 = \int d^{D-1}p_1 \frac{(2\pi)^{2-D}}{4E_1 E_2} \frac{1}{4q.k} \delta^D(E_1 + E_2 - E_q - E_k) . \quad (\text{C.13})$$

The integration over  $p_1$  can be performed by introducing  $D$ -dimensional spherical coordinates. Jacobi's determinant for this transformation is given by, [130],

$$J = \frac{\partial \vec{p}_1}{\partial(|\vec{p}_1|, \vec{\phi})} = p_1^{D-2} \sin^{D-3}(\phi_1) \sin^{D-4}(\phi_2) \dots \sin(\phi_{D-3}) . \quad (\text{C.14})$$

Defining

$$y := \cos(\phi_{D-3}) \quad (\text{C.15})$$

$$\phi_{D-3} \equiv \theta_{qp_1} , \quad (\text{C.16})$$

the scattering angle between  $q$  and  $p_1$  and integrating over all other angles gives

$$\int dR_2 = \int \frac{dp_1 dy 2\pi^{2-D}}{4E_1 E_2} \frac{1}{4q \cdot k} \frac{(2\pi)^{D/2-1}}{\Gamma(D/2-1)} p_1^{D-2} (1-y^2)^{D/2-2} \delta^D(E_1 + E_2 - E_q - E_k) . \quad (\text{C.17})$$

Finally, one integrates over the modulus of  $\vec{p}_1$

$$\int dR_2 = \int \frac{dy 2^{3-D} \pi^{1-D/2}}{4q \cdot k} \frac{(1-y^2)^{D/2-2}}{\Gamma(D/2-1)} \frac{(p'_{cm})^{D-3}}{4\sqrt{s}} . \quad (\text{C.18})$$

Now one may specialize to the process considered. The mass of the gluon is equal to zero and the off-shell mass of the virtual photon is given by  $q^2 = -Q^2$ . Since the same flavor of quarks is produced, their masses are equal. From (C.10) it follows that

$$p_{cm} = \frac{s + Q^2}{2\sqrt{s}} = \frac{q \cdot k}{\sqrt{s}} \quad (\text{C.19})$$

$$p'_{cm} = \frac{1}{2\sqrt{s}} . \quad (\text{C.20})$$

The final expression for the  $D$ -dimensional case now reads

$$\int dR_2 = \int \frac{(p'_{cm})^{D-3}}{32\pi s p_{cm}} \frac{(1-y^2)^{D/2-2}}{2^{D-4} \pi^{D/2-2} \Gamma(D/2-1)} dy . \quad (\text{C.21})$$

In the remainder  $y$  is used as reference variable. Since  $y = \cos \theta_{qp_1}$ , it has to be integrated from  $-1$  to  $1$ . It is useful to recall the relations for  $y$  and the Mandelstam-variable  $t$

$$t = m^2 - \frac{Q^2}{2x} (1 - vy) , \quad (\text{C.22})$$

where  $v$  is the velocity of the produced quarks in the cms, see (153). Due to this, it is possible to evaluate the integral by integrating over  $y$ , to obtain an expression which contains Bjorken- $x$ . In the massive case, see section 5, the phase space integral evaluates as follows: For  $D = 4$  one obtains

$$\int dR_2 = \int \frac{1}{32s} \frac{p'_{cm}}{p_{cm}} dy . \quad (\text{C.23})$$

From the definition of  $t$  follows

$$t = (q - p_1)^2 = -Q^2 + m_1^2 - 2E_q E_1 + 2p_{cm} p'_{cm} \cos(\theta_{qp_1}) \quad (\text{C.24})$$

$$\implies dt = 2p_{cm} p'_{cm} d \cos(\theta_{qp_1}) = 2p_{cm} p'_{cm} dy . \quad (\text{C.25})$$

Changing variables from  $y$  to  $t$  and referring to the physical region of  $t$ , [129], yields

$$\int dR_2 = \int_{t^-}^{t^+} \frac{dt}{64\pi s p_{cm}^2} , \quad (\text{C.26})$$

$$t^\pm = \frac{s + Q^2}{2} \pm \frac{s + Q^2}{2} \cdot v . \quad (\text{C.27})$$

## D Color Factors in $SU(N)$

The gauge symmetry group of QCD is the Lie-Group  $SU(3)$ . We will consider the general case of  $SU(N)$ . The non-commutative generators are denoted by  $t^a$ , where  $a$  runs from 1 to  $N^2 - 1$ . The generators can be represented by Hermitian, traceless matrices [28]. The structure constants  $f^{abc}$  and  $d^{abc}$  of  $SU(N)$  are defined via the commutation and anti-commutation relations of its generators [79]

$$[t^a, t^b] = if^{abc}t^c \quad (\text{D.1})$$

$$\{t^a, t^b\} = d^{abc}t^c + \frac{1}{N}\delta_{ab} . \quad (\text{D.2})$$

The indexes of the color matrices, in a certain representation, are denoted by  $i, j, k, l, \dots$ . Up to the 2-loop level only 3 color invariants can appear. They are given by

$$\delta_{ab}C_A = f^{acd}f^{bcd} \quad (\text{D.3})$$

$$\delta_{ij}C_F = t_{il}^a t_{lj}^a \quad (\text{D.4})$$

$$\delta_{ab}T_R = t_{ik}^a t_{ki}^b . \quad (\text{D.5})$$

These constants evaluate to

$$C_A = N \quad (\text{D.6})$$

$$C_F = \frac{N^2 - 1}{2N} \quad (\text{D.7})$$

$$T_R = \frac{1}{2} . \quad (\text{D.8})$$

For QCD,  $C_A = 3$  ,  $C_F = 4/3$  are obtained.

## E Results for the Individual Diagrams

In this Appendix, the results for the different diagrams as shown in Figures 6-9 are given for the matrix elements  $A_i^{Qg}$ ,  $A_i^{Qq}$  and  $A_i^{qq}$ . The index  $i$  denotes the label of the respective graphs in the corresponding Figure. Symmetry factors have been accounted for. The projections (205-208) have been applied. There is an overall factor

$$\hat{a}_s^2 S_\varepsilon^2 \left( \frac{\hat{m}^2}{\mu_0^2} \right)^\varepsilon, \quad (\text{E.1})$$

which is not written explicitly. In (E.1),  $\hat{a}_s$  denotes the bare strong coupling constant, Eq. (119),  $S_\varepsilon$  is the spherical factor, Eq. (120),  $\mu_0$  is the renormalization scale, (118), and  $\varepsilon = D - 4$ . The singlet results are

$$A_a^{Qq} = T_R C_F \left\{ \frac{1}{\varepsilon^2} \frac{16}{N^2(N+1)} + \frac{8}{\varepsilon} \frac{2N^3 - N - 2}{N^3(N+1)^2(N+2)} + \frac{8}{N^2(N+1)} S_2(N) \right. \\ \left. + \frac{4}{N^2(N+1)} \zeta_2 + \frac{4P_1(N)}{N^4(N+1)^3(N+2)^2} \right\}, \quad (\text{E.2})$$

$$P_1(N) = 7N^6 + 18N^5 + 18N^4 - 3N^3 - 21N^2 - 16N - 4.$$

$$A_b^{Qq} = T_R C_F \left\{ \frac{1}{\varepsilon^2} \left[ -\frac{32}{N} S_1(N) + \frac{32}{N} \right] + \frac{1}{\varepsilon} \left[ \frac{24S_2(N) - 8S_1^2(N)}{N} \right. \right. \\ \left. \left. + 16 \frac{N^2 + 7N + 2}{N(N+1)(N+2)} S_1(N) - 32 \frac{N^2 + 5N + 2}{N(N+1)(N+2)} \right] - \frac{16}{N} S_{2,1}(N) + \frac{40}{3N} S_3(N) \right. \\ \left. - \frac{4}{N} S_1(N) S_2(N) - \frac{4}{3N} S_1^3(N) - \frac{8}{N} S_1(N) \zeta_2 + 4 \frac{N^2 + 7N + 2}{N(N+1)(N+2)} S_1^2(N) \right. \\ \left. + 4 \frac{N^2 - 9N + 2}{N(N+1)(N+2)} S_2(N) + \frac{8}{N} \zeta_2 - 16 \frac{N^3 + 9N^2 + 8N + 4}{N^2(N+2)^2} S_1(N) \right. \\ \left. + 32 \frac{N^5 + 10N^4 + 30N^3 + 37N^2 + 18N + 4}{N(N+1)^3(N+2)^2} \right\}. \quad (\text{E.3})$$

$$A_c^{Qq} = T_R C_F \left\{ -\frac{1}{\varepsilon^2} \frac{8}{N} + \frac{1}{\varepsilon} \frac{4(13N^4 + 82N^3 + 82N^2 + N - 6)}{N^2(N+1)(N+2)(N+3)} + \frac{20}{N} S_2(N) - \frac{2}{N} \zeta_2 \right. \\ \left. - \frac{2P_2(N)}{N^3(N+1)^2(N+2)^2(N+3)} \right\}, \quad (\text{E.4})$$

$$P_2(N) = 16N^7 + 176N^6 + 520N^5 + 600N^4 + 257N^3 + 7N^2 + 16N + 12.$$

$$A_d^{Qq} = T_R C_F \left\{ -\frac{1}{\varepsilon^2} \frac{16}{N} + \frac{1}{\varepsilon} \left[ -\frac{8}{N} S_1(N) + 8 \frac{N^3 + 10N^2 + 59N + 42}{N(N+1)(N+2)(N+3)} \right] - \frac{2}{N} [S_2(N) + S_1^2(N)] \right. \\ \left. - \frac{4}{N} \zeta_2 + 4 \frac{N^4 + 8N^3 + 43N^2 + 36N + 12}{N^2(N+1)^2(N+2)} S_1(N) \right\}$$

$$\left. -\frac{8P_3(N)}{N(N+1)^3(N+2)^2(N+3)} \right\}, \quad (\text{E.5})$$

$$P_3(N) = N^6 + 10N^5 + 99N^4 + 350N^3 + 486N^2 + 274N + 60.$$

$$\begin{aligned} A_e^{Qq} = T_R \left[ C_F - \frac{C_A}{2} \right] & \left\{ \frac{1}{\varepsilon^2} \frac{16(N+3)}{(N+1)^2} + \frac{1}{\varepsilon} \left[ -\frac{8(N+2)}{N(N+1)} S_1(N) \right. \right. \\ & - 8 \frac{3N^3 + 9N^2 + 12N + 4}{N(N+1)^3(N+2)} \left. \right] - 2 \frac{9N^4 + 40N^3 + 71N^2 - 12N - 36}{N(N+1)^2(N+2)(N+3)} S_2(N) \\ & - 2 \frac{N^3 - N^2 - 8N - 36}{N(N+1)(N+2)(N+3)} S_1^2(N) + 4 \frac{(N+3)}{(N+1)^2} \zeta_2 \\ & + 4 \frac{4N^5 + 19N^4 + 31N^3 - 30N^2 - 44N - 24}{N^2(N+1)^2(N+2)(N+3)} S_1(N) \\ & \left. + \frac{4P_4(N)}{N^2(N+1)^4(N+2)^2(N+3)} \right\}, \quad (\text{E.6}) \end{aligned}$$

$$P_4(N) = 16N^7 + 111N^6 + 342N^5 + 561N^4 + 536N^3 + 354N^2 + 152N + 24.$$

$$\begin{aligned} A_f^{Qq} = T_R \left[ C_F - \frac{C_A}{2} \right] & \left\{ \frac{1}{\varepsilon^2} \left[ \frac{64}{(N+1)(N+2)} S_1(N) - \frac{64}{(N+1)(N+2)} \right] \right. \\ & + \frac{1}{\varepsilon} \left[ -\frac{16}{N} S_2(N) + 16 \frac{5N+2}{N^2(N+1)(N+2)} S_1(N) - \frac{32}{(N+1)^2(N+2)} \right] \\ & + \frac{16}{N} S_{2,1}(N) - \frac{8}{N} S_3(N) + \frac{16}{(N+1)(N+2)} S_1(N) \zeta_2 \\ & + 4 \frac{(9N+2)(2N-3)}{N^2(N+1)(N+2)} S_2(N) + 4 \frac{2N^2 - 3N + 2}{N^2(N+1)(N+2)} S_1^2(N) \\ & - \frac{16}{(N+1)(N+2)} \zeta_2 - 8 \frac{17N^2 + 32N + 12}{N(N+1)^2(N+2)^2} S_1(N) \\ & \left. + 16 \frac{2N^3 + 12N^2 + 23N + 18}{(N+1)^3(N+2)^2} \right\}. \quad (\text{E.7}) \end{aligned}$$

$$\begin{aligned} A_g^{Qq} = T_R C_F & \left\{ \frac{1}{\varepsilon^2} \frac{32}{(N+1)(N+2)} + \frac{1}{\varepsilon} \left[ \frac{8}{(N+1)(N+2)} S_1(N) \right. \right. \\ & - 8 \frac{17N^2 + 47N + 28}{(N+1)^2(N+2)^2} \left. \right] - \frac{38}{(N+1)(N+2)} S_2(N) + \frac{2}{(N+1)(N+2)} S_1^2(N) \\ & + \frac{8}{(N+1)(N+2)} \zeta_2 - 4 \frac{3N^3 + 31N^2 + 45N + 8}{N(N+1)^2(N+2)^2} S_1(N) \\ & \left. + 36 \frac{4N^4 + 26N^3 + 55N^2 + 43N + 8}{(N+1)^3(N+2)^3} \right\}. \quad (\text{E.8}) \end{aligned}$$

$$\begin{aligned}
A_h^{Qq} = T_R \left[ C_F - \frac{C_A}{2} \right] & \left\{ -\frac{1}{\varepsilon^2} \frac{32}{(N+1)(N+2)} + \frac{1}{\varepsilon} \left[ 16 \frac{N+3}{N(N+1)(N+2)} S_1(N) \right. \right. \\
& - 8 \frac{N^2+7N+8}{(N+1)^2(N+2)^2} \left. \right] - 4 \frac{N^2-18N+9}{N(N+1)(N+2)(N+3)} S_2(N) \\
& - 4 \frac{N^2-2N+9}{N(N+1)(N+2)(N+3)} S_1^2(N) - \frac{8}{(N+1)(N+2)} \zeta_2 \\
& + 4 \frac{3N^4+N^3-27N^2-85N-84}{N(N+1)^2(N+2)^2(N+3)} S_1(N) \\
& \left. - 4 \frac{(N-1)(14N^4+110N^3+337N^2+463N+240)}{(N+1)^3(N+2)^3(N+3)} \right\}. \tag{E.9}
\end{aligned}$$

$$\begin{aligned}
A_i^{Qq} = T_R C_A & \left\{ \frac{1}{\varepsilon^2} \left[ \frac{16}{(N+1)(N+2)} S_1(N) - \frac{16(N+4)}{(N+1)(N+2)^2} \right] + \frac{1}{\varepsilon} \left[ \frac{32}{(N+2)} S_{-2}(N) \right. \right. \\
& + \frac{4(4N+3)}{(N+1)(N+2)} S_2(N) - \frac{4}{(N+1)(N+2)} S_1^2(N) \\
& + 8 \frac{N^3+9N^2+17N+8}{N(N+1)^2(N+2)^2} S_1(N) - 8 \frac{2N^3+8N^2+19N+16}{(N+1)^2(N+2)^3} \left. \right] - \frac{32}{N+2} S_{-2,1}(N) \\
& - \frac{8(2N+1)}{(N+1)(N+2)} S_{2,1}(N) + \frac{16}{N+2} S_{-3}(N) + \frac{4(18N+17)}{3(N+1)(N+2)} S_3(N) \\
& + \frac{32}{N+2} S_{-2}(N) S_1(N) + \frac{2(8N+7)}{(N+1)(N+2)} S_2(N) S_1(N) - \frac{2}{3(N+1)(N+2)} S_1^3(N) \\
& + \frac{4}{(N+1)(N+2)} \zeta_2 S_1(N) - \frac{16(N^2-N-4)}{(N+1)(N+2)^2} S_{-2}(N) \\
& - 2 \frac{4N^4+N^3-7N^2+7N+8}{N(N+1)^2(N+2)^2} S_2(N) + 2 \frac{3N^3+7N^2-3N-8}{N(N+1)^2(N+2)^2} S_1^2(N) \\
& - \frac{4(N+4)}{(N+1)(N+2)^2} \zeta_2 - 4 \frac{4N^5+36N^4+114N^3+174N^2+137N+48}{N(N+1)^3(N+2)^3} S_1(N) \\
& \left. + 4 \frac{8N^5+68N^4+247N^3+449N^2+403N+144}{(N+1)^3(N+2)^4} \right\} \\
& + T_R C_F \left\{ \frac{1}{\varepsilon} \left[ -\frac{16}{(N+1)(N+2)} S_2(N) + \frac{16}{(N+1)(N+2)} S_1^2(N) \right. \right. \\
& - \frac{64}{N(N+2)} S_1(N) + \frac{128}{(N+1)(N+2)} \left. \right] - \frac{32}{3(N+1)(N+2)} S_3(N) \\
& + \frac{8}{(N+1)(N+2)} S_2(N) S_1(N) + \frac{8}{3(N+1)(N+2)} S_1^3(N) \\
& + \frac{8(3N+2)}{N(N+1)(N+2)} S_2(N) - \frac{8(3N-2)}{N(N+1)(N+2)} S_1^2(N) \\
& \left. + \frac{16(5N^2+9N+6)}{N(N+1)^2(N+2)} S_1(N) - \frac{192}{(N+1)(N+2)} \right\}. \tag{E.10}
\end{aligned}$$



$$A_j^{Qq} = T_R C_A \left\{ -\frac{1}{\varepsilon^2} \frac{8(4N^2 + 4N - 5)}{N^2(N+1)^2} + \frac{1}{\varepsilon} \frac{4(4N^5 + 22N^4 + 11N^3 + 13N^2 + 35N + 10)}{N^3(N+1)^3(N+2)} \right. \\ \left. - 4 \frac{4N^2 + 4N - 5}{N^2(N+1)^2} S_2(N) - 2 \frac{4N^2 + 4N - 5}{N^2(N+1)^2} \zeta_2 - \frac{2P_5(N)}{N^4(N+1)^4(N+2)^2} \right\}, \quad (\text{E.11})$$

$$P_5(N) = 20N^7 + 64N^6 + 120N^5 + 94N^4 - 140N^3 - 253N^2 - 100N - 20.$$

$$A_k^{Qq} = T_R C_A \left\{ \frac{1}{\varepsilon^2} \frac{8(3N^2 - 23N - 20)}{(N-1)N(N+1)^2(N+2)} - \frac{1}{\varepsilon} \frac{4(10N^4 + 7N^3 + 51N^2 + 172N + 112)}{(N-1)N(N+1)^3(N+2)^2} \right. \\ \left. + 4 \frac{3N^2 - 23N - 20}{(N-1)N(N+1)^2(N+2)} S_2(N) + 2 \frac{3N^2 - 23N - 20}{(N-1)N(N+1)^2(N+2)} \zeta_2 \right. \\ \left. + \frac{2P_6(N)}{(N-1)N(N+1)^4(N+2)^3} \right\}, \quad (\text{E.12})$$

$$P_6(N) = 14N^6 + 56N^5 + 153N^4 + 139N^3 - 414N^2 - 908N - 448.$$

$$A_l^{Qq} = T_R C_A \left\{ \frac{1}{\varepsilon^2} \left[ \frac{16}{N} S_1(N) + 8 \frac{2N^3 + 5N^2 + 4N + 2}{N^2(N+1)^2} \right] + \frac{1}{\varepsilon} \left[ \frac{4}{N} S_2(N) + \frac{4}{N} S_1^2(N) \right. \right. \\ \left. \left. - \frac{16}{N(N+1)} S_1(N) - 4 \frac{4N^6 + 30N^5 + 55N^4 + 38N^3 + 4N^2 - 10N - 4}{N^3(N+1)^3(N+2)} \right] \right. \\ \left. + \frac{8}{N} S_{2,1}(N) + \frac{4}{3N} S_3(N) + \frac{2}{N} S_2(N) S_1(N) + \frac{2}{3N} S_1^3(N) + \frac{4}{N} S_1(N) \zeta_2 \right. \\ \left. - 4 \frac{2N^3 + 2N^2 - N - 2}{N^2(N+1)^2} S_2(N) - \frac{4}{N(N+1)} S_1^2(N) + 2 \frac{2N^3 + 5N^2 + 4N + 2}{N^2(N+1)^2} \zeta_2 \right. \\ \left. - 4 \frac{(N+2)(2N+1)}{N^2(N+1)^2} S_1(N) + 2 \frac{P_7(N)}{N^4(N+1)^4(N+2)} \right\}, \quad (\text{E.13})$$

$$P_7(N) = 8N^8 + 68N^7 + 164N^6 + 171N^5 + 78N^4 + 12N^3 + 14N^2 + 14N + 4.$$

$$A_m^{Qq} = T_R C_F \left\{ \frac{1}{\varepsilon^2} \frac{8(N^2 - 2N - 2)}{N^2(N+1)^2} - \frac{1}{\varepsilon} \frac{4(2N^5 + 11N^4 + 12N^3 + 2N^2 + 6N + 4)}{N^3(N+1)^3(N+2)} \right. \\ \left. + 4 \frac{N^2 - 2N - 2}{N^2(N+1)^2} S_2(N) + 2 \frac{N^2 - 2N - 2}{N^2(N+1)^2} \zeta_2 + \frac{2P_8(N)}{N^4(N+1)^4(N+2)} \right\}, \quad (\text{E.14})$$

$$P_8(N) = 2N^6 + 7N^5 + 12N^4 + 6N^3 - 8N^2 - 10N - 4.$$

$$A_n^{Qq} = T_R C_A \left\{ \frac{1}{\varepsilon^2} \left[ 8 \frac{2N^2 + 3N + 2}{N(N+1)(N+2)} S_1(N) - 8 \frac{N(N+3)}{(N+1)^2(N+2)} \right] \right. \\ \left. + \frac{1}{\varepsilon} \left[ -16 \frac{N-1}{N(N+1)} S_{-2}(N) - 2 \frac{10N^2 + 21N + 6}{N(N+1)(N+2)} S_2(N) \right. \right. \\ \left. \left. + 2 \frac{2N^2 + 3N + 2}{N(N+1)(N+2)} S_1^2(N) - 4 \frac{N^5 + 6N^4 + 4N^3 - 30N^2 - 40N - 8}{N^2(N+1)^2(N+2)^2} S_1(N) \right] \right\}$$

$$\begin{aligned}
& +4 \frac{2N^4 + 11N^3 + 15N^2 + 12N + 8}{(N+1)^3(N+2)^2} \Big] + 16 \frac{N-1}{N(N+1)} S_{-2,1}(N) \\
& +4 \frac{4N^2 + 5N - 2}{N(N+1)(N+2)} S_{2,1}(N) - 8 \frac{N-1}{N(N+1)} S_{-3}(N) \\
& -2 \frac{28N^2 + 45N - 14}{3N(N+1)(N+2)} S_3(N) - 16 \frac{N-1}{N(N+1)} S_{-2}(N) S_1(N) \\
& - \frac{6N^2 + 5N - 18}{N(N+1)(N+2)} S_2(N) S_1(N) + \frac{2N^2 + 3N + 2}{3N(N+1)(N+2)} S_1^3(N) \\
& +2 \frac{2N^2 + 3N + 2}{N(N+1)(N+2)} \zeta_2 S_1(N) + 16 \frac{N^2 - N - 4}{(N+1)^2(N+2)} S_{-2}(N) \\
& + \frac{7N^5 + 26N^4 + 16N^3 - 58N^2 - 88N - 24}{N^2(N+1)^2(N+2)^2} S_2(N) \\
& - \frac{N^5 + 6N^4 + 4N^3 - 30N^2 - 40N - 8}{N^2(N+1)^2(N+2)^2} S_1^2(N) - 2 \frac{N(N+3)}{(N+1)^2(N+2)} \zeta_2 \\
& +2 \frac{P_9(N)}{N(N+1)^3(N+2)^3} S_1(N) - 2 \frac{P_{10}(N)}{(N+1)^4(N+2)^3} \Big\} , \tag{E.15}
\end{aligned}$$

$$\begin{aligned}
P_9(N) &= 2N^6 + 20N^5 + 40N^4 - 45N^3 - 170N^2 - 100N + 8 , \\
P_{10}(N) &= 4N^6 + 32N^5 + 91N^4 + 123N^3 + 62N^2 - 32N - 40 .
\end{aligned}$$

$$\begin{aligned}
A_o^{Qg} &= T_{RC_A} \left\{ \frac{1}{\varepsilon^2} \left[ -\frac{16}{N(N+2)} S_1(N) - 8 \frac{N^2 + 7N + 8}{(N+1)^2(N+2)^2} \right] \right. \\
& + \frac{1}{\varepsilon} \left[ -\frac{4}{N(N+2)} S_2(N) - \frac{4}{N(N+2)} S_1^2(N) + 4 \frac{2N^2 + 9N + 12}{N(N+1)(N+2)^2} S_1(N) \right. \\
& + 4 \frac{(11N^3 + 56N^2 + 92N + 49)N}{(N+1)^3(N+2)^3} \Big] - \frac{8}{N(N+2)} S_{2,1}(N) \\
& - \frac{4}{3N(N+2)} S_3(N) - \frac{2}{N(N+2)} S_2(N) S_1(N) - \frac{2}{3N(N+2)} S_1^3(N) \\
& - \frac{4}{N(N+2)} S_1(N) \zeta_2 + \frac{10N^3 + 31N^2 + 41N + 28}{N(N+1)^2(N+2)^2} S_2(N) \\
& + \frac{2N^2 + 9N + 12}{N(N+1)(N+2)^2} S_1^2(N) - 2 \frac{N^2 + 7N + 8}{(N+1)^2(N+2)^2} \zeta_2 \\
& \left. + 2 \frac{4N^4 + 16N^3 - 4N^2 - 61N - 48}{N(N+1)^2(N+2)^3} S_1(N) - 2 \frac{P_{11}(N)}{(N+1)^4(N+2)^4} \right\} , \tag{E.16}
\end{aligned}$$

$$P_{11}(N) = 28N^6 + 222N^5 + 684N^4 + 1038N^3 + 811N^2 + 321N + 64 .$$

$$\begin{aligned}
A_p^{Qq} &= T_{RC_A} \left\{ \frac{1}{\varepsilon^2} \left[ -8 \frac{(N-4)}{N(N+1)(N+2)} S_1(N) - 8 \frac{N+4}{(N+1)(N+2)^2} \right] \right. \\
& \left. + \frac{1}{\varepsilon} \left[ 2 \frac{3N+4}{N(N+1)(N+2)} S_2(N) - 2 \frac{N-4}{N(N+1)(N+2)} S_1^2(N) \right] \right\}
\end{aligned}$$

$$\begin{aligned}
& \left. + 4 \frac{N^3 - 17N^2 - 41N - 16}{N(N+1)^2(N+2)^2} S_1(N) + 4 \frac{4N^3 + 26N^2 + 51N + 32}{(N+1)^2(N+2)^3} \right] \\
& - 4 \frac{N-4}{N(N+1)(N+2)} S_{2,1}(N) + \frac{2}{3} \frac{5N+4}{N(N+1)(N+2)} S_3(N) \\
& - \frac{1}{3} \frac{N-4}{N(N+1)(N+2)} S_1^3(N) - \frac{N-4}{N(N+1)(N+2)} S_1(N) S_2(N) \\
& - 2 \frac{N-4}{N(N+1)(N+2)} S_1(N) \zeta_2 - \frac{7N^3 + 17N^2 + 13N + 16}{N(N+1)^2(N+2)^2} S_2(N) \\
& + \frac{N^3 - 17N^2 - 41N - 16}{N(N+1)^2(N+2)^2} S_1^2(N) - 2 \frac{N+4}{(N+1)(N+2)^2} \zeta_2 \\
& + 2 \frac{2N^5 + 48N^4 + 174N^3 + 242N^2 + 161N + 64}{N(N+1)^3(N+2)^3} S_1(N) \\
& - 2 \frac{10N^5 + 92N^4 + 329N^3 + 581N^2 + 507N + 176}{(N+1)^3(N+2)^4} \left. \right\}. \tag{E.17}
\end{aligned}$$

$$A_q^{Qq} = 0. \tag{E.18}$$

$$A_r^{Qq} = 0. \tag{E.19}$$

$$A_{r'}^{Qq} = 0. \tag{E.20}$$

$$\begin{aligned}
A_s^{Qg} = T_R C_A \left\{ -\frac{1}{\varepsilon^2} \frac{8}{N^2(N+1)^2} + \frac{1}{\varepsilon} \frac{4(2N^3 + N^2 - 3N - 1)}{N^3(N+1)^3} - \frac{4}{N^2(N+1)^2} S_2(N) \right. \\
\left. - \frac{2}{N^2(N+1)^2} \zeta_2 - \frac{2P_{12}(N)}{N^4(N+1)^4(N+2)} \right\}, \tag{E.21}
\end{aligned}$$

$$P_{12}(N) = 4N^6 + 4N^5 - 8N^4 - 2N^3 + 16N^2 + 9N + 2.$$

$$\begin{aligned}
A_t^{Qg} = T_R C_A \left\{ \frac{1}{\varepsilon^2} \frac{8(N^2 + 3N + 4)}{(N-1)N(N+1)^2(N+2)} - \frac{1}{\varepsilon} \frac{4(2N^4 + 5N^3 - 3N^2 - 20N - 16)}{(N-1)N(N+1)^3(N+2)^2} \right. \\
+ 4 \frac{N^2 + 3N + 4}{(N-1)N(N+1)^2(N+2)} S_2(N) + 2 \frac{N^2 + 3N + 4}{(N-1)N(N+1)^2(N+2)} \zeta_2 \\
\left. + \frac{2P_{13}(N)}{(N-1)N(N+1)^4(N+2)^3} \right\}, \tag{E.22}
\end{aligned}$$

$$P_{13}(N) = 2N^6 + 4N^5 - 13N^4 - 35N^3 + 14N^2 + 92N + 64.$$

The pure-singlet results are

$$A_a^{Qq} = T_R C_F \left\{ -\frac{1}{\varepsilon^2} \frac{16(N^2 + N - 2)}{N^2(N+1)^2} - \frac{1}{\varepsilon} \frac{8(5N^3 - 5N^2 - 16N - 4)}{N^3(N+1)^3(N+2)} \right. \\ \left. - 8 \frac{N^2 + N - 2}{N^2(N+1)^2} S_2(N) - 4 \frac{N^2 + N - 2}{N^2(N+1)^2} \zeta(2) + \frac{4P_{14}(N)}{N^4(N+1)^4(N+2)^2} \right\}, \quad (\text{E.23})$$

$$P_{14}(N) = N^8 + 7N^7 + 16N^6 - 9N^5 - 26N^4 + 61N^3 + 110N^2 + 44N + 8.$$

$$A_b^{Qq} = T_R C_F \left\{ -\frac{1}{\varepsilon^2} \frac{128}{(N-1)N(N+1)(N+2)} - \frac{1}{\varepsilon} \frac{128(3+2N)}{(N-1)N(N+1)^2(N+2)^2} \right. \\ \left. - \frac{64}{(N-1)N(N+1)(N+2)} S_2(N) - \frac{32}{(N-1)N(N+1)(N+2)} \zeta_2 \right. \\ \left. + \frac{32(N^4 + 6N^3 + N^2 - 24N - 24)}{(N-1)N(N+1)^3(N+2)^3} \right\}. \quad (\text{E.24})$$

The non-singlet results are

$$A_a^{qq,Q} = T_R C_F \left\{ -\frac{1}{\varepsilon^2} \frac{8(N^2 - 2 + N)}{3N(N+1)} - \frac{1}{\varepsilon} \frac{8(N^4 + 2N^3 - 10N^2 - 5N + 3)}{9N^2(N+1)^2} \right. \\ \left. - 4 \frac{11N^6 + 33N^5 - 34N^4 - 57N^3 + 5N^2 + 6N - 9}{27N^3(N+1)^3} - 2 \frac{N^2 - 2 + N}{3N(N+1)} \zeta_2 \right\}. \quad (\text{E.25})$$

$$A_b^{qq,Q} = T_R C_F \left\{ \frac{1}{\varepsilon^2} \left[ -\frac{32}{3} S_1(N) + \frac{32}{3} \right] + \frac{1}{\varepsilon} \left[ \frac{16}{3} S_2(N) - \frac{80}{9} S_1(N) + \frac{32}{9} \right] \right. \\ \left. - \frac{8}{3} S_3(N) - \frac{8}{3} \zeta_2 S_1(N) + \frac{40}{9} S_2(N) + \frac{8}{3} \zeta_2 - \frac{224}{27} S_1(N) + \frac{176}{27} \right\}. \quad (\text{E.26})$$

$$A_c^{qq,Q} = T_R C_F \left\{ -\frac{2}{\varepsilon} - \frac{5}{6} \right\}. \quad (\text{E.27})$$

The results for the 1-particle reducible diagrams  $u$  and  $v$  at  $O(a_s^2)$  follows. Only in these two cases, all prefactors are written explicitly.

$$A_u^{Qg} = a_s^2 S_\varepsilon^2 \left\{ \frac{8}{3\varepsilon} T_R \left( 1 + \frac{\zeta_2}{8} \varepsilon^2 \right) \sum_{i=1}^3 \left( \frac{m_i^2}{\mu^2} \right)^{\varepsilon/2} \right\} \left\{ -8 T_R \left( \frac{m^2}{\mu^2} \right)^{\varepsilon/2} \left( \frac{1}{\varepsilon} \frac{N^2 + 3N + 2}{N(N+1)(N+2)} - \frac{1}{(N+1)(N+2)} + \varepsilon \left( \frac{1}{2(N+1)(N+2)} + \frac{\zeta_2}{8N} \right) \right) \right\}, \quad (\text{E.28})$$

$$A_v^{Qg} = a_s^2 S_\varepsilon^2 \left\{ \frac{8}{3\varepsilon} T_R \left( 1 + \frac{\zeta_2}{8} \varepsilon^2 \right) \sum_{i=1}^3 \left( \frac{m_i^2}{\mu^2} \right)^{\varepsilon/2} \right\} \left\{ 16 T_R \left( \frac{m^2}{\mu^2} \right)^{\varepsilon/2} \times \left( \frac{1}{\varepsilon} - \frac{1}{2} + \varepsilon \left( \frac{1}{4} + \frac{\zeta_2}{8} \right) \right) \frac{1}{(N+1)(N+2)} \right\}. \quad (\text{E.29})$$

The sum of the last two diagrams then reads

$$\begin{aligned} A_u^{Qg} + A_v^{Qg} &= a_s^2 S_\varepsilon^2 \left\{ \frac{8}{3\varepsilon} T_R \left( 1 + \frac{\zeta_2}{8} \varepsilon^2 \right) \sum_{i=1}^3 \left( \frac{m_i^2}{\mu^2} \right)^{\varepsilon/2} \right\} \\ &\quad \left\{ T_R \left( \frac{m^2}{\mu^2} \right)^{\varepsilon/2} 8 \frac{N^2 + N + 2}{N(N+1)(N+2)} \left( -\frac{1}{\varepsilon} - \varepsilon \frac{\zeta_2}{8} \right) \right\} \\ &= a_s^2 S_\varepsilon \left\{ \frac{8}{3\varepsilon} T_R \left( 1 + \frac{\zeta_2}{8} \varepsilon^2 \right) \sum_{i=1}^3 \left( \frac{m_i^2}{\mu^2} \right)^{\varepsilon/2} \right\} \hat{A}_{Qg}^{(1)}. \end{aligned} \quad (\text{E.30})$$

Note that for diagram  $u$  and  $v$  the sum runs over all heavy quark flavors.

## F Momentum Integrals in $D$ dimensions

In order to perform momentum integrals in Minkowski-space, the Wick rotation is applied to obtain the  $D$ -dimensional integral in Euclidean space for all  $D$ -momenta appearing, [28], via

$$p_{0,M} \rightarrow ip'_{0,E} , \quad (\text{F.1})$$

where  $i$  is the imaginary unit and  $M, E$  label the Minkowski and Euclidean space vectors, respectively. At the end of the calculation, this rotation has to be undone for all momenta which were not integrated over. The following integration formulae are all given in Euclidean space and the subscripts  $M, E$  are omitted [79]. The Feynman-parametrization to combine propagators is given by

$$\frac{1}{A_1^{j_1} \dots A_n^{j_n}} = \frac{\Gamma(\sum_{i=1}^n j_i)}{\Gamma(j_1) \dots \Gamma(j_n)} \int_0^1 \dots \int_0^1 dx_1 \dots dx_n \frac{x_1^{j_1-1} \dots x_n^{j_n-1}}{(x_1 A_1 + \dots x_n A_n)^{\sum_{i=1}^n j_i}} \delta\left(\sum_{i=1}^n x_i - 1\right) . \quad (\text{F.2})$$

Symmetric integration in  $D$  dimensions is performed using the following relations, [79]:

$$\int d^D q q^{\nu_1} \dots q^{2\nu_n+1} f(q^2) \equiv 0 , \quad (\text{F.3})$$

$$\int d^D q q^{\nu_1} q^{\nu_2} f(q^2) = \frac{g_{\nu_1 \nu_2}}{D} \int d^D q q^2 f(q^2) , \quad (\text{F.4})$$

$$\int d^D q q^{\nu_1} q^{\nu_2} q^{\nu_3} q^{\nu_4} f(q^2) = \frac{g_{\nu_1 \nu_2} g_{\nu_3 \nu_4} + g_{\nu_1 \nu_3} g_{\nu_2 \nu_4} + g_{\nu_1 \nu_4} g_{\nu_2 \nu_3}}{D(D+2)} \int d^D q q^4 f(q^2) . \quad (\text{F.5})$$

Here  $g_{\nu_1 \nu_2}$  denotes the metric tensor and  $f$  is any function of the type

$$f(q^2) = \frac{(q^2)^r}{(q^2 + R^2)^m} . \quad (\text{F.6})$$

Momentum integrals in  $D$  dimensions, [79, 109]:

$$\int \frac{d^D q}{(2\pi)^D} \frac{(q^2)^r}{(q^2 + R^2)^m} = \frac{\Gamma(r + D/2) \Gamma(m - r - D/2)}{(4\pi)^{D/2} \Gamma(D/2) \Gamma(m)} (R^2)^{r+D/2-m} \quad (\text{F.7})$$

$$\int \frac{d^D q}{(2\pi)^D} \frac{1}{(q^2)^m} = 0 \quad (\text{F.8})$$

Having applied (F.2) when dealing with composite operators, one often encounters integrals of the type

$$I_M := \int \frac{d^D q}{(2\pi)^D} (\Delta q + \Delta p)^M f(q^2) , \quad (\text{F.9})$$

where  $p, \Delta$  are  $D$ -dimensional vectors, and  $\Delta^2 = 0$ ,  $M \in \mathbb{N}$ . One decomposes the sum and the dot product via

$$\begin{aligned} (\Delta q + \Delta p)^M &= \sum_{j=0}^M \binom{M}{j} (\Delta q)^j (\Delta p)^{M-j} \\ &= \sum_{j=0}^M \binom{M}{j} \left\{ \prod_{i=1}^j \Delta_{\nu_i} q^{\nu_i} \right\} (\Delta p)^{M-j} , \end{aligned} \quad (\text{F.10})$$

which yields

$$\begin{aligned}
I_M &= \sum_{j=0}^M \binom{M}{j} (\Delta p)^{M-j} \left\{ \prod_{i=1}^j \Delta_{\nu_i} \right\} \int \frac{d^D q}{(2\pi)^D} \left\{ \prod_{i=1}^M q^{\nu_i} \right\} f(q^2) \\
&= (\Delta p)^M \int \frac{d^D q}{(2\pi)^D} f(q^2),
\end{aligned} \tag{F.11}$$

applying (F.5) and  $\Delta^2 = 0$ .

## G Sums

For the calculation of the following sums, the techniques described in section 7.3 have been applied and use has been made of various results given in [70, 71, 115–117]. Parts of the results are known in the literature, the respective results are listed for convenience.  $N, L, A$  denote arbitrary integers and  $a$  is a complex number.

### G.1 Sums involving Harmonic Sums

$$\sum_{i=1}^{\infty} \frac{S_1(i)^2}{i} = \frac{5}{3}\zeta_3 + \frac{1}{3}\sigma_1^3, \quad (\text{G.1})$$

$$\sum_{i=1}^{\infty} \frac{S_1(i)^2}{i^2} = \frac{17}{10}\zeta_2^2, \quad (\text{G.2})$$

$$\sum_{i=1}^{\infty} \frac{S_1(i)^2}{i+1} = \frac{1}{3}\sigma_1^3 - \frac{4}{3}\zeta_3, \quad (\text{G.3})$$

$$\sum_{i=1}^{\infty} \frac{S_1(i)^2}{i+2} = \frac{1}{3}\sigma_1^3 - \frac{4}{3}\zeta_3 - \zeta_2 - 1, \quad (\text{G.4})$$

$$\sum_{i=1}^{\infty} \frac{S_{1,1}(i)}{i+1} = \frac{1}{6}\sigma_1^3 + \frac{1}{2}\sigma_1\zeta_2 - \frac{5}{3}\zeta_3, \quad (\text{G.5})$$

$$\sum_{i=1}^{\infty} \frac{S_{1,1}(i)}{i+2} = \frac{1}{6}\sigma_1^3 + \frac{1}{2}\sigma_1\zeta_2 - \frac{5}{3}\zeta_3 - \zeta_2, \quad (\text{G.6})$$

$$\sum_{i=1}^{\infty} \frac{1}{i+N} = \sigma_1 - S_1(N), \quad (\text{G.7})$$

$$\sum_{i=1}^{\infty} \frac{S_1(i)}{i+N} = \frac{1}{2}\sigma_1^2 - \frac{1}{2}\zeta_2 - S_{1,1}(N-1), \quad (\text{G.8})$$

$$\sum_{i=1}^{\infty} \frac{S_1(i+N)}{i} = \frac{1}{2}\sigma_1^2 + \frac{1}{2}\zeta_2 + S_{1,1}(N), \quad (\text{G.9})$$

$$\sum_{i=1}^{\infty} \frac{S_1(i+N)}{i^2} = -S_{2,1}(N) + \zeta_2 S_1(N) + 2\zeta_3, \quad (\text{G.10})$$

$$\sum_{i=1}^{\infty} \frac{S_1(i+N)}{i^3} = S_{3,1}(N) - \zeta_2 S_2(N) + \zeta_3 S_1(N) + \frac{1}{2}\zeta_2^2, \quad (\text{G.11})$$

$$\sum_{i=1}^{\infty} \frac{S_1(N+i)}{i+L} = \frac{1}{2}\sigma_1^2 + S_{1,1}(N-L) - \sum_{m=1}^L \frac{S_1(N-L+m)}{m} + \frac{1}{2}\zeta_2, \quad L < N, \quad (\text{G.12})$$

$$\sum_{i=1}^{\infty} \frac{S_1(i+N)}{N+i} = \frac{1}{2}\sigma_1^2 - S_{1,1}(N) + \frac{1}{2}\zeta_2, \quad (\text{G.13})$$

$$\sum_{i=1}^{\infty} \frac{S_1(i+N)}{N+i+1} = \frac{1}{2}\sigma_1^2 - S_{1,1}(N+1) + S_2(N+1) - \frac{1}{2}\zeta_2, \quad (\text{G.14})$$



$$\sum_{i=1}^{\infty} \frac{S_1(i+N)}{N+i+2} = \frac{1}{2}\sigma_1^2 - S_{1,1}(N+2) + S_2(N+2) - \frac{1}{2}\zeta_2 - \frac{1}{N+2}, \quad (\text{G.15})$$

$$\begin{aligned} \sum_{i=1}^{\infty} \frac{S_1(i)^2}{i+N} &= \frac{1}{3}\sigma_1^3 - 2S_{1,1,1}(N-1) + S_{2,1}(N-1) - \zeta_2 S_1(N-1) \\ &\quad - \frac{4}{3}\zeta_3, \end{aligned} \quad (\text{G.16})$$

$$\sum_{i=1}^{\infty} \frac{S_{1,1}(i+N)}{i} = \frac{1}{6}\sigma_1^3 + \frac{1}{2}\sigma_1\zeta_2 + 2S_{1,1,1}(N) + \frac{1}{3}\zeta_3, \quad (\text{G.17})$$

$$\sum_{i=1}^{\infty} \frac{S_{1,1}(i+N)}{i^2} = -2S_{2,1,1}(N) - S_{1,2,1}(N) + \zeta_2 S_{1,1}(N) + 2\zeta_3 S_1(N) + \frac{6}{5}\zeta_2^2, \quad (\text{G.18})$$

$$\sum_{i=1}^{\infty} \frac{S_{1,1}(i+N)}{i+1} = \frac{1}{6}\sigma_1^3 + \frac{1}{2}\sigma_1\zeta_2 + 2S_{1,1,1}(N-1) + \frac{1}{3}\zeta_3 - S_{1,1}(N), \quad (\text{G.19})$$

$$\begin{aligned} \sum_{i=1}^{\infty} \frac{S_{1,1}(i+N)}{i+2} &= \frac{1}{6}\sigma_1^3 + \frac{1}{2}\sigma_1\zeta_2 + 2S_{1,1,1}(N-2) + \frac{1}{3}\zeta_3 - S_{1,1}(N-1) \\ &\quad - \frac{S_{1,1}(N)}{2}, \end{aligned} \quad (\text{G.20})$$

$$\sum_{i=1}^{\infty} \frac{S_2(i)}{i+N} = \sigma_1\zeta_2 - S_1(N-1)\zeta_2 + S_{2,1}(N-1) - 2\zeta_3, \quad (\text{G.21})$$

$$\sum_{i=1}^{\infty} \frac{S_2(i+N)}{i} = \sigma_1\zeta_2 + S_3(N) + S_1(N)S_2(N) - \zeta_2 S_1(N) - \zeta_3, \quad (\text{G.22})$$

$$\sum_{i=1}^{\infty} \frac{S_2(i+N)}{i^2} = -S_{2,2}(N) - 2S_{3,1}(N) + 2\zeta_2 S_2(N) + \frac{7}{10}\zeta_2^2, \quad (\text{G.23})$$

$$\sum_{i=1}^{\infty} \frac{S_1(i+N)S_1(i)}{i} = \frac{1}{3}\sigma_1^3 - S_{2,1}(N) + S_{1,1,1}(N) + \zeta_2 S_1(N) + \frac{5}{3}\zeta_3, \quad (\text{G.24})$$

$$\sum_{i=1}^{\infty} \frac{S_1(i+N)S_1(i)}{i^2} = -S_{2,1,1}(N) + S_{3,1}(N) - \zeta_2 S_2(N) + 2\zeta_3 S_1(N) + \frac{17}{5}\zeta_2^2, \quad (\text{G.25})$$

$$\sum_{i=1}^{\infty} \frac{S_1(i+N)S_1(i)}{i+1} = \frac{1}{3}\sigma_1^3 + S_{1,1,1}(N-1) - \frac{1}{3}\zeta_3, \quad (\text{G.26})$$

$$\sum_{i=1}^{\infty} \frac{S_1(i+N)S_1(i)}{i+2} = \frac{1}{3}\sigma_1^3 + S_{1,1,1}(N-2) - S_1(N-1) - \frac{S_1(N-1)}{N-1} - \frac{1}{3}\zeta_3, \quad (\text{G.27})$$

$$\sum_{i=1}^{\infty} \frac{S_1(i+N)S_1(i)}{i(i+N)} = -\frac{S_{2,1}(N)}{N} + 3\frac{S_{1,1,1}(N)}{N} - 2\frac{S_{1,1}(N)}{N^2} + \zeta_2\frac{S_1(N)}{N} + 2\frac{\zeta_3}{N}, \quad (\text{G.28})$$

$$\sum_{i=1}^N i = \frac{(N+1)N}{2}, \quad (\text{G.29})$$

$$\sum_{i=1}^N S_1(i) = S_1(N)(N+1) - N, \quad (\text{G.30})$$

$$\sum_{i=1}^N iS_1(i) = S_1(N)\frac{(N+1)N}{2} + \frac{N(1-N)}{4}, \quad (\text{G.31})$$

$$\sum_{i=1}^N S_2(i) = S_2(N)(N+1) - S_1(N), \quad (\text{G.32})$$

$$\sum_{i=1}^N iS_2(i) = S_2(N)\frac{(N+1)N}{2} + \frac{S_1(N) - N}{2}, \quad (\text{G.33})$$

$$\sum_{i=1}^N \frac{S_1(i)}{N+1-i} = 2S_{1,1}(N+1) - 2S_2(N+1), \quad (\text{G.34})$$

$$\sum_{i=1}^N \frac{S_2(i)}{N+1-i} = 2S_{2,1}(N+1) + S_{1,2}(N+1) - 3S_3(N+1), \quad (\text{G.35})$$

$$\begin{aligned} \sum_{i=1}^N \frac{S_3(i)}{N+1-i} &= 2S_{3,1}(N+1) + S_{2,2}(N+1) + S_{1,3}(N+1) \\ &\quad - 4S_4(N+1), \end{aligned} \quad (\text{G.36})$$

$$\begin{aligned} \sum_{i=1}^N \frac{S_{1,2}(i)}{N+1-i} &= 2S_{1,1,2}(N+1) + 2S_{1,2,1}(N+1) - 3S_{1,3}(N+1) \\ &\quad - S_{2,2}(N+1), \end{aligned} \quad (\text{G.37})$$

$$\begin{aligned} \sum_{i=1}^{\infty} i \left[ S_1(i) - S_1(i+N) \right] &= -N\sigma_0 + \sigma_1 \frac{N(N+1)}{2} - S_1(N) \frac{N(N+1)}{2} \\ &\quad - \frac{N(1-N)}{4}, \end{aligned} \quad (\text{G.38})$$

$$\sum_{i=1}^{\infty} \left[ S_1(i) - S_1(i+N) \right]^2 = -2S_{1,1}(N) + (N+1)S_2(N) - S_1(N) + N\zeta_2, \quad (\text{G.39})$$

$$\begin{aligned} \sum_{i=1}^{\infty} i \left[ S_1(i) - S_1(i+N) \right]^2 &= \sigma_1 N^2 + \frac{3}{2}N^2 + S_1(N) \left( \frac{1}{2} - N^2 \right) \\ &\quad - \frac{N(N+1)}{2} \left[ S_2(N) + \zeta_2 \right], \end{aligned} \quad (\text{G.40})$$

$$\sum_{i=1}^{\infty} \left[ S_2(i) - S_2(i+N) \right] = (N+1)S_2(N) - N\zeta_2 - S_1(N), \quad (\text{G.41})$$

$$\sum_{i=1}^{\infty} \left[ S_1(i) - S_1(i+N) \right] = -N\sigma_1 + (N+1)S_1(N) - N, \quad (\text{G.42})$$

$$\begin{aligned} \sum_{i=1}^{\infty} i \left[ S_2(i) - S_2(i+N) \right] &= -N\sigma_1 - \frac{(N+1)N}{2} S_2(N) + N(N+1) \frac{\zeta_2}{2} \\ &\quad + S_1(N) \left( N + \frac{1}{2} \right) - \frac{N}{2}, \end{aligned} \quad (\text{G.43})$$

$$\sum_{k=1}^{\infty} \sum_{i=1}^{\infty} \frac{S_1(k+i+N)}{(k+i)(N+k)k} = \frac{1}{2}\sigma_1^2 \frac{S_1(N)}{N} + 2 \frac{S_{1,1}(N)}{N^2} - \frac{1}{2}\zeta_2 \frac{S_1(N)}{N} - \frac{2\zeta_3}{N}. \quad (\text{G.44})$$

## G.2 Sums involving Beta-Functions

$$\sum_{i=1}^{\infty} \frac{B(N, i)}{i} = \zeta_2 - S_2(N-1), \quad (\text{G.45})$$

$$\sum_{i=1}^{\infty} \frac{B(N, i)}{i+1} = 1 + [S_2(N-1) - \zeta_2](N-1), \quad (\text{G.46})$$

$$\sum_{i=1}^{\infty} \frac{B(N, i)}{i+2} = \frac{5-2N}{4} + [\zeta_2 - S_2(N-1)] \frac{(N-1)(N-2)}{2}, \quad (\text{G.47})$$

$$\begin{aligned} \sum_{i=1}^{\infty} \frac{B(N, i)}{i+3} &= \frac{6N^2 - 33N + 49}{36} \\ &+ [S_2(N-1) - \zeta_2] \frac{(N-1)(N-2)(N-3)}{6}, \end{aligned} \quad (\text{G.48})$$

$$\sum_{i=1}^{\infty} \frac{B(N, i)}{i^2} = \zeta_3 - \zeta_2 S_1(N-1) + S_{1,2}(N-1), \quad (\text{G.49})$$

$$\sum_{i=1}^{\infty} \frac{B(N, i)}{i^3} = \frac{2}{5}\zeta_2^2 + \zeta_2 S_{1,1}(N-1) - S_{1,1,2}(N-1) - \zeta_3 S_1(N-1), \quad (\text{G.50})$$

$$\sum_{i=1}^{\infty} \frac{B(N, i)}{N+i} = \frac{1}{N^2}, \quad (\text{G.51})$$

$$\sum_{i=1}^{\infty} \frac{B(N, i)}{1+N+i} = \frac{N^2 + N + 1}{N^2(N+1)^2}, \quad (\text{G.52})$$

$$\sum_{i=1}^{\infty} \frac{B(N, i)}{2+N+i} = \frac{N^4 + 4N^3 + 7N^2 + 6N + 4}{N^2(N+1)^2(N+2)^2}, \quad (\text{G.53})$$

$$\sum_{i=1}^{\infty} \frac{B(N, i)}{3+N+i} = \frac{N^6 + 9N^5 + 34N^4 + 69N^3 + 85N^2 + 66N + 36}{N^2(N+1)^2(N+2)^2(N+3)^2}, \quad (\text{G.54})$$

$$\begin{aligned} \sum_{i=1}^{\infty} \frac{B(N, i)}{4+N+i} &= \frac{P(N)}{N^2(N+1)^2(N+2)^2(N+3)^2(N+4)^2}, \\ P(N) &= N^8 + 16N^7 + 110N^6 + 424N^5 + 1013N^4 + 1576N^3 \\ &+ 1660N^2 + 1200N + 576, \end{aligned} \quad (\text{G.55})$$

$$\sum_{i=1}^{\infty} \frac{B(N, i)}{(N+i+1)^2} = \frac{(-1)^N}{N(N+1)} [2S_{-2}(N) + \zeta_2] + \frac{N-1}{N(N+1)^3}, \quad (\text{G.56})$$

$$\sum_{i=1}^{\infty} \frac{B(N, i)}{(2+N+i)^2} = 2(-1)^N \frac{2S_{-2}(N+2) + \zeta_2}{N(N+1)(N+2)} + \frac{N^2 + N + 1}{N(N+1)^2(N+2)^2}, \quad (\text{G.57})$$

$$\sum_{i=1}^{\infty} \frac{B(N, i)}{(N+i+1)^3} = \frac{(-1)^N}{N(N+1)} \left[ \zeta_3 + S_1(N+1)\zeta_2 - \zeta_2 + 2S_{1,-2}(N+1) - 2S_{-2}(N+1) + S_{-3}(N+1) \right], \quad (\text{G.58})$$

$$\sum_{i=1}^{\infty} \frac{B(N+1, i)}{N+i} = (-1)^N \left[ 2S_{-2}(N) + \zeta_2 \right], \quad (\text{G.59})$$

$$\sum_{i=1}^{\infty} \frac{B(N+2, i)}{N+i} = (N+1)(-1)^N \left[ 2S_{-2}(N) + \zeta_2 \right] - \frac{1}{N+1}, \quad (\text{G.60})$$

$$\sum_{i=1}^{\infty} \frac{B(N+1, i)}{(N+i)^2} = (-1)^N \left[ \zeta_3 + S_1(N)\zeta_2 + 2S_{1,-2}(N) + S_{-3}(N) \right]. \quad (\text{G.61})$$

### G.3 Sums involving Beta-Functions and Harmonic Sums

$$\sum_{i=1}^{\infty} B(N, i)S_1(i) = \zeta_2 - S_2(N-2), \quad (\text{G.62})$$

$$\sum_{i=1}^{\infty} \frac{B(N, i)S_1(i)}{i} = 2\zeta_3 + S_1(N-1)S_2(N-1) - \zeta_2 S_1(N-1) - S_{2,1}(N-1), \quad (\text{G.63})$$

$$\sum_{i=1}^{\infty} \frac{B(N, i)S_1(i)}{i^2} = \frac{1}{2}\zeta_2^2 + \zeta_2 S_{1,1}(N-1) - 2\zeta_3 S_1(N-1) - S_{1,1,2}(N-1) + S_{1,3}(N-1), \quad (\text{G.64})$$

$$\sum_{i=1}^{\infty} \frac{B(N, i)S_1(i)}{N+i} = \frac{\zeta_2 - S_2(N-1)}{N}, \quad (\text{G.65})$$

$$\sum_{i=1}^{\infty} \frac{B(N, i)S_1(i)}{N+i+1} = \frac{\zeta_2 - S_2(N-1)}{N+1} + \frac{1}{N^3(N+1)}, \quad (\text{G.66})$$

$$\sum_{i=1}^{\infty} \frac{B(N, i)S_1(i)}{N+i+2} = \frac{\zeta_2 - S_2(N+1)}{N+2} + \frac{2N^3 + 2N^2 + 3N + 1}{N^3(N+1)^3}, \quad (\text{G.67})$$

$$\sum_{i=1}^{\infty} \frac{B(N+1, i)S_1(i)}{N+i} = \frac{\zeta_2 - S_2(N)}{N} + (-1)^N \left[ \zeta_3 + S_{-3}(N) - 2\frac{S_{-2}(N)}{N} + 2S_{1,-2}(N) - \frac{\zeta_2}{N} + \zeta_2 S_1(N) \right], \quad (\text{G.68})$$

$$\sum_{i=1}^{\infty} B(N, i)S_1(N+i) = \frac{S_1(N-1)}{N-1} + \frac{2N^2 - 2N + 1}{N^2(N-1)^2}, \quad (\text{G.69})$$

$$\sum_{i=1}^{\infty} \frac{B(N, i)S_1(N+i)}{i} = 2\zeta_3 - 2S_3(N) + S_1(N) \left[ \zeta_2 - S_2(N) \right] + \frac{S_1(N)}{N^2} + \frac{1}{N^3}, \quad (\text{G.70})$$

$$\sum_{i=1}^{\infty} \frac{B(N, i)S_1(N+i-1)}{i} = 2\zeta_3 - 2S_3(N-1) + S_1(N-1) \left[ \zeta_2 - S_2(N-1) \right], \quad (\text{G.71})$$

$$\sum_{i=1}^{\infty} \frac{B(N, i)S_1(N+i)}{N+i} = \frac{S_1(N-1)}{N^2} + \frac{2}{N^3}, \quad (\text{G.72})$$

$$\sum_{i=1}^{\infty} \frac{B(N, i)S_1(N+i)}{N+1+i} = \frac{N^2 + N + 1}{N^2(N+1)^2} S_1(N) - \frac{(-1)^N}{N(N+1)} \left[ 2S_{-2}(N) + \zeta_2 \right] + \frac{1}{N^3}, \quad (\text{G.73})$$

$$\sum_{i=1}^{\infty} \frac{B(N, i)S_1(N+i-1)}{N+1+i} = \frac{N^2 + N + 1}{N^2(N+1)^2} S_1(N) - \frac{(-1)^N}{N(N+1)} \left[ 2S_{-2}(N) + \zeta_2 \right] + \frac{2N+1}{N^3(N+1)^2}, \quad (\text{G.74})$$

$$\begin{aligned} \sum_{i=1}^{\infty} \frac{B(N, i)S_1(N+i)}{N+2+i} &= \frac{N^3 + 2N^2 + 5N + 2}{N^3(N+1)^2(2+N)} \\ &+ \frac{N^4 + 4N^3 + 7N^2 + 6N + 4}{N^2(N+1)^2(N+2)^2} S_1(N) \\ &- \frac{2(-1)^N}{N(N+1)(N+2)} \left[ 2S_{-2}(N) + \zeta_2 \right], \end{aligned} \quad (\text{G.75})$$

$$\begin{aligned} \sum_{i=1}^{\infty} \frac{B(N, i)S_1(N+i-1)}{(N+1+i)^2} &= \frac{(-1)^N}{N(N+1)} \left[ 2S_{-2,1}(N+1) - 2S_{1,-2}(N+1) \right. \\ &+ 4S_{-2}(N+1) + 2\zeta_2 + \zeta_3 - \zeta_2 S_1(N+1) \left. \right] \\ &+ \frac{S_1(N+1)}{N(N+1)^2} + \frac{1}{N(N+1)^3}, \end{aligned} \quad (\text{G.76})$$

$$\sum_{i=1}^{\infty} \frac{B(N+1, i)S_1(N+i)}{N+i} = (-1)^N \left[ 2S_{-2,1}(N) + S_{-3}(N) + 2\zeta_3 \right], \quad (\text{G.77})$$

$$\begin{aligned} \sum_{i=1}^{\infty} \frac{B(N, i)S_1(N+i)}{i^2} &= \frac{1}{2}\zeta_2^2 + \zeta_3 \left[ \frac{2}{N} - S_1(N) \right] + \zeta_2 \left[ \frac{S_1(N)}{N} - 2S_{1,1}(N) \right] \\ &+ S_{2,2}(N) + 2S_{1,3}(N) + S_1(N)S_{1,2}(N) - 2\frac{S_3(N)}{N} \\ &- \frac{S_1(N)S_2(N)}{N}, \end{aligned} \quad (\text{G.78})$$

$$\sum_{i=1}^{\infty} \frac{B(N, i) S_1(N + i - 1)}{i^2} = \frac{1}{2} \zeta_2^2 - \zeta_3 S_1(N - 1) - 2\zeta_2 S_{1,1}(N - 1) + S_{2,2}(N - 1) + 2S_{1,3}(N - 1) + S_1(N - 1) S_{1,2}(N - 1), \quad (\text{G.79})$$

$$\sum_{i=1}^{\infty} B(N, i) S_1(i)^2 = 3\zeta_3 - \zeta_2 S_1(N - 2) + S_{1,2}(N - 2) - 2S_3(N - 2), \quad (\text{G.80})$$

$$\sum_{i=1}^{\infty} B(N, i) S_2(i) = -S_1(N - 2) \zeta_2 + \zeta_3 + S_{1,2}(N - 2), \quad (\text{G.81})$$

$$\begin{aligned} \sum_{i=1}^{\infty} \frac{B(N, i) S_1^2(i)}{i} &= +\frac{17}{10} \zeta_2^2 - 3\zeta_3 S_1(N - 1) + \frac{1}{2} \zeta_2 \left[ S_1^2(N - 1) \right. \\ &\quad \left. - S_2(N - 1) \right] - S_{1,1,2}(N - 1) + S_{2,2}(N - 1) \\ &\quad + 2S_1(N - 1) S_3(N - 1) - 2S_{3,1}(N - 1), \end{aligned} \quad (\text{G.82})$$

$$\begin{aligned} \sum_{i=1}^{\infty} \frac{B(N, i) S_2(i)}{i} &= S_{2,2}(N - 1) - S_{1,1,2}(N - 1) + \zeta_2 S_{1,1}(N - 1) \\ &\quad - \zeta_2 S_2(N - 1) - \zeta_3 S_1(N - 1) + \frac{7}{10} \zeta_2^2, \end{aligned} \quad (\text{G.83})$$

$$\sum_{i=1}^{\infty} \frac{B(N, i) S_2(i)}{N + i} = \frac{-S_1(N - 1) \zeta_2 + \zeta_3 + S_{1,2}(N - 1)}{N}, \quad (\text{G.84})$$

$$\sum_{i=1}^{\infty} \frac{B(N, i) S_2(i)}{1 + N + i} = \frac{-S_1(N) \zeta_2 + \zeta_3 + S_{1,2}(N)}{N + 1} - \frac{S_2(N) - \zeta_2}{N^2}, \quad (\text{G.85})$$

$$\begin{aligned} \sum_{i=1}^{\infty} B(N, i) S_{1,1}(N + i) &= \frac{S_{1,1}(N - 1)}{N - 1} + \frac{S_1(N - 1)}{(N - 1)^2} + \frac{1}{(N - 1)^3} \\ &\quad + \frac{S_1(N - 1)}{N^2} + \frac{2}{N^3}, \end{aligned} \quad (\text{G.86})$$

$$\sum_{i=1}^{\infty} B(N, i) S_{1,1}(N + i - 1) = \frac{S_{1,1}(N - 1)}{N - 1} + \frac{S_1(N - 1)}{(N - 1)^2} + \frac{1}{(N - 1)^3}, \quad (\text{G.87})$$

$$\begin{aligned} \sum_{i=1}^{\infty} \frac{B(N, i) S_{1,1}(N + i)}{i} &= S_{1,1}(N) \left[ \zeta_2 - S_2(N) \right] + \frac{6}{5} \zeta_2^2 - 3S_4(N) \\ &\quad + 2S_1(N) \left[ \zeta_3 - S_3(N) \right] + \frac{S_1(N)}{N^3} + \frac{S_{1,1}(N)}{N^2} + \frac{1}{N^4}, \end{aligned} \quad (\text{G.88})$$

$$\begin{aligned} \sum_{i=1}^{\infty} \frac{B(N, i) S_{1,1}(N + i - 1)}{i} &= S_{1,1}(N - 1) \left[ \zeta_2 - S_2(N - 1) \right] + \frac{6}{5} \zeta_2^2 - 3S_4(N - 1) \\ &\quad + 2S_1(N - 1) \left[ \zeta_3 - S_3(N - 1) \right], \end{aligned} \quad (\text{G.89})$$

$$\sum_{i=1}^{\infty} \frac{B(N, i) S_{1,1}(N+i)}{N+i} = \frac{1}{N} \left[ \frac{S_{1,1}(N)}{N} + \frac{S_1(N)}{N^2} + \frac{1}{N^3} \right], \quad (\text{G.90})$$

$$\begin{aligned} \sum_{i=1}^{\infty} \frac{B(N, i) S_{1,1}(N+i)}{N+i+1} &= \frac{S_1(N)}{N^3} + \frac{S_{1,1}(N)(N^2+N+1)}{N^2(N+1)^2} + \frac{1}{N^4} \\ &\quad - \frac{(-1)^N}{N(N+1)} \left[ 2\zeta_3 + S_{-3}(N) + 2S_{-2,1}(N) \right], \end{aligned} \quad (\text{G.91})$$

$$\begin{aligned} \sum_{i=1}^{\infty} \frac{B(N, i) S_{1,1}(N+i-1)}{N+i+1} &= \frac{S_1(N-1)}{N^2(N+1)} + \frac{S_{1,1}(N-1)(N^2+N+1)}{N^2(N+1)^2} \\ &\quad - \frac{(-1)^N}{N(N+1)} \left[ \zeta_2 + 2\zeta_3 + 2S_{-2}(N-1) \right. \\ &\quad \left. + S_{-3}(N-1) + 2S_{-2,1}(N-1) \right], \end{aligned} \quad (\text{G.92})$$

$$\begin{aligned} \sum_{i=1}^{\infty} B(N, i) S_1(i) S_1(N+i) &= S_1(N-1) \left[ \zeta_2 - S_2(N-1) \right] + 2 \left[ \zeta_3 - S_3(N-1) \right] \\ &\quad + \frac{\zeta_2}{N} - \frac{S_2(N-1)}{N} + \frac{S_1(N-1)}{(N-1)^2} + \frac{2}{(N-1)^3}, \end{aligned} \quad (\text{G.93})$$

$$\begin{aligned} \sum_{i=1}^{\infty} \frac{B(N, i) S_1(i) S_1(N+i)}{i} &= \frac{17}{10} \zeta_2^2 + 2 \frac{\zeta_3}{N} - \zeta_2 \left[ \frac{1}{N^2} + \frac{S_1(N-1)}{N} + 2S_{1,1}(N-1) \right] \\ &\quad + \frac{S_2(N-1)}{N^2} - \frac{S_3(N-1)}{N} + \frac{S_{1,2}(N-1)}{N} \\ &\quad + S_1(N-1) \left( S_3(N-1) + S_{1,2}(N-1) \right) \\ &\quad + S_2(N-1)^2 - S_{2,2}(N-1) - 2S_{3,1}(N-1), \end{aligned} \quad (\text{G.94})$$

$$\begin{aligned} \sum_{i=1}^{\infty} \frac{B(N, i) S_1(i) S_1(N+i)}{N+i} &= \frac{1}{N} \left\{ S_1(N) \left[ \zeta_2 - S_2(N) \right] + 2 \left[ \zeta_3 - S_3(N) \right] \right. \\ &\quad \left. + \frac{S_1(N)}{N^2} + \frac{2}{N^3} \right\}, \end{aligned} \quad (\text{G.95})$$

$$\begin{aligned} \sum_{i=1}^{\infty} \frac{B(N, i) S_1(i) S_1(N+i)}{1+N+i} &= \frac{(-1)^{N+1}}{N(N+1)} \left[ \zeta_3 + \zeta_2 S_1(N) + S_{-3}(N) + 2S_{1,-2}(N) \right] \\ &\quad + \frac{\zeta_2 S_1(N)}{N+1} + S_1(N) \left[ \frac{1}{N^3} - \frac{S_2(N)}{N+1} \right] + \frac{2\zeta_3}{N+1} \\ &\quad - \frac{2S_3(N)}{N+1} + \frac{2}{N^4}, \end{aligned} \quad (\text{G.96})$$

$$\begin{aligned} \sum_{k=1}^{\infty} \sum_{i=1}^{\infty} \frac{(N)_k}{(1)_k} \frac{B(k+i, N)}{k} \frac{S_1(i)}{i} &= \frac{17}{10} \zeta_2^2 - 2\zeta_3 S_1(N-1) + S_{2,2}(N-1) \\ &\quad + S_1(N-1) S_{2,1}(N-1) - 2S_{2,1,1}(N-1). \end{aligned} \quad (\text{G.97})$$

## G.4 Sums involving Beta-Functions and Harmonic Sums with two Free Indexes

$$\sum_{i=1}^{\infty} B(N-a, i+a) = B(1+a, N-1-a), \quad (\text{G.98})$$

$$\begin{aligned} \sum_{i=1}^{\infty} \frac{B(N, i+k)}{i} &= -\frac{d}{dN} B(k, N) \\ &= B(k, N) \left[ S_1(k+N-1) - S_1(N-1) \right], \end{aligned} \quad (\text{G.99})$$

$$\begin{aligned} \sum_{i=1}^{\infty} \frac{B(N, i+k)}{i} S_1(i+N+k-1) &= B(k, N) \left[ 2S_{1,1}(k+N-1) - S_2(N-1) \right. \\ &\quad \left. - S_1(N+k-1)S_1(N-1) \right], \end{aligned} \quad (\text{G.100})$$

$$\begin{aligned} \sum_{i=1}^{\infty} \frac{B(N, i+k)}{i} S_1(i+k-1) &= B(k, N) \left[ S_1(k+N-1)S_1(k-1) - S_2(N-1) \right. \\ &\quad \left. - S_1(k-1)S_1(N-1) + \zeta_2 \right]. \end{aligned} \quad (\text{G.101})$$

## G.5 Sums involving Binomials

$$\sum_{k=0}^{N-1} \binom{N-1}{k} (-1)^k \frac{1}{k+A} = B(N, A), \quad (\text{G.102})$$

$$\sum_{k=0}^{N-1} \binom{N-1}{k} (-1)^k \frac{1}{(k+A)^2} = B(N, A) \left[ S_1(N+A-1) - S_1(A-1) \right], \quad (\text{G.103})$$

$$\begin{aligned} \sum_{k=0}^{N-1} \binom{N-1}{k} (-1)^k \frac{1}{(k+A)^3} &= \frac{B(N, A)}{2} \left[ \left\{ S_1(N+A-1) - S_1(A-1) \right\}^2 \right. \\ &\quad \left. - S_2(A-1) + S_2(N+A-1) \right], \end{aligned} \quad (\text{G.104})$$

$$\sum_{k=1}^{N-1} \binom{N-1}{k} (-1)^k \frac{1}{k} = \lim_{\varepsilon \rightarrow 0} \left\{ B(N, \varepsilon) - \frac{1}{\varepsilon} \right\} = -S_1(N-1), \quad (\text{G.105})$$

$$\sum_{k=1}^{N-1} \binom{N-1}{k} (-1)^k \frac{1}{k^2} = -S_{1,1}(N-1), \quad (\text{G.106})$$

$$\sum_{k=1}^{N-1} \binom{N-1}{k} (-1)^k \frac{1}{k^3} = -S_{1,1,1}(N-1), \quad (\text{G.107})$$

$$\sum_{k=1}^{N-1} \binom{N-1}{k} (-1)^k \frac{1}{(k+1)^2} = \frac{S_1(N)}{N} - 1, \quad (\text{G.108})$$



$$\sum_{k=1}^{N-1} \binom{N-1}{k} (-1)^k \frac{1}{(k+2)^2} = \frac{S_1(N)}{N(N+1)} - \frac{1}{(N+1)^2} - \frac{1}{4}, \quad (\text{G.109})$$

$$\sum_{k=1}^{N-1} \binom{N-1}{k} (-1)^k \frac{1}{(k+3)^2} = \frac{2S_1(N)}{N(N+1)(N+2)} - \frac{5+3N}{(N+1)^2(N+2)^2} - \frac{1}{9}, \quad (\text{G.110})$$

$$\sum_{k=1}^{N-1} \binom{N-1}{k} (-1)^k \frac{1}{(k+1)^3} = \frac{S_{1,1}(N)}{N} - 1, \quad (\text{G.111})$$

$$\sum_{k=1}^{N-1} \binom{N-1}{k} (-1)^k \frac{1}{(k+2)^3} = \frac{S_{1,1}(N)}{N(N+1)} - \frac{S_1(N)}{(N+1)^2} - \frac{1}{(N+1)^3} - \frac{1}{8}, \quad (\text{G.112})$$

$$\begin{aligned} \sum_{k=1}^{N-1} \binom{N-1}{k} (-1)^k \frac{1}{(k+3)^3} &= \frac{2S_{1,1}(N)}{N(N+1)(N+2)} - \frac{(5+3N)S_1(N)}{(N+1)^2(N+2)^2} \\ &+ \frac{N^3 - 8N - 9}{(N+1)^3(N+2)^3} - \frac{1}{27}, \end{aligned} \quad (\text{G.113})$$

$$\sum_{k=1}^{N-1} \binom{N-1}{k} (-1)^k \frac{1}{(k+1)^4} = \frac{S_{1,1,1}(N)}{N} - 1,$$

$$\begin{aligned} \sum_{k=1}^{N-1} \binom{N-1}{k} (-1)^k \frac{1}{(k+2)^4} &= \frac{S_{1,1,1}(N)}{N(N+1)} - \frac{S_{1,1}(N)}{(N+1)^2} - \frac{S_1(N)}{(N+1)^3} - \frac{1}{(N+1)^4} \\ &- \frac{1}{16}, \end{aligned} \quad (\text{G.114})$$

$$\begin{aligned} \sum_{k=1}^{N-1} \binom{N-1}{k} (-1)^k \frac{1}{(k+3)^4} &= \frac{2S_{1,1,1}(N)}{N(N+1)(N+2)} - \frac{(5+3N)S_{1,1}(N)}{(N+1)^2(N+2)^2} \\ &+ \frac{(N^3 - 8N - 9)S_1(N)}{(N+1)^3(N+2)^3} \\ &+ \frac{-17 - 21N - 2N^2 + 6N^3 + 2N^4}{(N+1)^4(N+2)^4} - \frac{1}{81}. \end{aligned} \quad (\text{G.115})$$

## G.6 Sums involving Binomials and Harmonic Sums

Keep in mind that  $S_A(0) := 0$ . Therefore the sums below may begin at  $k = 0$ .

$$\sum_{k=0}^{N-1} \binom{N-1}{k} (-1)^k \frac{S_1(k+A)}{k+A} = B(N, A) \left[ S_1(N+A-1) - S_1(N-1) \right], \quad (\text{G.116})$$

$$\begin{aligned} \sum_{k=0}^{N-1} \binom{N-1}{k} (-1)^k \frac{S_1(k)}{k} &= \lim_{\varepsilon \rightarrow 0} \left\{ B(N, \varepsilon) \left[ S_1(N+\varepsilon-1) - S_1(N-1) \right] \right\} \\ &= \zeta_2 - S_2(N-1), \end{aligned} \quad (\text{G.117})$$

$$\sum_{k=1}^{N-1} \binom{N-1}{k} (-1)^k \frac{S_1(k)}{k^2} = -S_{1,2}(N-1), \quad (\text{G.118})$$

$$\sum_{k=0}^{N-1} \binom{N-1}{k} (-1)^k \frac{S_1(k+1)}{(k+1)^2} = \frac{S_2(N)}{N}, \quad (\text{G.119})$$

$$\sum_{k=0}^{N-1} \binom{N-1}{k} (-1)^k \frac{S_1(k+2)}{(k+2)^2} = \frac{S_2(N)}{N(N+1)} - \frac{1}{(N+1)^3}, \quad (\text{G.120})$$

$$\sum_{k=0}^{N-1} \binom{N-1}{k} (-1)^k \frac{S_1^2(k+1)}{k+1} = -\frac{S_1(N)}{N^2} + \frac{2}{N^3}, \quad (\text{G.121})$$

$$\sum_{k=0}^{N-1} \binom{N-1}{k} (-1)^k \frac{S_1^2(k+2)}{k+2} = -\frac{2N+1}{N^2(N+1)^2} S_1(N) + \frac{N^3+6N^2+6N+2}{N^3(N+1)^3}, \quad (\text{G.122})$$

$$\sum_{k=1}^{N-1} \binom{N-1}{k} (-1)^k \frac{S_2(k)}{k} = -S_{2,1}(N-1), \quad (\text{G.123})$$

$$\sum_{k=1}^{N-1} \binom{N-1}{k} (-1)^k \frac{S_2(k)}{k+1} = -\frac{S_{1,1}(N)}{N} + \frac{S_1(N)}{N^2}, \quad (\text{G.124})$$

$$\sum_{k=1}^{N-1} \binom{N-1}{k} (-1)^k \frac{S_2(k)}{2+k} = -\frac{S_{1,1}(N)}{N(N+1)} + \frac{1-N}{N^2} S_1(N) + \frac{1}{N+1}, \quad (\text{G.125})$$

$$\begin{aligned} \sum_{k=1}^{N-1} \binom{N-1}{k} (-1)^k \frac{S_2(k)}{3+k} &= -\frac{2S_{1,1}(N)}{N(N+1)(N+2)} - \frac{N^2+4N-4}{2(N+2)N^2} S_1(N) \\ &\quad + \frac{N+11}{4(N+1)(N+2)}, \end{aligned} \quad (\text{G.126})$$

$$\sum_{k=1}^{N-1} \binom{N-1}{k} (-1)^k \frac{S_2(k)}{(1+k)^2} = \frac{S_{2,1}(N)}{N} - \frac{S_{1,1,1}(N)}{N}, \quad (\text{G.127})$$

$$\begin{aligned} \sum_{k=1}^{N-1} \binom{N-1}{k} (-1)^k \frac{S_2(k)}{(2+k)^2} &= \frac{S_{2,1}(N)}{N(N+1)} - \frac{S_{1,1,1}(N)}{N(N+1)} + \frac{S_{1,1}(N)}{(N+1)^2} - \frac{N+2}{N(N+1)} S_1(N) \\ &\quad + \frac{2N+3}{(N+1)^2}, \end{aligned} \quad (\text{G.128})$$

$$\begin{aligned} \sum_{k=1}^{N-1} \binom{N-1}{k} (-1)^k \frac{S_2(k)}{(3+k)^2} &= \frac{2S_{2,1}(N)}{N(N+1)(N+2)} - \frac{2S_{1,1,1}(N)}{N(N+1)(N+2)} \\ &\quad + \frac{(3N+5)S_{1,1}(N)}{(N+1)^2(N+2)^2} - \frac{40+38N+9N^2+N^3}{4N(N+1)(N+2)^2} S_1(N) \\ &\quad + \frac{59+66N+18N^2+N^3}{4(N+1)^2(N+2)^2}, \end{aligned} \quad (\text{G.129})$$

$$\sum_{k=0}^{N-1} \binom{N-1}{k} (-1)^k \frac{S_{1,1}(k+A)}{k+A} = \frac{B(N,A)}{2} \left[ \left\{ S_1(N+A-1) - S_1(N-1) \right\}^2 + S_2(N-1+A) - S_2(N-1) \right], \quad (\text{G.130})$$

$$\sum_{k=0}^{N-1} \binom{N-1}{k} (-1)^k \frac{S_{1,1}(k)}{k} = \zeta_3 - S_3(N-1), \quad (\text{G.131})$$

$$\sum_{k=1}^{N-1} \binom{N-1}{k} (-1)^k \frac{S_3(k)}{k} = -S_{2,1,1}(N-1), \quad (\text{G.132})$$

$$\sum_{k=1}^{N-1} \binom{N-1}{k} (-1)^k \frac{S_3(k)}{k+1} = -\frac{S_{1,1,1}(N-1)}{N}, \quad (\text{G.133})$$

$$\sum_{k=1}^{N-1} \binom{N-1}{k} (-1)^k \frac{S_3(k)}{2+k} = -\frac{S_{1,1,1}(N)}{N(N+1)} + \frac{1-N}{N^2} S_{1,1}(N) + \frac{S_1(N)}{N} - \frac{1}{N+1}, \quad (\text{G.134})$$

$$\sum_{k=1}^{N-1} \binom{N-1}{k} (-1)^k \frac{S_3(k)}{3+k} = -\frac{2S_{1,1,1}(N)}{N(N+1)(N+2)} - \frac{N^2+4N-4}{2(N+2)N^2} S_{1,1}(N) + \frac{S_1(N)(N+10)}{4N(N+2)} - \frac{N+19}{8(N+1)(N+2)}, \quad (\text{G.135})$$

$$\sum_{k=0}^{N-1} \binom{N-1}{k} (-1)^k \frac{S_{1,1,1}(k+A)}{k+A} = -\frac{1}{6} \frac{d^3}{dN^3} B(N,A), \quad (\text{G.136})$$

$$\sum_{k=0}^{N-1} \binom{N-1}{k} (-1)^k \frac{S_{1,1,1}(k)}{k} = \frac{2}{5} \zeta_2^2 - S_4(N-1), \quad (\text{G.137})$$

$$\sum_{k=0}^{N-1} \binom{N-1}{k} (-1)^k \frac{S_{2,1}(k)}{k} = \frac{7}{10} \zeta_2^2 - S_{2,2}(N-1), \quad (\text{G.138})$$

$$\begin{aligned} & \sum_{k=0}^{N-1} \binom{N-1}{k} (-1)^k \left\{ -\frac{\zeta_3}{k} + 2\frac{\zeta_2}{k^2} - 2\frac{S_1(k)}{k^3} - \frac{S_{1,1}(k)}{k^2} \right\} \\ &= -\frac{7}{10} \zeta_2^2 + \zeta_3 S_1(N-1) - 2\zeta_2 S_{1,1}(N-1) + S_{1,3}(N-1) + 2S_{1,1,2}(N-1). \end{aligned} \quad (\text{G.139})$$

## G.7 Sums involving Binomials with Two Free Indexes

$$\sum_{k=0}^{L+1} \binom{L+1}{k} \frac{(-1)^k}{N-L+k} = B(N-L, L+2), \quad (\text{G.140})$$

$$\sum_{k=0}^{L+1} \binom{L+1}{k} \frac{(-1)^k}{(N-L+k)^2} = B(N-L, L+2) \left[ S_1(N+L) - S_1(N-L-1) \right], \quad (\text{G.141})$$

$$\sum_{k=0}^{L+1} \binom{L+1}{k} (-1)^k \frac{S_1(N-L+k)}{N-L+k} = B(N-L, L+2) \left[ S_1(N+1) - S_1(L+1) \right], \quad (\text{G.142})$$

$$\begin{aligned} \sum_{k=0}^{L+1} \binom{L+1}{k} (-1)^k \frac{S_1(N-L+k)}{1+N-L+k} &= B(N-L+1, L+2) \left[ S_1(N-L) - S_1(L+1) \right] \\ &= -\frac{d}{dL} B(N-L+1, L+2), \end{aligned} \quad (\text{G.143})$$

## G.8 Other Sums

$$\begin{aligned} \sum_{k=1}^{\infty} \frac{B(k+\varepsilon/2, N+1)}{N+k} &= (-1)^N \left[ 2S_{-2}(N) + \zeta_2 \right] \\ &+ \frac{\varepsilon}{2} (-1)^N \left[ -\zeta_3 + \zeta_2 S_1(N) + 2S_{1,-2}(N) - 2S_{-2,1}(N) \right] \\ &+ \frac{\varepsilon^2}{4} (-1)^N \left[ \frac{2}{5} \zeta_2^2 - \zeta_3 S_1(N) + \zeta_2 S_{1,1}(N) + 2 \left\{ S_{1,1,-2}(N) \right. \right. \\ &\left. \left. + S_{-2,1,1}(N) - S_{1,-2,1}(N) \right\} \right] + O(\varepsilon^3), \end{aligned} \quad (\text{G.144})$$

## G.9 Some Techniques

Consider the sum

$$T_1(N, L) := \sum_{i=1}^{\infty} B(N+L+1, i) A(i+N), \quad (\text{G.145})$$

where  $A$  is some function of  $i+N$ , possibly as well of  $L$ .  $L$  is a fixed integer. If the result for

$$T_2(N, L) := \sum_{i=1}^{\infty} B(N+L, i) A(i+N) \quad (\text{G.146})$$

is known, a difference equation may be formed. Define

$$F(j) := \sum_{i=1}^{\infty} B(j+L+1, i) A(i+j). \quad (\text{G.147})$$

Then

$$\begin{aligned}
& F(j+1) + F(j) \\
&= \sum_{i=1}^{\infty} \int_0^1 dx (1-x)^{j+1+L} x^{i-1} A(i+1+j) + \sum_{i=1}^{\infty} \int_0^1 dx (1-x)^{j+L} x^{i-1} A(i+j) \\
&= \sum_{i=2}^{\infty} \int_0^1 dx (1-x)^{j+1+L} x^{i-2} A(i+j) + \sum_{i=2}^{\infty} \int_0^1 dx (1-x)^{j+L} x^{i-1} A(j+i) \\
&+ \int_0^1 dx (1-x)^{j+L} A(j+1) \\
&= \sum_{i=2}^{\infty} \int_0^1 dx (1-x)^{j+L} A(i+j) \left[ x^{i-2} - x^{i-1} + x^{i-1} \right] + \frac{A(j+1)}{j+L+1} \\
&= \sum_{i=2}^{\infty} \int_0^1 dx (1-x)^{j+L} A(i+j) x^{i-2} + \frac{A(j+1)}{j+L+1} \\
&= \sum_{i=2}^{\infty} B(j+L+1, i-1) A(i+j) + \frac{A(j+1)}{j+L+1} \\
&= \sum_{i=1}^{\infty} B(j+L+1, i) A(i+1+j) + \frac{A(j+1)}{j+L+1}.
\end{aligned}$$

Referring to

$$F(0) := \sum_{i=1}^{\infty} B(L+1, i) A(i), \quad (\text{G.148})$$

the final result can be obtained by summing over  $j$

$$\begin{aligned}
T_1(N, L) &= \sum_{j=1}^N (-1)^{N-j} \left[ F(j) + F(j-1) \right] + (-1)^N F(0) \\
&= \sum_{j=1}^N (-1)^{N-j} \left[ \sum_{i=1}^{\infty} B(j+L, i) A(i+j) + \frac{A(j)}{j+L} \right] + (-1)^N F(0) \\
&= \sum_{j=1}^N (-1)^{N-j} \left[ T_2(j, L) + \frac{A(j)}{j+L} \right] + (-1)^N F(0).
\end{aligned}$$

For  $L = 0$ , this relation takes the form:

$$\begin{aligned}
T_1(N, 0) &= \sum_{i=1}^{\infty} B(N+1, i) A(i+N) = \sum_{j=1}^N (-1)^{N-j} \left[ T_2(j, 0) + \frac{A(j)}{j} \right] + (-1)^N F(0) \\
&= \sum_{j=1}^N (-1)^{N-j} \left[ \sum_{i=1}^{\infty} B(j, i) A(i+j) + \frac{A(j)}{j} \right] + (-1)^N F(0),
\end{aligned}$$

where

$$F(0) = \sum_{i=1}^{\infty} B(1, i) A(i).$$

## H The $\Gamma$ -Function and Related Functions

In the following we summarize relations for the Euler  $\Gamma$ -function and related quantities, cf. [131]. The  $\Gamma$ -function is analytic in the whole complex plane except at simple poles at the non-positive integer arguments. Its inverse is given by Euler's infinite product

$$\frac{1}{\Gamma(z)} = z \exp(\gamma_E z) \prod_{i=1}^{\infty} \left[ \left(1 + \frac{z}{i}\right) \exp(-z/i) \right]. \quad (\text{H.1})$$

The residues of the  $\Gamma$ -function at its poles are given by

$$\text{Res}[\Gamma(z)]_{z=-N} = \frac{(-1)^N}{N!}, \quad N \in \mathbb{N} \cup 0. \quad (\text{H.2})$$

In case of  $\text{Re}(z) > 0$ , it can be expressed by Euler's integral

$$\Gamma(z) = \int_0^{\infty} \exp(-t) t^{z-1} dt, \quad (\text{H.3})$$

from which one can infer the well known functional equation of the  $\Gamma$ -function

$$\Gamma(z+1) = z\Gamma(z). \quad (\text{H.4})$$

Around  $z = 1$ , the series expansion is obtained from

$$\Gamma(1-\varepsilon) = \exp(\varepsilon\gamma_E) \exp\left\{ \sum_{i=2}^{\infty} \zeta_i \frac{\varepsilon^i}{i} \right\}, \quad (\text{H.5})$$

$$|\varepsilon| < 1. \quad (\text{H.6})$$

Here and in (H.1),  $\gamma_E$  denotes the Euler-Mascheroni constant, see Eq. (121). It is related to the spherical factor  $S_\varepsilon$ , section 4.1, as

$$S_\varepsilon^2 = \frac{\exp(\gamma_E)}{(4\pi)^\varepsilon}. \quad (\text{H.7})$$

In (H.5) Riemann's  $\zeta$ -values are given by

$$\zeta_k = \sum_{i=1}^{\infty} \frac{1}{i^k}, \quad 2 \leq k \in \mathbb{N}. \quad (\text{H.8})$$

Functions closely related to the  $\Gamma$ -function are the function  $\psi(z)$ , the Beta-function  $B(A, C)$  and the function  $\beta(z)$ .

The Beta-function is defined as a fraction of  $\Gamma$ -functions as

$$B(A, C) = \frac{\Gamma(A)\Gamma(C)}{\Gamma(A+C)}. \quad (\text{H.9})$$

If  $\text{Re}(A), \text{Re}(C) > 0$ , the following integral representation is valid

$$B(A, C) = \int_0^1 dx x^{A-1} (1-x)^{C-1}. \quad (\text{H.10})$$

For arbitrary values of  $A$ ,  $C$ , (H.10) can be continued analytically by using (H.9, H.1) and expanded around pole terms via (H.2, H.5). Further the Beta-function is related to multiple harmonic sums via, [71],

$$NB(N, 1 - \varepsilon) = 1 + \sum_{l=1}^{\infty} \varepsilon^l \underbrace{S_{1, \dots, 1}}_l(N), \quad |\varepsilon| < 1. \quad (\text{H.11})$$

The  $\psi$ -function is defined as the logarithmic derivative of the  $\Gamma$ -function

$$\psi(x) = \frac{1}{\Gamma(x)} \frac{d}{dx} \Gamma(x). \quad (\text{H.12})$$

$\psi(x)$  and its derivatives can be expressed via single harmonic sums with positive index, cf. (237, 238). The small  $\beta$ -function is given by

$$\beta(x) = \frac{1}{2} \left[ \psi \left( \frac{x+1}{2} \right) - \psi \left( \frac{x}{2} \right) \right]. \quad (\text{H.13})$$

$\beta(x)$  and its derivatives are related to single harmonic sums with negative index, cf. (239,240).

# I Generalized Hypergeometric Series

The generalized hypergeometric function  ${}_P F_Q$  is defined by, cf. [69],

$${}_P F_Q \left[ \begin{matrix} (a_1) \dots (a_P) \\ (b_1) \dots (b_Q) \end{matrix}; z \right] = \sum_{i=0}^{\infty} \frac{(a_1)_i \dots (a_P)_i}{(b_1)_i \dots (b_Q)_i} \frac{z^i}{\Gamma(i+1)}. \quad (\text{I.1})$$

Here  $(c)_n$  is Pochhammer's symbol

$$(c)_n = \frac{\Gamma(c+n)}{\Gamma(c)}. \quad (\text{I.2})$$

In (I.1) there are  $P$  numerator parameters  $a_1 \dots a_P$ ,  $Q$  denominator parameters  $b_1 \dots b_Q$  and one variable  $z$ , all of which may be real or complex. Additionally, the denominator parameters must not be negative integers, since in that case (I.1) is not defined. The generalized hypergeometric series  ${}_P F_Q$  are evaluated at a certain value of  $z$ , which in this thesis is always  $z = 1$ .

Gauss was the first to study this kind of functions, introducing the Gauss function  ${}_2 F_1$ . He proved the theorem, cf. [69],

$${}_2 F_1[a, b; c; 1] = \frac{\Gamma(c)\Gamma(c-a-b)}{\Gamma(c-a)\Gamma(c-b)}, \quad \text{Re}(c-a-b) > 0 \quad (\text{I.3})$$

which is called Gauss' theorem. An integral representation for the Gauss function is given by the integral, cf. [69],

$${}_2 F_1 \left[ \begin{matrix} a, b+1 \\ c+b+2 \end{matrix}; z \right] = \frac{\Gamma(c+b+2)}{\Gamma(c+1)\Gamma(b+1)} \int_0^1 dx x^b (1-x)^c (1-zx)^{-a}, \quad (\text{I.4})$$

provided that the conditions

$$|z| < 1, \quad \text{Re}(c+1), \text{Re}(b+1) > 0, \quad (\text{I.5})$$

are obeyed. All parameter integrals emerging in this calculation may be cast into the form (I.4). Subsequent parameter integrations yield the final result in form of a generalized hypergeometric series, except for some integrals stemming from diagrams  $f$ ,  $n$  and  $i$ . The series can then be expanded in the dimensional regularization parameter  $\varepsilon$ , provided that the series is convergent if one sets  $\varepsilon = 0$ . If this is not the case, one has to find a way to calculate the hypergeometric series explicitly to extract the  $\varepsilon$  dependence. Let us consider e.g.

$${}_2 F_1 \left[ \begin{matrix} 1, 1 \\ 2 + \varepsilon \end{matrix}; 1 \right] = \frac{\Gamma(2+\varepsilon)\Gamma(\varepsilon)}{\Gamma(1+\varepsilon)^2} = \frac{1}{\varepsilon} + 1, \quad (\text{I.6})$$

where Gauss's theorem has been used. Therefore this series is divergent as  $\varepsilon \rightarrow 0$ , which can be seen by

$${}_2 F_1 \left[ \begin{matrix} 1, 1 \\ 2 \end{matrix}; 1 \right] = \sum_{i=0}^{\infty} \frac{1}{i+1} = \sigma_1 = \infty. \quad (\text{I.7})$$

However, this case only occurred in the simple case of a Gauss series as described above, of which a closed expression is known.



Expanding a hypergeometric series in  $\varepsilon$  amounts to expanding the Pochhammer symbol. In doing so, one has to keep in mind that

$$(\varepsilon)_0 \equiv 1 . \quad (\text{I.8})$$

Thus one cannot expand terms of the form  $(\varepsilon)_i$  as

$$(\varepsilon)_i = \Gamma(i)\varepsilon + O(\varepsilon^2) , \quad (\text{I.9})$$

if the summation parameter  $i$  runs from  $0 \dots \infty$ . Hence all terms of the infinite sums in which the argument of a Pochhammer symbol plus the value of the summation parameter are equal to a negative integer or 0 as  $\varepsilon \rightarrow 0$ , can only be expanded after assuming a specific value for  $i$ . One has to separate the respective sums into two different terms, one which has to be summed from  $a \dots \infty$  and one from  $0 \dots a$ , where  $a$  is an integer of fixed value, typically  $a = 0, 1, 2$ .

A shorthand notation for products of  $\Gamma$ -functions is

$$\Gamma \left[ \begin{matrix} a_1, \dots, a_i \\ b_1, \dots, b_j \end{matrix} \right] := \frac{\Gamma(a_1) \dots \Gamma(a_i)}{\Gamma(b_1) \dots \Gamma(b_j)} . \quad (\text{I.10})$$

The only generalized hypergeometric series which had to be dealt with was  ${}_3F_2[a, b, c; d, e; 1]$ , for which a variety of summation theorems exist in the literature, cf. [69]. One defines the parametric excess of the series by  $s := d + e - a - b - c$ . Saalschütz's theorem, cf. [69], states that

$${}_3F_2 \left[ \begin{matrix} a, b, c \\ d, e \end{matrix} ; 1 \right] = \Gamma \left[ \begin{matrix} d, 1 + a - e, 1 + b - e, 1 + c - e \\ 1 - e, d - a, d - b, d - c \end{matrix} \right] , \quad (\text{I.11})$$

provided that  $s = 1$  ( $\equiv$  the series is Saalschütizian) and one of the numerator parameters is equal to a negative integer.

Another theorem is a generalization of Dixon's theorem, [69],

$${}_3F_2 \left[ \begin{matrix} a, b, c \\ d, e \end{matrix} ; 1 \right] = \Gamma \left[ \begin{matrix} d, e, s \\ a, b + s, c + s \end{matrix} \right] {}_3F_2 \left[ \begin{matrix} d - a, e - a, s \\ s + b, s + c \end{matrix} ; 1 \right] . \quad (\text{I.12})$$

It can be used to recast sums in a more convenient way. Consider e.g. the following sum in which  $A$  and  $N$  are positive integers

$$\begin{aligned} \sum_{i=1}^{\infty} \frac{B(N, i)}{A + N + i} &= \frac{1}{N(A + N + 1)} {}_3F_2 \left[ \begin{matrix} 1, 1, A + N + 1 \\ A + N + 2, N + 1 \end{matrix} ; 1 \right] \\ &= \frac{1}{N(A + N + 1)} {}_3F_2 \left[ \begin{matrix} 1, 1, A + N + 1 \\ A + N + 2, N + 1 \end{matrix} ; 1 \right] \\ &= \frac{1}{N(A + N + 1)} \Gamma \left[ \begin{matrix} A + N + 2, N + 1, N \\ A + N + 1, N + 1, N + 1 \end{matrix} \right] {}_3F_2 \left[ \begin{matrix} -A, 1, N \\ N + 1, N + 1 \end{matrix} ; 1 \right] \\ &= \sum_{i=0}^A \binom{A}{i} (-1)^i \frac{B(N, i + 1)}{N + i} . \end{aligned} \quad (\text{I.13})$$

Some results for certain values of  $A$  are given in (G.51-G.55).

If one of the numerator parameters exceeds one of the denominator parameters by a positive integer constant, another relation can be proved by induction using Gauss' theorem. It has been also given in Ref. [132] recently and reads

**Corollary 1** *Let  $a, b, d, e \in \mathbf{C}$ ,  $\operatorname{Re}(e - a - b - 1 - k) > 0$ , then  $\forall k \in \mathbf{N}$*

$${}_3F_2 \left[ \begin{matrix} a, b, d+k \\ d, e \end{matrix}; 1 \right] = \Gamma \left[ \begin{matrix} e \\ e-a, e-b \end{matrix} \right] \left[ \sum_{i=0}^k \Gamma(e-a-b-i) \binom{k}{i} \frac{(a)_i (b)_i}{(d)_i} \right]. \quad (\text{I.14})$$

Proof: induction over  $k$

- $k = 0$

$$\begin{aligned} l.s. &= {}_3F_2[a, b, d; d, e; 1] = F_{2,1}[a, b; e; 1] = \Gamma \left[ \begin{matrix} e, e-a-b \\ e-a, e-b \end{matrix} \right] \\ r.s. &= \Gamma \left[ \begin{matrix} e \\ e-a, e-b \end{matrix} \right] \Gamma(e-a-b) = l.s., \quad \checkmark \end{aligned}$$

where (I.3) has been used.

- induction assumption:  
Up to some finite  $k \in \mathbf{N}$

$${}_3F_2[a, b, d+k; d, e; 1] = \Gamma \left[ \begin{matrix} e \\ e-a, e-b \end{matrix} \right] \left[ \sum_{i=0}^k \Gamma(e-a-b-i) \binom{k}{i} \frac{(a)_i (b)_i}{(d)_i} \right]$$

holds  $\forall a, b, d, e \in \mathbf{C}$ .

- $k \rightarrow k+1$

$$\begin{aligned} {}_3F_2[a, b, d+k+1; d, e; 1] &= \sum_{n=0}^{\infty} \frac{1}{n!} \frac{(a)_n (b)_n (d+k+1)_n}{(d)_n (e)_n} \\ &= {}_3F_2[a, b, d+k; d, e; 1] + \frac{1}{d+k} \sum_{n=0}^{\infty} \frac{n}{n!} \frac{(a)_n (b)_n (d+k)_n}{(d)_n (e)_n} \\ &= {}_3F_2[a, b, d+k; d, e; 1] + \frac{ab}{de} {}_3F_2[a+1, b+1, d+k+1; d+1, e+1; 1] = (*) \end{aligned}$$

Now the induction assumption is used

$$\begin{aligned}
(*) &= \Gamma \left[ \begin{matrix} e \\ e-a, e-b \end{matrix} \right] \left[ \sum_{i=0}^k \binom{k}{i} \frac{(a)_i (b)_i}{(d)_i} \Gamma(e-a-b-i) \right. \\
&\quad \left. + \frac{ab}{d} \sum_{i=0}^k \binom{k}{i} \frac{(a+1)_i (b+1)_i}{(d+1)_i} \Gamma(e-a-b-1-i) \right] \\
&= \Gamma \left[ \begin{matrix} e \\ e-a, e-b \end{matrix} \right] \left[ \sum_{i=0}^k \binom{k}{i} \frac{(a)_i (b)_i}{(d)_i} \Gamma(e-a-b-i) \right. \\
&\quad \left. + \sum_{i=1}^{k+1} \binom{k}{i-1} \frac{(a)_i (b)_i}{(d)_i} \Gamma(e-a-b-i) \right] \\
&= \Gamma \left[ \begin{matrix} e \\ e-a, e-b \end{matrix} \right] \left[ \sum_{i=0}^{k+1} \binom{k+1}{i} \frac{(a)_i (b)_i}{(d)_i} \Gamma(e-a-b-i) \right], \tag{I.15}
\end{aligned}$$

where the identity

$$\binom{k}{i} + \binom{k}{i-1} = \binom{k+1}{i} \tag{I.16}$$

has been used.

This ends the proof. □

For the Gauss function, there exists a representation in terms of a complex integral over  $\Gamma$ -functions. It is given by, cf. [69],

$${}_2F_1 \left[ \begin{matrix} a, b \\ c \end{matrix}; z \right] = \frac{\Gamma(c)}{2\pi i \Gamma(a)\Gamma(b)} \int_{-i\infty+\alpha}^{i\infty+\alpha} \frac{\Gamma(a+s)\Gamma(b+s)\Gamma(-s)}{\Gamma(c+s)} (-z)^s ds, \tag{I.17}$$

under the conditions

$$|z| < 1, \quad |\arg(-z)| < \pi. \tag{I.18}$$

(I.17) only holds if one chooses the integration contour in the complex plane and the positive constant  $\alpha$  in such a way that the poles of the  $\Gamma$ -functions containing  $+s$  are separated from those arising from the  $\Gamma$ -functions containing  $-s$  and closes the contour to the right.

Setting  $b = 1$ ,  $c = 1$  in (I.17) one obtains

$${}_1F_0[a; z] = \frac{1}{(1-z)^a}, \tag{I.19}$$

which gives the Mellin-Barnes transformation, cf. [120, 133],

$$\frac{1}{(X+Y)^\lambda} = \frac{1}{2\pi i \Gamma(\lambda)} \int_{-i\infty+\alpha}^{+i\infty+\alpha} ds \Gamma(\lambda+s)\Gamma(-s) \frac{Y^s}{X^{\lambda+s}}. \tag{I.20}$$

The contour has to be chosen as in (I.17) and the conditions  $0 < \alpha < \text{Re}(\lambda)$ ,  $|\arg(x)| < \pi$  have to be fulfilled.

By applying Mellin-Barnes transformations one can express sums of parameters raised to some power in the denominator by their product, thus rendering the evaluation of a parameter integral trivial. One is left with a complex integration, which is usually more complicated than (I.20) and involves several nested integrations. In some cases analytic results for the Mellin-Barnes integrals exist, e.g. Barnes' second lemma, [69],

$$\frac{1}{2\pi i} \int_{-i\infty+\alpha}^{i\infty+\alpha} \Gamma \left[ \begin{matrix} a+s, b+s, c+s, d-s, -s \\ e+s \end{matrix} \right] = \Gamma \left[ \begin{matrix} a, b, c, d+a, d+b, d+c \\ e-a, e-b, e-c \end{matrix} \right], \quad (\text{I.21})$$

provided  $a+b+c+d=e$ ,  $\text{Re}(c+s) > 0$ , and that the integration contour can be chosen in such a way that it separates the poles as outlined above. In a more general case, the first condition might not be fulfilled, but be of the form

$$a+b+c+d+k=e, \quad k \in \mathbb{N}. \quad (\text{I.22})$$

Integrals of this type can be evaluated recursively via the equality, [69],

$$\Gamma \left[ \begin{matrix} a, b, d-a, d-b \\ d \end{matrix} \right] {}_3F_2[a, b, c; d, e; 1] = \Gamma \left[ \begin{matrix} e \\ e-c \end{matrix} \right] \frac{1}{2\pi i} \int_{-i\infty+\alpha}^{+i\infty+\alpha} ds \Gamma \left[ \frac{a+s, b+s, d-a-b-s, e-c+s, -s}{e+s} \right], \quad (\text{I.23})$$

which holds under the condition  $\text{Re}(e-c+s) > 0$  and that the contour separates minus- and plus-poles. Setting  $c=d$  in (I.23) yields Barnes' second lemma via (I.3), whereas  $c=d+k$  yields an expression for the integral in (I.21) under the condition (I.22). By using (I.14) to evaluate the hypergeometric series, one arrives at

$$\begin{aligned} & \frac{1}{2\pi i} \int_{-i\infty+\alpha}^{+i\infty+\alpha} ds \Gamma \left[ \begin{matrix} a+s, b+s, d-a-b-s, e-d-k+s, -s \\ e+s \end{matrix} \right] \\ &= \Gamma \left[ \begin{matrix} a, b, d-a, d-b, e-d-k \\ d, e-a, e-b \end{matrix} \right] \left[ \sum_{i=0}^k \binom{k}{i} \frac{(a)_i (b)_i}{(d)_i} \Gamma(e-a-b-i) \right]. \end{aligned}$$

Substituting  $d \rightarrow d+a+b$ ,  $e \rightarrow c+d+k$ , defining  $e := a+b+c+d+k$ , one observes the new conditions  $\text{Re}(c+d+k-1) > 0$  and  $\text{Re}(c+s) > 0$ , stemming from (I.3, I.23). This yields

$$\begin{aligned} & \frac{1}{2\pi i} \int_{-i\infty+\alpha}^{+i\infty+\alpha} ds \Gamma \left[ \begin{matrix} a+s, b+s, c+s, d-s, -s \\ e+s \end{matrix} \right] \\ &= \Gamma \left[ \begin{matrix} a, b, c, d+a, d+b, d+c \\ e-a, e-b, e-c \end{matrix} \right] \left[ \sum_{i=0}^k \binom{k}{i} (a)_i (b)_i (c+d)_{k-i} (d+a+b+i)_{k-i} \right]. \quad (\text{I.24}) \end{aligned}$$

which holds only if  $a+b+c+d+k=e$ . For  $k=1, 2, 3$ , (I.24) can be found in [120].

## J Parameter Integrals

In the following, we present some sample calculations used in the evaluation of the individual diagrams.

After having performed the momentum integration, one has to take care of the boundaries of the emerging parameter integrals. At most one has to consider the following integral

$$I_1 := \int_0^1 dw \int_0^1 dv \int_0^1 dy f(w, v, y) \delta(y + v + w - 1), \quad (\text{J.1})$$

where  $f$  is any function of the variables  $w, v, y$ . Using the properties of the  $\delta$ -distribution, one can perform the  $y$  integration, yielding

$$\begin{aligned} I_1 &= \int_0^1 dw \int_0^1 dv \int_{-\infty}^{\infty} dy f(w, v, y) \delta(y + v + w - 1) \theta(y) \theta(1 - y) \\ &= \int_0^1 dw \int_0^{1-w} dv f(w, v, 1 - v - w) \\ &= \int_0^1 dv \int_0^{1-v} dw f(w, v, 1 - v - w). \end{aligned} \quad (\text{J.2})$$

When combining five propagators using the Feynman parametrization, one obtains after the momentum integration a four-fold parameter integral. In all diagrams but  $f, n$  and  $i$ , two further parameters can be integrated quite easily, e.g. the general integral of diagram  $d$  looks like

$$I_d = \int_0^1 dx \int_0^1 dw \int_0^{1-w} dv \frac{v^e w^a x^b (1-x)^c}{(x+w-xw)^d}, \quad (\text{J.3})$$

where  $a, b, c, d, e \in \mathbf{R}$ ,  $e \neq -n$ ,  $n \in \mathbf{N}$ . This gives

$$I_d = \frac{1}{e+1} \int_0^1 dx \int_0^1 dw \frac{(1-w)^{e+1} w^a x^b (1-x)^c}{(x+w-xw)^d}, \quad (\text{J.4})$$

and thus one is left with a two-parameter integral. The parameters  $a, b, c, d$ , and  $e$  are in general given in terms of the Mellin-variable  $N \in \mathbf{N}$ , the dimensional regularization parameter  $\varepsilon$  and further additive fixed integers. If  $\varepsilon = 0$ , these integrals diverge in general. In order to isolate the  $\varepsilon$ -dependences explicitly, i.e. to obtain the final result as a Laurent-series in  $\varepsilon$ , analytic continuation has to be performed. This is done by rewriting the integral as a function, of which the behavior in the complex plane is well defined and can therefore be expanded in  $\varepsilon$ . This expansion always amounts to expanding  $\Gamma$ -functions, see Appendix H, and is frequently used in this calculation. The simplest cases of analytic continuation are then obtained by using the integral representation of the Beta-function, see Eq. (H.10). Let us consider e.g. the following divergent integral as  $\varepsilon \rightarrow 0$ ,

$$\int_0^1 dx x^{\varepsilon-1} (1-x)^N = B(\varepsilon, N+1) = \frac{1}{\varepsilon} - S_1(N) + O(\varepsilon). \quad (\text{J.5})$$

This series in  $\varepsilon$  cannot be obtained by simply expanding the integrand of (J.5), which would yield up to  $O(\varepsilon^0)$

$$\int_0^1 dx \left(\frac{1}{x}\right) (1-x)^N = \infty. \quad (\text{J.6})$$

In order to analytically continue more difficult integrals, one makes use of the fact that integrals of the type (J.4) can be rewritten as a hypergeometric series, see Appendix I. Consider e.g.

$$I_1 = \int_0^1 dx \int_0^1 dw \frac{(1-w)^a w^b x^c (1-x)^d}{(x+w-xw)^e}, \quad (\text{J.7})$$

A change of variables  $y := 1 - x$  yields

$$I_1 = \int_0^1 dy \int_0^1 dw (1-w)^a w^b (1-y)^c y^d (1-y(1-w))^{-e}.$$

The  $y$ -integral can be carried out by using the integral representation of the hypergeometric function  ${}_2F_1[a, b; c; z]$ , Eq. (I.4), [69],

$$\begin{aligned} I_1 &= B(d+1, c+1) \int_0^1 dw (1-w)^a w^b {}_2F_1 \left[ \begin{matrix} e, d+1 \\ 2+d+c \end{matrix}; 1-w \right] \\ &= B(d+1, c+1) \sum_{k=0}^{\infty} \frac{(e)_k (d+1)_k}{k! (2+d+c)_k} \int_0^1 dw (1-w)^{a+k} w^b \\ &= B(d+1, c+1) B(a+1, b+1) {}_3F_2 \left[ \begin{matrix} e, d+1, a+1 \\ 2+d+c, 2+a+b \end{matrix}; 1 \right]. \end{aligned} \quad (\text{J.8})$$

This expression can now be safely expanded in  $\varepsilon$ , isolating the pole terms and carrying out the infinite summation afterwards, provided that the generalized hypergeometric series is finite if one sets  $\varepsilon = 0$ , see Appendix I.

In case of  $e = -N$ ,  $N \in \mathbb{N}$  in (J.7), one can derive the expression (J.8) easily by applying the binomial theorem. Thus

$$I_2 = \int_0^1 dx \int_0^1 dv w^a (1-w)^b x^c (1-x)^d (x+w-xw)^N, \quad (\text{J.9})$$

becomes

$$\begin{aligned} I_2 &= \sum_{i=0}^N \binom{N}{i} (-1)^i \int_0^1 dx \int_0^1 dv w^a (1-w)^{b+i} x^c (1-x)^{d+i} \\ &= \sum_{i=0}^N \binom{N}{i} (-1)^i B(a+1, b+i+1) B(c+1, d+i+1) \\ &= B(d+1, c+1) B(a+1, b+1) {}_3F_2 \left[ \begin{matrix} -N, d+1, a+1 \\ 2+d+c, 2+a+b \end{matrix}; 1 \right], \end{aligned} \quad (\text{J.10})$$

see (J.8). Here, one has used the relation, cf. [69],

$$\begin{aligned} (N+1)_{-i} &= \frac{(-1)^i}{(-N)_i}, \\ \rightarrow \binom{N}{i} (-1)^i &= \frac{(-N)_i}{\Gamma(i+1)}. \end{aligned} \quad (\text{J.11})$$

As an illustrative example let us consider now the complete calculation of the scalar five propagator integral of diagram  $e$ . In Minkowski-space it is given by

$$I_{e,a} : = \iint \frac{dq dk}{(2\pi)^{2D}} \frac{(\Delta q)^{N-1}}{(q^2 - m^2)^a ((q-p)^2 - m^2) (k^2 - m^2) ((k-p)^2 - m^2) ((k-q)^2)}. \quad (\text{J.12})$$

Here  $a$  denotes the power of the propagator and is equal to  $a = 1, 2$ . After performing a Wick-rotation for all occurring momenta into Euclidean space and performing the Feynman parametrization to combine the denominators containing the momentum  $k$ , see Appendix F, one obtains

$$I_{e,a} = (-1)^{N+a} \int \frac{dq}{(2\pi)^D} \frac{(\Delta q)^{N-1}}{(q^2 + m^2)^a ((q-p)^2 + m^2)} \int_0^1 dx dy dz \delta(1-x-y-z) \int \frac{dk}{(2\pi)^D} \frac{2}{(k^2 + (x+y)m^2 - 2ykp - 2zqk + zq^2)^3}. \quad (\text{J.13})$$

Now shift  $k \rightarrow k' + zq + yp$ . Using symmetric integration and the fact that  $\Delta^2 = 0$ , see (F.9-F.11), one can perform the  $k$ -integration in  $D$  dimensions

$$I_{e,a} = \frac{(-1)^{N+a} \Gamma(3 - D/2)}{(4\pi)^{D/2}} \int_0^1 dy dz \theta(1-y-z) \int \frac{dq}{(2\pi)^D} \frac{(\Delta q)^{N-1}}{(q^2 + m^2)^a ((q-p)^2 + m^2)} \frac{(z(1-z))^{D/2-3}}{(q^2 + \frac{m^2}{z} - 2\frac{yqp}{1-z})^{3-D/2}}. \quad (\text{J.14})$$

In order to get rid of the Heaviside-function, one shifts  $y \rightarrow (1-z)y'$ . Then one performs another Feynman parametrization to combine the remaining propagators

$$I_{e,a} = \frac{(-1)^{N+a} \Gamma(4 + a - D/2)}{(4\pi)^{D/2}} \int_0^1 dy dz \int_0^1 du dv dw \delta(1-u-v-w) \int \frac{dq}{(2\pi)^D} \frac{(\Delta q)^{N-1} w^{2-D/2} (z(1-z))^{D/2-3} (1-z) u^{a-1}}{(q^2 + m^2(u+v+\frac{w}{z}) - 2qp(v+wy))^{4+a-D/2}}.$$

Shifting  $q \rightarrow q' + (v+wy)p$ , and observing that  $\Delta^2 = 0$ , one can perform the  $q$ -integration, which yields

$$\begin{aligned} I_{e,a} &= \frac{(-\Delta p)^{N+a} \Gamma(4 + a - D/2)}{(4\pi)^{D/2}} \int_0^1 dy dz \int_0^1 du dv dw \delta(1-u-v-w) \\ &\int \frac{dq}{(2\pi)^D} \frac{(v+wy)^{N-1} w^{2-D/2} (z(1-z))^{D/2-3} (1-z) u^{a-1}}{(q^2 + m^2(u+v+\frac{w}{z}))^{4+a-D/2}} \\ &= \frac{(-\Delta p)^{N+a} \Gamma(4 + a - D)}{(4\pi)^D (m^2)^{4+a-D}} \int_0^1 dy dz \int_0^1 dv dw \theta(1-v-w) \\ &\frac{(v+wy)^{N-1} w^{2-D/2} (1-z)^{D/2-2} z^{1+a-D/2} (1-v-w)^{a-1}}{(z+w-wz)^{4+a-D}}. \end{aligned} \quad (\text{J.15})$$

We undo the Wick rotation for the momenta  $p$  and  $\Delta$ , insert  $D = 4 + \varepsilon$  and shift  $v \rightarrow (1 - w)v'$ . The  $y$  integration can then be performed and gives

$$\begin{aligned}
I_{e,a} &= (-1)^{a+1} \frac{(\Delta p)^{N-1} \Gamma(a - \varepsilon)}{(4\pi)^{4+\varepsilon} (m^2)^{a-\varepsilon}} \int_0^1 dy dz dv dw \\
&\quad \frac{((1-w)v + wy)^{N-1} (1-w) w^{-\varepsilon/2} (1-z)^{\varepsilon/2} z^{a-1-\varepsilon/2} (1 - (1-w)v - w)^{a-1}}{(z + w - wz)^{a-\varepsilon}} \\
&= (-1)^{a+1} \frac{(\Delta p)^{N-1} \Gamma(a - \varepsilon)}{N(4\pi)^{4+\varepsilon} (m^2)^{a-\varepsilon}} \int_0^1 dz dv dw \left[ ((1-w)v + w)^N - (1-w)^N v^N \right] \\
&\quad \frac{(1-w)^a w^{-1-\varepsilon/2} (1-z)^{\varepsilon/2} z^{a-1-\varepsilon/2} (1-v)^{a-1}}{(z + w - wz)^{a-\varepsilon}}. \tag{J.16}
\end{aligned}$$

Due to the presence of  $a$ , integrating  $v$  would require to introduce an additional sum. However, only the values  $a = 1, 2$  are needed in this calculation. Setting  $a = 1$ , the  $v$  integration is trivial and yields

$$\begin{aligned}
I_{e,1} &= \frac{(\Delta p)^{N-1} \Gamma(1 - \varepsilon)}{N(N+1)(4\pi)^{4+\varepsilon} (m^2)^{1-\varepsilon}} \int_0^1 dz dw \\
&\quad \frac{(1-w) w^{-1-\varepsilon/2} (1-z)^{\varepsilon/2} z^{-\varepsilon/2}}{(z + w - wz)^{1-\varepsilon}} \left[ \frac{1 - w^{N+1}}{1-w} - (1-w)^N \right] \\
&= \frac{(\Delta p)^{N-1} \Gamma(1 - \varepsilon)}{N(N+1)(4\pi)^{4+\varepsilon} (m^2)^{1-\varepsilon}} \int_0^1 dz dw \\
&\quad \frac{w^{-1-\varepsilon/2} (1-z)^{\varepsilon/2} z^{-\varepsilon/2}}{(z + w - wz)^{1-\varepsilon}} \left[ 1 - w^{N+1} - (1-w)^{N+1} \right]. \tag{J.17}
\end{aligned}$$

The integral is now in the standard form (J.7) and can be rewritten as a generalized hypergeometric series. Further one extracts the spherical factor  $S_\varepsilon$ , see section 4.

$$\begin{aligned}
I_{e,1} &= \frac{S_\varepsilon^2}{(4\pi)^4 (m^2)^{1-\varepsilon}} \frac{(\Delta p)^{N-1}}{N(N+1)} \exp \left\{ \sum_{i=2}^{\infty} \zeta_i \frac{\varepsilon^i}{i} \right\} \left\{ \right. \\
&\quad B(\varepsilon/2 + 1, 1 - \varepsilon/2) B(1, -\varepsilon/2) {}_3F_2 \left[ \begin{matrix} 1 - \varepsilon p, 1, 1 + \varepsilon/2 \\ 2, 1 - \varepsilon/2 \end{matrix}; 1 \right] \\
&\quad - B(\varepsilon/2 + 1, 1 - \varepsilon/2) B(1, N + 1 - \varepsilon/2) {}_3F_2 \left[ \begin{matrix} 1 - \varepsilon p, 1, 1 + \varepsilon/2 \\ 2, N + 2 - \varepsilon/2 \end{matrix}; 1 \right] \\
&\quad \left. - B(\varepsilon/2 + 1, 1 - \varepsilon/2) B(N + 2, -\varepsilon/2) {}_3F_2 \left[ \begin{matrix} 1 - \varepsilon p, N + 2, 1 + \varepsilon/2 \\ 2, N + 2 - \varepsilon/2 \end{matrix}; 1 \right] \right\}. \tag{J.18}
\end{aligned}$$

The generalized hypergeometric series can now be expanded in  $\varepsilon$ . Note that two of the three individual terms in (J.18) contain a single pole term in  $\varepsilon$ . These terms cancel in the complete expression, as has to be expected from dimensional counting. The final sum which has to be



calculated then is

$$\begin{aligned}
I_{e,1} &= \frac{-S_\varepsilon^2}{(4\pi)^4(m^2)^{1-\varepsilon}} \frac{(\Delta p)^{N-1}}{N(N+1)} \exp \left\{ \sum_{i=2}^{\infty} \zeta_i \frac{\varepsilon^i}{i} \right\} \sum_{s=0}^{\infty} \left\{ \frac{S_1(s) - S_1(1+N+s)}{(1+s)} + \frac{B(N+1, s+1)}{(1+s)} \right\} + O(\varepsilon) \\
&= \frac{-S_\varepsilon^2}{(4\pi)^4(m^2)^{1-\varepsilon}} \frac{(\Delta p)^{N-1}}{N(N+1)} \sum_{s=1}^{\infty} \left\{ \frac{S_1(s-1) - S_1(N+s)}{s} + \frac{B(N+1, s)}{s} \right\} + O(\varepsilon) \\
&= \frac{-S_\varepsilon^2}{(4\pi)^4(m^2)^{1-\varepsilon}} \frac{(\Delta p)^{N-1}}{N(N+1)} \sum_{s=1}^{\infty} \left\{ -\frac{1}{s^2} + \frac{S_1(s)}{s} - \frac{S_1(N+s)}{s} + \frac{B(N+1, s)}{s} \right\}. \quad (\text{J.19})
\end{aligned}$$

Here we dropped higher orders in  $\varepsilon$ . Using the sums given in Appendix G one finally obtains

$$\begin{aligned}
I_{e,2} &= \frac{-S_\varepsilon^2}{(4\pi)^4(m^2)^{1-\varepsilon}} \frac{(\Delta p)^{N-1}}{N(N+1)} \sum_{s=1}^{\infty} \left\{ -\frac{1}{s^2} + \frac{S_1(s)}{s} - \frac{S_1(N+s)}{s} + \frac{B(N+1, s)}{s} \right\} \\
&= \frac{-S_\varepsilon^2}{(4\pi)^4(m^2)^{1-\varepsilon}} \frac{(\Delta p)^{N-1}}{N(N+1)} \left\{ -\zeta_2 - S_{1,1}(N) + \zeta_2 - S_2(N) \right\} \\
&= \frac{S_\varepsilon^2}{(4\pi)^4(m^2)^{1-\varepsilon}} (\Delta p)^{N-1} \left\{ \frac{S_1^2(N) + 3S_2(N)}{2N(N+1)} \right\}. \quad (\text{J.20})
\end{aligned}$$

The case  $a = 2$  can be treated in the same way but results in a somewhat longer expression. Performing the  $v$  integration, one obtains the following representation in terms of generalized hypergeometric series

$$\begin{aligned}
I_{e,2} &= \frac{S_\varepsilon^2}{(4\pi)^4(m^2)^{2-\varepsilon}} \frac{(\Delta p)^{N-1}}{N(N+1)(N+2)} \exp \left\{ \sum_{i=2}^{\infty} \zeta_i \frac{\varepsilon^i}{i} \right\} (1-\varepsilon) B(1+\varepsilon/2, 2-\varepsilon/2) \left\{ \right. \\
&\quad -B(-\varepsilon/2, 1) {}_3F_2 \left[ \begin{matrix} 2-\varepsilon, 1, 1+\varepsilon/2 \\ 3, 1-\varepsilon/2 \end{matrix}; 1 \right] \\
&\quad +B(-\varepsilon/2, N+3) {}_3F_2 \left[ \begin{matrix} 2-\varepsilon, N+3, 1+\varepsilon/2 \\ 3, N+3-\varepsilon/2 \end{matrix}; 1 \right] \\
&\quad +(N+1)B(N+1-\varepsilon/2, 2) {}_3F_2 \left[ \begin{matrix} 2-\varepsilon, 2, 1+\varepsilon/2 \\ 3, N+3-\varepsilon/2 \end{matrix}; 1 \right] \\
&\quad \left. +B(N+1-\varepsilon/2, 1) {}_3F_2 \left[ \begin{matrix} 2-\varepsilon, 1, 1+\varepsilon/2 \\ 3, N+2-\varepsilon/2 \end{matrix}; 1 \right] \right\}. \quad (\text{J.21})
\end{aligned}$$

This gives the final result

$$I_{e,2} = \frac{S_\varepsilon^2}{(4\pi)^4(m^2)^{2-\varepsilon}} (\Delta p)^{N-1} \left\{ \frac{S_1(N) - S_2(N) - S_{1,1}(N)}{N(N+1)(N+2)} - \frac{1}{(N+1)^2(N+2)} \right\}. \quad (\text{J.22})$$

## K Mellin Transforms and Polylogarithms

The Mellin transforms used in the present calculation may be found in [70, 115]. As a sample, we present some relations of harmonic sums and Mellin-transforms, which can be written in a more compact form, see also [47].

Define

$$\mathbf{M}[f(x)][N] := \int_0^1 dx f(x) x^{N-1}.$$

Then, cf. [47, 70],

$$\mathbf{M}\left[\frac{1}{1+x}\right][N] = (-1)^{N-1} [\ln(2) + S_{-1}(N-1)], \quad (\text{K.1})$$

$$\mathbf{M}[\text{Li}_4(1-x)][N] = -\frac{S_{1,1,2}(N)}{N} + \frac{\zeta_2 S_{1,1}(N)}{N} - \frac{\zeta_3 S_1(N)}{N} + \frac{2\zeta_2^2}{5N}, \quad (\text{K.2})$$

$$\begin{aligned} \mathbf{M}\left[\frac{\ln(x) \ln(1+x)}{1+x}\right][N] &= (-1)^N \left[ \frac{\zeta_3}{8} - \frac{\zeta_2}{2} S_1(N-1) + \ln(2) \{ S_{-2}(N-1) \right. \\ &\quad \left. - S_2(N-1) \} - S_1(N-1) S_{-2}(N-1) - S_{-3}(N-1) \right. \\ &\quad \left. + S_{-2,1}(N-1) - S_{2,-1}(N-1) \right], \end{aligned} \quad (\text{K.3})$$

$$\begin{aligned} \mathbf{M}\left[\frac{\text{Li}_2(-x)}{1+x}\right][N] &= (-1)^N \left[ -\frac{\zeta_3}{4} + \frac{\zeta_2}{2} \{ S_{-1}(N-1) + \ln(2) \} \right. \\ &\quad \left. + \ln(2) \{ S_2(N-1) - S_{-2}(N-1) \} \right. \\ &\quad \left. + S_{2,-1}(N-1) \right], \end{aligned} \quad (\text{K.4})$$

$$\int_0^1 dx \frac{\text{Li}_2(x)}{1-x} [1-x^N] = \zeta_2 S_1(N) - S_{2,1}(N), \quad (\text{K.5})$$

$$\frac{S_{2,1}(N)}{N} = \mathbf{M}[-2\text{Li}_3(1-x) + \ln(1-x)\text{Li}_2(1-x) + 2\zeta_3][N], \quad (\text{K.6})$$

$$\mathbf{M}[\ln(1+z)](N) = \frac{1}{N} [\ln(2) - \beta(N+1)], \quad (\text{K.7})$$

$$\mathbf{M}[\ln(z) \ln(1+z)](N) = -\frac{1}{N^2} [\ln(2) - \beta(N+1)] - \frac{1}{N} \beta'(N+1), \quad (\text{K.8})$$

$$\begin{aligned} \mathbf{M}[\ln^2(z) \ln(1+z)](N) &= \frac{2}{N^3} [\ln(2) - \beta(N+1)] + \frac{2}{N^2} \beta'(N+1) \\ &\quad - \frac{1}{N} \beta''(N+1), \end{aligned} \quad (\text{K.9})$$

$$\mathbf{M}[\text{Li}_2(-z)](N) = -\frac{\zeta_2}{2N} + \frac{1}{N^2} \left[ \ln(2) - \beta(N+1) \right], \quad (\text{K.10})$$

$$\begin{aligned} \mathbf{M}[\ln(z)\text{Li}_2(-z)](N) &= \frac{\zeta_2}{2N^2} - \frac{2}{N^3} \left[ \ln(2) - \beta(N+1) \right] \\ &\quad - \frac{1}{N^2} \beta'(N+1), \end{aligned} \quad (\text{K.11})$$

$$\mathbf{M}[\text{Li}_2(-z) + \ln(z) \ln(1+z)](N) = -\frac{1}{2N} \left[ \zeta_2 + 2\beta'(N+1) \right], \quad (\text{K.12})$$

$$\mathbf{M}[\text{Li}_3(-z)](N) = -\frac{3}{4N} \zeta_3 + \frac{1}{2N^2} \zeta_2 - \frac{1}{N^3} \left[ \ln(2) - \beta(N+1) \right], \quad (\text{K.13})$$

$$\begin{aligned} \mathbf{M}[\Phi_1(z)](N) &= \frac{1}{N} \left\{ 2\mathbf{M} \left[ \frac{\text{Li}_2(x)}{1+x} \right] (N) - \frac{2}{N} \zeta_2 + \frac{2}{N^2} S_1(N) \right. \\ &\quad \left. + 3\zeta_2 \beta(N+1) + 2S_1(N) \beta'(N+1) - \beta''(N+1) \right. \\ &\quad \left. + \frac{\zeta_3}{4} - \zeta_2 \ln(2) \right\}, \end{aligned} \quad (\text{K.14})$$

where

$$\Phi_1(z) = 2\text{Li}_2(-z) \ln(1+z) + \ln^2(1+z) \ln(z) + 2S_{1,2}(-z). \quad (\text{K.15})$$

$\mathbf{M} \left[ \text{Li}_2(x)/(1+x) \right] (N)$  is a basic function, cf. [88, 110].

Useful relations between Nielsen integrals are, [116, 117],

$$\frac{1}{2^{n-1}} \text{Li}_n(x^2) = \text{Li}_n(x) + \text{Li}_n(-x), \quad (\text{K.16})$$

$$\text{Li}_2(1-z) = -\text{Li}_2(z) - \ln(z) \ln(1-z) + \zeta_2, \quad (\text{K.17})$$

$$\text{Li}_3(1-z) = -S_{1,2}(z) - \ln(1-z) \text{Li}_2(z) - \frac{1}{2} \ln(z) \ln^2(1-z) + \zeta_2 \ln(1-z), \quad (\text{K.18})$$

$$S_{1,2}(1-z) = -\text{Li}_3(z) + \ln(z) \text{Li}_2(z) + \frac{1}{2} \ln(1-z) \ln^2(z) + \zeta_3, \quad (\text{K.19})$$

$$S_{1,3}(1-z) = -\text{Li}_4(z) + \ln(z) \text{Li}_3(z) - \frac{1}{2} \ln(z)^2 \text{Li}_2(z) - \frac{1}{6} \ln^3(z) \ln(1-z) + \zeta_4. \quad (\text{K.20})$$

## L Splitting Functions

We summarize the LO and NLO splitting functions in the  $\overline{\text{MS}}$ -scheme in Mellin space, which are needed to renormalize the operator matrix elements, [33–35, 59, 63–66], They naturally emerge in our calculation and provide partial checks.

$$P_{qq}^{(0)}(N) = 4C_F \left[ -2S_1(N-1) + \frac{(N-1)(3N+2)}{2N(N+1)} \right] \quad (\text{L.1})$$

$$\hat{P}_{qq}^{(0)}(N) = 8T_R \frac{N^2 + N + 2}{N(N+1)(N+2)} \quad (\text{L.2})$$

$$P_{gg}^{(0)}(N) = 8C_A \left[ -S_1(N-1) - \frac{N^3 - 3N - 4}{(N-1)N(N+1)(N+2)} \right] + 2\beta_0 \quad (\text{L.3})$$

$$P_{gq}^{(0)}(N) = 4C_F \frac{N^2 + N + 2}{(N-1)N(N+1)} \quad (\text{L.4})$$

$$\hat{P}_{qq}^{\text{PS},(1)}(N) = 16C_F T_R \frac{5N^5 + 32N^4 + 49N^3 + 38N^2 + 28N + 8}{(N-1)N^3(N+1)^3(N+2)^2} \quad (\text{L.5})$$

$$P_{qq,Q}^{\text{NS},(1)}(N) = \hat{P}_{qq}^{\text{NS},(1)} = C_F T_R \left\{ \frac{160}{9} S_1(N-1) - \frac{32}{3} S_2(N-1) - \frac{4(N-1)(3N+2)(N^2-11N-6)}{9N^2(N+1)^2} \right\} \quad (\text{L.6})$$

$$\begin{aligned} \hat{P}_{gg}^{(1)}(N) = & 8C_F T_R \left\{ 2 \frac{N^2 + N + 2}{N(N+1)(N+2)} [S_1^2(N) - S_2(N)] - \frac{4}{N^2} S_1(N) \right. \\ & \left. + \frac{5N^6 + 15N^5 + 36N^4 + 51N^3 + 25N^2 + 8N + 4}{N^3(N+1)^3(N+2)} \right\} \\ & + 16C_A T_R \left\{ -\frac{N^2 + N + 2}{N(N+1)(N+2)} [S_1^2(N) + S_2(N) - \zeta_2 - 2\beta'(N+1)] \right. \\ & \left. + 4 \frac{2N+3}{(N+1)^2(N+2)^2} S_1(N) + \frac{P_5(N)}{(N-1)N^3(N+1)^3(N+2)^3} \right\}, \quad (\text{L.7}) \end{aligned}$$

where

$$P_5(N) = N^9 + 6N^8 + 15N^7 + 25N^6 + 36N^5 + 85N^4 + 128N^3 + 104N^2 + 64N + 16. \quad (\text{L.8})$$

The splitting functions contribute to the expansion coefficients of the inverse operator renormalization constants  $Z_{O,ij}$  and the transition functions  $\Gamma_{ij}$  in the  $\overline{\text{MS}}$ -scheme, [55, 104, 105],

$$Z_{ij}(\varepsilon, a_s) = \delta_{ij} + a_s S_\varepsilon \left[ -\frac{1}{\varepsilon} P_{ij}^{(0)} \right] + a_s^2 S_\varepsilon^2 \left[ \frac{1}{\varepsilon^2} \left\{ \frac{1}{2} P_{ik}^{(0)} \otimes P_{kj}^{(0)} + (\beta_0 + \beta_{0,Q}) P_{ij}^{(0)} \right\} - \frac{1}{\varepsilon} \delta\alpha_s P_{ij}^{(0)} - \frac{1}{2\varepsilon} P_{ij}^{(1)} \right]. \quad (\text{L.9})$$

$$\Gamma_{ij}(\varepsilon, a_s) = \delta_{ij} + a_s S_\varepsilon \left[ \frac{1}{\varepsilon} P_{ij}^{(0)} \right] + a_s^2 S_\varepsilon^2 \left[ \frac{1}{\varepsilon} \left\{ \frac{1}{2} P_{ik}^{(0)} \otimes P_{kj}^{(0)} + \beta_0 P_{ij}^{(0)} \right\} + \frac{1}{2\varepsilon} P_{ij}^{(1)} \right]. \quad (\text{L.10})$$

For the definition of the  $\beta$ -function, see Eqs. (134, 135).





## References

- [1] E. Rutherford, *Phil. Mag.* **21** (1911) 669.
- [2] E. Rutherford, *Phil. Mag.* **37** (1919) 581.
- [3] J. Chadwick, *Nature* **129** (1932) 312.
- [4] H. Yukawa, *Proc. Phys. Math. Soc. Jap.* **17** (1935) 48.
- [5] R. Frisch and O. Stern, *Z. Phys.* **85** (1933) 4;  
L.W. Alvarez and F. Bloch, *Phys. Rev.* **57** (1940) 111.
- [6] R. Hofstadter and E.E. Chambers, *Phys. Rev.* **103** (1956) 1454;  
D.N. Olsen, H.F. Schopper, R.R. Wilson, *Phys. Rev. Lett.* **6** (1961) 286.
- [7] M. Gell-Mann, *Phys. Lett.* **8** (1964) 214.
- [8] G. Zweig, Preprints, CERN-TH-412 (1964).
- [9] V.E. Barnes et al., *Phys. Rev. Lett.* **12** (1964) 204.
- [10] O.W. Greenberg, *Phys. Rev. Lett.* **13** (1964) 598.
- [11] H. Fritzsche and M. Gell-Mann, *Proc. 16th Int. Conf. on High Energy Physics, Chicago-Batavia*, **2**, (1972) 135, [hep-ph/0208010](#).
- [12] M.Y. Han and Y. Nambu, *Phys. Rev.* **139** (1965) B1006;  
M. Gell-Mann, *Acta Phys. Austr. Suppl.* **9** (1972) 733.
- [13] Y. Nambu, in *Preludes in Theoretical Physics in Honour of V.F. Weisskopf*, ed. A. De-Shalit, H. Fehsbach and L. van Hove, (North-Holland, Amsterdam; Wiley New York, 1966), pp. 133.
- [14] R.E. Taylor, *Rev. Mod. Phys.* **63** (1991) 573;  
H.W. Kendall, *Rev. Mod. Phys.* **63** (1991) 597;  
J.I. Friedman, *Rev. Mod. Phys.* **63** (1991) 615.
- [15] D.H. Coward et al., *Phys. Rev. Lett.* **20** (1968) 292;  
W.K. H. Panofsky, SLAC-PUB-0502, Presented at 14th Int. Conf. on High Energy Physics, Vienna, Aug. 1968, pp. 23;  
E.D. Bloom et al., *Phys. Rev. Lett.* **23** (1969) 930;  
M. Breidenbach et al., *Phys. Rev. Lett.* **23** (1969) 935.
- [16] J.D. Bjorken, *Phys. Rev.* **179** (1969) 1547.
- [17] R.P. Feynman, unpublished;  
R.P. Feynman, *Phys. Rev. Lett.* **23** (1969) 1415;  
R.P. Feynman, *Photon-Hadron Interactions*, (Benjamin, Reading, MA, 1972).
- [18] J.D. Bjorken and E.A. Paschos, *Phys. Rev.* **185** (1969) 1975.
- [19] S. Weinberg, *Phys. Rev. Lett.* **19** (1967) 1264.

- [20] S.L. Glashow, Nucl. Phys. **22** (1961) 579.
- [21] A. Salam and J.C. Ward, Phys. Lett. **13** (1964) 168;  
A. Salam, Weak And Electromagnetic Interactions, in : N. Svartholm (ed.), Elementary Particle Theory, Proceedings Of The Nobel Symposium, (Stockholm, 1968).
- [22] G.'t Hooft and M.J.G. Veltman, Nucl. Phys. **B50** (1972) 318.
- [23] J. C. Taylor, Nucl. Phys. **B33**, 436 (1971);  
A. A. Slavnov, Theor. Math. Phys. **10** (1972) 99, [Teor. Mat. Fiz. **10** (1972) 153].
- [24] B.W. Lee and J. Zinn-Justin, Phys. Rev. **D5** (1972) 3121; 3137; 3155; Phys. Rev. **D7** (1973) 1049.
- [25] G. 't Hooft, Nucl. Phys. **B33** (1971) 173.
- [26] C.N. Yang and R.L. Mills, Phys. Rev. **96** (1954) 191.
- [27] H. Fritzsch, M. Gell-Mann and H. Leutwyler, Phys. Lett. **B47** (1973) 365.
- [28] T. Muta, Foundations of quantum chromodynamics, (World Scientific, Singapore, 2000).
- [29] D.J. Gross and F. Wilczek, Phys. Rev. Lett. **30** (1973) 1343.
- [30] H.D. Politzer, Phys. Rev. Lett. **30** (1973) 1346.
- [31] K.G. Wilson, Phys. Rev. **179** (1969) 1699;  
R.A. Brandt and G. Preparata, Fortschr. Phys. **18** (1970) 249;  
W. Zimmermann, Lect. on Elementary Particle Physics and Quantum Field Theory, Brandeis Summer Inst., Vol. **1**, (MIT Press, Cambridge, 1970), pp. 395;  
Y. Frishman, Ann. Phys. **66** (1971) 373.
- [32] D.J. Gross and S.B. Treiman, Phys. Rev. **D4** (1971) 1059.
- [33] D. J. Gross and F. Wilczek, Phys. Rev. **D8** (1973) 3633.
- [34] D.J. Gross and F. Wilczek, Phys. Rev. **D9** (1974) 980.
- [35] H. Georgi and H. D. Politzer Phys. Rev. **D9** (1974) 416.
- [36] Y. Watanabe et al., Phys. Rev. Lett. **35** (1975) 898.
- [37] C. Chang et al., Phys. Rev. Lett. **35** (1975) 901.
- [38] J.E. Augustin et al. [SLAC-SP-017 Collaboration], Phys. Rev. Lett. **33** (1974) 1406;  
G.S. Abrams et al., Phys. Rev. Lett. **33** (1974) 1453.
- [39] J.J. Aubert et al. [E598 Collaboration], Phys. Rev. Lett. **33** (1974) 1404.
- [40] Z. Maki and M. Nakagawa, Prog. Theor. Phys. **31** (1964) 115;  
Y. Hara, Phys. Rev. **134** (1964) B701;  
J.D. Bjorken and S.L. Glashow, Phys. Lett. **11** (1964) 255.
- [41] W.M. Yao et al. [Particle Data Group], J. Phys. **G33** (2006) 1.



- [42] S.W. Herb et al., Phys. Rev. Lett. **39** (1977) 252.
- [43] F. Abe et al. [CDF Collaboration], Phys. Rev. Lett. **73** (1994) 225; Phys. Rev. **D50** (1994) 2966; Phys. Rev. Lett. **74** (1995) 2626;  
S. Abachi et al. [D0 Collaboration], Phys. Rev. Lett. **74** (1995) 2632.
- [44] E. Witten, Nucl. Phys. **B104** (1976) 445;  
J. Babcock and D. Sivers, Phys. Rev. **D18** (1978) 2301;  
M.A. Shifman, A.I. Vainshtein, and V.I. Zakharov, Nucl. Phys. **B136** (1978) 157;  
J.P. Leveille and T. Weiler, Nucl. Phys. **B147** (1979) 147.
- [45] M. Glück, E. Hoffmann and E.Reya, Z. Phys. **C13** (1982) 119.
- [46] E. Laenen, S. Riemersma, J. Smith and W.L. van Neerven Nucl. Phys. **B392** (1993) 162, 229;  
B. W. Harris and J. Smith, Nucl. Phys. **B452** (1995) 109.
- [47] J. Blümlein, A. De Freitas, W. L. van Neerven and S. Klein, Nucl. Phys. **B755** (2006) 272.
- [48] S.I. Alekhin and J. Blümlein, Phys. Lett. **B594** (2004) 299.
- [49] L.W. Whitlow et al. Phys. Lett. **B250** (1990) 193;  
S. Dasu et al., [E140 collab.], Phys. Rev. **D49** (1994) 5641;  
L.H. Tao et al., [E140x collab.], Z. Phys. **C70** (1996) 387;  
M. Arneodo et al., [NMC collab.], Nucl. Phys. **B483** (1997) 3; **B487** (1997) 3;  
Y. Liang, M.E. Christy, R. Ent and C.E. Keppel, Phys. Rev. **C73** (2006) 065201.
- [50] C. Adloff et al., [H1 collab.], Phys. Lett. **B393** (1997) 452.
- [51] M. Klein, in : Proc of the 12th Int. Workshop on Deep Inelastic Scattering, DIS 2004, Strebske Pleso, 2004, pp. 309;  
J. Feltesse, On a measurement of the longitudinal structure function  $F_L$  at HERA, Proc. of the 2005 Ringberg Workshop on New Trends in HERA Physics, 2005, eds. B. Kniehl, G. Kramer, and W. Ochs.
- [52] S.B. Libby and G. Sterman, Phys. Rev. **D18** (1978) 3252, 4737;  
R.K. Ellis, H. Georgi, M. Machacek, H.D. Politzer and G.G. Ross, Phys. Lett. **B78** (1978) 281;  
D. Amati, R. Petronzio and G. Veneziano, Nucl. Phys. **B140** (1978) 54;  
J.C. Collins, D.E. Soper and G. Sterman, Nucl. Phys. **B261** (1985) 104;  
G.T. Bodwin, Phys. Rev. **D31** (1985) 2616 [Erratum-ibid. **D34** (1986) 3932].
- [53] J.C. Collins, D.E. Soper and G. Sterman, Factorization of Hard Processes in QCD, in : Perturbative QCD, A.H. Mueller, (ed.), (World Scientific, Singapore, 1989), hep-ph/0409313.
- [54] R.E. Taylor, in: Proceedings of the International Symposium on Lepton and Photon interaction at High Energies, Stanford, (1975) 679.
- [55] M. Buza, Y. Matiounine, J. Smith, R. Migneron and W. L. van Neerven, Nucl. Phys. **B472** (1996) 611;  
M. Buza, Y. Matiounine, J. Smith and W. L. van Neerven, Nucl. Phys. **B485** (1997) 420;  
M.D. Buza, PhD Thesis, Charm production in deep inelastic lepton hadron scattering (Amsterdam, 1997).

- [56] W. Furmanski and R. Petronzio, *Z. Phys.* **C11** (1982) 293;  
A. Zee, F. Wilczek, and S.B. Treiman, *Phys. Rev.* **D10** (1974) 2881.
- [57] D.W. Duke, J.D. Kimel, and G.A. Sowell, *Phys. Rev.* **D25** (1982) 71;  
A. Devoto, D.W. Duke, J.D. Kimel, and G.A. Sowell, *Phys. Rev.* **D30** (1984) 541;  
D.I. Kazakov and A.V. Kotikov, *Nucl. Phys.* **B307** (1988) 721; *Phys. Lett.* **B291** (1992) 171;  
D.I. Kazakov, A.V. Kotikov, G. Parente, O.A. Sampayo, and J. Sanchez Guillen *Phys. Rev. Lett.* **65** (1990) 1535;  
J. Sanchez Guillen, J. Miramontes, M. Miramontes, G. Parente, and O.A. Sampayo, *Nucl. Phys.* **B353** (1991) 337;  
S.A. Larin, J.A.M. Vermaseren, *Z. Phys.* **C57** (1993) 93.
- [58] W.L. van Neerven and E.B. Zijlstra, *Phys. Lett.* **B272** (1991) 127;  
E.B. Zijlstra and W.L. van Neerven, *Phys. Lett.* **B273** (1991) 476; *Nucl. Phys.* **B383** (1992) 525.
- [59] S.-O. Moch and J.A.M. Vermaseren, *Nucl. Phys.* **B573** (2000) 853.
- [60] S.A. Larin, T. van Ritbergen, and J.A.M. Vermaseren, *Nucl. Phys.* **B427** (1994) 41;  
S.A. Larin, P. Nogueira, T. van Ritbergen, and J.A.M. Vermaseren, *Nucl. Phys.* **B492** (1997) 338;  
A. Retey and J.A.M. Vermaseren, *Nucl. Phys.* **B604** (2001) 281;  
J. Blümlein and J.A.M. Vermaseren, *Phys. Lett.* **B606** (2005) 130.
- [61] S.-O. Moch, J.A.M. Vermaseren, and A. Vogt, *Phys. Lett.* **B606** (2005) 123.
- [62] J.A.M. Vermaseren, A. Vogt, and S.-O. Moch, *Nucl. Phys.* **B724** (2005) 3.
- [63] E. Fermi, *Z. Phys.* **29** (1924) 315;  
E.L. Williams, *Proc. Roy. Soc. London (A)* **139** (1933) 163; *Phys. Rev.* **45** (1934) 729;  
C.F. v. Weizsäcker, *Z. Phys.* **88** (1934) 612;  
L.N. Lipatov, *Sov. J. Nucl. Phys.* **19** (1974) 164 [*Yad. Fiz.* **19** (1974) 331];  
G. Altarelli and G. Parisi, *Nucl. Phys.* **B126** (1977) 298.
- [64] A. Gonzales-Arroyo, C. Lopez and F.J. Yndurain, *Nucl. Phys.* **B153** (1979) 161;  
A. Gonzales-Arroyo and C. Lopez, *Nucl. Phys.* **B166** (1980) 429.
- [65] E.G. Floratos, C. Kounnas and R. Lacaze, *Phys. Lett.* **B98** (1981) 89,285; *Nucl. Phys.* **B192** (1981) 417.
- [66] G. Curci, W. Furmanski and R. Petronzio, *Nucl. Phys.* **B175** (1980) 27;  
W. Furmanski and R. Petronzio, *Phys. Lett.* **B97** (1980) 437.
- [67] G. Chetyrkin and F.V. Tkachov, *Nucl. Phys.* **B192** (1981) 159.
- [68] N. Nielsen, *Nova Acta Leopoldina*, **90** (1909) 123;  
K.S. Kölbig, *Siam J. Math. Anal.*, **17** (1986) 5.
- [69] L.J. Slater *Generalized Hypergeometric Functions*, (Cambridge University Press, Cambridge, 1966),  
W.N. Bailey, *Generalized Hypergeometric Series*, (Cambridge University Press, Cambridge,

- 1935);  
D.B. Sears, Proc. Lond. Math. Soc. (2) **52** (1951) 467; **53** (1951) 138; 158; 181.
- [70] J. Blümlein and S. Kurth, Phys. Rev. **D60** (1999) 014018.
- [71] J.A.M. Vermaseren, Int. J. Mod. Phys. **A14** (1999) 2037.
- [72] J.A.M. Vermaseren, New features of FORM, math-ph/0010025.
- [73] J. Blümlein, On the Theoretical Status of Deep Inelastic Scattering, hep-ph/9512272;  
B. Lampe and E. Reya, Phys. Rept. **332** (2000) 1.
- [74] J. Blümlein, M. Klein, T. Naumann and T. Riemann, Proc. of DESY Theory Workshop on  
Physics at HERA, Hamburg, West Germany, Oct 12-14, ed. R.D. Peccei, PHE-88-01 (1987)  
39pp.
- [75] R. Hamberg, PhD Thesis, Second order gluonic contributions to physical quantities (Leiden,  
1991).
- [76] B. Povh, K. Rith, C. Scholz, F. Zetsche, Teilchen und Kerne, (Springer, Berlin, 1993).
- [77] E. Reya, Phys. Rep. **69** (1981) 195;  
R.G. Roberts, The structure of the proton, (Cambridge University Press, Cambridge, 1990).
- [78] J. Blümlein, B. Geyer and D. Robaschik, Nucl. Phys. **B560** (1999) 283.
- [79] F.J. Yndurain, Quantum Chromodynamics, (Springer-Verlag, New York, 1983).
- [80] J. Blümlein, Z. Phys. **C65** (1995) 293;  
A. Arbuzov, D.Y. Bardin, J. Blümlein, L. Kalinovskaya and T. Riemann, Comput. Phys.  
Commun. **94** (1996) 128.
- [81] R.D. Field, Applications of perturbative QCD, (The Perseus Books Group, New York, 1989).
- [82] C. Itzykson and J. Zuber, Quantum Field Theory, (Mc Graw-Hill Inc., New York, 1980).
- [83] J. Blümlein and N. Kochelev, Nucl. Phys. **B498** (1997) 285.
- [84] J. Blümlein and A. Tkabladze, Nucl. Phys. **B553** (1999) 427.
- [85] G. Sterman, An Introduction to Quantum Field Theory, (Cambridge University Press, 1993).
- [86] R.L. Jaffe, MIT-CTP-1261 Lectures presented at the Los Alamos School on Quark Nuclear  
Physics, Los Alamos, NM., June, 10-14, 1985.
- [87] L. D. Landau, Nucl. Phys. **13** (1959) 181.  
J. D. Bjorken, PhD Thesis, Stanford University, 1959.
- [88] J. Blümlein, Comput. Phys. Commun. **133** (2000) 76.
- [89] J. Blümlein and S.-O. Moch, Phys. Lett. **B614** (2005) 53.

- [90] C. Nash, Nucl. Phys. **B31** (1971) 419;  
P.V. Landshoff and J.C. Polkinghorne, Phys. Rept. **5** (1972) 1;  
J.D. Jackson, G.G. Ross and R.G. Roberts, Phys. Lett. **B226** (1989) 159;  
R.G. Roberts and G.G. Ross, Phys. Lett. **B373** (1996) 235;  
J. Blümlein and N. Kochelev, Phys. Lett. **B381** (1996) 296;  
J. Blümlein, V. Ravindran and W.L. van Neerven, Phys. Rev. **D68** (2003) 114004.
- [91] S.D. Drell and T.-M. Yan, Ann. Phys. **66** (1971) 578.
- [92] J. Blümlein, Lecture Notes: Introduction into QCD, DESY, (1997).
- [93] C.G. Callan jr. and D.J. Gross, Phys. Rev. Lett. **22** (1969) 156.
- [94] C. G. Bollini and J. J. Giambiagi, Nuovo Cim. **B12** (1972) 20;  
Phys. Lett. **B40** (1972) 566.
- [95] G. 't Hooft and M. J. G. Veltman, Nucl. Phys. **B44** (1972) 189.
- [96] J. F. Ashmore, Lett. Nuovo Cim. **4**, 289 (1972).
- [97] G. M. Cicuta and E. Montaldi, Lett. Nuovo Cim. **4**, 329 (1972).
- [98] E. R. Speer, J. Math. Phys. **15**, 1 (1974).
- [99] G. 't Hooft, Nucl. Phys. **B61** (1973) 455.
- [100] W. A. Bardeen, A. J. Buras, D. W. Duke and T. Muta, Phys. Rev. **D18** (1978) 3998.
- [101] D.R.T. Jones, Nucl. Phys. **B75** (1974) 531;  
W.E. Caswell, Phys. Rev. Lett. **33** (1974) 244;  
O.V. Tarasov, A.A. Vladimirov and A.Y. Zharkov, Phys. Lett. **B93** (1980) 429;  
T. van Ritbergen, J.A.M. Vermaseren and S.A. Larin, Phys. Lett. **B400** (1997) 379.
- [102] S. Bethke, J. Phys. **G26** (2000) R27.
- [103] K.G. Chetyrkin, B.A. Kniehl and M. Steinhauser, Phys. Rev. Lett. **79** (1997) 2184.
- [104] R. Mertig and W.L. van Neerven, Z. Phys. **C70** (1996) 637.
- [105] E.B. Zijlstra and W.L. van Neerven, Nucl. Phys. **B383** (1992) 525.
- [106] J. Blümlein in : Working Group I: Parton distributions: Summary report for the HERA LHC,  
Workshop Proceedings. M. Dittmar et al. hep-ph/0511119.
- [107] J. Blümlein, in preparation.
- [108] I. Bierenbaum, J. Blümlein and S. Klein, Nuc. Phys. (Proc. Suppl.) **B160** (2006) 85.
- [109] J.C. Collins, Renormalization, (Cambridge University Press, Cambridge, 1984).
- [110] J. Blümlein, Comput. Phys. Commun. **159** (2004) 19.
- [111] L. Euler, Novi Comm. Acad. Sci Petropolitanae, **1** (1775) 140.

- [112] D. Zagier, in : Proc. First European Congress Math. Vol. II, (Birkhäuser, Boston, 1994), pp. 497.
- [113] J.M. Borwein, D.M. Bradley, D.J. Broadhurst and P. Lisonek, Trans. Am. Math. Soc. **353** (2001) 907.
- [114] For a uniqueness theorem see, E. Carlson, Thesis, Univ. Uppsala, 1914;  
E.C. Titchmarsh, Theory of Functions, (Oxford University Press, Oxford, 1939), Chapt. 9.5.
- [115] J. Blümlein and H. Kawamura, Nucl. Phys. **B708** (2005) 467.
- [116] J. Blümlein, Collection of Polylog-Integrals, unpublished.
- [117] A. Devoto and D. W. Duke, Riv. Nuovo Cim. **7N6** (1984) 1.
- [118] L.M. Milne-Thomson, The Calculus of finite Differences, (MacMillan, London, 1960).
- [119] V.A. Smirnov, Phys. Lett. **B460** (1999) 397;  
J.B. Tausk, Phys. Lett. **B469** (1999) 225;  
V.A. Smirnov and O.L. Veretin, Nucl. Phys. **B566** (2000) 469;  
V.A. Smirnov, Phys. Lett. **B547** (2002) 239; V.A. Smirnov, Nucl. Phys. Proc. Suppl. **135** (2004) 252;  
M. Czakon, J. Gluza and T. Riemann, Nucl. Phys. **B751** (2006) 1.
- [120] V.A. Smirnov, Evaluating Feynman Integrals, (Springer, Berlin Heidelberg New York, 2004).
- [121] I. Bierenbaum and S. Weinzierl, Eur. Phys. J. **C32** (2003) 67;  
I. Bierenbaum, Dissertation, Univ. Mainz, 2005.
- [122] D. Kreimer, Phys. Rept. **363** (2002) 387;  
A. Connes and D. Kreimer, Annales Henri Poincare **3** (2002) 411.
- [123] M. Czakon, Comput. Phys. Commun. **175** (2006) 559.
- [124] S. Weinzierl, Comput. Phys. Commun. **145** (2002) 357.
- [125] S.-O. Moch and P. Uwer, Comput. Phys. Commun. **174** (2006) 759.
- [126] J. Blümlein, Nucl. Phys. (Proc. Suppl.) **135** (2004) 225;  
J. Blümlein and V. Ravindran, Nucl. Phys. **B716** (2005) 128; Nucl. Phys. **B749** (2006) 1.
- [127] M. Glück, E. Reya and M. Stratmann, Nucl. Phys. **B422** (1994) 37.
- [128] E. G. Floratos, D. A. Ross and C. T. Sachrajda, Nucl. Phys. **B129**, 66 (1977), [Erratum-  
ibid. **B139**, 545 (1978)].
- [129] E. Byckling and K. Kajantie, Particle Kinematics, (John Wiley & Sons, London, 1973).
- [130] G.M. Fichtenholz, Differential- und Integralrechnung, Vol. 3, (Johann Ambrosius Barth, Leipzig, 1992).
- [131] M. Abramowitz and I. A. Stegun, Handbook of Mathematical Functions, (Dover Publications, Inc., New York, 1972).

- [132] M.W. Coffey, On hypergeometric series reductions from integral representations, the Kampé de Fériet function, and elsewhere [math-ph/0608048](#).
- [133] E.W. Barnes, Proc. Lond. Math. Soc. (2) **6** (1907) 141; Quart. J. Math. **41** (1910) 136;  
R.B. Paris and D. Kaminski, *Asymptotics and Mellin-Barnes Integrals*, (Cambridge University Press, Cambridge, 2001).







## Zusammenfassung

Diese Diplomarbeit behandelt die Beiträge der Erzeugung von schweren Quarks zu den Koeffizientenfunktionen der tief-inelastischen Streuung bis zu  $O(a_s^2)$  bei grossen Virtualitäten  $Q^2$ . Die Korrekturen zu den Strukturfunktionen durch schwere Quarks sind relativ groß und können 20–40 Prozent des Gesamtergebnisses ausmachen. Im Falle der unpolarisierten Lepton–Nukleon Streuung bei Ein-Photon Austausch wird der Wirkungsquerschnitt der tief-inelastischen Streuung durch die Strukturfunktionen  $F_2(x, Q^2)$  und  $F_L(x, Q^2)$  beschrieben. Innerhalb der Lichtkegelentwicklung erhält man für Twist  $\tau = 2$  eine Darstellung der Strukturfunktionen als Mellin-Faltung der leichten Parton-Dichten mit den Wilson-Koeffizienten für schwere Quarks. Die Parton-Dichten sind prozessunabhängige nicht-störungstheoretische Grössen, wohingegen die Wilson-Koeffizienten prozessabhängig sind und die Parton-Photon Wechselwirkung beschreiben, welche bei hinreichend grossem  $Q^2$  im Rahmen der Störungstheorie berechnet werden können. Die Berechnung des perturbativen Anteils der Strukturfunktionen vergrössert unser Wissen über die Quantenchromodynamik. Zum Beispiel können hierdurch die universellen Twist  $\tau = 2$  Parton-Dichten aus experimentellen Daten bestimmt und somit die Vorhersagen aus verschiedenen Experimenten verglichen werden. Auch kann der gegenwärtige theoretische Fehler der QCD-Skala  $\Lambda_{QCD}$  durch genauere Kenntnis dieser Beiträge verkleinert werden.

Für die massiven Wilson-Koeffizienten erhält man im Limes  $Q^2 \gg m^2$  eine weitere Faktorisierung. Mittels der Lichtkegelentwicklung kann man zeigen, dass diese dann durch eine Mellin-Faltung der masselosen Wilson-Koeffizienten und der massiven partonischen Operatormatrixelemente gegeben sind. Dies erlaubt die Berechnung der logarithmischen Massenkorrekturen  $\ln^k(Q^2/m^2)$ , sowie des konstanten Terms, jedoch nicht von Potenzkorrekturen der Form  $(m^2/Q^2)^k$ . Die logarithmischen Korrekturen sind mittels der Renormierungsgruppengleichung durch die wohlbekannteren Spaltungsfunktionen und die masselosen Wilson-Koeffizienten gegeben, während der konstante Term sich aus der Berechnung der Operatormatrixelemente bestimmt. Die Berechnung der massiven 2–Schleifen Operatormatrixelemente und insbesondere des konstanten Terms der Massenkorrekturen zu den Wilson-Koeffizienten ist der Hauptteil dieser Arbeit. Hierfür waren massive 2–Schleifen 2–Punkt Integrale mit einem einlaufenden masselosen Teilchen zu berechnen. Diese Integrale enthalten zusätzlich eine von der Lichtkegelentwicklung stammende Operatoreinsetzung. Es handelt sich um die erste Nachrechnung des konstanten Terms, der zuvor in Ref. [55] berechnet wurde. Im Gegensatz zu Ref. [55] haben wir auf die Verwendung der partiellen Integrationsmethode für die Impulsintegrale verzichtet und dadurch eine sehr grosse Anzahl von Zwischenergebnissen vermieden und die Berechnung entscheidend kompaktifiziert. Ebenso konnte eine weitestgehende Automatisierung der Rechnung mittels Computer-Algebra Programmen erreicht werden. Zusätzlich haben wir unsere Berechnungen im Mellin-Raum durchgeführt und nicht im  $z$ -Raum, wie in Ref. [55]. Dadurch konnten wir die Integration von Nielsen-Integralen mit teilweise komplizierten Argumenten vermeiden. Stattdessen ist es uns in fast allen Fällen gelungen, eine Darstellung in Form von generalisierten hypergeometrischen Reihen zu finden, wobei als komplexeste Reihe  ${}_3F_2$  auftrat. Daraus ergeben sich unendliche Summen über einfache harmonische Summen, Beta-Funktionen und Binomialkoeffizienten mit einem freien Parameter, Mellin- $N$ . Diese führen im Ergebnis wiederum auf im Allgemeinen verschachtelte harmonische Summen. Unser Ergebnis im Mellin-Raum stimmt mit dem Mellin-transformierten Ergebnis von Ref. [55] überein. Die Komplexität der Mellin-Darstellung ist jedoch wesentlich geringer als die der  $z$ -Raum Darstellung. Statt 48 verschiedenen Nielsen-Integralen im  $z$ -Raum besteht unser Ergebnis nur noch aus 6 verschiedenen harmonischen Summen im Mellin-Raum, von denen nur eine einzige verschachtelt ist. Es scheint so zu sein, dass die Mellin-Darstellung der Symmetrie des Problems am ehesten gerecht wird.

## Acknowledgement

I am deeply grateful to J. Blümlein for putting very much time and effort in supervising me and invoking my interest in particle physics.

I would like to thank W.L. van Neerven and J. Smith for the opportunity to compare with their results for the individual Feynman diagrams.

Additionally I would like to thank DESY for giving me the opportunity to work on my thesis at Zeuthen and supporting me.

Further thanks go to I. Bierenbaum, F. Haas and U. Rühling for reading the manuscript.

Diese Diplomarbeit beinhaltet Beiträge zu folgenden Publikationen:

The longitudinal heavy quark structure function  $F_L^{Q\bar{Q}}$  in the region  $Q^2 \gg m^2$  at  $O(\alpha_s^3)$ ,  
J. Blümlein, A. De Freitas, W. L. van Neerven and S. Klein,  
Nucl. Phys. **B755** (2006) 272-285.

Evaluating two-loop massive operator matrix elements with Mellin-Barnes integrals,  
I. Bierenbaum, J. Blümlein and S. Klein,  
Nucl. Phys. (Proc. Suppl.) **B160** (2006) 85-90,

und 2 Publikationen in Vorbereitung.

## Selbstständigkeitserklärung

Hiermit erkläre ich, dass ich diese Arbeit im Rahmen der Betreuung am Deutschen Elektronen-Synchrotron in Zeuthen ohne unzulässige Hilfe Dritter verfasst und alle Quellen als solche gekennzeichnet habe.

Sebastian Klein, Potsdam den 27. Oktober 2006.